

JOURNAL OF THE  
**Electrochemical  
Society**

Vol. 101, No. 6

June 1954



DUPLICATE COPY  
RECEIVED

JUN 2 1954

SAVANNAH RIVER PLANT  
LIBRARY - T. I. S.

แผนกห้องสมุด กรมวิทยาศาสตร์  
กระทรวงอุตสาหกรรม



# Chlorine...

## for the Petrochemical Industry

Chlorine is of swiftly growing importance in the production of many new and revolutionary petrochemicals.

Swiftly growing, too, is the use of uniformly high quality GLC GRAPHITE ANODES—in helping the electrolytic industry meet the increasing civilian and defense needs for chlorine and caustic soda.

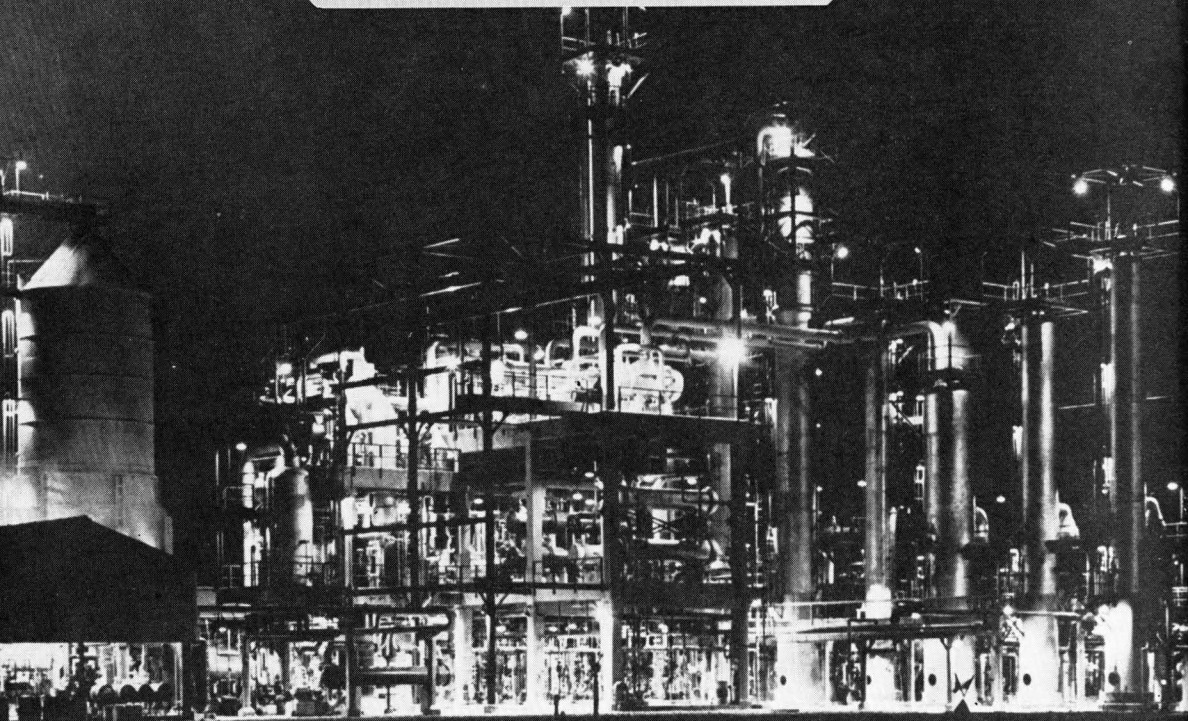
ELECTRODE DIVISION

**Great Lakes Carbon Corporation**

Niagara Falls, N. Y.



Morganton, N. C.



*Courtesy Jefferson Chemical Company Inc.*

### Graphite Electrodes, Anodes, Molds and Specialties

**Sales office:** Niagara Falls, N. Y.    **Other offices:** New York, N. Y., Oak Park, Ill., Pittsburgh, Pa.

Sales Agents: J. B. Hayes, Birmingham, Ala.; George O'Hara, Long Beach, Cal.; Great Northern Carbon & Chemical Co., Ltd., Montreal, Canada

Overseas Carbon & Coke Company, Inc., Geneva, Switzerland; Great Eastern Carbon & Chemical Co., Inc., Chiyoda-Ku, Tokyo

## EDITORIAL STAFF

R. M. BURNS, *Chairman*  
NORMAN HACKERMAN, *Technical Editor*  
RUTH G. STERNS, *Managing Editor*  
CECIL V. KING, *Associate Editor*  
U. B. THOMAS, *News Editor*  
NATALIE MICHALSKI, *Assistant Editor*

## DIVISIONAL EDITORS

J. V. PETROCELLI, *Corrosion*  
ABNER BRENNER, *Electrodeposition*  
W. C. VOSBURGH, *Battery*  
H. C. FROELICH, *Electronics*  
W. C. GARDINER, *Industrial Electrolytic*  
S. J. SINDEBAND, *Electrothermic*  
JOHN J. CHAPMAN, *Electric Insulation*  
CARL WAGNER, *Theoretical*  
SHERLOCK SWANN, JR., *Electro-Organic*

## REGIONAL EDITORS

JOSEPH SCHULEIN, *Pacific Northwest*  
J. C. SCHUMACHER, *Los Angeles*  
O. W. STOREY, *Chicago*  
G. W. HEISE, *Cleveland*  
PAUL S. BRALLIER, *Niagara Falls*  
OLIVER OSBORN, *Houston*  
EARL A. GULBRANSEN, *Pittsburgh*  
A. C. HOLM, *Canada*  
J. W. CUTHBERTSON, *Great Britain*  
T. L. RAMA CHAR, *India*



## ADVERTISING OFFICE

JACK BAIN  
*Advertising Manager*  
545 Fifth Avenue  
New York 17, N. Y.

PHONE—Murray Hill 2-5345

# Journal of the Electrochemical Society

216 West 102nd Street, New York 25, N.Y.

JUNE 1954

VOL. 101 • NO. 6

## CONTENTS

### Editorial

The Gerontological Outlook . . . . . 143C

### Technical Papers

- ✓ Preparation of High Purity Lead. *Ray C. Hughes* . . . . . 267  
Mathematical Studies on Galvanic Corrosion, I. Coplanar Electrodes with Negligible Polarization. *J. T. Waber* . . . . . 271  
Intensity Anomalies in Electron Diffraction Patterns of CuO. *J. M. Cowley* . . . . . 277  
Reduction of Oxidation-Ions in Hydrocarbons. *Andrew Gemant* . . . . . 281  
✓ High Purity Silicon. *Felix B. Litton and Holger C. Andersen* . . . . . 287  
Phenomena Observed in the Melting and Solidification of Germanium. *S. E. Bradshaw* . . . . . 293  
✓ Preparation and Examination of Beryllium Carbide. *M. W. Mallett, E. A. Durbin, M. C. Udy, D. A. Vaughan, and E. J. Center* . . . . . 298  
Ionic Mass Transfer and Concentration Polarization at Rotating Electrodes. *M. Eisenberg, C. W. Tobias, and C. R. Wilke* . . . . . 306  
Electrochemical Polarization of Titanium in Aqueous Solutions of Sodium Chloride. *Norman Hackerman and Colby D. Hall, Jr.* . . . . . 321  
The Nature of the Zinc-Containing Ion in Strongly Alkaline Solutions. *Theodora P. Dirkse* . . . . . 328  
DISCUSSION SECTION . . . . . 332

### Technical Review

The Problem of Correct Thermal Insulation of Bottom Linings of Aluminum Furnaces. *J. Wleugel and O. C. Böckman* . . . . . 145C

### Current Affairs

- News Notes in the Electrochemical Field . . . . . 151C  
Section News . . . . . 152C Book Reviews . . . . . 155C  
Personals . . . . . 154C Recent Patents . . . . . 159C  
Letter to the Editor . . . . . 155C Literature from Industry . . . . . 160C  
Meetings of Other Organizations . . . . . 155C New Products . . . . . 161C  
Employment Situation . . . . . 162C

Published monthly by The Electrochemical Society, Inc., Mount Royal and Guilford Aves., Baltimore 2, Md., combining the JOURNAL and TRANSACTIONS OF THE ELECTROCHEMICAL SOCIETY. Editorial office: 216 West 102nd Street, New York 25, N. Y. Statements and opinions given in articles and papers in the JOURNAL OF THE ELECTROCHEMICAL SOCIETY are those of the contributors, and The Electrochemical Society assumes no responsibility for them. Subscription \$11.25 to members, \$15.00 to nonmembers. Single copies \$1.25 to members, \$1.50 to nonmembers. Copyright 1954 by The Electrochemical Society, Inc. Entered as second-class matter November 15, 1947, at the Post Office at Baltimore, Md., under the act of August 24, 1912.

# CHECK THE FACTS..

## ON NATIONAL CARBON'S FULL LINE OF "KARBATE" PIPE AND FITTINGS FOR CORROSIVE SERVICES

IF YOU NOW USE "Karbate" pipe and fittings, you know their many advantages:

- Excellent Corrosion Resistance
- Freedom from Metallic Contamination
- High Resistance to Thermal Shock
- Light Weight
- Easy Machining and Fabrication

If you're not familiar with this material, get the facts . . . give them careful consideration when planning layouts where "Karbate" impervious graphite's remarkable combination of properties is required for efficient, trouble-free operation.

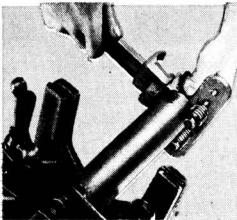
"Karbate" pipe and fittings feature standard stock items in a wide range of sizes . . . designed to make their *proper application* both simple and economical.



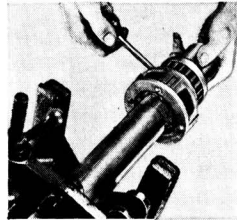
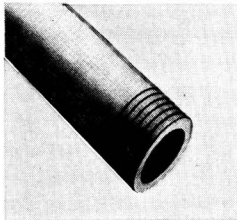
### EFFICIENT HAND TOOLS CUT FIELD ASSEMBLY COST

The light-weight hand tools shown below, developed specifically for threading and serrating "Karbate" pipe, contribute to ease and economy

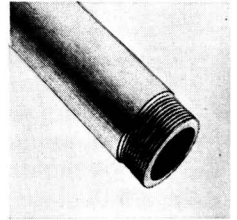
of field-fabrication . . . pay for themselves on the first sizeable job. Another reason to check - and *choose* "Karbate" impervious graphite equipment!



**SERRATING**



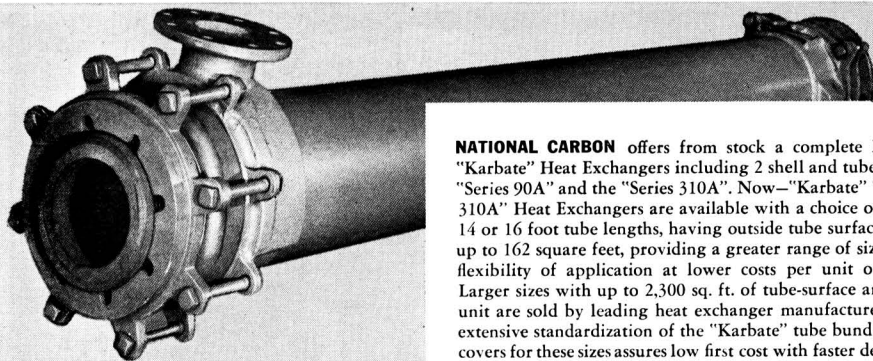
**THREADING**



# ...CHOOSE "KARBATE"

BRAND

## IMPERVIOUS GRAPHITE PROCESS EQUIPMENT



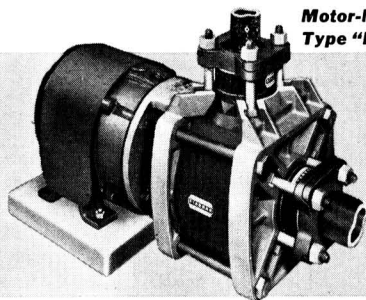
"Karbate" Heat Exchangers

**NATIONAL CARBON** offers from stock a complete line of "Karbate" Heat Exchangers including 2 shell and tube units: "Series 90A" and the "Series 310A". Now—"Karbate" "Series 310A" Heat Exchangers are available with a choice of 9, 12, 14 or 16 foot tube lengths, having outside tube surface areas up to 162 square feet, providing a greater range of sizes and flexibility of application at lower costs per unit of area. Larger sizes with up to 2,300 sq. ft. of tube-surface area per unit are sold by leading heat exchanger manufacturers. An extensive standardization of the "Karbate" tube bundles and covers for these sizes assures low first cost with faster delivery.

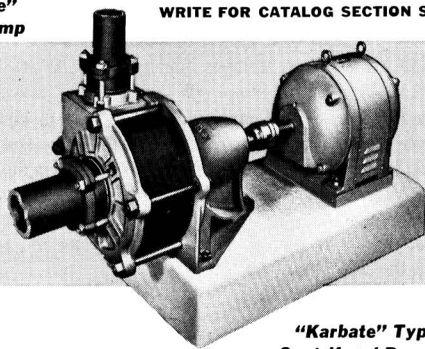
WRITE FOR CATALOG SECTION S-6740

**FEATURING** improved designs in a broad range of capacities, "Karbate" pumps are your best buy for the widest span of corrosive fluids, including

even mildly corrosive services. Ruggedly built, these new pumps are meeting the toughest requirements, virtually eliminating pump down-time.



Motor-Mounted "Karbate"  
Type "F" Centrifugal Pump



WRITE FOR CATALOG SECTION S-7250

"Karbate" Type "C"  
Centrifugal Pump

*The term "Karbate" is a registered trade-mark  
of Union Carbide and Carbon Corporation*

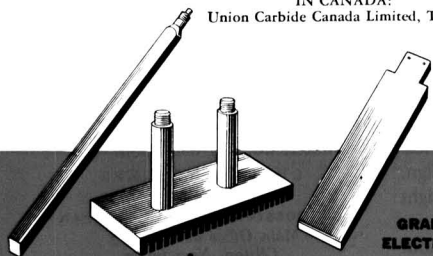
### **NATIONAL CARBON COMPANY**

A Division of Union Carbide and Carbon Corporation  
30 East 42nd Street, New York 17, N. Y.

District Sales Offices: Atlanta, Chicago, Dallas, Kansas City,  
New York, Pittsburgh, San Francisco

IN CANADA:

Union Carbide Canada Limited, Toronto



GRAPHITE ANODES FOR  
ELECTROLYTIC PROCESSES

IMPERVIOUS GRAPHITE  
**KARBATE**  
TRADE-MARK  
PROCESS EQUIPMENT  
**NATIONAL CARBON COMPANY**  
A Division of Union Carbide and Carbon Corporation.



TB 134

## How Improved Balance Design *Speeds Laboratory Work*

To appreciate how time—and tempers—can be saved in daily use of laboratory balances, let's go through a typical weighing operation, using a balance of modern design.

First of all, there's no time wasted in adjusting the zero point of the balance. Any slight variation from zero is quickly corrected. You just shift the index plate by Autodex, a control operated from outside the case.

Raising the front door, you'll notice there's plenty of hand room—no corner posts to get in your way, and no vertical chain column to restrict your access to the right pan. Loading of pans is fast and easy.

Now you have your sample and weights on the pans and you've closed the door. At this point, you'll find the adjustable Alnico damper helpful. It's vernier graduated for rapid duplication of settings—a feature especially welcomed by those who use the balance many times throughout the day.

To release the pans, simply turn the

knob. The individual pan arrest, with positive stop and even release, is mounted under the base plate and adjustable from above. This permits centering of bows after weights are placed on the pans and reduces knife edge wear.

Beam arrestment is easy and positive. The beam arrest arms and beam are pivoted about a common axis. This insures positive alignment and contact between knife edges and bearings with no dulling of agate edges.

In final balancing, you don't take your reading from a chain column as in previous balance designs. You refer, instead, to the easy-to-read Chainomatic dial, with its large numerals at convenient, constant eye-level position.

There are other sight-saving features, too, in modern balance design. The case is tapered to focus light on the working area. White matte inside finish adds brightness without glare. And white opal back glass elim-

inates background distraction.

It's a revelation, users tell us, how much faster, more effectively, they can work with these improved balances. Christian Becker makes a full range of 23 models, meeting virtually all laboratory needs.

If, on the other hand, you have an unusual problem, where a non-standard balance seems to be indicated, Christian Becker will adapt one of the present models or develop an entirely new design to answer your requirements.

Christian Becker also offers complete repair and reconditioning services. Just send in your old or damaged Christian Becker balance for a firm quotation—without charge or obligation—on the cost of restoring it to topnotch working condition.

**CHRISTIAN BECKER**

*Division of*

**THE TORSION BALANCE COMPANY**

*Main Office and Factory*

*Clijton, New Jersey*

*Sales Offices: Chicago — San Francisco*



## The Gerontological Outlook

“*COMPULSORY* retirement limits are old-fashioned” according to Dr. Martin Gumpert, the eminent geriatrician. He goes on to point out that the retirement practise, still followed by the majority of employers, causes tremendous economic waste, destroys the consumer capacity of a steadily growing segment of our population, and is grossly unjust and physically and emotionally deleterious to the retired individual of physical and mental vigor. There is no doubt that the rapidly increasing proportion of the population 65 years of age and over presents a problem of growing magnitude. As a result of the contributions of chemistry and medicine toward the elimination of infectious diseases, life expectancy of the newly born has risen in the past half century from 47 to 67 for men and 71 for women. During this period, the population of the United States has doubled, but the number who are 65 and over has quadrupled and is at present increasing at the rate of four hundred thousand a year.

Four choices are open to individuals upon retirement. They may continue in gainful employment and about 40% do so. The other choices for them are leisure, idleness, or recreation. Owing to the unnecessary intellectual shrinkage that many undergo in middle life, the leisure of later years all too often degenerates into idleness. Most people have less capacity for leisure than they have for work. With no established place in the cultural and recreational life of their community and no role in the economic system, many spend the later years in loneliness and insecurity. As a consequence, gerontological endeavor in many localities is being directed toward providing for medical care, recreation, appropriate housing, opportunities for gainful employment, and greater participation in the social and cultural activities of the community. Lending emphasis to the movement was the Governor of New York's designation of May as Senior Citizens' Month.

It is becoming recognized that individuals are only as old as their chemistry and that this bears little direct relationship to chronological age. Biochemical and medical research are now directed principally toward discovering the processes of aging and the reactions responsible for the onset of arteriosclerosis, degenerative heart disease, cancer, and obesity. No doubt the complicated and fascinating chemistry of living organisms pertinent to these ailments will provide difficulties as well as excitement to experimental scientists. Progress will be slow, but one may expect the next increase in life expectancy to be in the later years that have not shared appreciably in the gains of the past half century. Thus it may well be that the predicted figure of twenty-five million senior citizens in our population at the end of the century will be exceeded.

Preparation for senior citizenship should begin in early middle life. That is the time to broaden intellectual interests, develop hobbies and serious avocations. So much the better if some of these activities are capable of later expansion into financially profitable endeavors. The main problem, however, is to stay alive mentally and while in the prime of life to grow in intellectual appetite and stamina. He whose sole interest is his job usually does not long survive retirement from it. By the middle years, most people are established in their principal occupations and should be ready for the stimulation of new adventure. They can learn to paint or play a musical instrument, read extensively in the field of art or archeology, study geology or astronomy, learn a foreign language, delve into the records and remains of ancient civilizations, excavate fossils, learn mechanical arts, take up skiing and mountain climbing, collect books, start a greenhouse and experiment with growing orchids—even become an editor! All such activities and many more can make the later years the best of life and probably contribute to the vigor and durability so well exemplified in Horace Walpole's favorite character, the countess who was killed by falling out of an apple tree at the age of 126.

—RMB



**Model 622—Ultra-Sensitive Instruments**  
Portable d-c and a-c thermo instruments for precision measurement of potentials and minute currents in electronics or laboratory research.



**Model 901**  
**Portable Test Instruments**  
Available in d-c, Model 901—and a-c, Model 904, single and multiple ranges of wide coverage. Excellent scale readability and shielding. Accuracy within  $\frac{1}{2}$  of 1%.



**A-C Clamp Volt-Ammeter**  
(Model 633, Type VA-1) For convenient and rapid measurement of a-c voltage and current without breaking the circuit. Jaws take insulated or non-insulated conductors up to 2" diameter. Safe, rugged, versatile. Also available as a-c clamp ammeter, without voltage ranges.

*Specialized and Multi-purpose*

## INSTRUMENTS

for ● RESEARCH  
● PRODUCTION  
● MAINTENANCE

For complex, or just routine measurement jobs, these and other specialized WESTON Instruments save time and assure dependable measurements. For information on the complete line, see your local Weston representative, or write . . . WESTON Electrical Instrument Corp., 614 Frelinghuysen Ave., Newark 5, N. J.

**WESTON**  
*Instruments*



### Sensitive Relays

A line of sensitive relays including the Model 705 which provides positive operation at levels as low as  $\frac{1}{2}$  microampere. Non-chattering magnetic contacts handle up to 10 watts at 120 volts.

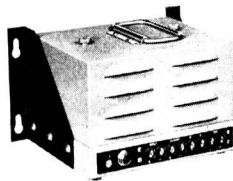


### Panel and Switchboard Instruments

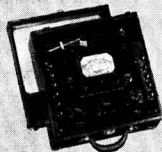
A complete line of instruments in all types, sizes and ranges required for switchboard and panel needs . . . including d-c, a-c power frequencies and radio frequency, rectifier types and D.B. meters.



**Model 697 Volt-Ohm-Milliammeter**  
One of a line of pocket-size meters, Model 697 combines a selection of a-c and d-c current, and resistance ranges. Ideal for maintenance testing and many inspection requirements.

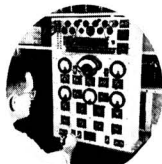


**Model 1411 Inductronic D-C Amplifier**  
Stable amplifier provides high degree of resolution even at fractional loads. Reaches steady full scale deflection in a fraction of a second. Interchangeable plug-in range standards for either microamperes or millivolts.



### Industrial Circuit Tester—Model 785

A multi-range, multi-purpose, ultra-sensitive analyzer, for laboratory and industrial checking of electrical and electronic circuits. Has 28 practical scale ranges; measures d-c and a-c voltage, d-c and a-c current, and resistance. Accessories available to extend ranges. Compact and portable; furnished in either oak or steel case.



### Model 686 Electronic Tube Analyzer

Tests tubes under exact operating potentials. Accurately determines true mutual conductance of all tubes, in accordance with manufacturers' rated operating conditions, or under special operating conditions.



### High Frequency Electronic Analyzer Model 769

A three-in-one instrument providing a self-contained Volt-Ohm-Milliammeter, a high impedance electronic D-C Volt-Ohmmeter, and a probe type Vacuum Tube Voltmeter for use to 300 megacycles. Exceptionally stable and accurate. Has specially designed extremely small RF and D-C probes.



# Preparation of High Purity Lead<sup>1,2</sup>

RAY C. HUGHES

*Philips Laboratories, Inc., Irvington-on-Hudson, New York*

## ABSTRACT

Previously published methods for the preparation of high purity lead are critically reviewed. The presumably more effective of these methods were subjected to trial and analytical evaluation. Based on these analytical results, a combination of procedures is described which produces lead of extremely high purity. The method employed involves electrolytic displacement of bismuth and other elements from lead salt in solution by treatment with lead metal, coprecipitation of numerous impurities on lead sulfide, conversion to metal, and final vacuum distillation.

## INTRODUCTION

Efforts to prepare pure samples of lead and its compounds date back to the work of Stas (1) in 1860. Pure samples have been required for atomic weight determinations, study of the properties of the element and its compounds, and as an analytical aid, especially in assays for gold and in standards for spectrographic analysis. Numerous publications and several reviews on the subject have appeared. However, none of the original publications has presented adequate analytical evidence as to the purity attained. Consequently, the reviews do not clearly establish relative efficacy of the various methods described and, in addition, all are incomplete to a greater or lesser extent.

The purpose of this paper is to present an analytical evaluation of previously described methods and to describe in detail a combination of methods for preparation of pure lead.

### *Review of Previous Methods*

Mellor (2) and Vanino (3) described a method employed by Stas (1) for preparing high purity lead. It comprises purification of a lead acetate solution and several subsequent precipitations and resolutions to obtain a pure lead carbonate which is reduced to metal with potassium cyanide. No adequate analytical data are available for the metal made by this method.

Mellor also refers to the use of vacuum distillation by Lambert and Cullis (4) to purify further lead produced by the Stas method. Baxter and Grover (5) and Richards and Wadsworth (6) purified lead by recrystallization from nitrate solution; the yield from such a method is quite low, and quality of the product questionable. Archibald (7)

reviews early work in preparing samples for atomic weight determinations; Schopper (8) presents a rather comprehensive review of work done to 1939 on preparation of high purity lead. He considers the method of Haber and Jaenicke (9) to be superior; this method depends on coprecipitation of impurities with lead sulfide. Russell (10) developed an electrolytic method using a perchlorate solution.

Lead of high purity (99.998+ %), with the only impurities being iron and copper,<sup>3</sup> has been reported (11). McLellan (12) generously supplied the following details:

1. A new storage battery box with three anodes and two cathodes makes a good cell. Anodes about  $\frac{3}{4}$  in. thick with supporting lugs are cast from bismuth-free lead.<sup>4</sup> Cathodes, made from pure lead deposited on rolled lead<sup>4</sup> starting sheets equal in area to the anodes, are supported by heavy Pyrex rods.

2. Ideally, the electrolyte, which does not require stirring, has a specific gravity of 1.21; it is composed of 67 g/l Pb as  $\text{PbSiF}_6$  and 95 g/l  $\text{H}_2\text{SiF}_6$ .<sup>5</sup> Lead should be introduced in the form of bismuth-free  $\text{PbCO}_3$ .<sup>4</sup> Pure glue in a minimum of hot water is added daily. A reasonable current density is 0.5 amp/in.<sup>2</sup>

3. Wash cathodes thoroughly in distilled water then melt in a spun iron crucible and cast. Remelt in a glass or pure iron container. Gradually add pure red phosphorus while stirring constantly. Keeping the temperature around 350°C, tap off from the bottom most of the decopperized lead. Melt in a spun iron crucible and add reagent grade NaOH and  $\text{NaNO}_3$ . Stir 15 min at 400°C and cool. Dissolve caustic skin in distilled water, remelt lead, and granulate in distilled water. Remelt in a beaker, using reagent sodium acetate and NaOH as slag

<sup>1</sup> Manuscript received December 17, 1951. This paper was prepared for delivery before the Montreal Meeting, October 26-30, 1952.

<sup>2</sup> This work was supported in part under Contract W33-038 AC-15141 with the Air Materiel Command.

<sup>3</sup> Prepared in Research Department, American Smelting and Refining Company, Barber, New Jersey.

<sup>4</sup> St. Joe brand.

<sup>5</sup> Merck reagent grade.

cover. Introduce clean air or oxygen to the lead through a Pyrex tube; skim slag and repeat with fresh slag materials.

Details of a method for preparation of rather pure lead, and a sample of lead so produced, have been supplied by G. K. Williams (13) and associates.<sup>6</sup> The method has been described by Green (14).

Vacuum distillation has been investigated by Lambert and Cullis (4) and Tamman and Dreyer (15). Kroll (16), Leitgeb (17), and Dushman (18) present reviews on vacuum evaporation of metals and considerations involving purification of lead by such methods. A study of all available data on vacuum distillation of lead indicates that, except for bismuth and possibly antimony, impurities should remain in the initial and final distillate of such a process.

Haber and Jaenicke (9) use a method which appears to have considerable merit for the preparation of pure lead. It is essentially a coprecipitation of contaminants with a small amount of lead (from a solution of lead salt) according to principles which have been elucidated by Hahn (19). Experimental work (see later) shows that not all impurities are adequately removed by this method.

#### EXPERIMENTAL INVESTIGATION OF METHODS

An experimental investigation was made of the more promising methods selected from those just reviewed. In general, the methods were applied to small samples of lead (or a compound) of low impurity content. Starting materials, purified samples, and concentrates obtained during sample purification were all examined and compared by spectrographic methods developed to give maximum sensitivity. Details of the method have been published elsewhere (20). The following sensitivities of detection (in ppm) were obtained in the direct analysis of a lead sample: Ag, 0.01; Cu, 0.03; Bi, 0.3; Fe, 0.1; Cd, 0.03; Sn, 0.3; Zn, 0.05. Additional sensitivity of at least one order of magnitude was obtainable in specific cases by use of fractions separated from the sample.

As, Se, and Te were not included in the analytical investigation due to the known low sensitivity of spectrographic detection of these elements. The behavior of antimony has not been adequately determined because of its relatively low sensitivity of detection.

Throughout the experimental work extensive precautions were taken to avoid contamination of samples. Water and acids were redistilled from a fused quartz still. Dust-proof fused quartz, high purity alumina, and platinum containers were

used. All vessels were cleaned thoroughly in hot dilute nitric acid and rinsed with redistilled water. When these precautions were not observed, contamination from dust and containers (such as Pyrex glass and porcelain) was detected.

#### *Sulfide Coprecipitation*

Experimental work was initiated with a study of the sulfide coprecipitation method of Haber and Jaenicke (9). It was found that Ag, Fe, Mo, and Cu are strongly concentrated in the precipitate and efficiently removed. Bi, Cd, Sb, Sn, and Zn either preferentially remain in solution, or are about equally distributed between the two phases; thus they are not effectively eliminated.

#### *Vacuum Distillation*

In view of the foregoing, other methods were tested, one of which was high vacuum distillation. A sample of lead containing approximately 1 ppm each of Ag and Bi, 2 ppm each of Cu and Fe, and 0.1 and 0.5 ppm, respectively, of Cd and Zn was employed. A single distillation in fused quartz at 700°–800°C and 10<sup>-6</sup> mm resulted in lowering the Fe, Cu, and Ag content below the limit of spectrographic detectability. Reheating the distillate at approximately 500°C caused volatilization of a small amount of material which condensed in the pump leads and gave strong spectra of cadmium and zinc. Residual lead gave no spectroscopic evidence of cadmium or zinc. Bismuth was distributed about equally between distillate and residue. Therefore, except for bismuth and possibly antimony for which no data were obtained, high vacuum distillation is an effective and convenient method for removal of impurities from lead. A combination of the Haber and Jaenicke process and vacuum distillation leaves only bismuth and antimony.

#### *Electrolytic Displacement*

At this stage it became evident that bismuth is by far the most persistent impurity, and that for which no proved effective method of removal is available. According to the method employed by Stas (1), Sb, Bi, Cu, Ag, Au, and the platinum metals should be displaced from solution by the action of metallic lead. However, no quantitative data exist as to its efficacy.

The method was studied by use of lead acetate filtrate from a prior trial of the sulfide coprecipitation method. To a neutral solution containing 500 grams lead acetate and 500 ml redistilled water, 1 gram finely chipped, high purity lead was added, and the solution heated overnight at the boiling point. The lead was separated and portions of it and the solution analyzed spectrographically. Treat-

<sup>6</sup> Broken Hill Associated Smelter's Proprietary Limited, Port Pirie, South Australia.

ment with 1-gram portions of lead was repeated several times.

In a single treatment, bismuth was removed from the solution to an extent such that it no longer gave spectrographic evidence of its presence. The metal, of course, gave strong lines of bismuth. Several successive treatments resulted in removal of progressively smaller quantities of bismuth, although after the first treatment the solution must have contained less than 0.3 ppm bismuth based on lead content. Copper and silver were also efficiently removed. Cadmium, zinc, and antimony are not removed by this treatment.

#### PROCEDURE FOR THE PREPARATION OF HIGH PURITY LEAD AND ITS COMPOUNDS

Due to failure of any single procedure to remove all impurities from lead, a combination of procedures was selected as most suitable for the production of a pure sample. These procedures are applied in proper sequence to avoid reintroduction of contaminants previously removed.

Lead acetate is the most convenient and suitable starting material; however, the metal, nitrate, or other compound may be employed, provided it is eventually converted to the acetate. Technical acetate is of acceptable purity for the starting material.

Preparation of pure lead consists of three processes: (a) treatment of lead acetate or lead nitrate with lead metal, primarily for elimination of bismuth. This may be the first or second step, or it is eliminated if removal of bismuth is not required; (b) lead sulfide coprecipitation specifically for removal of copper, silver, gold, selenium, and tellurium;<sup>7</sup> (c) high vacuum distillation is required for elimination of cadmium and zinc. It is also effective for removal of practically all metallic elements except bismuth and possibly antimony. Further, this reduces the gas content to a low level.

For step (a) the solution should be highly concentrated, e.g., about 100 ml water to each 200 grams acetate, and contained in a fused quartz or silica flask. Finely divided lead is added in the proportion 1 g/100 g Pb in solution. For 12–24 hr the solution is heated in contact with the lead. The solution is decanted, a fresh quantity of lead is added, and the procedure repeated for a total of five treatments, or until spectrographic analysis of residual lead shows that further treatment removes

<sup>7</sup> Conversion to metal by ignition of the purified acetate probably aids in elimination of alkalis, alkaline earths, silica, and other soluble impurities which escape precipitation as sulfides, and which are not readily reduced to the elemental condition. However, this is not relied upon for separation of any impurity.

no more impurities. Lead employed for each treatment must be prepared from acetate solution by ignition, unless pure lead is available from a previous preparation. Considerable care must be exercised to avoid copper contamination from vessels or water during this treatment. Addition of water during the last several treatments should be avoided.

To the solution obtained from the above treatment, 1 gram thiourea/100 grams lead in solution is added. The solution, again contained in fused silica or quartz, is heated at the boiling point on a hot plate until it darkens and begins to deposit lead sulfide. Heating is continued 1–2 hr. The solution is then filtered through a fritted silica filter. (Pyrex may be substituted since the exposure is brief.) The solution is again heated for a similar period and filtered. Under these conditions it should be possible to obtain four small precipitates of lead sulfide. Finally, the solution is heated for 12–24 hr, to ensure complete decomposition of thiourea, and filtered. Spectrographic analysis of the precipitates should show that, after the third, there is no further concentration of impurities in the precipitate.

The purified solution is now transferred to a dense, high purity, aluminum oxide crucible, which initially should be no more than  $\frac{1}{5}$  full. The solution is cautiously evaporated at gradually increasing temperature until a solid residue of lead acetate is obtained. The crucible is transferred to a pot-type crucible furnace and the temperature of the crucible gradually increased to approximately 700°C. (Close control of temperature is not required.) During heating, the acetate melts, becomes viscous, foams, and finally decomposes to a mixture of metal, oxide, and carbon. Fresh lead acetate solution is dropped onto the lead-lead oxide mixture while heating is continued. The previously formed oxide is now largely reduced. Contact of cold solution with the hot crucible wall should be avoided. Crucible contents should have free access to air in order to oxidize the carbon residue. It is convenient to stir the residue and keep it compacted with a rod of aluminum oxide or spectroscopically pure graphite. Ignition should be conducted in a hood. At some stages, fumes may burn above the crucible. When prepared in this manner, a large proportion of lead is formed with relatively little oxide. The lead may be separated from the oxide by pouring off into a clean silica or Pyrex container; remelting and mechanical separation by pouring into a clean container three or four times results in elimination of all visible oxide.<sup>8</sup>

<sup>8</sup> If oxide or other compound of lead is desired, the ignition may be carried out at 300°C in fused quartz without subsequent addition of fresh quantities of acetate. Under these conditions, pure lead oxide is formed. However, it should be noted that zinc and cadmium may still be present.

For the final step in purification, lead prepared as described above is transferred to a fused quartz still and redistilled under high vacuum at 700°–800°C. Head and end fractions (1–2% of total) should be discarded.

Lead produced by the procedure described here contains no spectrographically detectable impurities within the sensitivity limits given earlier. Traces of Si, Ca, Mg, Cu, and Fe which are occasionally detected spectrographically are believed to originate from even the best obtainable graphite electrodes. All available evidence would indicate that this lead is probably of the highest purity which has been attained. The methods employed are relatively convenient, rapid, and allow high recovery.

#### ACKNOWLEDGMENT

It is a pleasure to acknowledge the encouragement of O. S. Duffendack, President and Director of Research of this Laboratory, throughout this work; the assistance of J. S. Schulz with all phases of the experimental work; and the kindness of R. D. McLellan and G. K. Williams, for permission to publish details of methods supplied by them.

Any discussion of this paper will appear in a Discussion Section, to be published in the December 1954 issue of the JOURNAL.

#### REFERENCES

1. J. S. STAS, *Bull. acad. roy. sci. Belg.*, (2), **10**, 295 (1860).
2. J. W. MELLOR, "A Comprehensive Treatise on Inorganic and Theoretical Chemistry," Vol. VII, p. 508, Longmans, Green and Co. Ltd., London (1947).
3. L. VANINO, "Handbuch der Preparativen Chemie," Band 1, pp. 610–2, Ferdinand Enke, Stuttgart (1925).
4. B. LAMBERT AND H. E. CULLIS, *J. Chem. Soc.*, **107**, 210 (1915).
5. G. P. BAXTER AND F. L. GROVER, *J. Am. Chem. Soc.*, **37**, 1027 (1915).
6. T. W. RICHARDS AND C. WADSWORTH, *J. Am. Chem. Soc.*, **38**, 221 (1916).
7. E. H. ARCHIBALD, "The Preparation of Pure Inorganic Substances," pp. 219–23, John Wiley and Sons, Inc., New York (1932).
8. W. SCHOPPER, in "Reine Metalle," (A. E. van Arkel, Editor), pp. 501–15, Julius Springer, Berlin (1939).
9. F. HABER AND J. JAENICKE, *Z. anorg. u. allgem. Chem.*, **147**, 156 (1925).
10. R. S. RUSSELL, *Proc. Australasian Inst. Mining and Met.*, N.S., No. 95, 125 (1934).
11. T. A. WRIGHT, "Spectroscopy in Science and Industry," pp. 47–50, John Wiley and Sons, Inc., New York (1938).
12. R. D. McLELLAN, Private communications.
13. G. K. WILLIAMS, J. MURRIE, F. A. GREEN, AND N. G. READ, Private communications.
14. F. A. GREEN, Symposium on Refining Non-Ferrous Metals 1949, Inst. Mining and Met. (London), 281–36 (1950).
15. G. TAMMAN AND K. L. DREYER, *Z. anorg. u. allgem. Chem.*, **190**, 53 (1930).
16. W. J. KROLL, *Trans. Electrochem. Soc.*, **87**, 571 (1945).
17. LEITGEBEL, *Z. anorg. u. allgem. Chem.*, **202**, 317 (1931); *Metal U. Erz*, **32**, 206 (1935).
18. S. DUSHMAN, "Scientific Foundations of Vacuum Technique," pp. 740–78, John Wiley & Sons, New York (1949).
19. O. HAHN, "Applied Radiochemistry," The Collegiate Press, Menasha, Wisconsin (1936).
20. R. C. HUGHES, *Spectrochim. Acta*, **5**, 210 (1952).

# Mathematical Studies on Galvanic Corrosion

## I. Coplanar Electrodes with Negligible Polarization<sup>1</sup>

J. T. WABER

*Los Alamos Scientific Laboratory of the University of California, Los Alamos, New Mexico*

### ABSTRACT

Distribution of potential within an electrolyte produced by a coplanar arrangement of electrodes has been determined mathematically. Only the limiting case of negligible anodic and cathodic polarization is considered. Distribution of corrosion attack on the anode has been derived from this potential distribution.

### INTRODUCTION

A mathematical study of a typical case of galvanic corrosion is presented in this discussion. Two coplanar electrodes placed in juxtaposition are considered. The arrangement is characteristic of local cells that occur frequently in corrosion. Pertinent galvanic cells may consist either of many tiny electrodes imbedded in a metal or, in some cases, of large pieces of different metals connected electrically. It is possible to distinguish more satisfactorily, in a qualitative way, between microscopic and macroscopic galvanic cells on the basis of current density distribution. In microscopic cells, current density is relatively uniform over each electrode, whereas in macroscopic cells it varies significantly.

In a given environment, and irrespective of its physical size, a galvanic cell may behave as though it were "macroscopic" or "microscopic," depending on whether its critical dimension is much larger or much smaller than a polarization parameter,  $\xi$ . This critical dimension is that which affects distribution of current density most strongly and thus depends upon the geometry of the cell. In certain cases, it may be the separation of electrodes and, in others, the smallest dimension of one electrode. This parameter<sup>2</sup> has the dimension of length and is defined by Wagner (1) as

$$\xi_i = K \left| \frac{d\Delta E_i}{dJ_i} \right| \quad [1]$$

where  $K$  is the specific conductivity of the corrodent,  $\Delta E_i$  is the overvoltage of the  $i$ th metal or electrode, and  $J_i$  is the current density. The vertical bars denote the absolute value of the derivative.

<sup>1</sup> Manuscript received February 23, 1953. This paper was prepared for delivery before the Detroit Meeting, October 9 to 12, 1951.

<sup>2</sup> The symbol  $\xi$  is used to emphasize the dimensional character of this parameter and to remove any possible confusion with  $K$  which is commonly used to denote conductivity.

### DERIVATION OF RESULTS

Only the limiting case in which polarization can be neglected is considered. It is equivalent to assuming that  $\xi$  is negligibly small. Such would be the case if the electrolyte resistance were very high, or if the smallest critical dimension,  $\lambda$ , of the galvanic cell were large in comparison with  $\xi$ . Hence, because  $\lambda/\xi$  is large, such galvanic cells behave as though they were macroscopic, irrespective of their physical size. If the electrolyte resistance is very large, almost all electrodes behave macroscopically. On the contrary, under corrosive conditions that permit strong polarization of the electrodes ( $\xi$  large), arrays of macroscopic elements may behave as though they were of microscopic dimensions. Solutions of high conductivity can also produce the same effect.

#### *Distribution of Potential*

Distribution of potential throughout the electrolyte is given by Laplace's equation because space charges and sources or sinks for ions are not present in bulk corrosive media. The exact potential distribution depends on the geometry of electrodes as well as their voltages. Electrodes are considered to be part of the boundary of the electrolyte. In order to calculate the distribution of the potential, one must solve a boundary-value problem for which the values of potential imposed on the boundary of the electrolyte, as well as the geometry of the boundary, are specified.

Fourier series and conformal mapping are two methods which may be used for solving such problems. Fourier series and conformal mapping are discussed by Churchill (2) among others, while a less mathematical approach to various boundary value problems is given by Jakob (3) on heat transfer.

One may calculate the local corrosion intensity by evaluating the normal gradient of the potential at one electrode. The numerical evaluation may be difficult and tedious in some cases.

### Boundary Conditions

For corrosion by local cells, a coplanar arrangement of electrodes is pertinent and illustrates the principal features needed for an analysis. The primary interest lies in the effects due to the anode-cathode junctions. In order to eliminate other edge effects it is assumed: (a) that long, narrow strips of each electrode are juxtaposed to form an infinite, alternating array, (b) that the array has even symmetry, and (c) that the length in the  $Z$  direction is so large as to have no effect on the current distribution. Such an arrangement is shown in Fig. 1a. At the center of each anode (or cathode) one can see intuitively that there must be no net current flow since the flow of ions changes direction to either side of the center. We shall choose the origin in the center of one of the anodes. Since there is no variation in potential in the  $Z$  direction, and

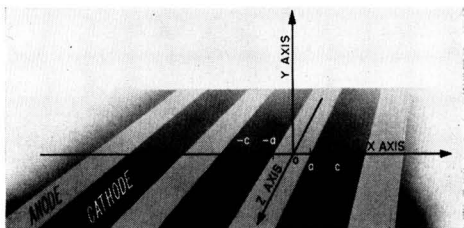


Fig. 1a. Perspective view illustrating relative orientation and shape of the electrodes.

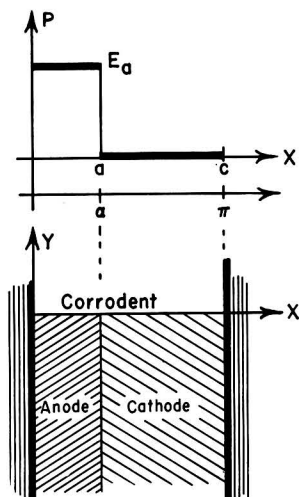


Fig. 1b. Distribution of potential assumed as the boundary conditions is shown in the upper drawing. In the lower drawing the anode and cathode arrangement is illustrated. At the remote edges of the electrodes, boundary conditions are equivalent to assuming insulation.

consequently none in the current density, we may restrict our attention to the two-dimensional flow problem. Because of the highly symmetrical arrangement, only a semi-infinite strip of liquid lying in the first quadrant of the  $XY$  plane above the array needs to be considered. The width of this strip is equal to half of the sum of the anode and cathode widths. Geometric relations are illustrated in Fig. 1b.

There can be no flow of electrons across the boundary formed by the  $Y$  axis, and on this boundary the gradient of the potential in the  $X$  direction is zero. This statement is mathematically equivalent to assuming insulation of the boundary. A similar argument shows that the horizontal gradient in Fig. 1b is zero at the boundary,  $x = c$ .

The potential is measured with respect to the unpolarized cathode. The anodic potential in excess of the cathodic potential, i.e., the potential difference, is designated as  $E_a$  and the potential in the solution as  $P(x, y)$ .

The pertinent boundary conditions are:

$$\lim_{y \rightarrow \infty} P(x, y) < \text{const.} \quad [2]$$

$$\left. \frac{\partial P}{\partial x} \right|_{x=0} = \left. \frac{\partial P}{\partial x} \right|_{x=c} = 0 \quad [3]$$

$$P(x, 0) = \begin{cases} E_a & 0 \leq x \leq a \\ 0 & a \leq x \leq c \end{cases} \quad [4]$$

### Solution by Fourier Series

A Fourier series, which satisfies Laplace's equation and conditions [2] and [3], is

$$P(x, y) = A_0 + \sum_{n=1}^{\infty} A_n \exp(-nhy) \cos(nhx) \quad [5]$$

where the constants  $A_0$  and  $A_n$  are determined by boundary condition [4]. In [5],  $n$  is an integer and  $h$  is a reciprocal length equal to

$$h = \pi/c \quad [6]$$

One may employ the orthogonal properties of a cosine series to obtain the coefficient  $A_n$ . That is, both sides of [5] are multiplied by  $\cos mhx$  and then integrated termwise with respect to  $x$  over the range  $x = 0$  to  $x = c$ . Thus

$$A_m = \frac{2h}{\pi} \int_0^c P(x, 0) \cos(mhx) dx \quad [7]$$

$$= \left( \frac{2E_a}{\pi^m} \right) \sin(mha)$$

$$A_0 = \frac{1}{c} \int_0^c P(x, 0) dx = E_a(a/c) \quad [8]$$

After substitution, the potential at any point is given by

$$P(x, y) = \frac{E_a \alpha}{c} + \frac{2E_a}{\pi} \sum_{n=1}^{\infty} \exp(-nhy) \frac{\sin(nha)}{n} \cos(nhx) \quad [9]$$

The equations can be simplified slightly by defining the dimensionless variables.

$$\begin{aligned} \xi &= hx \\ \eta &= hy \\ \alpha &= ha \end{aligned} \quad [10]$$

Hence,

$$P(\xi, \eta) = E_a \alpha + \frac{2E_a}{\pi} \sum_{n=1}^{\infty} \frac{1}{n} \exp(-n\eta) \sin(n\alpha) \cos(n\xi) \quad [11]$$

The normal gradient is the  $\eta$ -derivative of  $P$ . Therefore the local anodic corrosion rate,  $r(\xi)$ , at any point on the electrode surface is

$$r(\xi) = - \left( \frac{\pi R_o}{2} \right) \frac{\partial P}{\partial \eta} \Big|_{\eta=0} \quad [12]$$

where the constant  $R_o$  is defined as

$$R_o = \frac{2KM}{\pi Fv} \quad [13]$$

In [13],  $M$  is the atomic weight of the anodic metal ion,  $v$  is its charge, and  $F$  is Faraday's number. Substitution of [11] into [12] leads to

$$r(\xi) = R_o E_a \sum_{n=1}^{\infty} \sin(n\alpha) \cos(n\xi) \quad [14]$$

Series [14] does not converge and hence it cannot be used for evaluating the corrosion current. Substitution of a small nonzero value of  $\eta_o$  into the derivative of [12] leads to small bounded values of a series similar to [14]. However, it is preferable to evaluate the derivative at zero by a different method, and not to depend upon a limiting value as  $\eta_o$  approaches zero.

*Solution by Conformal Mapping*

A closed analytic expression which is bounded over most of the anodic region may be obtained for the  $\eta$ -derivative by conformal mapping. Wagner (4) has applied this technique to the solution of similar problems in cathodic protection.

The semi-infinite strip of corrodent in Fig. 1b may be regarded as the complex  $Z$  plane by letting

$$z = x + iy$$

where  $i$  is the imaginary square root of minus one. Mathematical transformations are used to rearrange the electrode positions into one for which the potential distribution is well known. The four steps necessary to transform the arrangement of electrodes shown in Fig. 2a into that shown in Fig. 2b are defined below. The effect of each transformation is shown in Fig. 3. The quantity

$$\gamma = \sin \left( \frac{\pi}{2} \cdot \frac{2a - c}{c} \right) \quad [15]$$

is used in the following equations for convenience. The first transformation is an expansion which changes the scale,

$$z^i = \frac{\pi}{2} \left( \frac{2z - c}{c} \right) \quad [16]$$

The second transforms the strip into a semi-infinite plane,

$$z^{ii} = \sin z^i \quad [17]$$

The third shifts the origin by  $\gamma$  units,

$$z^{iii} = z^{ii} - \gamma \quad [18]$$

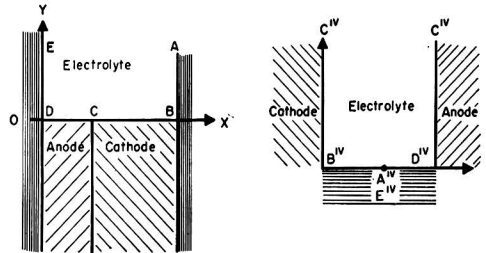


FIG. 2. Net change in relative anode and cathode positions brought about by the series of transformations. Fig. 2a (left) shows the initial location and Fig. 2b (right) shows the final location.

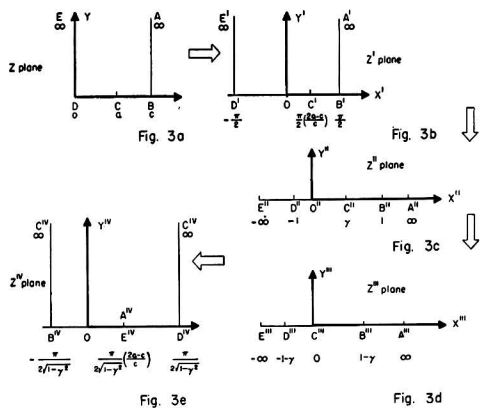


FIG. 3. Detailed effects of each transformation from the  $Z$  plane in Fig. 3a to the  $Z^{iv}$  plane in Fig. 3e.

The fourth transforms the semi-infinite plane back into a strip, but with a relocation of the vertices, i.e., corners. It is a special type of Schwartz-Christoffel transformation.

$$z^{iv} = \int \frac{dz^{iii}}{z^{iii}(z^{iii} - 1 + \gamma)^{\frac{1}{2}}(z^{iii} + 1 + \gamma)^{\frac{1}{2}}} \quad [19]$$

Integration of [19] gives

$$z^{iv} = \frac{1}{\sqrt{1 - \gamma^2}} \arcsin \left( \gamma - \frac{1 - \gamma^2}{z^{iii}} \right) \quad [20]$$

It can be shown that boundary condition [4] transforms to

$$P = 0 \text{ for } x^{iv} = \frac{-\pi}{2\sqrt{1 - \gamma^2}} \quad [21]$$

$$P = E_a \text{ for } x^{iv} = \frac{\pi}{2\sqrt{1 - \gamma^2}}$$

as long as  $Y^{iv}$  is positive and finite. The solution of the problem in the  $Z^{iv}$  plane is well known and gives isopotential lines parallel to the  $Y^{iv}$  axis.

The boundary conditions are satisfied by

$$P = E_a \operatorname{Re} \left( \frac{1}{2} + \frac{z^{iv} \sqrt{1 - \gamma^2}}{\pi} \right) \quad [22]$$

where **Re** stands for the real part of the enclosed expression. By reversing the sequence of transformations one can show that

$$P = E_a \operatorname{Re}$$

$$\left\{ \frac{1}{2} + \frac{\arcsin \left[ \gamma - \frac{1 - \gamma^2}{\sin \frac{\pi}{2} \left( \frac{2z - c}{c} \right) - \gamma} \right]}{\pi} \right\} \quad [23]$$

Equation [23] has an advantage in permitting direct calculation of the  $Y$  derivative; whereas the equivalent Fourier representation [14] does not converge at  $y = 0$ . The derivative can be shown to be

$$\frac{\partial P}{\partial y} \Big|_{y=0} = \frac{E_a}{c} \left\{ \frac{\cos \left( \frac{\pi}{2} \cdot \frac{2a - c}{c} \right)}{\sin \left( \frac{\pi}{2} \cdot \frac{2x - c}{c} \right) - \sin \left( \frac{\pi}{2} \cdot \frac{2a - c}{c} \right)} \right\} \quad [24]$$

if one notes that

$$\frac{\partial P}{\partial y} = \left( \frac{dP}{dz} \cdot \frac{\partial z}{\partial y} \right) = \operatorname{Re} \left( i \frac{dP}{dz} \right) \quad [25]$$

It may be seen that this derivative goes to infinity at  $x = a$ . Practically, current density remains finite because of polarization, but this factor has been ignored in the idealized analysis presented here.

### Potential of a Composite Electrode

The potential in solution of a galvanic cell with respect to an infinitely remote reference electrode can be derived from equation [9]. The potential at infinite  $y$  and any value of  $x$  is:

$$P(x, \infty) = E_a(a/c) = E_a(\alpha/\pi) \quad [26]$$

Under such conditions, the potential of a composite metal or of a galvanic cell depends on the percentage of anodic material or phase present. This highly important result may also be derived from [23].

### NUMERICAL EVALUATION

Potential fields have been calculated for the  $\alpha$ -value of  $\pi/2$ ,  $\pi/4$ , and  $\pi/8$ ; that is, for values of the ratios of the anodic to the cathodic width of 1,  $1/3$ , and  $1/7$ .

Expression [11] or [23] may be used and, in a number of cases, tabulated values of  $P(x, y)$  have been checked with both expressions.

### Evaluation of Equation [23]

The real and imaginary parts of the arcsin must be separated in order to facilitate direct calculation. For a slightly simpler calculation procedure, the reader is referred to Hawelka's tables (5) of the sines and cosines of complex numbers. However, the following equations are evaluated easily and depend only upon the usual trigonometric functions of a real variable. Two variables,  $s$  and  $t$ , are defined such that

$$P(x, y) = E_a \left\{ \frac{1}{2} + \frac{1}{\pi} \operatorname{Re} \sin^{-1} \left( \gamma - \frac{1 - \gamma^2}{t + is} \right) \right\} \quad [27]$$

Hence,

$$s = \cos \left( \xi - \frac{\pi}{2} \right) \sinh \eta \quad [28]$$

$$t = -\gamma + \sin \left( \xi - \frac{\pi}{2} \right) \cosh \eta \quad [29]$$

It may then be shown that

$$P(x, y) = E_a \left\{ \frac{1}{2} + \frac{1}{\pi} \operatorname{Re} \sin^{-1} (\mu - i\nu) \right\} \quad [30]$$

where the quantities  $\mu$  and  $\nu$  are

$$\mu = \frac{\gamma(t^2 + s^2) - t(1 - \gamma^2)}{t^2 + s^2} \quad [31]$$

$$\nu = \frac{s(1 - \gamma^2)}{t^2 + s^2} \quad [32]$$

The real part of the arcsin is

$$\operatorname{Re} \sin^{-1}(\mu - i\nu) = \sin^{-1} \left\{ \frac{2\mu}{\sqrt{(1 + \mu)^2 + \nu^2} + \sqrt{(1 - \mu)^2 + \nu^2}} \right\} \quad [33]$$



Although the expression for the potential in terms of  $s$  and  $t$  is cumbersome to write, only 40 arithmetic operations are involved in calculating the potential at a given point.

Potential Fields

Waber has tabulated elsewhere (6) values of the dimensionless parameter representing potential,  $P(x, y)/E_a$ , for the values of  $\alpha$  equal to  $\pi/2$ ,  $\pi/4$ , and  $\pi/8$ .

The potential fields are presented as perspective drawings in Fig. 4, 5, and 6. Regard that portion of these fields which has a potential in excess of  $E_a/2$  as "anodic" and the remainder as "cathodic." The equipotential line,  $P = E_a/2$ , is concave toward the anode if  $\alpha < \pi/2$ . Thus, considerable portions of the corrodent are left at potentials near that of the cathode. Shrinkage of the anodic portion toward the anode, as  $\alpha$  decreases, is illustrated in these figures. Daniel-Bek's (7) and Copson's (8) experi-

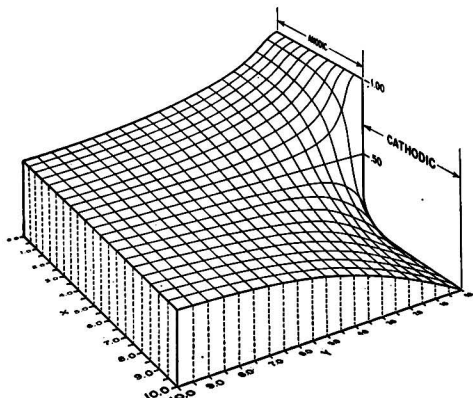


FIG. 4. Perspective drawing of the distribution of potential for equal relative anode and cathode areas.

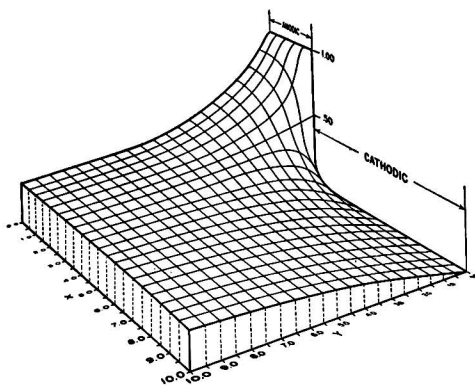


FIG. 5. Perspective drawing of the distribution of potential where  $\alpha = \pi/4$ , that is, where the anode is one third the width of the cathode.

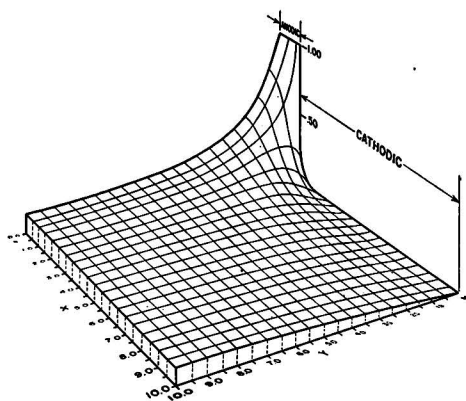


FIG. 6. Perspective drawing of the distribution of potential where  $\alpha = \pi/8$ , that is, where the anode is one seventh the width of the cathode.

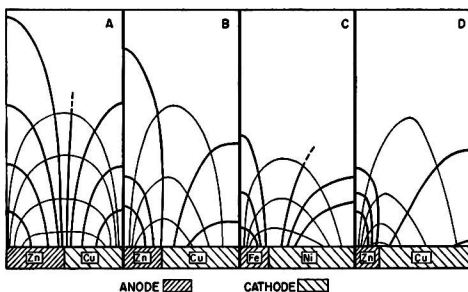


FIG. 7. A diagrammatic summary of measurements by Daniel-Bek and by Copson illustrating the effect of relative anodic size on potential distribution in a corrodent. (A) Equal anode and cathode areas for Cu-Zn couple in NaCl; (B) relative anode area  $\alpha = \pi/3$  for Cu-Zn couple in NaCl; (C) relative anode area  $\alpha = \pi/4$  for Fe-Ni couple in Bayonne tap water; (D) relative anode area  $\alpha = \pi/5$  for Cu-Zn couple in NaCl. Horizontal dimensions of various test specimens have been replaced by a common scale. The ordinate in the graph is the relative distance perpendicular to the metallic surface. Heavy lines are the equipotential lines and the others are the flow lines of the ions.

TABLE I. Relative corrosion current density  $r(x)/E_a R_0 h$

$x$	$\alpha = \pi/2$	$\alpha = \pi/4$	$\alpha = \pi/8$
0*	0.5000	1.207	2.515
0.5	0.5098	1.227	2.554
1.0	0.5411	1.292	2.684
1.5	0.6013	1.415	2.930
2.0	0.7074	1.631	3.363
2.5	0.9003	2.023	4.150
3.0	1.3068	2.789	5.799
3.5	2.5628	5.365	11.372
3.75	5.0968	10.429	21.026
4.00	$\infty$	$\infty$	$\infty$

\* Anodic region assumed to be 4 units wide.

mental data which are summarized on a common relative scale in Fig. 7, qualitatively show this shrinkage of the anodic field. In slightly different terms the equipotential line that corresponds to  $E_a(a/c)$  and goes to infinity is straight where  $\alpha = \pi/2$ . However, this line becomes concave toward the anode if  $\alpha$  is less than  $\pi/2$ . Daniel-Bek (7) made this conclusion on the basis of his experimental studies.

#### Evaluation of the Current Density

The local corrosion rate is given by equation [12]. The constant,  $R_o$ , includes the effect of conductivity of the corroding medium as well as the valence type and atomic weight of the anodic metal. It is desirable to work with dimensionless parameters so that the tabulated values may be applied to all similar problems. To this end,  $r(\xi)$  is divided by  $E_a R_o$ . Use of simple algebra results in

$$\frac{r(\xi)}{E_a R_o} = \frac{r(x)}{E_a R_o h} = \left( \frac{c}{2E_a} \right) \frac{\partial P}{\partial y} \Big|_{y=0} \quad [34]$$

Values for the right hand side of [34] are given in Table I for three percentages of anodic material. For application to a specific experimental problem to be discussed in a subsequent report, the anodic region was assumed to be four units wide. The width of the cathode was adjusted so that the three values of  $\alpha$  were  $\pi/2$ ,  $\pi/4$ , and  $\pi/8$ .

As  $\alpha$  decreases (for fixed  $a$ ), the relative corrosion current density increases somewhat faster than does the sum of the half widths  $c$ .

#### SUMMARY

An expression has been derived for the distribution of potential within a solution brought about by the

immersion of a coplanar galvanic couple in the solution, and numerical values have been obtained. Only the limiting case of negligible polarization is discussed. The local corrosion rate was calculated from the normal derivative of the potential evaluated at the electrodes.

#### ACKNOWLEDGMENTS

The fruitful suggestions and kind advice of Carl Wagner are gratefully acknowledged. Also appreciated are the help of S. F. Waber and the assistance of several members of the Computing Group in the Theoretical Physics Division of the Los Alamos Scientific Laboratory in certain phases of the calculations. This work was initiated at Illinois Institute of Technology and the author would like to thank most heartily Hugh J. McDonald for his continuing encouragement.

Any discussion of this paper will appear in a Discussion Section to be published in the December 1954 issue of the JOURNAL.

#### REFERENCES

1. C. WAGNER, *This Journal*, **98**, 116 (1951).
2. R. CHURCHILL, "Fourier Series and Boundary Value Problems," p. 94, McGraw-Hill Book Co., New York (1941).
3. M. JAKOB, "Heat Transfer," Vol. I, John Wiley & Sons, Inc., New York (1949).
4. C. WAGNER, *This Journal*, **99**, 1 (1952).
5. R. HAWELKA, "Vierstellige Tafeln der Kreis- und Hyperbelfunktionen sowie ihrer Umkehrfunktionen," F. Vieweg Braunschweig (1931).
6. J. T. WABER, AEC Document LA 1488, Jan. 26, 1953.
7. V. S. DANIEL-BEK, *Zhur. Fiz. Khim.*, **18**, 250 (1944).
8. H. R. COPSON, *Trans. Electrochem. Soc.*, **84**, 71 (1943).

# Intensity Anomalies in Electron Diffraction Patterns of CuO<sup>1</sup>

J. M. COWLEY

*Chemical Physics Section, Division of Industrial Chemistry, Commonwealth Scientific and Industrial Research Organization, Melbourne, Australia*

## ABSTRACT

The oxide layer, giving the so-called CuO' electron diffraction pattern and formed by heating copper in air at 600°C, has been examined by high-resolution electron diffraction and electron microscopy. It is shown that the intensity anomalies which differentiate the CuO' pattern from the normal CuO pattern are not due to impurities as has been suggested. The oxide grows in the form of long needle-like spines approximately perpendicular to the copper surface, with one or more screw dislocations along the axis of each spine. Each spine is a single crystal of CuO, about 1000 Å in diameter, elongated along the (110) zone axis. Intensity anomalies of the CuO' pattern result from this particular morphology.

## INTRODUCTION

Since Murison (1) first reported that the electron diffraction pattern obtained from copper surfaces heated in air at 300°–600°C is often not that of normal CuO, but, instead, a "three-ring" pattern, a number of authors have repeated his observations and offered various explanations for the anomaly. The three-ring pattern, or "CuO' pattern," as it has been called, has the same dimensions as the normal CuO ring pattern and so appears to be given by a similar monoclinic crystal lattice with unit cell dimensions of the normal CuO,  $a = 4.65$ ,  $b = 3.41$ ,  $c = 5.11$  Å, and  $\beta = 99^{\circ}29'$ . The relative intensities of the rings are, however, markedly different. In particular, the innermost ring, the (110) with  $d = 2.73$  Å, is strong instead of weak, and the (11 $\bar{2}$ ) ring with  $d = 1.95$  Å is also stronger than normal.

Murison concluded that the pattern is given by another crystal form of CuO. Other suggestions have been that it is given by an oxide with the CuO structure, but with an excess of oxygen or copper, or, more specifically, by an oxide intermediate between CuO and Cu<sub>2</sub>O. Honjo (2) showed that the rings of the CuO' pattern are usually arced and suggested that anomalous intensities result from a preferred orientation of crystallites of normal CuO, due to the preferential development of certain crystal faces in the growing oxide layer.

Recently, Gulbransen and McMillan (3) studied the oxidation of pure copper and examined conditions under which the CuO' pattern appeared. They found a dependence on the purity of the copper used, in that intensity anomalies were less pronounced for high purity copper than for less pure copper. They concluded that the high intensities of the rings at  $d = 2.73$  and  $1.95$  Å result from the

superposition of strong rings from oxides of other metals present as impurities in the copper.

A series of observations made in this laboratory during the early part of 1951 provides ample evidence that, at least in the case of the oxides studied by the author, the explanation given by Gulbransen and McMillan cannot be correct, and that, in fact, abnormally intense rings are given by the same material as the other rings. The author used an electron diffraction camera of high resolving power (4) and obtained arc patterns and single-crystal patterns from the oxide formed on a fine copper gauze by heating it in air. Some of the specimens were examined in the RCA Model EMU electron microscope.

Abnormal intensities of the rings may be explained in terms of the particular morphology of crystals of normal CuO growing in the form of thin spines around screw dislocations. This has become evident in the course of an investigation on the influence of screw dislocations on crystal morphology and electron diffraction intensities, with special reference to CuO and ZnO smoke crystals (5).

## EXPERIMENTAL OBSERVATIONS

Electrolytic copper grids, with 200 meshes to the inch, such as are sometimes used to support electron microscope specimens, were heated in air at 600°C for periods of up to 25 hr. The grids then appeared jet black in color, with an obvious decrease in the size of the holes, indicating a thick oxide layer. When the electron beam was limited to a small region along the edge of a hole in the mesh, an arc pattern, such as that shown in Fig. 1a, was obtained by transmission of the beam through projecting oxide crystals. From the positions of the arcs it can be deduced that crystals of CuO are preferentially oriented with the (110) zone axis perpendicular to

<sup>1</sup> Manuscript received August 18, 1953.

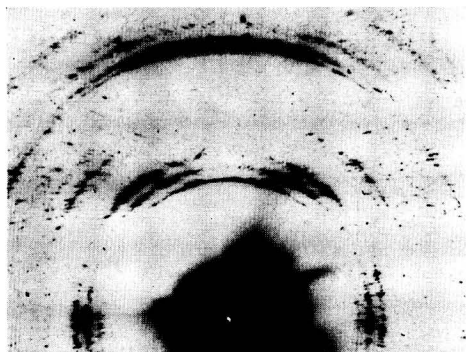


FIG. 1a. Part of an arc pattern from CuO crystals grown on a copper mesh.



FIG. 1b. Enlargement of single-crystal spots from an arc pattern such as Fig. 1a.

the copper surface. Individual arcs are resolved into a large number of single-crystal spots, each of which is elongated in a direction perpendicular to the (110) zone axis. An examination of individual elongated spots under very high resolution conditions (Fig. 1b) shows that elongation is due to extended "shape transforms" similar to those previously described in patterns of ZnO smoke (6). It may therefore be concluded that the oxide grows in the form of long thin needles perpendicular to the copper surface, with the long axis of the needles parallel to the (110) zone axis.

Electron micrographs of similar regions, Fig. 2, confirm that the oxide is in the form of long thin needles growing approximately perpendicular to the surface. Average diameter of the needles is a little over 1000 Å; lengths are very much greater. In some cases, a spine was observed to extend right across one of the grid apertures.

Some single-crystal diffraction patterns were obtained by using a very fine electron probe to pick

out individual needles. Fig. 3 shows such a pattern obtained with the beam in the  $(\bar{1}10)$  direction. The  $(00l)$  reflections give the closely spaced line of spots through the central spot. Of these, the reflections with  $l$  odd are "forbidden" in that the intensity calculated for them from the known structure of CuO is zero. The fact that they appear with appreciable intensity implies that considerable secondary scattering or "dynamic interaction" has taken place. This is to be expected for CuO crystals more than 100 Å thick. Weak, continuous lines running between the spots of the pattern indicate that there is a considerable amount of disorder in the crystal. The lines are stronger near the spots of the pattern. Lines running near to the central spot are less pronounced than those further out. The direction of the lines is perpendicular to the axis of the needle. These observations suggest that the disorder in the crystal may take the form of screw dislocations along the axes of the needle-like CuO crystals. Wilson (7) has examined diffraction effects given by a screw dislocation along the axis of a cylindrical crystal. The apparent crystal size is, in effect, decreased in directions perpendicular to the axis. This effect is zero for reflections from planes parallel to the dislocation axis, and the more marked, the greater is the angle between the reflecting plane and this axis. In a single-crystal pattern, such as Fig. 3, this would result in an elongation of the spots in a direction perpendicular to the long crystal axis, as observed. Each needle-like crystal of CuO may therefore be considered to contain one or more screw dislocations along its axis. The rapid growth of the crystals in the (110) direction may then be attributed to growth about screw dislocations.

Observations were also made by "reflection" from the surface of a copper block which had been heated in the same way as the copper mesh. The patterns

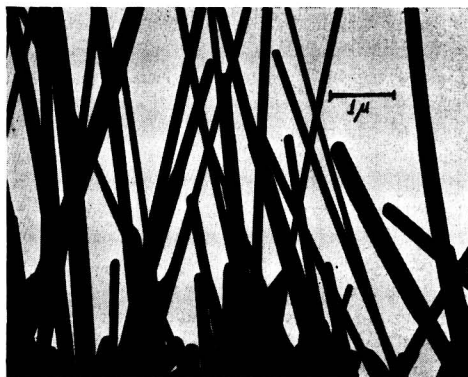


FIG. 2. Electron micrograph of CuO crystals growing from the side of an aperture of a fine copper mesh.

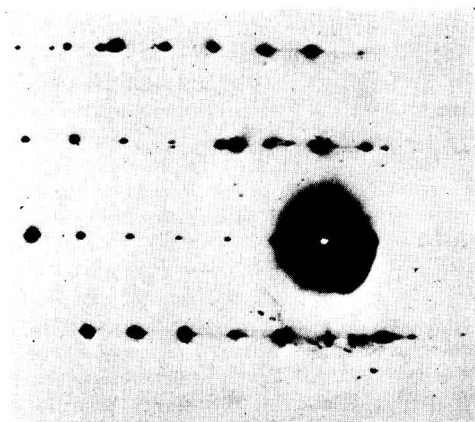


FIG. 3. Single crystal pattern obtained from a needle-like CuO crystal. A background of spots given by other crystals has been removed by masking.

obtained are similar to that of Fig. 1 except that more than half of the pattern is obscured by the shadow of the block, and the arcing of the rings is not quite so pronounced. The individual spots are elongated in the same way, indicating that the same acicular crystal habit is present. The general appearance is exactly that of the CuO' patterns previously obtained by reflection methods. The two broad (110) arcs form an almost-continuous inner ring which is of about the same strength as the next two rings. These rings are actually composite, the first being made up of (002) and (111) arcs, the second being a combination of (200) and (111) arcs. The merging of the several arcs on these strong rings gives the appearance of continuous rings even in the presence of a considerable degree of orientation. As Honjo has pointed out, this fortuitous circumstance has prevented many authors from realizing that a preferred orientation is present.

Relative intensities of the arcs in the patterns obtained from the heated copper grids are the same as in these CuO' reflection patterns. It is therefore clear that, in the present case at least, the three-ring pattern is given by thin needle-like crystals of CuO growing approximately perpendicular to the copper surface.

#### DISCUSSION

The evidence from which it may be concluded that the intensity anomalies are not due to impurities may be summarized as follows:

1. The arcing of the (110) and (11 $\bar{2}$ ) rings is consistent with that of the other rings of the pattern. It is unlikely that an impurity would give arcs in the same positions even if the crystals of the impurity had a similar preferred orientation.

2. The fine structure of single crystal spots which make up the (110) and (11 $\bar{2}$ ) arcs is similar to that of spots in other arcs, indicating that these arcs are given by crystals of the same size, shape, and degree of imperfection.

3. Intensities of the (110) and (11 $\bar{2}$ ) arcs are high enough to account for the appearance of abnormally intense rings in a reflection pattern from crystals with a concealed preferred orientation.

Differences between the normal CuO and the CuO' patterns are, therefore, differences which occur in single-crystal patterns, and it is unnecessary to postulate the presence of an impurity. The observation of Gulbrandsen and McMillan that the intensities of the (110) and (11 $\bar{2}$ ) rings are dependent on the purity of the copper used may perhaps be explained if the purity is considered to affect the habit, degree of orientation, or degree of imperfection of the crystals.

The idea that the anomalous intensities are the result of a defect or excess of copper atoms in the lattice need not be considered in detail. Such a high concentration of defects or excess atoms would be required to give the observed modification of the intensities that either the lattice symmetry or the unit cell dimensions, and hence the ring diameters, would be appreciably changed.

Honjo suggested that the intensity anomalies follow from preferred orientation of the crystallites, but orientation by itself cannot give rise to the observed intensities. This is apparent from the calculated structure factors which are given in the diagrammatic representation of the arc patterns, Fig. 4. On the first layer line, the intensity of the (110) arc should be much less than that of the neighboring arcs for a normal CuO lattice, whereas in Fig. 1, the (110) arc is almost as strong as its neighbors. The abnormal intensity of the (110) arc must, therefore, be a result of the previously unsuspected spine-like habit of the oxide.

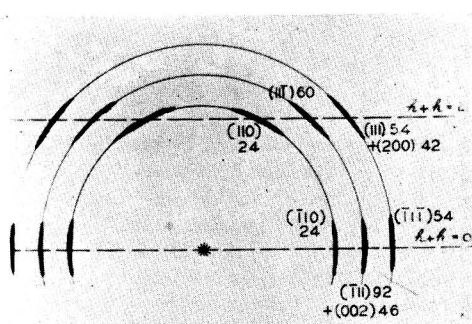


FIG. 4. Diagram showing the indices (in brackets) and structure factors for the normal CuO structure, for the arcs on the inner three rings of Fig. 1a (not to scale).

The average thickness of the spines is about 1000 Å. A perfect single crystal of this thickness would not give diffraction intensities according to the simple kinematic theory. Dynamic effects would be strong. Intensities would be proportional to the first power, rather than the square of the structure factors, and dynamic interaction effects would be expected to even out the intensities, making strong reflections weaker and weak reflections stronger. Thus the (110) arc would not be as weak, compared to its neighbors, as would be expected from the kinematic theory.

Because of the spine-like habit of the crystals, the average thickness of crystal traversed will vary appreciably for reflections from different planes. The spines vary widely in orientation. Planes perpendicular to the spine axis can reflect only when the spine is perpendicular to the electron beam. Planes parallel to the spine axis can reflect for any orientation of the spine. For planes perpendicular to the spine axis the average thickness will be least. The greater the thickness of crystal traversed, the more the intensity of a reflection will be reduced by extinction, absorption (inelastic scattering), and dynamic interaction. The intensities of the (110) arcs on the first layer line, which are given by planes nearly perpendicular to the spine axis, should therefore be reduced less than the intensities of other arcs. The arcs on the zero layer line should be weakened most, since they are given by reflections from planes parallel to the spine axis.

Imperfections of the crystal lattice, presumably taking the form of screw dislocations parallel to the axes of the spines, will modify the intensities in much the same way. Wilson's analysis of the case of a screw dislocation along the axis of a cylinder, showed that, in effect, the apparent crystal size is smaller for reflections from planes more nearly

perpendicular to the axis of the dislocation. Thus, extinction effects will reduce intensities much more for reflections from planes nearly parallel to the axis than for reflections from planes nearly perpendicular to the axis.

The relative intensities of the various arcs on the innermost ring in the pattern, Fig. 1a, give a clear indication that some such modification of the intensities has occurred. The ( $\bar{1}10$ ) arc (planes parallel to the spine axis) is very much weaker than the (110) arc (planes almost perpendicular to the spine axis), although the two reflections have the same structure factor. Similar differences are evident on other rings. Therefore, it seems probable that a complete explanation of the intensity anomalies of the CuO' pattern may be possible in terms of the particular morphology of normal CuO crystals, resulting from growth about screw dislocations.

#### ACKNOWLEDGMENTS

The writer wishes to thank Mr. J. L. Farrant for taking the electron micrographs and Mr. J. A. Spink who took a number of the electron diffraction patterns.

Any discussion of this paper will appear in a Discussion Section to be published in the December 1954 issue of the JOURNAL.

#### REFERENCES

1. C. A. MURISON, *Phil. Mag.*, **17**, 96 (1934).
2. G. HONJO, *J. Phys. Soc. Japan*, **4**, 330 (1949).
3. E. A. GULBRANSEN AND W. R. McMILLAN, *This Journal*, **99**, 393 (1952).
4. J. M. COWLEY AND A. L. G. REES, *J. Sci. Instr.*, **30**, 33 (1953).
5. A. L. G. REES, J. L. FARRANT, AND J. M. COWLEY, To be published.
6. A. L. G. REES AND J. A. SPINK, *Acta Cryst.*, **3**, 316 (1950); *Nature*, **165**, 645 (1950).
7. A. J. C. WILSON, *Acta Cryst.*, **5**, 318 (1952).

# Reduction of Oxidation-Ions in Hydrocarbons<sup>1</sup>

ANDREW GEMANT

*Engineering Laboratory and Research Department, The Detroit Edison Company, Detroit, Michigan*

## ABSTRACT

The formation of oxidation-ions, resulting from oxidation of aromatic ortho dihydroxyl compounds in hydrocarbons, is shown to be either completely or partially reversed upon reduction. Compounds studied were catechol, butylcatechol, and 1,2-naphthalenediol. Among the oxidizing agents, ozone was studied in detail. Reduction was by hydrogen at atmospheric pressure and room temperature.

From the easy reduction of ions it appears that a large fraction of them are relatively simple molecules; their possible structures are indicated. Ortho derivatives of aromatics containing additional side chains are likely to be parents of oxidation-ions.

## SCOPE OF STUDY

A preceding study (1) attempted to identify the ions causing increase in electrical conductivity of hydrocarbons upon oxidation. An attempt was made to find a group of easily oxidizable compounds which possess known oxidation products and show increased conductivity upon oxidation. Such a group was considered to be chemically representative of what can be termed a parent of oxidation-ions.

Compounds of these characteristics were found among the hydroquinones, particularly in the ortho position. In concentrations of a few millimoles per liter of hydrocarbon solvent and on mild oxidation, a marked increase in conductivity takes place. It is not yet possible to assign with certainty a structure to the oxidation-ions formed. They were tentatively identified as originating from semiquinone radicals as oxidation intermediates, stabilized by addition or loss of an electron. It is realized, however, that this explanation might be modified by future work.

If this explanation is correct, it should be possible to reverse by suitable means, at least partly, the observed increase in electrical conductivity. It was this question to which the present investigation was devoted. Since the ions are formed by oxidation, it was concluded that subsequent reduction should eliminate the ionic species formed and cause conductivity to decrease. It is known that *o*-quinone is readily reduced by agents like potassium iodide (2, 3). The same probably holds for intermediate products which form the ions.

In addition to the process of reduction, the present study was also concerned with ion generation by means of oxidation with ozone. Results obtained by this method throw added light on the nature of oxidation-ions.

<sup>1</sup> Manuscript received November 16, 1953. This paper was prepared for delivery before the Chicago Meeting, May 2 to 6, 1954.

## REDUCTION OF OXIDATION-IONS FROM CATECHOL

Reduction was carried out with hydrogen at room temperature and atmospheric pressure on a platinum black catalyst. A small glass container was used for the reduction; it contained 10 cc of solution into which were lowered platinum plates which were electrolytically coated with platinum black and a glass tube with fritted glass at the lower end. Hydrogen was bubbled through the solution via this tube. Reduction was under rather mild conditions.

A typical result is presented in Fig. 1. Catechol, 5 millimole/l in dioxane, was oxidized by silver oxide for 2 hr. The increase in conductivity (corrected for change in dielectric constant) is drawn as a dotted line, since only initial and end values were measured, the general trend of the curve being known from previous data (1). The solution, which had a reddish-brown coloration due to *o*-quinone, was decanted from solid silver oxide and subjected to reduction. After 2 hr the conductivity level was about the same as before oxidation; the color at the same time faded markedly. The quinone was, therefore, reduced to a considerable extent. After 18 hr the conductivity was nearly the same as before,  $2.0 \times 10^{-12}$  mho/cm. According to later experiments, dioxane is not very suitable as a solvent involving reduction; the peroxide content of some batches apparently interferes with the reduction process.

Further results along similar lines are assembled in Fig. 2, referring to 3 millimole/l *p*-*tert*-butylcatechol (recrystallized from the Eastman product). In curves 1 and 2 oxidation time was 10 min, and in curve 3 it was 20 min. Immediately after oxidation, which utilized  $\text{KMnO}_4$ , reduction was achieved using a hydrogen stream. Oxidation, accompanied by green coloration, increased conductivity; reduction, accompanied by decoloration, reduced conductivity. The final level in the case of benzene and octane

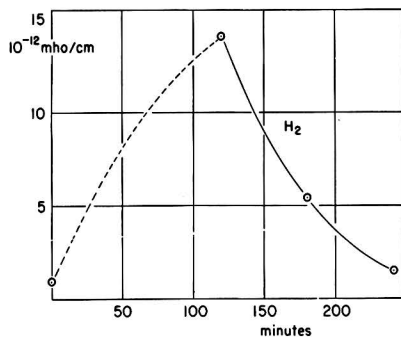


Fig. 1. Electrical conductivity vs. time of oxidation and reduction of 5 millimole/l catechol in dioxane.

was close to the initial one, but somewhat higher for xylene. No correction was applied to these data because of the small change in dielectric constant.

It has been pointed out (1) that intermediate oxidation products, which form ions, are not always stable; conductivity may change with time. It was of interest, therefore, to compare oxidized samples that were undergoing reduction with samples of the same batch that were allowed to stand after oxidation. Two results of this kind are shown in Fig. 3. Group 1 shows an oxidation curve for 20 min, followed by a branching of the curve. The bottom branch refers to reduction, and the top branch to a sample that was allowed to stand after initial oxidation. Group 2 shows a curve for an oxidation time of 135 min, followed by two branches analogous to those in the first group. While the top branches show only little change, the reduction curves exhibit sharp drops. These drops are, therefore, not caused by inherent instability of oxidation-ions.

It was also of interest to ascertain whether reversals could be effected by repeating oxidation and reduction processes. One of the tests carried out for

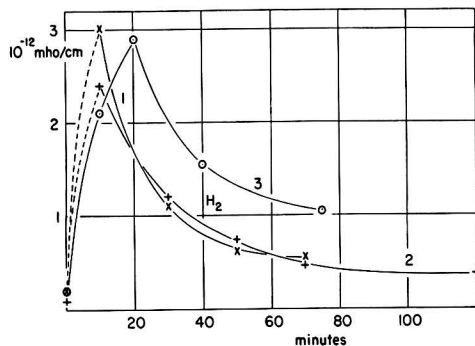


Fig. 2. Conductivity vs. time of oxidation and reduction of 3 millimole/l butylcatechol in benzene (curve 1), *n*-octane (curve 2), and xylene (curve 3).

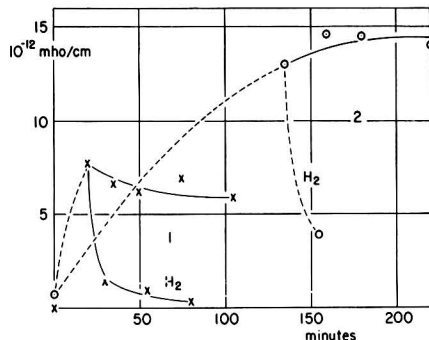


Fig. 3. Conductivity vs. time for oxidation, reduction, and standing after oxidation. Group 1: butylcatechol in benzene; group 2: catechol in dioxane.

this purpose, using the benzene-butylcatechol system, is reproduced in Fig. 4. It shows four oxidation peaks and four corresponding reduction drops, indicating that the initial condition was restored after each reduction. The peaks are of different magnitude because no effort was made to keep conditions of oxidation constant (amount and particle size of  $\text{KMnO}_4$  crystals, conditions of stirring, and the like). At each oxidation the greenish color of the quinone appeared, disappearing at each reduction.

#### REDUCTION OF OXIDATION-IONS FROM *o*-NAPHTHALENEDIOL

All work up to this point was carried out with dihydroxyl derivatives of benzene. The following was an attempt to extend the work to a naphthalene derivative. Ortho naphthalenediol is not readily available, so 1,2-(or  $\beta$ -) naphthoquinone (Eastman product) was used. The compound was dissolved in benzene and the clear filtered red solution used; in some tests it was previously recrystallized from ether. In order to obtain the corresponding ortho diol, the quinone solution was reduced in the apparatus described above. The color faded to a faint pink hue.

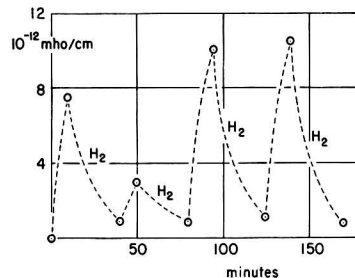


Fig. 4. Repeated oxidations and reductions in a 4 millimole/l butylcatechol solution in benzene.



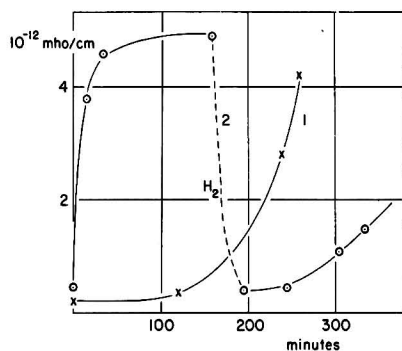
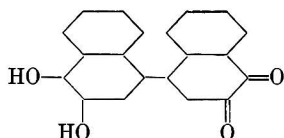


FIG. 5. Oxidation and reduction of  $\beta$ -naphthoquinone. Curve 1: 2.5 millimole/l 1,2-naphthalenediol in benzene-dioxane; curve 2: 5 millimole/l  $\beta$ -naphthoquinone in benzene.

When such a solution was diluted by an equal part of dioxane (final concentration of the diol being 2.5 millimole/l) and oxidized with silver oxide, curve 1 of Fig. 5 was obtained. In contrast to previous curves it shows an induction period of about 2 hr, after which a rapid increase of conductivity takes place, the solution assuming a reddish color.

A somewhat unexpected observation was made with  $\beta$ -naphthoquinone. If no reduction precedes oxidation, but the original benzene solution (concentration 5 millimole/l) is used and oxidized with  $\text{Ag}_2\text{O}$ , an immediate increase in conductivity takes place, as shown in the first part of curve 2. This solution was next subjected to reduction, showing a rapid drop of conductivity. Repeated oxidation with  $\text{Ag}_2\text{O}$  produces the same type of oxidation curve as in curve 1, as expected.

The chemical nature of intermediate ions in this case is probably similar to that postulated for the case of *o*-benzoquinone (1). It is known (4) that *o*-naphthoquinone upon standing forms a quinhydrone type compound, (3,4-dioxynaphthyl-1)-naphthoquinone-1,2, of the following probable constitution:



The compound, a dimer of *o*-naphthoquinone, is a dark powder, moderately soluble in benzene. When this is oxidized, the hydroxylated benzene ring acts as a catechol molecule, leading to semiquinone radicals. This is the probable cause of ion formation, as shown in the first part of curve 2, when the quinone, and not its reduced form, was used.

#### OXIDATION BY OZONE

A further group of experiments was concerned with ozone as oxidizing agent, and subsequent reduction. The results are instructive in providing further support for the hypothesis that ions are intermediate chemical forms between the fully reduced and fully oxidized form.

Referring to the reduction arrangement described earlier, for oxidation the tube could be connected to a cylindrical glass ozonizer, the outer electrode of which consisted of aluminum foil, and the inner of water. High voltage to the ozonizer was supplied by a transformer using a primary voltage regulator, and oxygen was fed from a tank.

Results on oxidation by ozone are presented in Fig. 6, curve 1, which refers to a 6 millimole/l butyl-catechol solution in xylene. Ozone has an advantage over solid oxidants in that its concentration can be easily varied. This is done by varying the electric field across the gap (4 mm) between the two glass cylinders of the ozonizer. Curve 1 consists of various sections, each referring to periods of 30 min in which the field was increased in steps as indicated; the figures give effective kilovolts per centimeter. Concentration of ozone in the oxygen stream increases with increasing electric field, as was ascertained by the intensity of darkening of KI-starch paper. Hence, it may be seen that the conductivity effect depends upon the concentration of  $\text{O}_3$ , going through a maximum at about 26 kv<sub>eff</sub>/cm. The increasing part of the curve seems obvious, but the decreasing part is unexpected. A possible explanation is that oxidation of catechol then proceeds too vigorously; the relatively unstable intermediate ionic stages are then further oxidized to the end product.

Curve 2 of Fig. 6 is a control test with xylene, without butylcatechol, carried out at the same field intensities as the previous test. Increase in con-

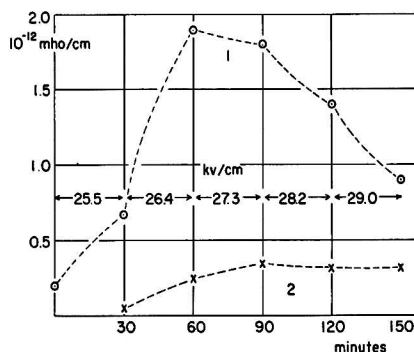


FIG. 6. Oxidation by means of ozone at various field intensities in the ozonizer. Curve 1: 6 millimole/l butyl-catechol in xylene; curve 2: xylene only.

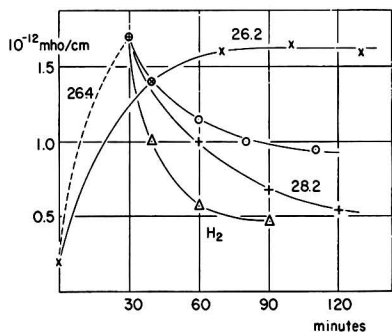


FIG. 7. Conductivity changes upon oxidation by ozone at various field intensities, upon standing, and upon reduction by hydrogen after oxidation; 6 millimole/l butylcatechol in xylene.

ductivity is small, hence the major portion of the effect shown in curve 1 is due to the presence of catechol, i.e., conductivity is due to ions formed from catechol.

Further results, using ozone as oxidant, are presented in Fig. 7. All data refer to a 6 millimole/l butylcatechol solution in xylene. The curve marked 26.2 refers to an oxidation test at the optimum field intensity. After the maximum conductivity of  $1.6 \times 10^{-12}$  mho/cm is reached, it remains constant with continued oxidation, indicating a dynamic equilibrium between ion generation and annihilation.

The other group of curves has a 30-min oxidation section at the optimum field. From this point on, three branches are shown. The top branch refers to standing of the solution, showing a decrease of conductivity due to inherent instability of the ionic species. The next branch gives further oxidation data at a higher than optimum field intensity, showing a more rapid drop than on standing. The third branch refers to reduction by hydrogen; this drop is the steepest, indicating rapid annihilation of ions.

#### CONCLUSIONS CONCERNING STRUCTURE OF IONS

Before discussing some conclusions that may be drawn from the results on reduction, two pertinent points are mentioned.

One is that only ortho compounds exhibit the effect of prompt conductivity changes on oxidation. This was shown by previous work (1) and also in Fig. 8, comparing butylcatechol (curve 1) with butylhydroquinone (curve 2). The absence of any increase of conductivity in curve 2 proves the point in question. A possible explanation is given later.

The second point is whether or not ions are formed in thermodynamic equilibrium with the fully reduced and oxidized parent compounds. From experimental material available it appears that such an equilibrium could at best account for a small

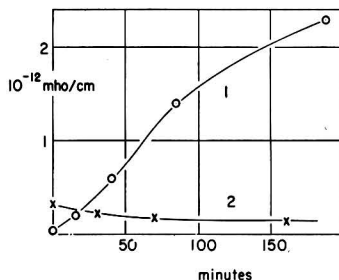


FIG. 8. Comparison of butylcatechol (curve 1) and butylhydroquinone (curve 2) in benzene, oxidized by  $\text{KMnO}_4$ .

fraction of ions present and that the major fraction are intermediates of relative stability. It is realized that this conclusion is not final and may be subject to revision. Michaelis (5) found equilibrium between quinones and semiquinones, but conditions in hydrocarbons are certainly different from those in aqueous solutions. An experimental indication of the absence of an equilibrium in the present case is presented in Fig. 9.

Curves 1 and 2 refer to phenanthrenequinone solutions in xylene and xylene-dioxane 1:1. The left parts of the curves reproduce data during reduction of the yellow quinone solution, in the course of which the colorless 9,10-phenanthrenediol was formed. The right parts refer to oxidation by  $\text{KMnO}_4$ , converting the colorless diol back into yellow quinone. The diol in solution is known to be unstable (6), oxidizing very rapidly to quinone. Such rapid oxidation precludes the presence at any moment of a noticeable concentration of intermediate ionic species, as mentioned above, and accordingly there is no increase of conductivity observable in the course of curves 1 and 2. The absence of such increase during the entire course of curves 1 and 2 seems to indicate, moreover, that the mere presence of the reduced and oxidized forms, even if they are present simultaneously, does not lead by

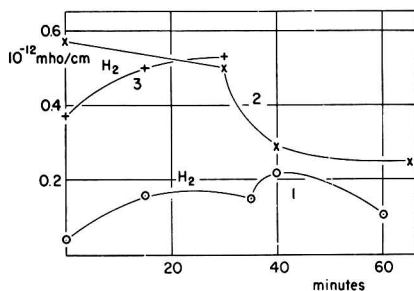


FIG. 9. Reduction and oxidation of phenanthrenequinone in xylene (curve 1) and dioxane-xylene (curve 2). Reduction of butyl-*o*-quinone (curve 3).

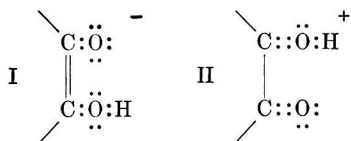
means of an equilibrium to a marked concentration of ionic species.

Curve 3 refers to reduction of red butyl-*o*-quinone, prepared from the corresponding catechol (7). No significant increase in conductivity occurs, in spite of the fact that in the course of the reduction both quinone and catechol were present. From the standpoint of the explanation based on ionic intermediates, the result shown in curve 3 seems surprising. One would expect ions to form also during reduction. If the observation is confirmed in further studies, then it shows that reduction follows a path different from that of the oxidation. Considering the many different ways in which a net reaction can and does occur, this is not improbable.

The observed effect of reduction on conductivity shows that oxidation-ions are reduced to nonionic molecules. The observed effect is in many cases complete, in others partial. It is perhaps safe to assume that the ions that are promptly reduced by hydrogen at atmospheric pressure and room temperature are chemically simple compounds, whereas those that are more resistant to reduction are secondary molecules of more complicated structure or higher molecular weight. The ionic species generated from aromatic dihydroxyl compounds appear, therefore, to be simple molecules. In a subsequent paper on this study, cases will be presented that exhibit a partial effect upon reduction, indicating that only part of the ions are primary products.

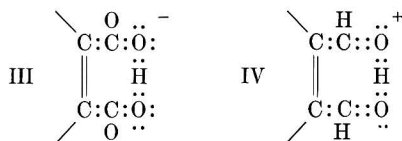
Sticher and Piper (8) subjected the reaction product of electron-bombarded decalin to hydrogenation with nickel as catalyst at about 240°C and 200 atm; a decrease of conductivity in a ratio 1:7 was observed. Since reduction in their work was carried out under severe conditions, a direct comparison with the present work is not possible. However, the two results appear to be in agreement, and it may be that the conductivity in their work was of a kind described here.

The chemical nature of the ions can only be tentatively inferred from the various observations. If the ions are intermediate compounds, they are of the nature of semiquinone radicals. The group with two ortho carbon atoms thus has the formula  $C_2O_2H$ . The molecule must exist in two forms, an anion and a cation; since both are relatively stable, the oxygen atoms must have completed electronic octets. The probable structure of the ortho groups in question is then the following:



The remainder of the molecule depends, of course, on the original compound present, and may, in addition, have the structure of a dimer, tetramer, and the like, if such were formed in the course of oxidation. Continued oxidation of the radicals and the ions leads to quinones; reduction, to ortho diols. As may be seen, the assumed structures are a diol anion and an oxonium type cation. The kinetics of their formation cannot be derived with certainty from experimental results of this study.

The ionic group does not need to be always the same. There can be longer side chains than those shown above. Since only ortho diols lead to ion formation, there is a likelihood that the hydrogen is situated between the two oxygen atoms, in other words, there may be a hydrogen bond in such ions. Such an anion, derived from phthalic acid, is shown in III, and a cation, as an oxonium ion of phthalic aldehyde, in IV.



The anion structure shown by III is similar to the chelate structure of anions of dicarboxylic acids in aqueous solution, discussed by McDaniel and Brown (9).

When the starting compound is not a diol, hydroxyl groups might form as the first step of oxidation, and ion formation is then a secondary process. Side chains in the ortho position, like in *o*-xylene, substantially facilitate such a process. A single hydroxyl group, as in phenol, favors formation of a second hydroxyl in the ortho position. Experimental results along these lines will be given in a subsequent paper.

It is quite likely that not all oxidation ions in hydrocarbons have the assumed structures of a diol anion and an oxonium cation. Other possibilities, such as formation of ion-radicals, should be kept in mind.

Presence of ortho substituents in the benzene ring is not the only criterion for a substance to be an ion parent. In order to be stable, ions need solvating action on the part of solvent molecules. This action is partly nonspecific, dependent on the dielectric constant of the solvent, partly specific, dependent on the chemical constitution of both solvent and solute. This latter action on the ions is analogous to the solvent action on the parent molecule which causes its greater or lesser solubility. The more soluble a compound in a solvent, the more likely it will

form ions. Hence a reasonably good solubility is a second essential criterion.

This is illustrated by catechol, which does not give an effect in benzene, but does so in dioxane. Butylcatechol, the solubility of which in benzene is considerably greater than that of catechol, gives a positive effect in benzene. Since side chains generally increase the solubility of hydroxyl compounds in hydrocarbons, alkyl substituted compounds in hydrocarbon mixtures facilitate the formation of oxidation-ions.

Any discussion of this paper will appear in a Discussion Section to be published in the December 1954 issue of the JOURNAL.

## REFERENCES

1. A. GEMANT, *This Journal*, **100**, 320 (1953); *Z. Elektrochem.*, **57**, 277 (1953).
2. R. WILLSTÄTTER AND F. MÜLLER, *Ber.*, **41**, 2580 (1908).
3. J. SCHMIDLIN, J. WOHL, AND H. THOMMEN, *Ber.*, **43**, 1302 (1910).
4. W. STEGMUND, *Monatsh. Chem.*, **29**, 1096 (1908).
5. L. MICHAELIS AND M. P. SCHUBERT, *Chem. Rev.*, **22**, 437 (1938).
6. "Beilstein Handbook of Organic Chemistry," Springer (Berlin) **6**, 1036 (1923).
7. E. DYER AND O. BAUDISCH, *J. Biol. Chem.*, **95**, 483 (1932).
8. J. STICHER AND J. D. PIPER, *Ind. Eng. Chem.*, **33**, 1567 (1941).
9. D. H. McDANIEL AND H. C. BROWN, *Science*, **118**, 370 (1953).

# High Purity Silicon<sup>1</sup>

FELIX B. LITTON AND HOLGER C. ANDERSEN

*Foote Mineral Company, Research and Development Laboratories, Berwyn, Pennsylvania*

## ABSTRACT

Thermal decomposition of silicon tetraiodide was investigated in both standard iodide (de Boer) and intermittent flow systems for potential use as a method for preparing high purity silicon metal.

Purity of metal obtained from operation of a standard iodide process cell appeared to be a function of impurities in crude silicon source material. Iodide metal having resistivities from 0.5-3 ohm-cm in the single crystal form was produced from Electro-Metallurgical high purity silicon. When iodide metal was used as silicon source material, the resistivity of single crystals of doubly refined metal varied from 3-8 ohm-cm.

Silicon of higher purity was obtained through thermal decomposition of fractionally distilled silicon tetraiodide in an intermittent flow system. After preparation of tetraiodide by reaction of resublimed iodine and Electro-Metallurgical high purity silicon, it was subjected to a 16 step distillation at 200 mm pressure in a packed quartz column. The modified iodide process silicon was *p*-type, and the resistivity varied in seven preparations from 30-200 ohm-cm

## INTRODUCTION

Becket (1) and Tucker (2) are credited with the first successful attempt to produce high purity silicon in commercial quantities. Using metal prepared by their process, Scaff (3) observed that different impurities segregated at various rates in directionally solidified metal, and that this procedure could be used for controlling distribution of impurities and, consequently, electrical properties of the metal. In 1949, Lyon, Olson, and Lewis (4) reported preparation of "hyper-pure" silicon by vapor-phase reduction of silicon tetrachloride with zinc.

Other methods have been investigated for the preparation of silicon in small quantities. Van Arkel (5) and Hölbling (6) studied hydrogen reduction of the tetrachloride. Silicon was prepared by reduction of potassium fluosilicate with potassium (7) and electrolysis of fused potassium fluosilicate (8). Von Wartenberg (8) thermally decomposed silicon tetraiodide on a graphite rod, while Stock (9) investigated thermal decomposition of silanes.

The objective of this research was to prepare silicon of the highest possible purity by the iodide process (10-12).

## EXPERIMENTAL WORK

### *General Consideration*

It is known that extremely small amounts of impurity elements decrease resistivity of silicon metal (13). Elements in groups III and V have a pronounced effect on electrical properties. The

effect of impurity elements from other groups is not as clearly defined.

During this investigation, thermodynamic calculations were made in order to estimate the order of thermal stability of groups III and V metal iodides relative to silicon tetraiodide. Brewer's data (14) were used for reference purposes. A filament temperature of 982°C and an iodide cell pressure of 10 $\mu$  were assumed to represent normal iodide process cell operation.

Calculations indicated that iodides of P, As, and Sb were less stable, and that those of Al, In, Ga, B, and Bi were more stable, than silicon tetraiodide. Therefore, it was anticipated that the concentration of the latter elements would decrease and that the former elements would not decrease in concentration in iodide metal relative to the concentration of those elements in the source silicon.

### *Factors Influencing Rate of Silicon Formation in the Iodide Process Cell*

Rate of silicon deposition through thermal decomposition of silicon tetraiodide on a heated wire in a standard de Boer type iodide cell was studied as a function of three operating variables: (a) amount of iodine introduced in the cell, (b) cell temperature, and (c) filament (hot-wire) temperature.

Initial experiments were carried out in an Inconel cell, 4 in. in diameter by 12 in. long, similar to that previously described (12). Low-aluminum grade silicon metal<sup>2</sup> was used as crude source material and was supported at the cell wall by means of a molybdenum screen. A U-shaped molybdenum wire, 0.060 in. in diameter by 10 in. long, attached to

<sup>1</sup> Manuscript received June 12, 1953. This paper was prepared for delivery before the Chicago Meeting, May 2 to 6, 1954.

<sup>2</sup> Obtained from Electro-Metallurgical Division, Union Carbide and Carbon Corporation.

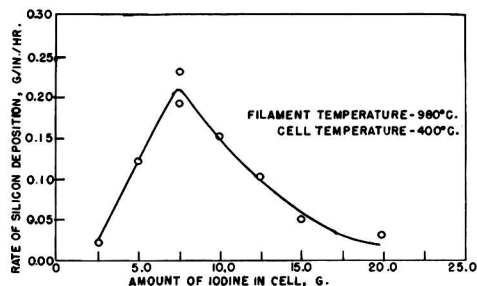


Fig. 1. Effect of iodine on rate of silicon deposition. Filament temperature, 980°C; cell temperature, 400°C.

the head of the cell through suitable electrode connections, served as the surface for thermally decomposing tetraiodide. The head was also fitted with a  $\frac{1}{2}$ -in. diameter evacuation tube, a sight glass for optically determining filament temperature, and a thermocouple well for measuring the temperature of the source material.

After crude silicon was placed in the annular space between the molybdenum screen and cell wall, the filament was attached and the head bolted in position. The cell was leak-tested at 40 psi internal pressure, after which it was evacuated at 500°C to 0.05 $\mu$ . When the cell had cooled to room temperature, a weighed amount of iodine was admitted and the evacuation tube sealed off. Before adjustment of the filament and cell temperatures to desired operating values, the cell was reheated to 400°C for one hour to form silicon tetraiodide. When the experiment was completed, the filament was weighed and the rate of decomposition calculated. The crude silicon charge was washed with dilute nitric and hydrofluoric acids before it was reused for subsequent experiments.

The influence of iodine addition on rate of silicon formation at constant filament and cell temperatures is shown in Fig. 1. In the iodine weight range of 2.5–7.5 grams, the rate increased with increased

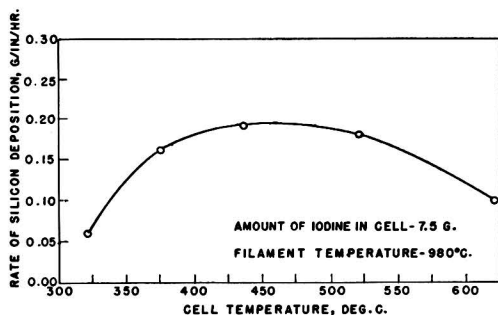


Fig. 2. Influence of cell temperature on rate of silicon deposition. Amount of iodine in cell, 7.5 grams; filament temperature, 980°C.

iodine addition, then decreased with further iodine addition.

The effect of varying the cell temperature using constant iodine addition and filament temperature is shown in Fig. 2. Data indicated that maximum rate of silicon formation occurred at 460°C. Even though an optimum cell temperature was observed, its influence on rate of silicon formation was not as critical as the amount of iodine added to the cell for the deposition process.

The influence of filament temperature on the rate of silicon formation, using 7.5 grams iodine addition and cell temperature of 460°C, is shown in Fig. 3. Data showed that 770°C was the minimum temperature at which measurable decomposition of the tetraiodide occurred, and that the rate increased with increasing temperature to the highest value studied (1040°C).

#### Standard Iodide Process Silicon

*Apparatus.*—An Inconel iodide process cell, 18 in. in diameter by 12 in. deep, was fabricated as the initial step in preparing silicon in approximately one-pound quantities for test purpose. The cell was designed to operate with a flat spiral filament of 0.10-in. diameter tantalum wire, 240 in. in length, suspended above the crude silicon starting material, which was distributed at the bottom of the cell. Vacuum seal and head arrangement similar to those used for the smaller cell were incorporated in the larger unit. Operating temperature was manually controlled by means of strip heaters in contact with the cell.

*Cell operation.*—Prior to operating this cell, filaments were prepared from molybdenum, tungsten, tantalum, and carbon for silicon formation experiments. When molybdenum was used, a continuous alloy zone 0.070 mm thick formed between the filament wire and silicon deposit. Metal droplets, assumed to be silicon-tungsten alloy, formed during the initial stage of deposition on a tungsten filament.

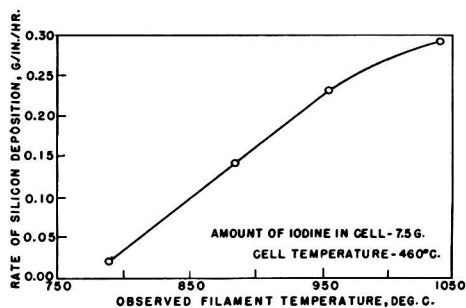


Fig. 3. Effect of filament temperature on rate of silicon deposition. Amount of iodine in cell, 7.5 grams; cell temperature, 460°C.



FIG. 4. View of a typical iodide process silicon, actual size.

A discontinuous alloy layer 0.017 mm thick formed between the silicon deposit and tantalum wire, showing that tantalum was to be preferred over either molybdenum or tungsten for filament material. In the case of carbon, a reaction zone 0.70 mm thick was formed.

The cell was operated on a charge of 5 lb of high purity grade silicon<sup>2</sup> and 50 grams of resublimed iodine. The following operational data were obtained from a typical preparation: tantalum wire temperature, 982°C; filament length, 170 in.; cell temperature, 450°C; preparation time, 74.5 hr; silicon obtained, 472 grams.

The "as deposited" iodide metal was polycrystalline, and vitreous in appearance. A view of a typical preparation is shown in Fig. 4.

*Spectrochemical analysis.*—Total impurities as reported from spectrochemical analyses on 16 deposits produced from high purity silicon showed that the metal contained 1–120 ppm detectable impurities which were one or more of the following elements: Fe, Al, Ca, Mg, Mn, Cu, and Na.

*Electrical properties.*—Resistivity and type rectification of iodide process silicon prepared from three different source materials are shown in Table I. Results are average values obtained on at least four preparations from measurements on "as deposited" and single crystal specimens.

Specific resistance was determined by measuring the voltage drop across 0.10 in. of the specimen with a L&N Type 7651 potentiometer. Rectification type was indicated by direction of current flow in a simple thermoelectric circuit.

These data indicated that silicon purification was

<sup>2</sup> Obtained from Electro-Metallurgical Division, Union Carbide and Carbon Corporation.

TABLE I. Resistivity and type rectification of iodide process silicon

Source material	Form	Resistivity, ohm-cm	Type rectification
High Purity (Electro-Metallurgical) . . . . .	As deposited	0.5–3.0	<i>p</i> and <i>n</i>
High Purity (Electro-Metallurgical) . . . . .	Single crystal*	0.1–3.0	<i>p</i> and <i>n</i>
Iodide process silicon . . . . .	As deposited	5.0–8.0	<i>n</i>
Iodide process silicon . . . . .	Single crystal*	3.0–8.0	<i>p</i>
High Purity (Sylvania Electric)† . . . . .	As deposited	3.0–7.0	<i>n</i>
High Purity (Sylvania Electric) . . . . .	Single crystal*	0.2–6.0	<i>n</i>

\* Drawn from quartz crucibles.

† Metal prepared from zinc reduction of silicon tetrachloride; 99.85% minimum Si content.

obtained, but that both donor and acceptor elements were transferred in the standard iodide process cell from a given source material. It was not possible to obtain either the degree of purification desired, or to determine which elements transferred in this work, due to unreliability of chemical procedure in the analytical range of interest.

#### *Preparation of Silicon from Fractionally Distilled Silicon Tetraiodide in an Intermittent Flow System*

*Preparation and properties of silicon tetraiodide.*—Silicon tetraiodide was prepared by allowing iodine to react with silicon at 700°–850°C in quartz apparatus, similar to that employed by Schwarz and Pflugmacher (15). Resublimed iodine was vaporized from a heated flask and carried by tank argon through a 1-in. reaction tube containing high purity silicon. Silicon tetraiodide, a clear yellow liquid (mp 122°C), condensed in the downstream portion of the apparatus and was retained in a receiving flask.

The yield of tetraiodide was essentially quantitative with respect to iodine in the presence of excess silicon. However, only 45–65% of the silicon charge was utilized in a given iodination experiment.

Tetraiodide is strongly hygroscopic and corrosive, and gradually assumes a red color on exposure to air.

Vapor pressure of fractionally distilled silicon tetraiodide measured in a static isoteniscope as reported elsewhere (16) was expressed by the equation

$$\log P_{\text{mm}} = 23.3809 - \frac{3,862.7}{T} - 4.9934 \log T$$

where  $T$  is in degrees Kelvin. The normal boiling point was calculated to be 301.5°C, compared with 290°C reported by Friedel (17). The liquid density, measured in a small, sealed pycnometer over the range 128°–243°C was expressed by the equation:  $\rho = 3.40 - 2.5 \times 10^{-3} (t-120) \text{ g/cc}$ ,  $t = \text{°C}$  (16).

*Fractional distillation of silicon tetraiodide.*—After exploratory work on fractionation of silicon tetraiodide in a 3.7 step distillation, a column containing 16 theoretical plates was assembled to obtain metal more efficiently in 50-gram quantities for test and melting purposes.

The transparent fused quartz column, 6 ft in length by 1 $\frac{3}{8}$  in. in diameter, was randomly packed with  $\frac{3}{16}$  in. diameter by  $\frac{3}{16}$  in. long quartz Raschig rings, and during operation kept adiabatic by conventional means. Reflux was controlled and fractions obtained with a quartz du Pont type swinging funnel reflux splitter (18), the former actuated by an adjustable electric timer. A 9:1 reflux ratio was used in distillation experiments. Pressure in the column was controlled by a manostat in combination with a vacuum pump and tank argon bleed.

The column was calibrated by fractionally distilling a 20 mole % carbon tetrachloride-benzene mixture, and analyzing simultaneously collected distillate and residue samples with an Abbé refractometer. The number of theoretical steps was determined by the McCabe-Thiele (19) method, and, for comparison, calculated by the Fenske equation (20), using an average relative volatility of 1.134. It was observed that the number of theoretical steps increased with increased throughput, and varied from 16–42 at throughputs of 23 and 72 ml/min, respectively. Inasmuch as the turbulence noted at lower throughput approximated that in silicon tetraiodide distillation, the more conservative number of steps was selected to describe the performance of this column.

A pressure of 200 mm Hg was chosen for column operation, corresponding to a boiling temperature of 238.1°C for silicon tetraiodide. Referring to Table II, showing the boiling point and vapor pressure of

TABLE II. Boiling point at 200 mm and vapor pressure at 238°C of groups III and V metal iodides

Compound	Boiling point at 200 mm pressure, °C	Vapor pressure at 238°C, mm Hg	Relative volatility	Reference
BI <sub>3</sub>	157	1360	6.8	(16)
PI <sub>3</sub>	169	910	4.6	(21)
GaI <sub>3</sub>	299	36	0.18	(21)
Al <sub>2</sub> I <sub>6</sub>	324	24	0.12	(21)
AsI <sub>3</sub>	336	24	0.12	(21)
SbI <sub>3</sub>	369	11	0.06	(21)
InI <sub>3</sub>	414	1.1	0.006	(21)

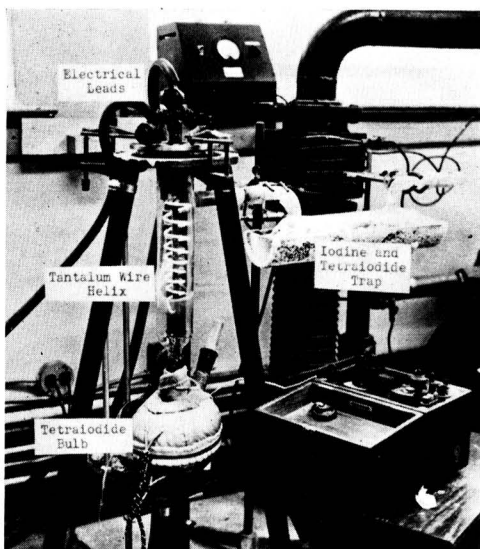


FIG. 5. View of apparatus for decomposing silicon tetraiodide.

groups III and V metal iodides, the relative volatility,  $\alpha$ , of these iodides in comparison to silicon tetraiodide indicated that, based on the assumption of Raoult's law, boron and phosphorus would segregate in the first distillate, while gallium, aluminum, arsenic, antimony, and indium would tend to remain in the still-pot residue. An enrichment of 4.6 and a depletion of 5.5 per equivalent plate was anticipated in the vapor respectively for phosphorus and gallium, the iodides having vapor pressures nearest to silicon tetraiodide.

*Thermal decomposition of fractionally distilled silicon tetraiodide.*—Thermal decomposition of fractionally distilled silicon tetraiodide was carried out in the apparatus shown in Fig. 5. A tantalum wire, 0.10 in. in diameter by 3 ft long, formed into a helix, which represented the most efficient form, was used

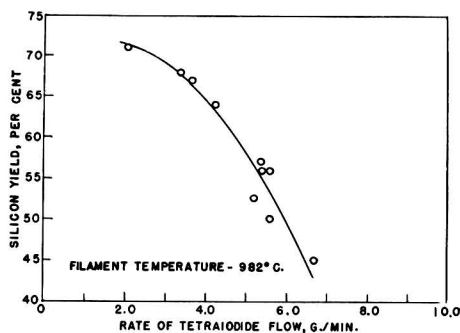


FIG. 6. Yield of silicon metal vs. flow rate of silicon tetraiodide. Filament temperature, 982°C.



for filament. Electrical connections were made to the filament through a flanged Inconel head and molybdenum electrodes. Neoprene gaskets were used for electrode insulation, and for sealing the head to the flanged quartz decomposition cell, which measured  $2\frac{3}{4}$  in. in diameter by 12 in. long.

The cell was attached to the vacuum system and the tetraiodide flask through 20 mm ground quartz joints. During cell operation, undecomposed tetraiodide and free iodine were collected at 28° and 0°C and returned to the decomposition cell and iodinator, respectively, for reuse.

Yield of silicon from a given quantity of tetraiodide varied with the flow rate of silicon tetraiodide through the decomposition cell at constant filament temperature. At a flow rate of 6.9 g/min tetraiodide, 45% was decomposed; by decreasing the flow rate to 2.15 g/min, 71% was decomposed. The efficiency of tetraiodide decomposition at various flow rates is shown in Fig. 6. Dependence of decomposition efficiency on flow rate could result either from increased pressure or decreased contact efficiency.

*Electrical properties.*—Resistivity and type rectification of silicon prepared from center distillates of fractionally distilled tetraiodide are shown in Table III. In each distillation, approximately 50% of the still charge was obtained as center distillate, with the balance equally distributed between first distillate and residue.

Resistivity and type rectification were also determined on silicon prepared from the first distillate and

residue tetraiodide obtained during processing silicon No. 1226 and 1234 (refer to Table III). The first distillate yielded metal having 8 ohm-cm and type-*p* rectification; 0.2 ohm-cm and type-*n* rectification were obtained on metal from the residue from silicon No. 1226. Similar values from processing silicon No. 1234 were 10 and 7 ohm-cm resistivity and type-*p* rectification, respectively, from first fraction and residue tetraiodides.

#### CONCLUSIONS

1. Rate of silicon formation in a standard iodide cell was observed to depend on the variables studied as follows: the rate reached a maximum with respect to amount of iodine used, then decreased with further iodine addition; the rate also reached a maximum with respect to cell temperature and rose continuously with filament temperature up to the highest value employed (1040°C).

2. Resistivity and type rectification of silicon prepared in a standard type iodide process cell showed that groups III and V elements were transferred in the iodide process.

3. Silicon prepared from fractionally distilled tetraiodide had resistivities of a higher order than standard process metal, indicating that the tetraiodide was purified through fractional distillational procedure. As work is in progress at the present time to determine the degree to which contaminating elements are removed and where they are segregated, no conclusion could be drawn relative to ultimate purification obtainable by this procedure.

#### ACKNOWLEDGMENT

The work described is part of a research project carried out by Foote Mineral Company on the preparation of high purity silicon under Contracts DA 36-039-sc-5550 and DA-36-039-sc-56693 for the Signal Corps Engineering Laboratories. The authors acknowledge permission to publish these data.

The authors gratefully acknowledge the assistance of Messrs. H. C. Daly, L. H. Belz, and Dr. R. J. Brumbaugh for the enthusiastic manner in which they performed separate phases of the work described.

Any discussion of this paper will appear in a Discussion Section, to be published in the December 1954 issue of the JOURNAL.

#### REFERENCES

1. F. M. BECKET (To Electro-Metallurgical Division, Union Carbide and Carbon Corp.), U. S. Pat. 1,386,227, August 2, 1951.
2. N. P. TUCKER, *J. Iron Steel Inst. (London)*, **15**, 412 (1927).
3. J. H. SCAFF (To Bell Telephone Laboratories, Inc.), U. S. Pat. 2,402,582, June 25, 1946.

TABLE III. Resistivity and type rectification of silicon prepared from center distillates of fractionally distilled silicon tetraiodide

Silicon No.	Resistivity, ohm-cm	Type rectification	Remarks
1226 <sup>a</sup>	18	<i>p</i>	SC <sup>e</sup>
1234 <sup>b</sup>	30	<i>p</i>	SC <sup>e</sup>
1420 <sup>c</sup>	30-200	<i>p</i>	SF <sup>f</sup>
1422 <sup>c</sup>	100	<i>p</i>	SC <sup>e</sup>
1464 <sup>c</sup>	35-95	<i>p</i>	PF <sup>f</sup>
1477 <sup>c</sup>	40-80	<i>p</i>	SF <sup>f</sup>
1479 <sup>c</sup>	37-98	<i>p</i>	PF <sup>f</sup>
1481 <sup>c</sup>	40-80	<i>p</i>	PF <sup>f</sup>
1486 <sup>c</sup>	44-51	<i>p</i>	PF <sup>f</sup>

<sup>a</sup> SiI<sub>4</sub> distilled in 3.7 step column.

<sup>b</sup> SiI<sub>4</sub> doubly distilled in 3.7 step column.

<sup>c</sup> SiI<sub>4</sub> distilled in 16 step column.

S—Single crystal.

P—Polycrystalline, with large faces.

F—Floating-zone technique.

C—Czochralski technique.

<sup>e</sup> Prepared by Dr. F. H. Horn, General Electric Research Laboratory.

<sup>f</sup> Prepared by Dr. P. H. Keck, Squier Signal Laboratory.

<sup>g</sup> Prepared by Dr. A. C. Sheekler, General Electric Company, Syracuse, N. Y.

4. D. W. LYON, C. M. OLSON, AND E. D. LEWIS, *This Journal*, **96**, 359 (1949).
5. A. E. VAN ARKEL, *Metallwirtschaft*, **13**, 405, 511 (1934).
6. R. HÖLBLING, *Z. angew. Chem.*, **40**, 655 (1927).
7. J. J. BERZELIUS, *Ann. Phys.*, Ser. II, **1**, 169 (1824).
8. H. VON WARTENBERG, *Z. anorg. u. allgem. Chem.*, **265**, 186 (1951).
9. A. STOCK AND C. SOMIESKI, *Ber.*, **49**, 111 (1916).
10. A. E. VAN ARKEL AND J. H. DE BOER, *Z. anorg. u. allgem. Chem.*, **141**, 289 (1924).
11. I. E. CAMPBELL, R. I. JAFFEE, J. M. BLOCHER, JR., JOSEPH GURLAND, AND B. W. GONSER, *This Journal*, **93**, 271 (1948).
12. F. B. LITTON, *ibid.*, **98**, 488 (1951).
13. H. C. TORREY AND C. A. WHITMER, "Crystal Rectifiers," pp. 64-67, (Radiation Laboratory Series 15) McGraw-Hill Book Co., Inc., New York (1948).
14. L. L. QUILL (Editor), "The Chemistry and Metallurgy of Miscellaneous Materials," Paper 6, p. 76, McGraw-Hill Book Co., Inc., New York (1950).
15. R. SCHWARZ AND A. PFLUGMACHER, *Ber.*, **75B**, 1062 (1942).
16. H. C. ANDERSEN AND L. H. BELZ, *J. Am. Chem. Soc.*, **75**, 4828 (1953).
17. C. FRIEDEL, *Liebigs Ann. Chem.*, **149**, 96 (1868).
18. A. S. CARTER AND F. W. JOHNSON (To E. I. du Pont de Nemours & Co.), U. S. Pat. 2,251,185, July 29, 1941.
19. J. H. PERRY, "Chemical Engineer's Handbook," McGraw-Hill Book Co., Inc., New York (1950).
20. M. P. FENSKE, *Ind. Eng. Chem.*, **24**, 482 (1932).
21. F. D. ROSSINI, D. D. WAGMAN, W. H. EVANS, S. LEVINE, AND I. JAFFE, Cir. No. 500, National Bureau of Standards, U. S. Government Printing Office, Washington, D. C. (1952).

# Phenomena Observed in the Melting and Solidification of Germanium<sup>1</sup>

S. E. BRADSHAW

*Research Laboratories of the General Electric Co. Ltd., Wembley, Middlesex, England*

## ABSTRACT

Small spheres of molten germanium, weighing around 10 mg, form pear-shaped solids on freezing, and a solidification mechanism is advanced to explain the shape and impurity distribution which occurs. Solids are shown to be substantially single crystal germanium.

The shape of a germanium ingot is shown to involve the ratio of the densities of liquid and solid germanium,  $d_L/d_S$ , at the melting point, and from the value of 1.13 obtained for  $d_L/d_S$ , it is deduced that the melting point of germanium is lowered by an increase of pressure. It is suggested that germanium may undergo an allotropic modification under pressure.

## INTRODUCTION

The melting and solidification of germanium are somewhat unusual processes. It is possible to arrange external conditions so that the solidification-front progresses uniformly through the mass of molten material, and the solid which results has the shape predicted by an analysis based on simple ideas. This can be illustrated by some practical methods employed in the preparation of germanium for use in semiconductor devices.

### *Globule Melting*

Small spheres of molten germanium, weighing around 10 mg, form pear-shaped solids, "globules," when allowed to solidify on a graphite support. The shape of a fraction of these globules closely approximates a right-circular cone standing on a hemispherical base, and the remainder possess shapes intermediate between this and a sphere; the germanium solidifies in such a way that the globule's cone-axis is roughly vertical.

It has been shown (1) that small spheres of molten germanium, solidifying in contact with a flat support, form slender right-circular cones due to uniform progress of a planar solidification front. It has also been shown (2) that small spheres of molten germanium can supercool by as much as 235°C. If it is assumed that the supercooled material nucleates at the graphite contact surface, rapid advance of the solidification front may be postulated as freezing in the original spherical shape, but since the solidification process liberates some 8 kcal/g-atom, the temperature of the remaining liquid rises; consequently the rate of solidification becomes smaller.

<sup>1</sup> Manuscript received May 20, 1953. This paper was prepared for delivery before the New York Meeting, April 12 to 16, 1953.

When the solidification front has slowed down sufficiently, the coning phenomenon results.

Thus, solidification of a small molten sphere of germanium to the shape formed by mounting a cone on a hemisphere requires a somewhat restricted set of conditions, and when these conditions are not satisfied, intermediate shapes of globules result.

### *Normal Freezing*

Progressive solidification of molten germanium in a horizontal direction results in an ingot whose cross section varies uniformly along its length, and for a horizontal crucible of constant cross section, the cross section of the ingot is smaller at the end first to solidify and larger at the end last to solidify.

If the effect due to surface tension is neglected and the phenomenon regarded as being due solely to the difference in density between solid and liquid germanium, the height,  $Y$ , of the ingot produced by a horizontal crucible of constant cross section is given by

$$(1 - x)^{(d_S/d_L)-1} = f(Y) \quad (1)$$

where  $x$  = fractional distance along the ingot from the end first to solidify,  $d_S$  = density of solid germanium at solidification temperature, and  $d_L$  = density of liquid germanium at solidification temperature. The function  $f(Y)$  depends on the cross section of the crucible employed and, for a rectangular cross section, is equal to  $Y/Y_0$  where  $Y_0$  is the height at  $x = 0$ .

If the crucible is tilted at an angle to the horizontal, the equation describing the shape of the ingot is too involved to be of direct value, but it can be shown that for certain angles of tilt the variation in cross section of ingots is a minimum. It is found in practice that tilting the crucible against the

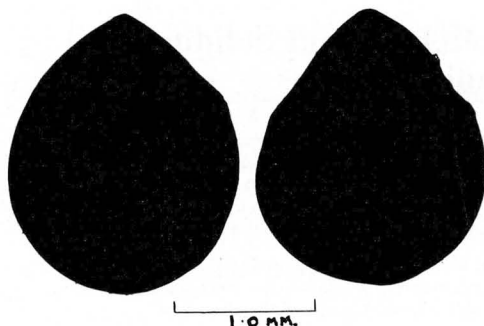


FIG. 1. Shapes of typical germanium globules

direction of solidification by about  $5^\circ$  gives optimum uniformity of ingot cross section.

#### Zone Melting

The shape of ingot which results from passage of a molten zone (3) along a charge-ingot contained in a horizontal crucible of constant cross section depends on shape of the charge ingot. When this is of constant cross section, passage of a single zone results in an ingot whose height is given by:

$$\left(\frac{d_L}{d_S}\right) - \left[\left(\frac{d_L}{d_S}\right) - 1\right] \exp(-d_S x / d_L c) = f(Y) \quad (\text{II})$$

where  $c$  is the zone length expressed as a fraction of the length of the ingot, and the previous notation is retained.

Now, if further zones are passed along this ingot, a limiting shape will be reached at which the shape of the ingot is unaltered by passage of a molten zone. The height of this ingot is given, to a close approximation, by

$$\exp 2\left[\left(\frac{d_L}{d_S}\right) - 1\right]x/c = f(Y) \quad (\text{III})$$

with the notation used in equation (II).

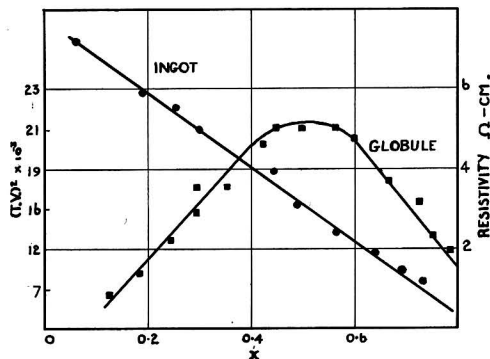


FIG. 2. The fraction of germanium solidified,  $x$ , at a point in a germanium globule vs. the mean value of (turn-over voltage)<sup>2</sup> occurring at this point.

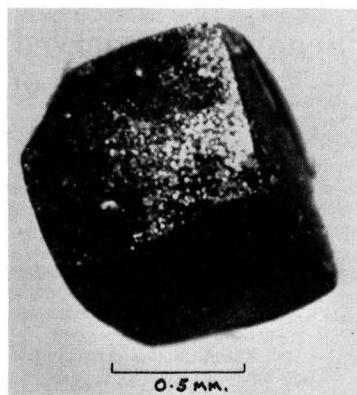


FIG. 3. Shape of the solid obtained by partial dissolution of a germanium globule.

Neither equation (II) nor (III) will hold for the last portion of the ingot to solidify. This will solidify normally with a height given by equation (I). Equation (III) indicates that the smaller the zone length the greater is the variation in the cross section of the ingot. For the length of zone commonly employed, however, tilting the crucible by about  $5-10^\circ$  against the motion of the zone gives optimum uniformity.

#### EXPERIMENTAL

A shallow depression in a graphite bar was filled with germanium in the form of a fine black powder and heated at  $1000^\circ\text{C}$  in an atmosphere of  $\text{N}_2$  for 15 min. At the end of this period, the bar was rapidly cooled by being brought into the cold part of the furnace; subsequently the globule, weighing about 10 mg, was removed from the depression. A prepared surface in which the axis of the cone lay was explored for turn-over voltage (t.v.), using a micro-manipulator and tungsten whiskers. In Fig. 1, the

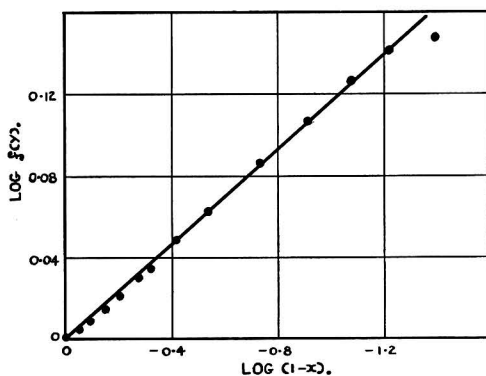


FIG. 4.  $\log f(Y)$  vs.  $\log (1-x)$  for a normally-frozen germanium ingot.

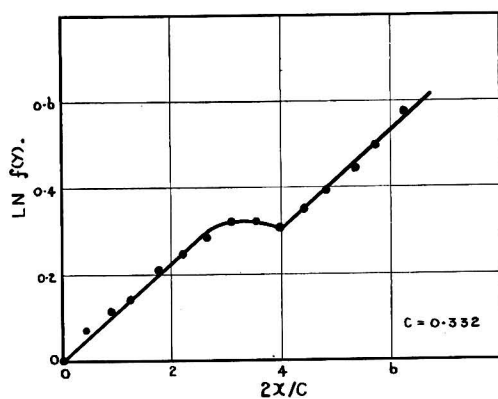


Fig. 5.  $\ln f(Y)$  vs.  $2x/c$  for a zone-melted germanium ingot, where  $c$  is 0.332.

shapes of typical surfaces are illustrated, and in Fig. 2 the fraction of germanium solidified at a certain distance along this axis is plotted against the mean value of  $(t.v.)^2$  occurring at this distance. Fig. 3 illustrates the shape obtained from a globule by partial dissolution in a solvent consisting of equal volumes of 4*N* sodium hydroxide solution and 4*N* sodium hypochlorite solution, the temperature being held at 80°C with vigorous stirring.

An ingot was produced from a horizontal graphite crucible of constant cross section by normal freezing, and its height,  $Y$ , measured for different values of  $x$ . A plot of  $\log f(Y)$  vs.  $\log(1 - x)$  is given in Fig. 4.

A similar procedure was employed with the zone-melting technique, and a plot of  $\ln f(Y)$  vs.  $2x/C$  is given in Fig. 5. The zone length,  $C$ , was taken as being the average distance between the two solid-liquid interfaces of the 24 zones passed along the ingot.

#### DISCUSSION

The mechanism of solidification of the globules results in a segregation of impurity analogous to that which occurs in an ingot (4) and varying rates of solidification are reflected in distribution of impurities obtained. For the initial rapid solidification, segregation is low and impurity concentration in the solid is high. As the solidification rate becomes smaller, and segregation becomes more effective, the impurity concentration in the solidifying germanium becomes smaller. Since, however, the concentration in the liquid fraction is now increasing, the concentration in the solid begins to increase at some point and continues to do so until all the germanium is solid.

An approximate theory of semiconductors indicates that  $(t.v.)^2$  is roughly inversely proportional to impurity concentration. For comparison, the result for a typical ingot is included in Fig. 2; the two

ordinate scales have been adjusted until they are approximately equivalent. It would appear that both shape of the globule and distribution of impurity within it are consistent with the solidification mechanism advanced.

Absence of a surrounding crucible for the solidifying germanium and presence of a planar solidification front are common to both the globule technique and the Czochralski pulling method used in the preparation of germanium single crystals (5). Cubes with truncated corners which are produced from the globules by preferential etching technique indicate that they are, in fact, substantially single crystals, and this was confirmed by an x-ray examination which showed the presence of some mosaic structure. The result illustrated in Fig. 3 is in harmony with the concept of a reciprocity between growth and dissolution (6) since it is known that the preferred direction of growth in germanium is [100].

Values of  $d_L/d_S$  calculated from Fig. 4 and 5 are 1.13 and 1.11, respectively, but uncertainty in the value of  $C$  probably makes the latter estimate less reliable. The value of 1.13 is intermediate between the value of 1.22 reported by Hall (7) and 1.05 found by Mokrovskii and Regel (8). The abrupt change in height of the zone-melted ingot, apparent in Fig. 5, is inherent in the process and occurs when the volume of liquid in the zone reaches the point where the balance of hydrostatic and surface-tension forces becomes unstable. Molten germanium then flows back over the trailing edge of the zone for a short distance, and the balance of forces is restored. From equation (III) it can be seen that if a limiting shape is rapidly regained, the slopes of the straight-line portions of the graph of  $2x/C$  vs.  $\ln f(Y)$  will be the same.

Among the elements, a value of  $d_L/d_S$  greater than one is the exception rather than the rule, and it is confined to those cases where bonding mechanism is substantially covalent. These strongly directive bonds result in a relatively open structure, and during melting the complete or partial collapse of the covalent bonds leads to an increase in density, the coordination number for germanium increasing from 4 to 8 during melting (9).

The Clausius-Clapeyron equation for phase changes,

$$\Delta S/\Delta V = dp/dT \quad (IV)$$

relates  $dp/dT$ , rate of increase of pressure with melting point, with  $\Delta S$ , entropy of fusion, and  $\Delta V$ , increase of volume on melting. At the melting point, the free-energy of fusion is zero and  $\Delta H = T\Delta S$  where  $\Delta H$  is the heat of fusion. Employing Greiner's values (10) ( $\Delta H = 8100$  cal/g-atom and  $T = 1209^\circ\text{K}$ ) gives  $\Delta S = 6.7$  cal/°C.  $\Delta V = -1.6$  cc is obtained by substituting  $(d_S/d_L - 1) = -0.115$ ,

$A = 72.6$ , and  $d_s = 5.25$  in  $\Delta V = A(d_s/d_L - 1)/d_s$ .<sup>2</sup> Substituting these values in equation (IV) gives

$$\frac{dp}{dT} = -4.2 \text{ cal/}^\circ\text{C/cc} = -1.8 \times 10^8 \text{ dynes/cm}^2/^\circ\text{C}.$$

The negative value for this differential coefficient implies that an increase of pressure lowers the melting point of germanium initially, but calculation of the melting point corresponding to any given pressure requires a knowledge of the dependence of this coefficient on pressure. For bismuth and gallium, Bridgman (11) found that  $d^2p/dT^2$  was negative and suggested that this indicated some sort of instability in structure. With bismuth, gallium, and antimony, which have  $d_L/d_s > 1$ , polymorphic transitions were found to occur under very high pressure. In the case of gallium a new solid phase appeared around  $10^{10}$  dynes/cm<sup>2</sup>, which was denser than the liquid (11). In the cases of carbon and tin, it is well known that the diamond structure is the thermodynamically unstable allotrope at normal temperatures and pressures, and a graphitic silicon has been reported (12). It would seem reasonable to suggest, therefore, that the diamond structure of germanium may not be stable under pressure, particularly for elevated temperatures.

Pressure exerted locally by the whisker of a point-contact diode is very high—of the order of  $10^{10}$  dynes/cm<sup>2</sup> for a 10-gram load on an apparent whisker area of  $10^{-6}$  cm<sup>2</sup>—and its effect upon structure or melting point of germanium may be of importance during such processes as the "forming" treatment, where it is known that temperatures in excess of  $500^\circ\text{C}$  may be attained. Whisker pressure alone may be sufficient to cause a small region of the germanium to undergo allotropic modification, and it is significant that Jordan (13) has reported that localized pressures of the order of  $10^{10}$  dynes/cm<sup>2</sup> can modify conduction characteristics of very restricted areas from *n*-type to *p*-type. This modification is permanent.

## APPENDIX

### DERIVATION OF EQUATION (I)

For a horizontal crucible of unit length and constant cross section, the cross section of the ingot at any point,  $x$ , is a function of the height of the ingot,  $Y$ , and some constants. Call this function  $g(Y)$ . If, during normal freezing, the charge is solid from  $x = 0$  to  $x = x$ , and liquid from

$x = x$  to  $x = 1$ , then, neglecting the effect of surface tension, the weight of liquid,  $W_L$ , is

$$W_L = d_L(1 - x)g(Y) \quad (\text{V})$$

In this equation,  $d_L$  is the density of liquid germanium at solidification temperature, and it is assumed that the germanium is at this temperature everywhere. Differentiating equation (V) with respect to  $x$  gives

$$-\frac{dW_L}{dx} = -d_L[(1 - x)g'(Y) - g(Y)] \quad (\text{VI})$$

where  $g'(Y)$  denotes the differential coefficient of  $g(Y)$  with respect to  $x$ . But if  $W_S$  is the weight of the solid,

$$\frac{-dW_L}{dx} = \frac{dW_S}{dx} = d_S g(Y) \quad (\text{VII})$$

where  $d_S$  is the density of solid germanium at solidification temperature. On combining (VI) and (VII),

$$\frac{-\left(\frac{d_S}{d_L} - 1\right)}{(1 - x)} = \frac{g'(Y)}{g(Y)} \quad (\text{VIII})$$

and integration of (VIII) gives

$$(1 - x)^{(d_S/d_L - 1)} = g(Y)/g(Y_0) \quad (\text{IX})$$

where  $Y_0$  is the height of the ingot at  $x = 0$ . Replacing  $g(Y)/g(Y_0)$  by  $f(Y)$  gives equation (I). For a crucible of rectangular cross section  $g(Y) = bY$ , where  $b$  is the breadth of the crucible; hence  $f(Y) = Y/Y_0$ .

### DERIVATION OF EQUATION (II)

If, during zone-melting, the charge has been zoned from 0 to  $x$ , is liquid in the zone  $x$  to  $x + c$ , and solid in the portion still to be zoned from  $x + c$  to 1, then

$$W_R = d_{LC} g(Y) + d_S(1 - x - c)g(\bar{Y})$$

and hence

$$-\frac{dW_R}{dx} = -d_{LC} g'(Y) + d_S g(\bar{Y}) \quad (\text{X})$$

Where  $g(\bar{Y})$  is uniform cross section of the charge ingot,  $W_R$  is weight of material to be zoned and in process of being zoned, and  $c$  is length of the molten zone, which is constant. The same assumptions are made as in the previous case. As before,

$$\frac{-dW_R}{dx} = \frac{dW_S}{dx} = d_S g(Y) \quad (\text{XI})$$

where  $W_S$  is the weight of germanium which has been zoned. Combining (XI) and (X) gives

$$\frac{d_S [g(Y) - g(\bar{Y})]}{d_L c} = g'(Y) \quad (\text{XII})$$

The weight of liquid in the first zone to be formed is  $d_{LC} g(Y_0)$ , and this zone was formed by melting a weight of the charge ingot  $d_S c g(\bar{Y})$ , hence

$$g(\bar{Y}) = \frac{d_L}{d_S} g(Y_0) \quad (\text{XIII})$$

Substituting (XIII) in (XII) gives

$$\frac{g(Y_0) - \frac{d_S}{d_L} g(Y)}{c} = g'(Y) \quad (\text{XIV})$$

<sup>2</sup> After this paper was written, a letter by R. G. Schulman and D. N. Van Winkle ["Pressure Welded *P-N* Junctions in Germanium," *J. Applied Phys.*, **24**, 224 (1953)] was published in which a volume change of 5% and a melting point of  $935^\circ\text{C}$  were quoted as having been obtained experimentally. Using these values and 110 cal/gram for the heat of fusion, they obtain  $dT/dP = -2.4 \times 10^{-3}$  degrees/kg/cm<sup>2</sup>.

and integration gives

$$(d_L/d_S) - [(d_L/d_S) - 1] \exp(-d_S x/d_L c) = g(Y)/g(Y_0) \quad (\text{XV})$$

Replacing  $g(Y)/g(Y_0)$  by  $f(Y)$  gives equation (II).

#### DERIVATION OF EQUATION (III)

Let the relationship between  $g(Y)$  and  $x$  for an ingot treated with a large number of zones be

$$g(Y) = \phi(x) \quad (\text{XVI})$$

Then the condition that this relationship will be unaltered by the passage of further zones is

$$\int_x^{x+c} \phi(x) dx = \frac{d_L}{d_S} c g(Y) \quad (\text{XVII})$$

An approximate solution of this equation is

$$\exp 2[(d_L/d_S) - 1]x/c = g(Y)/g(Y_0) \quad (\text{XVIII})$$

Substituting  $g(Y)/g(Y_0)$  by  $f(Y)$  gives equation (III).

Any discussion of this paper will appear in a Discussion Section, to be published in the December 1954 issue of the JOURNAL.

#### REFERENCES

1. J. W. RYDE AND B. S. COOPER, *Engineering*, **173**, 690 (1952).
2. D. TURNBULL AND R. E. CECHE, *J. Applied Phys.*, **21**, 804 (1950).
3. W. G. PFANN, *J. Metals*, **4**, 747 (1952).
4. G. L. PEARSON, J. D. STRUTHERS, AND H. C. THEURER, *Phys. Rev.*, **77**, 809 (1950).
5. G. K. TEAL AND J. B. LITTLE, *Phys. Rev.*, **78**, 647 (1950).
6. H. E. BUCKLEY, "Crystal Growth," p. 304, John Wiley & Sons, Inc., New York (1951).
7. R. N. HALL, *Science*, **112**, 419 (1950).
8. N. MOKROVSKII AND A. REGEL, *J. Tech. Phys. (U.S.S.R.)*, **22**, 1281 (1952).
9. H. HENDUS, *Z. Naturforsch.*, **2a**, 505 (1947).
10. E. S. GREINER, *J. Metals*, **4**, 1044 (1952).
11. P. W. BRIDGMAN, "The Physics of High Pressure," G. Bell & Sons, Ltd., London (1949).
12. F. HEYD, F. KOHL, AND A. KOCHANOVSKA, *Collection Czechoslov. Chem. Commun.*, **12**, 502 (1947).
13. J. P. JORDAN, *Elec. Eng.*, **71**, 619 (1952).

# Preparation and Examination of Beryllium Carbide<sup>1</sup>

M. W. MALLETT, E. A. DURBIN, M. C. UDY, D. A. VAUGHAN, AND E. J. CENTER

*Battelle Memorial Institute, Columbus, Ohio*

## ABSTRACT

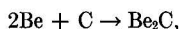
Properties of beryllium carbide were studied to determine its suitability as a high-temperature refractory. Various methods of preparing it were tried and a number of the physical and chemical properties of the resulting products were determined. Lots containing 85 weight % of useful product were prepared by the beryllium metal-carbon reaction. Because the material was to be fabricated into refractory bodies, particular attention was paid to the chemical analysis for unreacted BeO, beryllium metal, and free carbon; x-ray diffraction identification of the various phases present; and microscopical examination for mineral composition, crystal size, and crystal habit.

As a refractory, beryllium carbide has several disadvantages. It tends to hydrolyze in atmospheric moisture and to react with both oxygen and nitrogen, when heated.

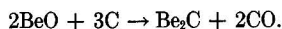
## INTRODUCTION

Because of recent interest in the use of unconventional refractories such as carbides, nitrides, and sulfides, an investigation was made of the suitability of beryllium carbide as a high-temperature refractory.

The earliest work on beryllium carbide appears to be that of Lebeau (1) in 1895. He prepared the carbide by two methods: (a) heating a mixture of beryllium and sugar charcoal in an electric furnace,



and (b) heating beryllium oxide with sugar charcoal in an electric furnace (40 kw) for about 10 min,



Lebeau gave it the formula  $\text{Be}_4\text{C}_3$ , but, after Henry (2) pointed out an error in the atomic weight and the valency of beryllium had been proven, he adopted the formula  $\text{Be}_2\text{C}$ . No other carbides seem to exist. This compound was described (3) as consisting of yellowish-brown transparent crystals with properties quite similar to those of aluminum carbide. It is so hard it scratches quartz easily.

The crystal structure of  $\text{Be}_2\text{C}$  was studied by Stackelberg and Quatram (4). X-ray investigation showed that  $\text{Be}_2\text{C}$  has an antifuorite ( $\text{CaF}_2$ ) lattice like  $\text{Mg}_2\text{Si}$ . The following constants were determined:  $a_0 = 4.33 \text{ \AA}$ ; x-ray density,  $d = 2.44$ ; Be - C distance =  $1.87 \text{ \AA}$ ; and C - C distance =  $3.06 \text{ \AA}$ .

Work described in the present paper was completed in 1948. Subsequently, Geller (5) summarized previously known data on physical and chemical properties of  $\text{Be}_2\text{C}$ , and Coobs and Koshuba (6) discussed fabrication of this compound. Procedures

for determination of the principal constituents and contaminants of  $\text{Be}_2\text{C}$  were recently described by Gallagher (7).

## PREPARATION

The  $\text{Be}_2\text{C}$  prepared for this investigation was made by the two basic methods used by Lebeau, that is, by heating an intimate mixture of BeO and carbon and by reacting beryllium metal and carbon.<sup>2</sup>

### *Apparatus*

A typical furnace setup is shown in Fig. 1. A semi-permanent graphite heater crucible was packed in the induction coil with Norblack powder insulation. Vent holes were formed by pushing twelve  $\frac{1}{8}$ -in.-diameter wires into the Norblack packing. The top of the packing was then sealed with Alundum cement before the wires were removed. Care was taken not to form the vent holes after applying the Alundum cement, because any oxide carried into the packing forms gas when heated and forces the Norblack out, sometimes explosively. A second graphite crucible containing the charge was slipped into the heater crucible. Holes were provided near the top of the inner crucible, into which a heavy iron wire bail could be placed for lifting the hot crucible from the assembly upon completion of a heat. Another crucible and charge could then be placed in the hot furnace and reacted without delay. A solid graphite cover rested on the charge, leaving about  $1\frac{1}{2}$  in. of space between this cover and a clay-graphite cover which rested on the top edge of the crucible. Into this space was flowed a continuous stream of argon through a fused-silica tube. This provided a

<sup>2</sup> A proposed method, which appears feasible but has not been tried, is a vapor-deposition method in which a mixture of a beryllium halide and a hydrocarbon gas, carried in a stream of hydrogen, would be reacted on contact with a hot filament depositing  $\text{Be}_2\text{C}$  on the filament.

<sup>1</sup> Manuscript received July 1, 1953. This paper was prepared for delivery before the Wrightsville Beach Meeting, September 13 to 16, 1953.



blanket of inert gas over the charge during heating. A second hole in the outer lid was used for making optical pyrometer readings on the inner lid. Occasional setups contained a graphite-tube sight-well ( $\frac{3}{4}$  in. ID x 1 in. OD) centrally located in the charge and extending downward through both covers to within one inch of the bottom of the charge. Lid temperatures were compared with "true" temperatures throughout the range of temperatures used. Lid temperatures varied from  $300^\circ\text{C}$  low at  $1700^\circ\text{C}$  to about  $600^\circ\text{C}$  low at  $2200^\circ\text{C}$ .

#### Experimental Procedure

In a small exploratory heat, a mixture of stoichiometric quantities of  $\text{BeO}^3$  ( $-200$  mesh) and graphite powder ( $-60$  mesh) was placed in a graphite crucible and heated in a vacuum furnace ( $<10^{-4}$  mm Hg). As the temperature was raised, the first indication of reaction occurred at  $1500^\circ\text{C}$ , when rapid gas evolution began. The reaction had not reached completion after two hours' heating at  $1650^\circ\text{C}$ . X-ray diffraction analysis indicated that considerable  $\text{BeO}$  and unreacted carbon still remained. Subsequent larger heats (600-gram charge) were made using a similar mixture except that fluorescent-grade  $\text{BeO}^4$  was substituted for the more refractory H. F.-grade  $\text{BeO}$ . Oxide and graphite were intimately mixed by ball milling together. This mixture was heated in an argon atmosphere to a minimum temperature of  $1900^\circ\text{C}$ . Even though a temperature of about  $2800^\circ\text{C}$  was reached in the hottest part of the charge, some unreacted  $\text{BeO}$  and carbon remained after four hours' heating. About 60% yield of material containing about 90%  $\text{Be}_2\text{C}$ , with the balance  $\text{BeO}$  and free carbon, was obtained.

The useful product of each heat or lot (described above or below) tended to form a sintered or semi-sintered mass which could be distinguished by color (metallic or red-brown) from the relatively loose unreacted charge. The unreacted material was usually confined to the upper part of the charge. The amount to be discarded was determined by visual inspection and was readily separated from the selected product. Percentage of yield was based on the weight of selected product and the theoretical weight of  $\text{Be}_2\text{C}$  to be expected from the beryllium content of the charge.

Several lots of  $\text{Be}_2\text{C}$  were prepared by heating a mixture of beryllium metal flake (Clifton Products, Inc.) and minus 60-mesh graphite powder. In some cases, carbon black (Norblack) was used in place of graphite. It was impossible to get uniform mixing because of the nature of the flakes which were about one inch in diameter and foil-like in thickness. How-

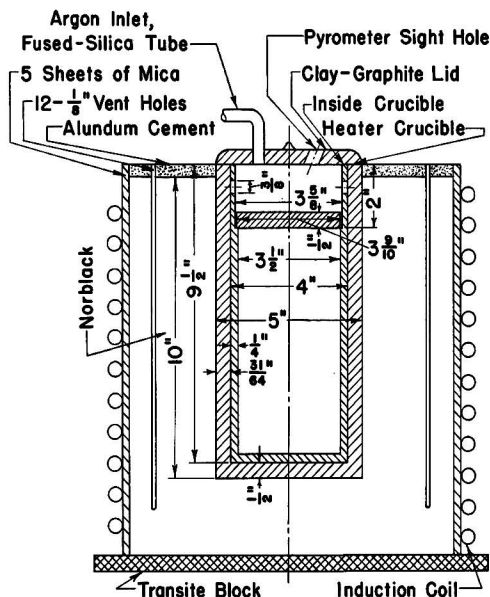


FIG. 1. Furnace setup for metal-carbon reaction

ever, this was inconsequential because the beryllium apparently vaporized during heating so that the end product consisted of a cylindrical mass, approximately  $3\frac{1}{2}$  in. in diameter by 8 in. in length, of loosely sintered  $\text{Be}_2\text{C}$  grains of about 30-mesh grain size. The product ranged from red, through tan, bronze, brown, or black according to the free-carbon content.

Later, a rather large supply of finely divided beryllium metal in the form of saw chips and turnings was available; this material was substituted for beryllium flake with similar results. Some advantage was gained in using the saw chips because about 650 grams of charge could be packed in a crucible which would hold only 500 grams using the bulkier flake.

Twenty to thirty minutes at  $1700^\circ\text{C}$  was found sufficient to complete the metal-carbon reaction. This was much more rapid than the  $\text{BeO}$ -carbon reaction and a greater percentage (85 weight %) of useful product was obtained. Therefore, this method was used to the exclusion of other methods and about 40 lots of beryllium carbide were prepared.

#### An Alternative Method

In addition to the above methods of producing  $\text{Be}_2\text{C}$ , several others were tried. Experience gained during the pouring of beryllium into hot graphite molds showed that beryllium reacts exothermically with graphite to form  $\text{Be}_2\text{C}$ . The reaction seemed to start about  $50^\circ\text{C}$  above the melting point of beryllium. Similar reactions were noted when beryllium melts in graphite crucibles were superheated. The

<sup>3</sup> Brush Beryllium Company H. F. grade.

<sup>4</sup> Clifton Products, Inc.

reaction could not always be brought about, apparently because, in some cases, a thin adherent layer of carbide formed on the inner surface of the crucible preventing further reaction.

When the reaction did occur, the melt solidified in spite of increasing temperature. This thickening or freezing of the melt was caused by the formation of many individual grains of  $\text{Be}_2\text{C}$  in the metal matrix. In many cases, 80–90% of the volume was comprised of these carbide crystals (see Fig. 2). Average particle size ran from about  $0.5 \mu$  to about  $100 \mu$ , depending, among other things, on the temperature of formation and time at temperature. Although grain size varied greatly from heat to heat, grains of an individual heat were all of the same approximate order of magnitude. Upon exposure of a polished section of this material to air for several days, carbide particles took on a pink color. Air etch was the result of hydrolysis of the carbide by the moisture of the atmos-

phere. Highlights in the large grains (Fig. 2A) are reflections from within the translucent  $\text{Be}_2\text{C}$  grains.  $\text{Be}_2\text{C}$  grains were separated by dissolving the beryllium metal matrix in dilute hydrochloric acid. Although smaller grains were greatly hydrolyzed, large well-formed crystals showed little attack. This method appears well suited for producing relatively pure  $\text{Be}_2\text{C}$ , although it has been used only on a small scale to date.

Sloman (8) found similar grains of  $\text{Be}_2\text{C}$  formed by the action of graphite on the metal during electrolysis. Remelting allowed carbide particles to segregate in the bottom of the beryllium ingot. Upon solution of the metal with very dilute HCl, pink crystals were obtained which were identified as  $\text{Be}_2\text{C}$  by chemical and x-ray analysis. Sloman states that, in metal containing segregated carbide, the carbides appear grayish-brown under ordinary vertical illumination. Using a wide-angle lens, an intense pink coloration was noted. He thought this pink color was caused by a trace of iron carbide. This is unlikely and, in view of observations made on many  $\text{Be}_2\text{C}$  materials, the pink color in reflected light is evidently due to the hydrolysis product on the surface of the carbide.

#### ANALYSIS AND PROPERTIES OF $\text{Be}_2\text{C}$

Various lots of  $\text{Be}_2\text{C}$  were examined and analyzed as they were made or processed. In addition to visual examination, the principal analyses made included: (a) chemical analysis for total and free carbon, water, and  $\text{Be}_2\text{C}$ ; (b) x-ray diffraction identification of phases; and (c) microscopic observations which included measurement of crystal size, identification of crystal types, identification of phases and estimation of percentage by area measurement, and adjusted mineral composition after correction for relative apparent densities of the constituents. In addition, observations were made on hardness, density, and melting point of  $\text{Be}_2\text{C}$ . Also, a technique was worked out for recording in natural color the appearance of the carbide under the microscope.

#### *Types of Beryllium Carbide*

Casual examination of the product of the usual oxide-carbon or metal-carbon reaction has led to varied descriptions of the carbide. It has been described as pink, red, yellow, orange, tan, bronze, brown, black, metallic, or gray. These designations taken alone are quite deceptive. As seen under the microscope, in either transmitted or reflected light,  $\text{Be}_2\text{C}$  appears as translucent amber grains. The masking power of black free-carbon particles is great. As little as 10% by area, as measured under the microscope, causes the product to look black to the naked eye.

The types of  $\text{Be}_2\text{C}$  observed in the investigation

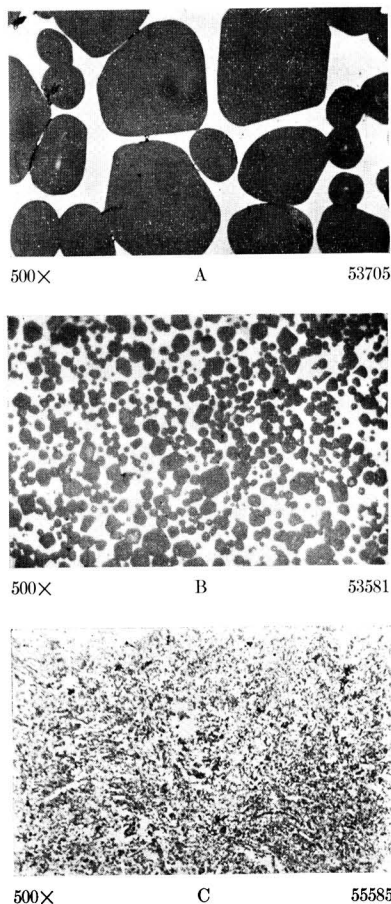


FIG. 2.  $\text{Be}_2\text{C}$  crystals in a beryllium metal matrix, illustrating differences in particle size.

may be described as: (a) coarsely crystalline, (b) microcrystalline (nodular), and (c) vermiculate (defined below). The coarsely crystalline  $\text{Be}_2\text{C}$  was obtained in several ways. One product containing 100% of this type of crystal was extracted from beryllium metal (see Fig. 2A) which had reacted with a graphite crucible. This was the purest carbide produced, containing only traces of opaque material (free carbon or metal) and a small amount of hydrolysis product resulting from the acid-extraction process. In lots of  $\text{Be}_2\text{C}$  made by the metal-carbon reaction at about 2000°C for 1 hr, 95–99% of the crystals were coarse and well formed (see Table I). In addition, this material usually contained 5–10% unreacted carbon. However, the  $\text{Be}_2\text{C}$  grains contained no internal free carbon (graphite flakes).

Microcrystalline  $\text{Be}_2\text{C}$  of the nodular or "grape cluster" type was produced by reacting beryllium metal and carbon at lower temperatures (1700°C) or for short times (20–30 min) at 2000°C. A few lots were made in which 98–99% of the  $\text{Be}_2\text{C}$  phase was microcrystalline (see Table I). This material, when crushed and pressed, showed better sintering characteristics than the more coarsely crystalline material. Nodular  $\text{Be}_2\text{C}$  is readily made by the metal-carbon reaction; whereas, in the oxide-carbon method, where a long time at temperature is required to complete the reaction, only coarse crystals are produced.

The term "vermiculate" applies primarily to the mass of wormlike tubes often produced when beryllium carbide heats are taken above 2200°C (see Fig. 3). These tubes appear to be formed from drippings of a viscous fluid. Although they intermingle, they do not adhere to each other. The interior of the hollow structure is an aggregate of angular reddish



FIG. 3. Vermiculate  $\text{Be}_2\text{C}$ . Top—core of high-temperature heat; bottom—individual tubes showing hollowness.

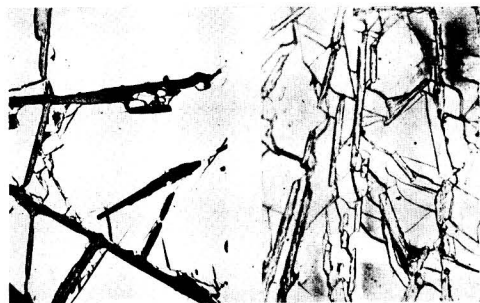
TABLE I. Preparation and crystal properties of beryllium carbide

Lot* No.	Preparation of material		Crystal sizes (microns)			Crystal habit	
	Time, min	Temp, °C	variation		Avg size	% "grape-cluster" finely crystalline nodules in calcined powder	% individual crystal grains plus crystals in calcined powder
			min.	max.			
1	30	1700	0.5	32	5	98–99	<2
2	30	2200	3.0	95	42	5	95
3	30	2020	0.5	50	13	90–95	5–10
4	30	2020	0.5	33	9	98–99	<2
5	30	2020	0.5	47	12	93–95	5–7
6	50	2020	1.0	249	82	5	95
7	15	2020	—	—	—	—	—
	+30	2200	4.0	230	83	Traces only	98–99
8	15	2020	—	—	—	—	—
	+30	2200	1.0	154	58	2–5	95–98

\* These products were made by the metal-carbon reaction using the stoichiometric ratio for  $\text{Be}_2\text{C}$ .

crystals, while the exterior is smooth and metallic in appearance. The metallic color is caused by a thin layer of highly oriented carbon crystals. Because of the similarity of the individual crystals of this and clinker-like porous material which exhibits the vermiform structure to a lesser degree, all high-temperature products with the metallic-appearing surface have been termed vermiculate.

Vermiculate  $\text{Be}_2\text{C}$  is evidently a decomposition product, formed by loss of beryllium through vaporization. This leaves an excess of carbon which precipitates as graphite flakes in a  $\text{Be}_2\text{C}$  matrix (see Fig. 4). In one case, graphite flakes were formed by heating "pure"  $\text{Be}_2\text{C}$  (no free carbon) to 2200°C. The vermiculate structure appears to have been formed by pressure (possibly CO) from within. The



250X

FIG. 4. Graphite flakes in a  $\text{Be}_2\text{C}$  matrix. Left, unetched, right, air etched.

fact that the tubes distort and conform to the contour of the crucible wall is evidence that incipient melting has occurred. However, this is not a useful melting point as the material cannot be cast at atmospheric pressure.

Samples of  $\text{Be}_2\text{C}$  powder contained in graphite capsules and heated in argon for 30 min at  $2400^\circ\text{C}$  formed a clinker-like product. Incipient fusion appeared to have taken place. At  $2300^\circ\text{C}$ , some sintering occurred, but no fusion. When similar samples were heated in closed graphite capsules in a vacuum at  $>2100^\circ\text{C}$ ,  $\text{Be}_2\text{C}$  sublimed and condensed as red crystals on the lid ( $2100^\circ\text{C}$ ) of the capsule which was slightly cooler than the bottom of the capsule. This sublimation seems to take place through dissociation of the carbide to its elements and recombination at a favorable temperature. A similar experiment at slightly higher temperature ( $2120^\circ\text{C}$  on the lid) yielded metallic appearing crystals. The metallic appearance was caused by a thin layer of vaporized carbon on the surface of the carbide crystals. It is apparent that, if  $\text{Be}_2\text{C}$  is to be melted, it must be done at high pressures in an inert atmosphere.

### Chemical Analysis

Various lots of  $\text{Be}_2\text{C}$  were analyzed for total and free carbon and soluble beryllium. The percentage of  $\text{Be}_2\text{C}$  was calculated from these figures. A list of the typical chemical analyses appears in Table II. Usually, a mineral balance (free carbon plus  $\text{Be}_2\text{C}$ ) of about 98% was obtained. The rest may be accounted for as  $\text{BeO}$ , as evidenced by the x-ray diffraction analysis and  $\text{Be}(\text{OH})_2$ , small amounts of which form by hydrolysis of  $\text{Be}_2\text{C}$  with atmospheric moisture. Total carbon was determined by combustion of a sample of  $\text{Be}_2\text{C}$  in  $\text{O}_2$  at  $2500^\circ\text{F}$  for 15 min.

Ingot iron was added as a flux for the  $\text{BeO}$ , combustion product, which otherwise tends to protect the carbide from complete oxidation. Carbon was collected as  $\text{CO}_2$  and weighed. The total carbon figure was not always reliable because, even with the precautions taken, the analyses appear low and often did not agree with the calculated  $\text{Be}_2\text{C}$ .

Soluble beryllium was determined by hydrolyzing  $\text{Be}_2\text{C}$  in 2.5N HCl near the boiling point until hydrocarbon evolution, as evidenced by bubble formation, ceased. Free carbon was filtered off and determined by combustion as above.

The free-carbon analyses appear reliable. Microscopic estimates of carbon are sometimes low. This is probably caused in part by the presence of colloidal carbon within the  $\text{Be}_2\text{C}$  crystals. This is measured by chemical means, but not by the microscope. For the soluble-beryllium analysis, it was assumed that the  $\text{BeO}$ , which was highly fired during production of the  $\text{Be}_2\text{C}$ , was insoluble. The presence of unreacted beryllium was ruled out because of the high vapor pressure (about 0.4 cm Hg) at the minimum reaction temperature,  $1700^\circ\text{C}$ . The only other soluble beryllium compound likely to be present was  $\text{Be}(\text{OH})_2$ . In our early work, no analysis was made for  $\text{H}_2\text{O}$ .

TABLE II. Analytical data on beryllium carbide

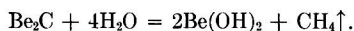
Lot No.	Petrographic Analysis*				Chemical analysis				X-ray diffraction analysis		
	Adjusted wt, % mineral composition after applying ratio factors				Total carbon (C), %	Free, uncombined carbon (C), %	Soluble beryllium compound ( $\text{Be}$ ), %	Calculated beryllium carbide ( $\text{Be}_2\text{C}$ ), %			
	Beryllium carbide ( $\text{Be}_2\text{C}$ )	Carbon (C)	Beryllium oxide ( $\text{BeO}$ )	Beryllium hydroxide [ $\text{Be}(\text{OH})_2$ ]					( $\text{Be}_2\text{C}$ )	( $\text{BeO}$ )	(C)
1	91.5	7.5	Trace†	None	44.8	9.6	53.1	88.5	S	VVF	MF
2	92.4	5.6	None	Trace†	45.3	10.2	53.6	89.4	VS	VVF	M
3	—	14.1	—	—	41.0	11.5	51.7	86.1	S	VF	MS
4	73.4	21.9	1.2	3.8	50.4	23.2	43.8	72.7	S	VF	VS
5	88.0	9.7	0.6	1.8	37.5	5.0	56.0	93.4	VVS	MF	S
6	—	9.1	—	—	39.2	9.0	52.8	87.9	VS	—	M
7	—	7.8	—	—	39.0	11.6	51.5	85.8	M	—	M
8	—	4.9	—	—	39.6	7.5	55.1	91.8	VS	MF	M

\* Two lots analyzed for beryllium silicate ( $2\text{BeO}\cdot\text{SiO}_2$ ) showed none in one case and a trace to  $<1\%$  in the other instance.

† Less than 1%, but visible.

and all soluble beryllium was assumed to be  $\text{Be}_2\text{C}$ . Later it was found that about 1%  $\text{H}_2\text{O}$  was picked up during handling even though the material was stored in tightly sealed containers immediately after being produced. Assuming that 1%  $\text{H}_2\text{O}$  is present as  $\text{BeO}\cdot\text{H}_2\text{O}$  (2.389%), then the  $\text{Be}_2\text{C}$  value is 0.833% high and the total assay 1.556% low. Thus, the  $\text{BeO}$  shown to be present by x-ray diffraction and the small amount of  $\text{Be}(\text{OH})_2$  which is probably present in all samples account for the difference between the total of the free carbon and  $\text{Be}_2\text{C}$  and 100%.

As indicated above,  $\text{Be}_2\text{C}$  has a strong tendency to hydrolyze. This reaction takes place according to the following reaction:



Hydrolysis has been particularly noticeable in connection with vermiculate (high temperature) carbide. Hard clinker-like lumps of this material, which were very difficult to break when first made, crumbled into small grains after exposure to air for one or two weeks. Samples of the clinker mounted in Bakelite hydrolyzed after several days in air and swelled to such an extent that the plastic was cracked into several pieces. Typical lots of -30 mesh  $\text{Be}_2\text{C}$ , as made and stored in covered fruit jars for several days, analyzed 1.0 weight %  $\text{H}_2\text{O}$ . A sample of  $\text{Be}_2\text{C}$  crystals (Fig. 2A), when extracted from Be metal with dilute  $\text{HCl}$ , washed with  $\text{H}_2\text{O}$ , and dried with ether, analyzed 6.5%  $\text{H}_2\text{O}$ . Hydrolysis appears unavoidable in this process. A sample of vermiculate material, which had hydrolyzed in air, was analyzed in the hydrolyzed condition and after drying at various temperatures. Before drying, it contained 4.2%  $\text{H}_2\text{O}$ ; drying at  $100^\circ\text{C}$  for 1 hr reduced this but slightly to 3.7%. Even drying at  $400^\circ\text{C}$  for 1 hr left appreciable  $\text{H}_2\text{O}$ , 0.71%. When the  $400^\circ\text{C}$  treatment was followed by an hour at  $650^\circ\text{C}$ , the  $\text{H}_2\text{O}$  fell to 0.20%. An additional hour at  $800^\circ\text{C}$  practically completed the drying, leaving only 0.09%  $\text{H}_2\text{O}$ . The  $\text{H}_2\text{O}$  analysis was made by collecting the  $\text{H}_2\text{O}$  evolved when  $\text{Be}_2\text{C}$  was heated at  $1000^\circ\text{C}$  for 15 min in a slow stream of dry oxygen.

It appears that certain porosity of beryllium castings, made in previously used graphite molds, may be attributed to hydrogen from hydrolysis products of  $\text{Be}_2\text{C}$ .  $\text{Be}_2\text{C}$  formed on the surface of the mold by previous castings may hydrolyze and, in spite of preheating to  $600^\circ\text{F}$  ( $316^\circ\text{C}$ ), may retain sufficient moisture to cause porosity. Preheating to at least  $1000^\circ\text{C}$  is recommended. After drying, the mold may, of course, be cooled to a lower temperature for use.

Chemical analysis of pressed bodies of  $\text{Be}_2\text{C}$  heated

in nitrogen at  $1100^\circ\text{C}$  showed an increase of nitrogen content (x-ray diffraction analysis showed the presence of  $\text{Be}_3\text{N}_4$ ). At lower temperatures, no nitrogen pickup was noted. Other compacts tended to oxidize when heated in air at  $800^\circ\text{C}$ .

#### *X-Ray Diffraction Analysis*

In general, the x-ray diffraction analyses of the major phases agreed with chemical analyses and with observations made using the microscope. Constituents present in quantities less than 5-10% are often not detectable by x-ray methods. However, in this series of analyses,  $\text{BeO}$  as low as 1% was detected.  $\text{Be}(\text{OH})_2$  was found in nearly all the samples examined by x-ray diffraction. This is probably, in part, the result of hydrolysis of the  $\text{Be}_2\text{C}$  during preparation of samples for x-ray analysis. The density of  $\text{Be}_2\text{C}$  determined from lattice parameter measurements agrees with the value  $d = 2.44$ , as reported by Stackelberg (4).

#### MICROSCOPY OF BERYLLIUM CARBIDE

The various phases present in the usual "as made" material were identified under a petrographic microscope and percentage estimates made by area measurement. An attempt was made to convert area measurements to weight percentages by use of conversion factors based on the apparent density of the constituents. The minimum, maximum, and average size of the carbide crystals were determined, and the physical nature of crystals of typical lots were assigned on the basis of crystal-size measurement. Results of microscopical examination, chemical analyses, and x-ray diffraction analysis are summarized in Table II. The agreement of the results by the three methods is self-evident.

#### *Identification of Phases*

Beryllium carbide does not occur in nature because of its strong tendency to hydrolyze. No optical data on beryllium carbide were found in the literature. It was found to crystallize in the isometric system and to exhibit an amber color in either reflected or transmitted light. The color in reflected light tends to be somewhat more red; whereas, in transmitted light the color is slightly more brown. Examined in plane polarized, transmitted light, the crystals are translucent. They are isotropic and so appear dark in polarized light between crossed nicols. A typical lot of coarsely crystalline  $\text{Be}_2\text{C}$ , produced from the metal-carbon reaction, is readily crumbled to minus 30-mesh grain size in the hand. The individual particles thus produced are, in certain cases to a large extent, single crystals.

Because  $\text{Be}_2\text{C}$  crystallizes in the isometric system,

it has only one index of refraction value. Through use of fused solid melts containing mixtures of selenium and sulfur, the average index of refraction of crystalline  $\text{Be}_2\text{C}$  was found to be  $N = 2.64_{\pm 0.01}$ . White light was employed for making index of refraction measurements because monochromatic yellow, sodium vapor light was absorbed within the dark-red embedding medium. Therefore, the refractive index measurements were made by means of the red wave band portion of the transmitted white light.

In addition to the carbide phase, the usual lot of "as made" beryllium carbide may contain free carbon, free beryllium metal,  $\text{BeO}$ , and  $\text{Be}(\text{OH})_2$ . It was not found possible to distinguish between beryllium metal and the black, opaque carbon particles. It may be possible that this could be done by some technique, such as mounting the material in clear plastic and examining polished sections under reflected light. However, if free metal occurred in the usual product, it must have been very minor compared to free carbon, as evidenced by x-ray examination data.

Area measurements of free carbon, including graphite flakes in the  $\text{Be}_2\text{C}$  matrix, were made. In order to convert these measurements to weight percentages for comparison purposes, a conversion factor for carbon was first determined. Comparison of microscopical area measurements and chemical free-carbon analyses of 30 samples of the product of the metal-carbon reaction indicated that, if the percentage of carbon by area measurement were divided by 1.6 to convert area percentage to weight percentage, satisfactory agreement between microscopical and chemical methods would be obtained. Having assigned a weight percentage value to carbon by this means, the area measurements of  $\text{Be}_2\text{C}$  and  $\text{Be}(\text{OH})_2$  were converted to weight percentage on the basis of their relative densities. Carbon could not be corrected on the basis of density alone because it is evidently present as porous, bulky particles of low apparent density. The carbon of materials from the high-temperature  $\text{BeO}$ -carbon reaction was even bulkier than that of the metal-carbon reaction and required use of a conversion factor of 3.0. A possible explanation of the difference is that the carbon of the metal-carbon reaction product is unreacted and may be considered as rough spheres comparable to the shape of the  $\text{Be}_2\text{C}$  particles, while the carbon in the  $\text{BeO}$ -carbon reaction product, which is present principally in the form of thin graphite flakes within the  $\text{Be}_2\text{C}$  matrix, retains some of its flaky nature even when ground to  $<10 \mu$  and so covers a greater area than an equal weight of spherical particles.

$\text{BeO}$  was occasionally present as prismatic crystals that were birefringent in polarized light between

crossed nicols. It apparently formed in the cooler regions of the charge because of incomplete shielding by the argon atmosphere.

Some carbide products appeared more subject to hydrolysis than others. In the typical hydrolyzed material,  $\text{Be}(\text{OH})_2$  completely enveloped the  $\text{Be}_2\text{C}$  crystals. The hydroxide appeared to possess a crypto-crystalline, fibrous structure that was birefringent in polarized light between crossed nicols.

#### *Crystallography of Beryllium Carbide*

Crystallographic properties of  $\text{Be}_2\text{C}$  appear to resemble closely those of fluorite ( $\text{CaF}_2$ ). Euhedral ( $\text{Be}_2\text{C}$ ) occurs as octahedrons, dodecahedrons, tetrahedrons, or as truncated octahedrons containing the usual 8 octahedral faces plus 6 "cubic" pinacoid faces, adding up to 14 faces in the completed form. Twinning of the truncated octahedrons can occur parallel to the cubic pinacoid face to form "accordion-like" structures. The crystalline phase of  $\text{Be}_2\text{C}$  exhibited perfect octahedral cleavage along four directions. Twinning of  $\text{Be}_2\text{C}$  occurred only in high-temperature, coarsely crystalline products. Threelings were the highest order of twinning observed to date, although fourlings are possible if all conditions for stable crystal twinning symmetry were satisfied. The threelings were joined together through two  $45^\circ$ -angle bends. Simple, contact-twin crystals of the Carlsbad or Siamese twin type were observed, as well as twolings composed of two crystals joined together at a  $45^\circ$  angle. Crystals also tended to form an open link-chain-type of structure composed of from 5–25 euhedral or subhedral crystals that adhere together in a continuous, irregular chain. Also, a closed-chain type of structure occasionally occurred in which individual crystals formed densely packed, parallel rows, having the appearance of a beaded fabric. Both porous and very dense nonporous chain-type structures were observed.

Other crystal structures include the individual euhedral and subhedral crystals mentioned previously and coarsely crystalline intergranular aggregates of these crystals. In addition, there is the microcrystalline "grape cluster" or nodular type of crystal aggregate that predominates in beryllium carbide produced by the metal-carbon reaction at relatively low reaction temperatures ( $1700^\circ\text{C}$ ). The grape clusters are composed of anhedral and subhedral crystals which form dense and nonporous aggregates.

#### *Colored Photographs of Beryllium Carbide*

Because of the difficulty of accurately describing in words the colors of beryllium carbide particles, a technique was worked out by which the appearance of several representative lots of  $\text{Be}_2\text{C}$  were recorded

in natural color on Ektochrome transparencies. A sample of the material was suspended in a cianthien red Y dye solution in nitrobenzene on a glass slide. Limited transmitted light produced a light brown background. Peripheral lighting from small fluorescent tubes illuminated the translucent Be<sub>2</sub>C grains. Exposures were made with a Bausch & Lomb research metallograph, each exposure requiring approximately 45 min. In the colored transparencies, one can distinguish among translucent, amber Be<sub>2</sub>C, the black opaque unreacted carbon, and precipitated flakes of graphite occurring within the Be<sub>2</sub>C crystals. Occasional grains of Be<sub>2</sub>C exhibited an olive green color, possibly caused by the presence of precipitated colloidal carbon. In other Be<sub>2</sub>C grains, the greenish color may be caused by the thinness of section.

#### HARDNESS MEASUREMENTS

Coarse crystals of Be<sub>2</sub>C were mounted in Lucite and polished. Knoop hardness numbers were then taken by means of a Tukon hardness tester. When a 100-gram load was used, crystals shattered or chipped away at the impression. Satisfactory readings were taken with lighter loads. Readings of 2678, 2520, and 2613 were obtained with a 50-gram load, and 2740 with a 25-gram load. It appears that the hardness of Be<sub>2</sub>C is greater than that of silicon carbide and approaches the hardness of boron carbide.

#### CONCLUSIONS

Be<sub>2</sub>C may be made by several methods, principal of which are the BeO-carbon and the Be-metal-carbon reactions. The metal-carbon reaction appears better when controlled crystal size is desired. The

true translucent amber color of Be<sub>2</sub>C is revealed only under the microscope. As a refractory, it has several disadvantages. It tends to hydrolyze even in atmospheric moisture. In heating, Be<sub>2</sub>C must be protected against both oxygen and nitrogen. It decomposes at about 2150°C with vaporization of the beryllium which reunites with carbon in cooler regions, or with oxygen or nitrogen, if present. Be<sub>2</sub>C has no useful melting point at atmospheric pressure.

#### ACKNOWLEDGMENT

This work was performed at Battelle Memorial Institute under the sponsorship of the Nepa Division of the Fairchild Engine and Airplane Corporation.

Any discussion of this paper will appear in a Discussion Section to be published in the December 1954 issue of the JOURNAL.

#### REFERENCES

1. P. LEBEAU, *Compt. rend.*, **121**, 496 (1895); *J. Soc. Chem. Ind.*, **15**, 141 (1895); *J. Chem. Soc.*, **70**, 169 (1895).
2. L. HENRY, *J. Chem. Soc.*, **70**, 169 (1895).
3. P. LEBEAU, *J. Phys. Chem.*, **4**, 222 (1899); *J. Chem. Soc.*, **76**, 554 (1899); *Z. Kryst.*, **34**, 629 (1899); also see: C. L. PARSONS, "Chemistry and Literature of Beryllium," The Chemical Publishing Co., New York (1909); J. N. FRIEND, "Textbook of Inorganic Chemistry," Vol. III, Pt. II, pp. 27-28, Charles Griffin & Co., Ltd., London (1926); J. W. MELLOR, "Treatise of Inorganic and Theoretical Chemistry," Vol. 5, p. 866, Longmans, Green and Company, London (1924).
4. M. V. STACKELBERG AND F. QUATRAM, *Z. physik. Chem.*, **27**, 50 (1934).
5. R. F. GELLER, *Nucleonics*, **7** (1950).
6. J. H. COOBS AND W. J. KOSHUBA, *This Journal*, **99**, 115 (1952).
7. M. GALLAGHER, *J. Southern Research*, **3**, No. 4, 14 (1951).
8. H. A. SLOMAN, *J. Inst. Metals*, **49**, No. 2, 365 (1932).

# Ionic Mass Transfer and Concentration Polarization at Rotating Electrodes<sup>1</sup>

M. EISENBERG,<sup>2</sup> C. W. TOBIAS, AND C. R. WILKE

*Department of Chemistry and Chemical Engineering, University of California, Berkeley, California*

## ABSTRACT

Rates of ionic mass transfer at nickel electrodes rotating about their axes in the center of stationary electrodes were studied using the ferri-ferrocyanide couple in alkaline solutions. A general mass transfer correlation was found to apply equally well to dissolution rates of rotating solids and to rates of ionic mass transfer at rotating electrodes. This correlation takes into account physical properties of the system as well as geometric and hydrodynamic factors. The correlation allows prediction of limiting currents and concentration polarization at rotating electrodes under a wide range of conditions.

The nature of polarization involved in reduction of  $\text{Fe}(\text{CN})_6^{-3}$  and oxidation of  $\text{Fe}(\text{CN})_6^{-4}$  was also investigated. Polarization was found to depend strongly on the presence of electrode poisons. With freshly prepared solutions, under exclusion of light, and with cathodically treated nickel electrodes, relatively small chemical polarizations were determined. For rotational speeds not exceeding Reynolds number 11,000, chemical polarization was found to be negligible in comparison with concentration polarization. Under such conditions, the ferro-ferricyanide couple can be conveniently used to obtain mass transfer rates for various hydrodynamic conditions, or conversely, to verify the validity of mass transfer equations by a comparison of experimental and calculated values of limiting currents and concentration polarization.

The rotating electrode model was found to be most suitable for studying the nature of electrolytic polarization phenomena because of uniformity of the current distribution and the hydrodynamic diffusion layer at the electrode surface.

## INTRODUCTION

Study of mass transfer at working electrodes is of fundamental importance (1, 2) in analysis of electrode phenomena and in consideration of concentration polarization, limiting currents, and rates of electrode reactions. Several typical cases have been analyzed by the methods of hydrodynamics and boundary layer theory, and for a few models, experimental results were successfully correlated (1, 2). The effect of natural convection in electrolysis was quantitatively evaluated by Wagner (3) and Wilke and coworkers (4) among others. Rotating disk electrodes were treated mathematically by Levich (5). This theory applies if the diffusion boundary layer at the disk is laminar. Along the lines suggested by Agar (6), Lin and coworkers (7) correlated limiting current densities for the inner electrode of an annular cell with streamline and turbulent longitudinal flow. An extension of this study for laminar and turbulent flow along flat plate electrodes was recently reported (8).

The present investigation is concerned with cylindrical central electrodes rotating in concentric

cylindrical cells. Among many possible methods of stirring, the case of a rotating electrode is noteworthy, not only because it affords experimental reproducibility, but also because it permits application of methods of hydrodynamics and mass momentum transfer analogy in interpretation and correlation of data (9-11). Theoretical analysis of this problem for electrodes is further facilitated by uniformity of current distribution resulting from the geometry of concentric cylindrical electrodes and uniform thickness of the diffusion layer formed on the rotating electrode.

Recently, rotated electrode surfaces have been used in chemical analysis and in corrosion studies in parallel with polarographic methods (12, 13). Industrial applications of this forced convection model are known, and further important uses are anticipated.

The effect of speed of rotation upon rate of mass transfer was first studied by Brunner (14, 15). He found that the diffusion layer thickness,  $\delta$ ,<sup>3</sup> decreases with the  $\frac{2}{3}$  power of the speed. However, he considered neither the effect of rotor diameter nor the dependence on physical properties of the electrolyte. Therefore, only qualitative conclusions can be drawn from these experimental results.

<sup>3</sup> A table of nomenclature is collected at the end of this paper.

<sup>1</sup> Manuscript received December 16, 1953. This paper was prepared for delivery at the Chicago Meeting, May 2 to 6, 1954.

<sup>2</sup> Present address: Stanford Research Institute, Stanford, California.



Eucken (16) analyzed the effect of laminar flow forced convection upon rate of mass transfer at an electrode. In his experiments the external vessel containing the solution was rotated, and laminar flow past the fixed inner flat plate electrode resulted. Eucken's mathematical analysis is valid only for this particular condition. Kambara and coworkers (17) adapted Eucken's treatment to a 0.5-mm diameter platinum wire electrode projecting perpendicularly 6 mm from the axis of a rotating glass rod. In the derivation, it is assumed that the velocity gradient at the electrode surface is proportional to rpm. This is valid for Eucken's model, where laminar flow exists in the entire region of flow, but is inadmissible for the turbulent flow case, where laminar flow is restricted to the boundary layer adjacent to the electrode surface.

For the sake of clarity, the term "rotating electrode" is used henceforth only in reference to cylindrical electrodes rotating about their axes in the center of stationary, circular, cylindrical electrodes. Recently, Roald and Beck (18) used such rotating electrodes in a study of dissolution rates of magnesium and its alloys in hydrochloric acid solutions. They found that rates of dissolution increase in low acid concentrations with the 0.71 power of the speed of rotation. At higher acid concentrations (1.4*M* and higher), the reaction rates become entirely independent of rotational speeds, as the stirring effect produced by hydrogen bubbles evolving at the metal interface becomes predominant. This stirring effect, however, should not be ignored even at low acid concentrations because of turbulence caused by hydrogen bubbles moving in the boundary layer adjacent to the dissolving magnesium rod. For this reason the work of Roald and Beck represents a rather special case of forced convection mass transfer.

In studies of dissolution and corrosion rates of rotated metal rods, King and coworkers (19-22) estimated the mass transfer coefficients employing King and Shack's earlier experimental finding (23), according to which "normal diffusion (or transport) control requires that rates be linear with peripheral speed above about 5000 cm/min" (22). King and Cathcart (24) indicated that the mass transfer coefficient is directly proportional to the 0.7 power of the diffusion coefficient of the reacting ionic species.

The effect of cylinder diameter, speed of rotation, diffusion coefficient, and viscosity on mass transfer rates has not been successfully incorporated into a single correlation, although the usefulness of the Chilton-Colburn analogy for correlating the pertinent variables was realized by King and coworkers in 1937 (25).

The present work was undertaken with the follow-

ing aims in mind: (a) to establish correlations between physical properties of a system, geometrical and hydrodynamic conditions, and rates at which a solute (ion) is transferred to or from a rotating electrode; (b) to determine whether such general mass transfer correlations enable prediction of concentration polarization and limiting currents in steady state electrolysis.

#### EXPERIMENTAL

To assure the latter objective it was important to choose an electrode reaction which occurs with negligible chemical polarization. For such an electrode process the total measured polarization ( $\Delta E_T$ )<sup>3</sup> would represent concentration polarization ( $\Delta E_{\text{conc}}$ ) only, and would make a comparison between theoretical prediction and experiment possible. However, most of the known electrode reactions take place with considerable chemical polarization ( $\Delta E_{\text{chem}}$ ) when finite currents are passed. Some oxidation-reduction reactions have long been suggested by investigators (26-28) to occur with negligible chemical polarization. Recently, Moll (29) found no measurable chemical polarization for the ferrous-ferric couple at gold and platinum electrodes freshly treated by hydrogen and oxygen discharge. Essin and coworkers (30) made similar studies on the ferrocyanide-ferricyanide couple at platinum and nickel electrodes and concluded that there is no appreciable chemical polarization "when the metal is free of all film that may form on the surface." In contrast, Carmody and Rohan (31) reported a measurable chemical polarization for this latter system on platinum. A similar conclusion was arrived at by Petrocelli and Paolucci (32) who studied this couple up to current densities of 25 ma/cm<sup>2</sup>. They found, however, that "cathodic activation," i.e., a hydrogen discharge treatment of the electrode, tends to decrease chemical polarization.

For the purposes of this study, smoothness of the electrode surface was important because of hydrodynamic considerations. In a redox electrolysis, unlike in a metal deposition process, the electrode surface remains physically unaltered. Another advantage of the redox reaction is that steady-state electrode potentials are attained in much shorter time than in a deposition reaction.

These findings, in addition to stability considerations of several contemplated couples, resulted in selection of the ferricyanide-ferrocyanide couple and nickel electrodes for the present studies. A large excess of sodium hydroxide was used in order to eliminate the contribution of ionic migration to mass transfer (1).

Solutions of potassium ferri- and ferrocyanide,

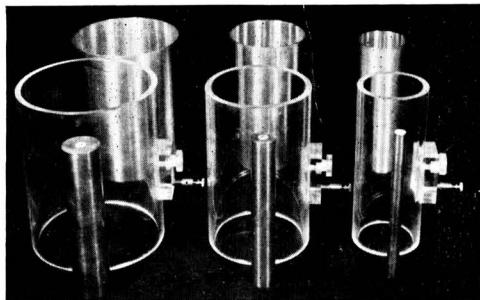
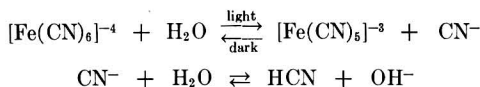


FIG. 1. Lucite cylinders, outer and inner nickel electrodes.

and particularly the ferrocyanide, are known to decompose slowly in light, resulting in formation of cyanide and hydroxide ions according to the following equations (33, 34):



In alkaline solutions kept in darkness, decomposition of these cyanide complexes is practically eliminated (35). Solutions used in these studies were freshly prepared for each series of runs in black Jena glass bottles.

#### Apparatus and Procedure

A concentric cylindrical cell, 6.16 in. high, built from acrylic plastic (Lucite), was equipped with grooved endplates which could hold as desired one of three cylindrical plastic tubes of 2.48, 4.00, 5.47 in. ID (Fig. 1 and 2). A  $\frac{1}{2}$ -in. diameter stainless steel driving shaft passing through a teflon packing gland in the top plate was equipped with a  $\frac{1}{4}$ -in. standard thread allowing nickel electrodes of 1.273, 2.48, and 5.024 cm diameter to be screwed onto it. The rotated electrode was supported from below by a guide pin and teflon lining in order to eliminate eccentric motion. Concentric outer cylindrical nickel electrodes of 6.07, 9.87, and 13.69 cm ID, all

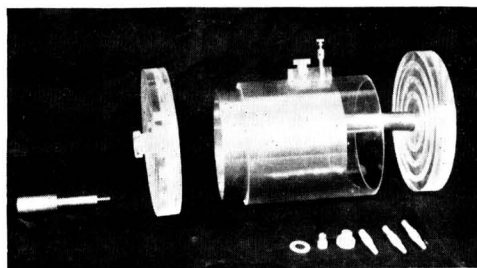


FIG. 2. Components of the cell

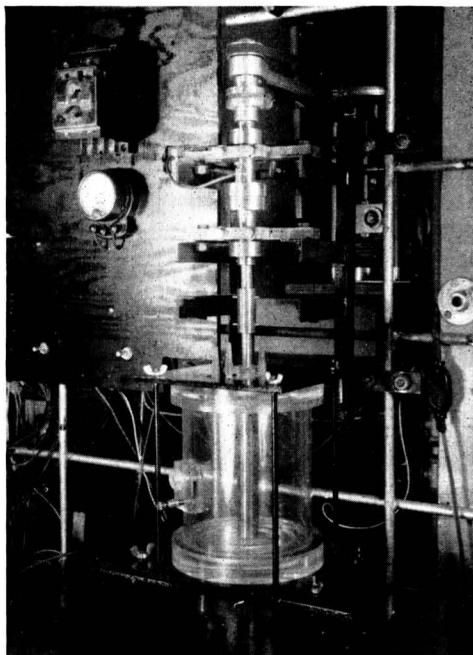


FIG. 3. Cell with supporting structure. (Outer electrode removed.)

15.11 cm long, were fitted tightly into corresponding Lucite tubes (Fig. 1 and 2). The cell was made liquid tight with neoprene rubber joint gaskets in the grooves. A ground glass joint thermometer fitted into the top plate with its bulb reaching about  $\frac{3}{4}$  in. into the cell. The assembled cell with supporting structure designed to eliminate vibrations is shown in Fig. 3.

Electrodes permitted a variation of the ratio of gap to the diameter of the inner electrode ranging from 0.104 to 4.88. A Lucite nipple on the top

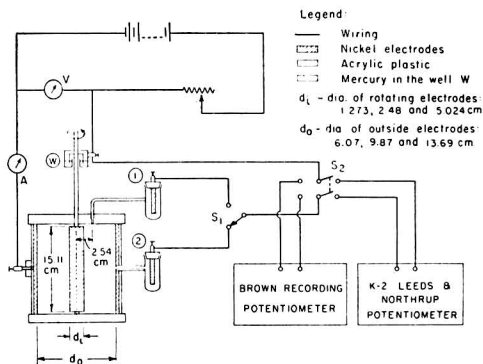


FIG. 4. Schematic diagram of the electrolyzing and measuring circuits used with the cell for rotating electrodes.

plate of the assembled cell was screwed into a small tapered hole which ended with a  $\frac{1}{4}$  mm diameter on the inside of the plate and was located 2.541 cm from the cell axis (Fig. 4). Through this hole and a piece of polyethylene tubing, a continuous liquid junction led to reference cell No. 1 equipped with a nickel electrode and filled with the same solution as that in the electrolytic cell. Reference cell No. 2 was connected with the cell by means of a teflon nipple ( $\frac{1}{4}$ -in. OD) leading through the center of the Lucite cylinder and ending flush with the inner surface of the outside electrode. Such arrangements of the liquid junction leading to reference electrodes are preferable for two reasons: (a) the flow pattern in the cell remains undisturbed, and (b) a distortion of current distribution over the electrode surface is avoided.

As can be seen from the diagram in Fig. 4, a potential measurement of the rotating electrode by means of reference electrode No. 1 involved an ohmic potential drop over the annular solution space between the radius of the rotating electrode and the distance of 2.54 cm at which the small opening leading to that reference cell was located. For a total current,  $i$ , this ohmic drop was therefore

$$iR_{(1)} = \frac{i}{2\pi\kappa h'} \ln \frac{2.54}{r_i} \quad (\text{Ia})$$

where  $R_{(1)}$  = resistance, ohms;  $r_i$  = radius of rotated inner electrode, cm;  $h'$  = height of cell, here 15.11 cm;  $\kappa$  = conductivity of solution,  $\text{ohm}^{-1} \text{cm}^{-1}$ .

Similarly a potential measurement of the rotated electrode by means of reference No. 2 involved an ohmic drop given by:

$$iR_{(2)} = \frac{i}{2\pi\kappa h'} \ln \frac{r_o}{r_i} \quad (\text{Ib})$$

Since  $r_o$ , internal radius of the outer electrode, was either 6.84, 4.94, or 3.035 cm, respectively, for series of runs I, II, and III, the ohmic drop could be computed more reliably by equation (Ib), i.e., using reference No. 2. This is particularly true since a small geometrical misalignment will cause a lesser relative error in the ratio  $r_o/r_i$  of equation (Ib).

In all runs, potential measurements of the rotating electrode were taken by means of both reference junctions selected one at a time with switch S-1 (Fig. 4). Net values obtained after subtracting  $iR_{(1)}$  and  $iR_{(2)}$  drops, respectively, rarely differed by more than 1%. However, for reasons stated above, in most cases measurements with reference electrode No. 2 were preferred over an arithmetic average of the two measurements.

Electrical connection to the rotating electrode

was accomplished by means of a mercury well (W in Fig. 4). A copper contact screw provided the connection to the outer stationary electrode. Current was measured with a d-c milliammeter<sup>4</sup> or a d-c ammeter.<sup>5</sup> All ammeters were carefully calibrated by means of standard resistors. Selector switch S-2 (Fig. 4) permitted measurements of potential by either (a) recording potentiometer<sup>6</sup> with five ranges, the largest being up to 500 mv, or a (b) manual potentiometer,<sup>7</sup> using a high sensitivity galvanometer as zero instrument.<sup>8</sup> The recorder was used first to ascertain whether steady-state polarization was achieved, then the final value was measured accurately by means of the manual potentiometer.

Sodium hydroxide, 2*N*, was used as neutral electrolyte in preparing five approximately equimolar potassium ferricyanide and potassium ferrocyanide solutions in the concentration range of 0.009 to 0.204 mole/l. C.P. reagents<sup>9</sup> were used throughout. Slight changes in concentrations of ferri- and ferrocyanide ions, caused by use of a solution up to limiting current densities, were followed up by strict analytical control. Ferricyanide was determined by the iodometric procedure (36) and ferrocyanide by permanganate titration (37).

Before introduction into the cell, each solution was alternately deaerated in a glass column by means of vacuum, and saturated with nitrogen several times to remove dissolved oxygen. Presence of a considerable amount of dissolved oxygen in the cell would have interfered with electrode reactions of ferricyanide and ferrocyanide, particularly at low concentrations. Furthermore, it was felt that, in absence of oxygen, nickel electrodes would remain in an "active" state longer.

Prior to each assembling of the cell, smooth electrodes were polished with rouge paper, washed with  $\text{CCl}_4$ , and treated cathodically in a 5% NaOH solution at a current density of 20 ma/cm<sup>2</sup> for 12–15 min.

The assembled cell was filled with a given solution at approximately 25°C, the inner electrode set into rotation at a selected speed. Value of the electrode potential at no current flow (ZCP) was measured with both references. These were later subtracted (with proper sign) from the "at current" values. Thus any "static" potential differences due to variations in surface structure of the electrodes could be accounted for. A relatively small current was applied, and the potential of the rotating elec-

<sup>4</sup> Weston (Model 45).

<sup>5</sup> Cenco (Model 6935).

<sup>6</sup> Minneapolis Honeywell Company (Model Y-153-X-12).

<sup>7</sup> Leeds and Northrup, Type K-2 (Model No. 7552).

<sup>8</sup> Leeds and Northrup (No. 2430).

<sup>9</sup> Merck and Company.

trode followed with a reference electrode and recording potentiometer until steady state was achieved. Final values were then measured with the manual potentiometer, using both reference electrodes consecutively. Steady-state polarization was obtained in a few seconds at high speeds and within 2-3 min at low speeds. Achievement of the steady state, while not essential for determination of limiting currents, was important for subsequent calculations of chemical polarization. A reliable comparison of concentration and chemical polarization can be made only under steady-state conditions. Current was increased in small increments until the limiting current, noted by a sudden rise in potential, was attained. At a given speed each run was first completed with the rotor as cathode. Then polarity was reversed and a run was carried out with the rotor as anode. When a series of runs with speeds ranging from 30 to 1650 rpm was complete, the cell was taken apart, the electrodes treated as described previously, and reassembled with another electrode diameter but with the same inner electrode. Thus the effect of the gap between concentric cylindrical electrodes was studied for a given solution, given diameter of rotating electrode, and given angular velocity. The temperature of  $25^{\circ}\text{C} \pm 0.3$  was maintained by blowing preheated or precooled air on the cell exterior. Physical properties required for correlative study were determined for each solution within the range  $20^{\circ}$ - $30^{\circ}\text{C}$ .

Conductivities were measured in a conventional conductivity cell, calibrated with 0.9996*M* KCl solution, using an audiooscillator<sup>10</sup> as power source for 1000 cycle A.C., a Wheatstone bridge, and an oscilloscope<sup>11</sup> as zero instrument.

Viscosities of solutions relative to water were measured at several temperatures in a thermostat with an Ubbelohde pipette, and absolute viscosities calculated using densities obtained by pycnometer determinations.

Diffusion coefficients for ferri-ferrocyanide ions were measured by the capillary method (38).

#### Methods of Calculation

*Ionic mass transfer.*—Potential values obtained for each run were first corrected by subtracting (with proper sign) the ZCP differences and the corresponding  $iR$  drops calculated by means of equation (1). These net resulting values represented  $\Delta E_T$ . From the known areas of rotating electrodes, current densities were calculated, and plots of current density,  $I$  (ma/cm<sup>2</sup>) vs.  $\Delta E_T$  (mv) were prepared. Limiting current densities were then determined for each run at the plateau of the curve. At this

point, in case of cathodic ferricyanide reduction runs, the consecutive electrode process was hydrogen evolution. This, however, did not take place before the potentials exceeded 600-700 mv. For anodic oxidation of ferrocyanide the plateau was shorter as the consecutive reaction (oxygen evolution) took place at  $\Delta E_T$  values of 200-250 mv. As illustrations, Fig. 5 and 6 show sets of cathodic and corresponding anodic runs for solution No. 9 at speeds up to 1650 rpm. The limiting cathodic current densities ( $I_c$ ) and the limiting anodic current densities ( $I_a$ ) are given in the corresponding figures.

At limiting current when interfacial concentration of reacting species becomes zero, the rate of ionic mass transfer of ferricyanide ion to the cathode or of ferrocyanide ion to the anode can be expressed as (1):

$$N = \frac{I_L}{nF} (1 - t_i) = k_L c_o \quad (II)$$

where  $I_L$  = cathodic ( $I_c$ ) or anodic ( $I_a$ ) limiting current densities, amp/cm<sup>2</sup>;  $n$  = valence change of reacting ion;  $F$  = the Faraday constant;  $c_o$  = bulk concentration of reacting ion, moles/cc;  $t_i$  = transference number of the reacting ion;  $k_L$  = average mass transfer coefficient, cm/sec. Since the estimated transference numbers of ferri- and ferrocyanide ions did not exceed 0.03 (and was usually much lower) due to excess NaOH used as the indifferent electrolyte, equation (II) can be rewritten as:

$$N = \frac{I_L}{nF} = k_L c_o \quad (IIa)$$

Thus by means of equation (IIa) the average mass transfer coefficient,  $k_c$  for the ferricyanide reduction and  $k_a$  for ferrocyanide oxidation, was calculated for each run.

From the measured values of viscosity,  $\mu$ , density,  $\rho$ , and diffusion coefficients,  $D$ , of ferrous and ferric cyanide, corrected to the temperature of given runs, the corresponding Schmidt groups  $Sc = \mu/\rho D$  were computed for anodic and cathodic experiments.

The Reynolds number, characterizing flow produced in the cell, was found to involve the rotating electrode diameter as the characteristic length dimension and not the gap between cylindrical electrodes (39). Accordingly, the Reynolds number was computed as:

$$R_d = \frac{V \cdot d_i}{\nu} \quad (III)$$

where  $V$  = peripheral velocity, cm/sec; and  $\nu$  = kinematic viscosity, cm<sup>2</sup>/sec.

*Concentration polarization and chemical polarization*

<sup>10</sup> Hewlett-Packard Model 200 C.

<sup>11</sup> RCA No. 155 A.

tion.—It is clear that as far as mass transfer studies are concerned, it is not necessary for the electrode reaction to take place with negligible chemical polarization. The mass transfer coefficient,  $k_L$ , could be calculated for any current density if in addition to the bulk concentration,  $c_o$ , the interfacial concentration,  $c_i$ , were known. Since an accurate experimental determination of  $c_i$  is extremely difficult, mass transfer coefficients are most conveniently obtained from limiting current measurements, as outlined above.

However, an electrode reaction with negligible chemical polarization was desirable in these studies in order to ascertain experimentally whether correct predictions of limiting currents and concentration polarization can be made from a general mass transfer correlation for rotating cylinders.

The ferri-ferrocyanide couple was therefore investigated as to the nature of polarization associated with both cathodic reduction of ferricyanide and anodic oxidation of ferrocyanide on nickel electrodes. This was done as follows.

(A) From graphs of  $I$  vs.  $\Delta E_T$  (of the type shown in Fig. 6 and 7), values of  $I$  and  $\Delta E_T$  were read off at equal current density increments and tabulated

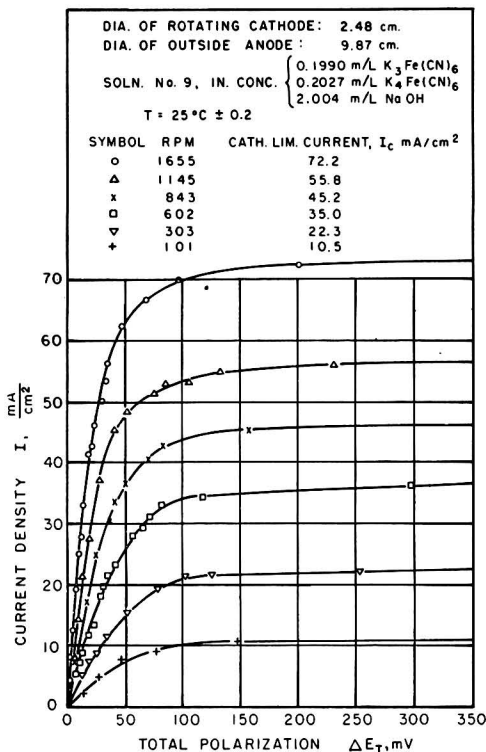


FIG. 5. Cathodic polarization curves of ferricyanide ion reduction.

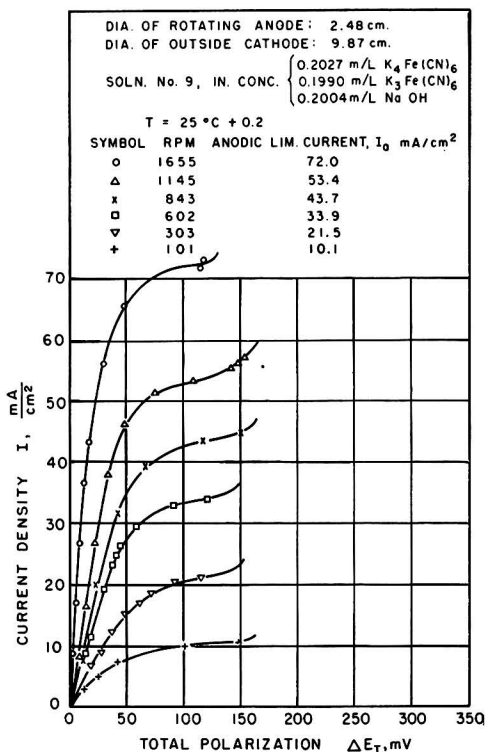


FIG. 6. Anodic polarization curves of ferrocyanide ion oxidation.

up to current densities equal to 70–75% of limiting current density.

(B) Using  $I_c$ , and  $I_a$  (both obtained for the same solution, cell geometry and speed),  $\Delta E_{conc}$  for this redox couple was calculated (30, 40) for each current density by the following equations<sup>12</sup>:

$$\Delta E_{conc} = \frac{RT}{nF} \ln \frac{1 - I/I_c}{1 + I/I_a} \quad (\text{for cathodic case}) \quad (IVa)$$

$$\Delta E_{conc} = \frac{RT}{nF} \ln \frac{1 + I/I_c}{1 - I/I_a} \quad (\text{for anodic case}) \quad (IVb)$$

(C)  $\Delta E_{chem}$  at each of the applied current densities was calculated by subtracting the calculated  $\Delta E_{conc}$  from the experimentally obtained  $\Delta E_T$ :

$$\Delta E_{chem} = \Delta E_T - \Delta E_{conc} \quad (V)$$

It is interesting to note that, from equations (IV) and (V) for the case of a redox electrode reaction with negligible chemical polarization, a plot of

<sup>12</sup> Actually the derivation of equation (IVa) assumes that the mass transfer coefficient is independent of current density. In forced convection such an assumption is well justified.

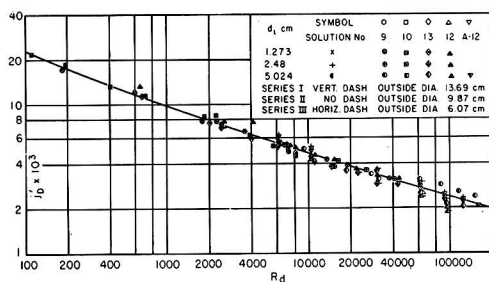


Fig. 7. Cathodic reduction of ferricyanide. Mass transfer at rotating electrodes.

$$j'_D = \frac{k_c}{V} (Sc)^{0.644} \text{ vs. } R_d$$

experimental values of  $\Delta E_T$  versus  $\log Q$ , where

$$Q = \frac{1 \mp I/I_c}{1 \pm I/I_a} \quad (\text{VI})$$

(upper sign for cathodic, lower for anodic case) should yield a straight line with slope  $2.303 RT/nF$ . For the ferri-ferrocyanide couple  $n = 1$ , and expressing potentials in millivolts, the slope for experiments performed at 25°C should be 59.1.

## RESULTS AND DISCUSSION

### Correlation of Mass Transfer Rates

Ionic mass transfer results presented here were part of a broader study involving dissolution of rotating cylinders cast from benzoic and cinnamic acid into water and aqueous glycerol solutions (39). A general type of correlation based on methods of momentum-mass transfer analogy was obtained using the following parameter:

$$j'_D = \frac{k_L}{V} (Sc)^{0.644} \quad (\text{VII})$$

in which  $Sc = \nu/D$  accounts for the physical properties of the system and  $k_L$  is given by equation (IIa).

Fig. 7 and 8 show logarithmic  $j'_D$  vs.  $R_d$  plots of mass transfer data for reduction of ferricyanide and oxidation of ferrocyanide, respectively. Table I gives a typical set of data,<sup>13</sup> including physical properties, for one of five solutions studied. Average deviations of points in Fig. 7 and 8 from the best line are  $\pm 7\%$  and  $\pm 6.6\%$  for the two electrode reactions. These experiments involved a Schmidt number variation of 2230 to 3650 and a Reynolds number range of 112.0–162,000 (peripheral velocities 1.17 to 426 cm/sec). Limiting current densities varied from 0.43 to 113 ma/cm<sup>2</sup>.

<sup>13</sup> Complete data are given in Reference (39).

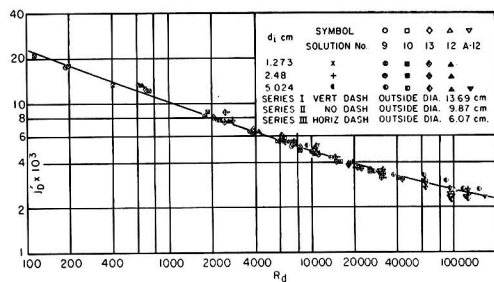


Fig. 8. Anodic oxidation of ferrocyanide. Mass transfer at rotating electrodes.

$$j'_D = \frac{k_a}{V} (Sc)^{0.644} \text{ vs. } R_d$$

In Fig. 9, lines correlating electrolytic data are compared with results obtained by solid dissolution studies. Results for the various systems agree with each other within 7% and all lie within experimental error involved in determination of frictional drag coefficient,  $f/2$ , obtained by Theodorsen and Regier (11).

Such an agreement is very encouraging in view of the Chilton-Colburn analogy (41) which suggests that

$$j_D = \frac{k_L}{V} \phi(Sc) = f/2 \quad (\text{VIII})$$

where  $\phi(Sc)$  represents a function of the Schmidt number. [For a detailed discussion see Reference (39).]

In Fig. 10, all mass transfer data for three solid dissolution systems and the two electrolytic redox reactions were plotted together. The best curve (within  $\pm 8.3\%$ ) through all points is represented by coordinates given in Table II.

In the Reynolds number range 1000–100,000 data are best represented by a straight line (dashed in Fig. 10) given by

$$j'_D = \frac{k_L}{V} Sc^{0.644} = 0.0791 R_d^{-0.30} \quad (\text{IX})$$

From equation (IX) a number of interesting practical relations may be derived.

Recalling that the mass transfer coefficient  $k_L = I_L/nF c_o$ , the following relations for limiting current density may be obtained:

$$\begin{aligned} I_L &= 0.0791 n F c_o V \left( \frac{V d_i}{\nu} \right)^{-0.30} \left( \frac{\nu}{D} \right)^{-0.644} \\ &= 0.0791 n F c_o V^{0.70} d_i^{-0.30} \nu^{-0.344} D^{0.644} \quad (\text{X}) \\ &= n F \frac{D c_o}{\delta} \text{ (amp/cm}^2\text{)} \end{aligned}$$

TABLE I. Mass transfer at rotating electrodes, ferri-ferrocyanide couple. (Sample data).\* Solution No. 9 (2.004N NaOH)

Run No.	V cm/sec	T °C	$\nu \times 10^2$ cm <sup>2</sup> /sec	$R_d$	Cathodic reduction of ferricyanide					Anodic oxidation of ferrocyanide						
					$C_{ferri} \times 10^3$ mole/cc	$I_a$ ma/cm <sup>2</sup>	$k_c \times 10^3$ cm/sec	$D \times 10^5$ cm <sup>2</sup> /sec	Sc	$j_b \times 10^3$	$C_{ferro} \times 10^3$ mole/cc	$I_a$ ma/cm <sup>2</sup>	$k_a \times 10^3$ cm/sec	$D \times 10^5$ cm <sup>2</sup> /sec	Sc	$j_b \times 10^3$
13a. $d_i = 1.273$ cm $A = 61.2$ cm <sup>2</sup> Ser. II ( $d_o = 9.87$ cm)																
—, 276A	114.9	25	1.423	10,280	—	—	—	—	—	0.2030	52.0	265.5	0.390	3,649	4.55	
277C, 278A	81.5	25	1.423	7,291	0.1988	42.2	219.8	0.454	3,134	4.82	0.2020	42.0	214.4	0.390	3,649	5.18
280C, 281A	40.4	25	1.423	3,614	0.1982	28.2	147.3	0.454	3,134	6.51	0.2028	26.0	132.6	0.390	3,649	6.46
284C, 285A	20.0	25	1.423	1,789	0.1976	16.6	87.0	0.454	3,134	7.76	0.2027	16.4	83.9	0.390	3,649	8.27
286C, 287A	6.8	25	1.423	608	0.1971	8.8	46.2	0.454	3,134	12.1	0.2026	8.9	45.4	0.390	3,649	13.1
290C, 291A	2.07	25	1.423	185	0.1961	3.75	19.9	0.454	3,134	17.1	0.2024	3.55	18.2	0.390	3,649	17.3
13b. $d_i = 2.48$ cm $A = 117.6$ cm <sup>2</sup> Ser. II ( $d_o = 9.87$ cm)																
133C, 134A	214.9	25	1.423	37,460	0.1990	72.2	376	0.454	3,134	3.12	0.2027	72.0	368	0.390	3,649	3.37
135C, 136A	148.7	25	1.423	25,920	0.1970	55.8	294	0.454	3,134	3.53	0.2026	53.4	273	0.390	3,649	3.62
137C, 138A	109.5	25	1.423	19,080	0.1960	45.2	239	0.454	3,134	3.89	0.2025	43.7	224	0.390	3,649	4.03
139C, 140A	78.2	25	1.423	13,630	0.1945	35.0	186	0.454	3,134	4.25	0.2024	33.9	174	0.390	3,649	4.37
141C, 142A	39.3	25	1.423	6,850	0.1935	22.3	119	0.454	3,134	5.41	0.2023	21.5	110.1	0.390	3,649	5.51
143C, 144A	13.1	25	1.423	2,283	0.1925	10.5	57	0.454	3,134	7.76	0.2023	10.1	51.8	0.390	3,649	7.77
13c. $d_i = 5.024$ cm $A = 236.4$ cm <sup>2</sup> Ser. II ( $d_o = 9.87$ cm)																
484C, 485A	26.6	25	1.423	9,391	0.1891	13.60	74.5	0.454	3,134	5.00	0.2030	13.80	70.4	0.390	3,649	5.22
486C, 487A	79.7	25	1.423	28,140	0.1904	27.8	151.3	0.454	3,134	3.39	0.2037	27.40	139.4	0.390	3,649	3.44
488C, 489A	172.8	25	1.423	61,010	0.1918	55.6	300.3	0.454	3,134	3.11	0.2044	55.6	281.9	0.390	3,649	3.21
490C, 491A	246.8	25	1.423	87,130	0.1930	73.3	393.8	0.454	3,134	2.84	0.2050	75.0	379.1	0.390	3,649	3.03
492C, 493A	332.8	25	1.423	117,500	0.1969	90.4	475.9	0.454	3,134	2.55	0.2024	87.0	445.4	0.390	3,649	2.64
494C, 495A	426.2	25.7	1.405	152,400	0.1963	109.0	575.6	0.461	3,048	2.37	0.2024	113.0	578.6	0.396	3,548	2.63

$$R_d = \frac{V d_i}{\nu} \quad j'_b = \frac{k_L}{\nu} (Sc)^{0.611}$$

$\delta$  (cm) is then given by:

$$\begin{aligned} \delta &= \frac{1}{0.0791 V^{0.70} d_i^{-0.30} \nu^{-0.344} D^{-0.356}} \\ &= 12.64 \times \frac{d_i^{0.30} \nu^{0.344} D^{0.356}}{V^{0.70}} \quad (XI) \\ &= 99.62 \frac{d_i^{0.40} \nu^{0.344} D^{0.356}}{S^{0.70}} \end{aligned}$$

where  $D$  = diffusion coefficient, cm<sup>2</sup>/sec; and  $S$  = rotational speed, rpm.

Thus,  $\delta$  depends not only on rotational speed, but also on rotor diameter as well as on viscosity and diffusivity. The latter three variables were not considered by Brunner (14).

Assuming  $\delta$  independent of rate (i.e., of the current density), as was suggested by Agar (6), one can write:

$$\frac{I}{nF} = \frac{D}{\delta} (c_o - c_i) \quad (XIIa)$$

\* See footnote (15), p. 315.

Hence for a given applied C.D.,  $c_i$  may be calculated by:

$$c_i = c_o - \frac{I}{nFD} \delta \quad (XIIb)$$

$\delta$  is obtained for a given geometry, speed and physical properties of the electrolyte by equation (XI).

Previous studies relating to mass transfer at rotating electrodes were limited in scope and can be compared to the present work only in respect to functional dependence on rotational speed. Roald and Beck (18) found for rotating magnesium electrodes:

$$k_L = \text{const } V^{0.7} \quad (XIII)$$

This is in agreement with results of the present study since equation (XIII) can be shown to follow from equation (IX) for a given system (constant  $\nu$  and  $Sc$ ) and given rotor diameter. Brunner (14) used rather impractical geometries and poorly defined experimental conditions; his results may be expressed in the form:

$$k_L = \text{const (rpm)}^{2/3} \quad (XIV)$$

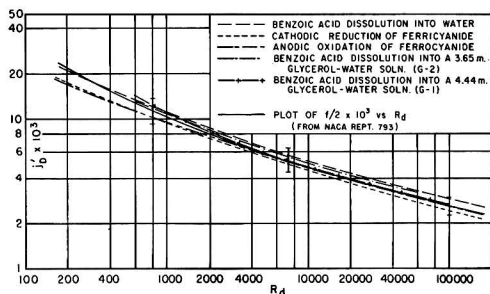


FIG. 9. Mass transfer correlation for inner rotating cylinder. Comparison of five systems studies with friction coefficients  $f/2$

For a given rotor diameter and given set of physical properties of the system, this relation is in approximate agreement with results of the present study.

A linear dependence of dissolution rates, or limiting currents on velocity of rotation as proposed by King and Shack (22, 23) is not substantiated by the present study.

#### Limiting Currents and Concentration Polarization

*The nature of polarization of a redox electrode.*—For  $\Delta E_T$  of a redox electrode Petrocilli (40) obtained a general equation<sup>14</sup> which in a somewhat modified form may be written as:

$$\Delta E_T = \frac{RT}{nF} \ln \left[ \frac{1 - I/I_c}{1 + I/I_a} - \frac{I \frac{I_a}{i_o}}{(I_a + I) \exp\left(-\alpha E_T \frac{nF}{RT}\right)} \right] \quad (\text{XV})$$

where  $\alpha$  = a constant between 0 and 1 (usually close to 0.5) representing the portion of the electrical potential difference across the activation energy barrier, which acts in the cathodic direction;  $i_o$  = exchange current density, representing the rate of forward (cathodic) and also backward (anodic) reaction at the reversible, or open circuit potential.

Using concepts of the absolute reaction rate theory (44) it is possible to show (40) that

$$i_o = \frac{nF kT}{N h} c_o \cdot e^{-\Delta F^*/RT} \quad (\text{XVI})$$

where  $\Delta F^*$  = standard free energy change of the activation process (at open circuit), ergs/mole;  $N$  = Avogadro number,  $6.023 \times 10^{23}$ , molecules/mole;  $h$  = Planck constant,  $6.624 \times 10^{-27}$ , erg-sec/mole-

<sup>14</sup> Analogous relations have recently been obtained by a number of investigators (42, 43).

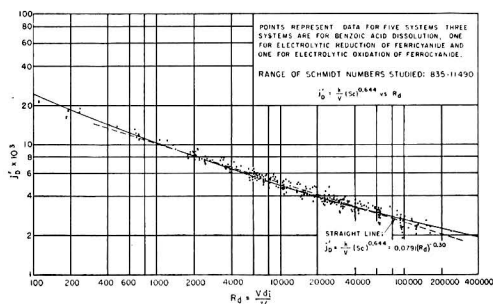


FIG. 10. General correlation for mass transfer at rotating cylinders.

cule;  $k$  = Boltzmann constant,  $1.3805 \times 10^{-6}$ , erg/ $^{\circ}$ K-molecule.

Thus, at constant  $T$ ,  $i_o$  depends only on  $\Delta F^*$  and  $c_o$ , of reacting ions. For a given electrode reaction the activation energy can be assumed to be constant provided electrode poisons are absent (29, 42). Under such conditions  $i_o$  depends only on  $c_o$ .

In equation (XV) the first term in the bracket represents the contribution of concentration polarization, and the second represents chemical polarization. Relative magnitude of this second term depends primarily on  $I_a/i_o$ .

For a given electrode system  $I_a$  increases with the 0.70 power of the rotational velocity, according to equation (X);  $i_o$ , however, remains unaffected. Hence at high rotational speeds, i.e., large values of  $I_a/i_o$ , chemical polarization should become significant in comparison with concentration polarization. It is obvious, therefore, that in order to ascertain experimentally whether a given electrolytic redox reaction comes close to thermodynamic reversibility, i.e., takes place with a comparatively small chemical polarization,  $\Delta E_T$  vs.  $I$  curves must be obtained at high rotational speeds. From such curves (see, for example, Fig. 5 and 6) plots of  $\Delta E_T$  against  $\log \frac{1 \mp I/I_c}{1 \pm I/I_a}$  can be prepared

TABLE II. Coordinates of the general mass transfer correlation curve for rotating cylinders (see Fig. 10)

$R_d$	$j_D \times 10^2$
200	18.4
500	13.0
1,000	10.2
4,000	6.53
10,000	4.88
30,000	3.54
60,000	2.96
100,000	2.61
200,000	2.24
300,000	2.05



as described previously. A comparison of equations (IV) and (XV) shows that if chemical polarization is negligible, i.e.,  $\Delta E_T \approx \Delta E_{conc}$ , experimental points in such plots should fall close to a straight line with a slope of 59.1 (at 25°C, expressing polarization in mv). This type of plot is very convenient, as the distance of a given point from the straight line with slope 59.1 gives directly the value of chemical polarization and demonstrates its importance relative to concentration polarization (see for instance in Fig. 13).

Table III<sup>15</sup> gives typical results for a given concentration, inner and outer diameter. Values of  $\Delta E_{conc}$  and  $\Delta E_{chem}$  were calculated according to equations (IV) and (V). Data for three experimental series were plotted in Fig. 11. Solutions used were only 0.05M and 0.01M in ferri- or ferrocyanide, hence, according to equations (XV) and (XVI) some chemical polarization may be expected. However, as Fig. 11 shows, even up to peripheral velocities of 157.3 cm/sec,  $\Delta E_T$  consists almost entirely, within limits of experimental accuracy, of concentration polarization.

The predominant importance of the stirring rate as represented by  $V$  is interestingly demonstrated in Fig. 13 for a solution of a relatively high concentration [number 9, approximately 0.20N of  $\text{Fe}(\text{CN})_6^{3-}$  and  $\text{Fe}(\text{CN})_6^{4-}$ ]. For runs up to a velocity of 115 cm/sec, data fall close to the straight line with a slope 59.1, the value for the so-called reversible electrode. At higher speeds, i.e., when the ratio  $I_a/i_o$  increases, chemical polarization becomes relatively significant. For instance at  $V = 333$  cm/sec, when the concentration polarization is 59.1 mv, the corresponding chemical polarization has already reached 19.4 mv (Fig. 13). Hence, in case of a reaction where  $I_a/i_o$  is not very small, it is possible to increase this ratio by increasing  $I_a$  with stirring (rotational speed). In this way a reaction in which polarization is predominantly controlled by mass transfer (i.e., concentration polarization) may be converted to one which is under activation control, involving large chemical polarization.

As shown previously,  $i_o$  depends greatly on the activation energy necessary for the reaction to proceed. The latter has been found by many investigators to increase in the presence of electrolytic poisons (29, 42). Thus, according to equation (XVI),

<sup>15</sup> An extended version of these tables has been deposited as Document 4212 with the ADI Auxiliary Publications Project, Photoduplication Service, Library of Congress, Washington 5, D. C. A copy may be secured by citing the Document number and by remitting \$1.25 for photoprints, or \$1.25 for 35-mm microfilm. Advance payment is required. Make checks or money orders payable to: Chief, Photoduplication Service, Library of Congress.

TABLE III. Concentration and chemical polarizations at various rotational speeds and current densities

[Sample data]<sup>15</sup>  
 Solution No. 13, Series II  
 Initial composition: (0.04996 m/l  $\text{K}_3\text{Fe}(\text{CN})_6$   
 (0.05052 m/l  $\text{K}_4\text{Fe}(\text{CN})_6$   
 (1.923 m/l NaOH  
 T = 25.0°C  
 Rotor diameter ( $d_i$ ) = 5.024 cm  
 Outer cylinder diameter ( $d_o$ ) = 9.87 cm

Run No.	I ma/cm <sup>2</sup>	Cathodic reduction of $\text{Fe}(\text{CN})_6^{3-}$			Anodic oxidation of $\text{Fe}(\text{CN})_6^{4-}$		
		$\Delta E_{conc}^{calc}$ (mv)	$\Delta E_T$ (meas) mv	$\frac{\Delta E_{chem}}{\Delta E_T} = \frac{\Delta E_T}{\Delta E_{conc}}$ (calc)	$\Delta E_{conc}^{calc}$ (mv)	$\Delta E_T$ (meas) mv	$\frac{\Delta E_{chem}}{\Delta E_T} = \frac{\Delta E_T}{\Delta E_{conc}}$ (calc)
1208 rpm; $V = 318$ cm/sec; $I_c = 22.00$ ma/cm <sup>2</sup> ; $I_a = 21.00$ ma/cm <sup>2</sup>							
15a	2	-4.5	-4.0	0.5	4.8	4.0	-0.8
	4	-9.6	-9.1	0.5	9.7	8.1	-1.6
	6	-14.6	-12.4	2.2	14.8	12.4	-2.4
	8	-19.9	-17.2	2.7	20.3	17.2	-3.1
	10	-25.6	-21.6	4.0	26.3	21.6	-4.7
	12	-31.9	-26.7	5.2	33.0	27.8	-5.2
	14	-39.1	-34.1	5.0	40.8	36.3	-4.5
	16	-47.9	-43.0	4.9	50.9	50.0	-0.9
	18	-59.8	-56.7	3.1	65.5	67.2	1.7
18.5	-63.6	-61.6	2.0	70.5	72.8	2.3	
302 rpm; $V = 79.4$ cm/sec; $I_c = 8.20$ ma/cm <sup>2</sup> ; $I_a = 8.10$ ma/cm <sup>2</sup>							
15b	1	-6.3	-6.4	-0.1	6.3	6.4	0.1
	2	-12.8	-13.0	-0.2	12.9	13.0	0.1
	3	-19.7	-20.3	-0.6	19.8	20.3	0.5
	4	-27.5	-28.9	-1.4	27.7	28.9	1.2
	5	-36.5	-39.7	-3.2	36.9	39.7	2.8
	6	-48.1	-53.9	-5.8	48.8	53.9	5.1
102 rpm; $V = 26.8$ cm/sec; $I_c = 3.96$ ma/cm <sup>2</sup> ; $I_a = 3.80$ ma/cm <sup>2</sup>							
15c	0.3	-4.0	-4.0	0.0	4.0	4.0	0.0
	0.6	-8.0	-7.9	0.1	8.0	7.9	-0.1
	0.9	-12.1	-12.1	0.0	12.2	12.1	-0.1
	1.2	-16.3	-16.7	-0.4	16.6	16.7	0.1
	1.5	-20.8	-20.9	-0.1	21.1	20.9	-0.2
	1.8	-25.5	-26.0	-0.5	26.1	26.0	-0.1
	2.1	-30.7	-31.2	-0.5	31.6	31.2	-0.4
	2.4	-36.6	-37.1	-0.5	37.9	37.1	-0.8
	2.7	-43.3	-44.2	-0.9	45.2	44.2	-1.0
	3.0	-51.4	-54.2	-2.8	54.5	54.2	-0.3
	3.3	-62.1	-68.0	-5.9	67.7	68.0	0.3
	3.36	-64.8	-71.0	-6.2	71.3	71.0	-0.3
	25 rpm; $V = 6.58$ cm/sec; $I_c = 1.81$ ma/cm <sup>2</sup> ; $I_a = 1.74$ ma/cm <sup>2</sup>						
15d	0.2	-5.8	-6.2	-0.4	5.8	6.2	0.4
	0.4	-11.7	-12.1	-0.4	11.8	12.1	0.3
	0.6	-17.8	-18.5	-0.7	17.8	18.5	0.7
	0.8	-24.7	-25.3	-0.6	25.2	25.3	0.1
	1.0	-32.3	-33.0	-0.7	33.3	33.0	-0.3
	1.2	-41.4	-42.6	-1.2	43.1	42.6	-0.5
	1.4	-53.3	-55.2	-1.9	56.7	57.0	-0.3
	1.5	-61.2	-64.7	-3.5	66.3	68.7	2.4

\*  $\Delta E_{conc}(\text{mv}) = 59.1 \log \frac{1 \mp I/I_c}{1 \pm I/I_a}$ . (Upper sign for cathodic case, lower for anodic.)

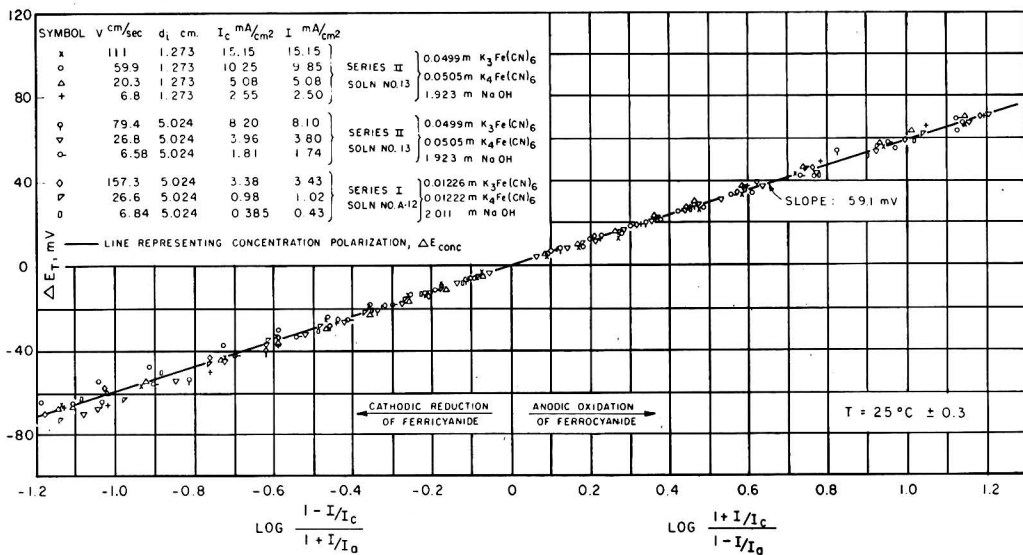


FIG. 11. Total polarization  $\Delta E_T$  vs.  $\log Q$

$i_0$  may be expected to decrease significantly under such conditions. In a special study on effects of better known electrode poisons, Gerischer (42) found that at platinum electrodes treated with a  $2 \times 10^{-6} M$   $H_2S$  solution for 1 min and 60 min, respectively,  $i_0$  for the  $Fe^{+3}/Fe^{+2}$  couple dropped to 10.8% and 1.7% of the original (active state) value, respectively. The highly alkaline solutions used in the present studies, when exposed to air, could dissolve an amount of  $H_2S$  sufficient to decrease  $i_0$  and consequently increase chemical polarization. Effects of other electrode poisons should, of course, be taken into account also. For instance, HCN formed through photochemical decomposition of ferrocyanide may exercise a powerful effect. Several investigators (45, 28) have also concluded that even electrodes made of "noble" metals such as gold, silver, and nickel become gradually covered with oxide films (when used in air-saturated solutions) causing a large increase in polarization.

In a special study designed to demonstrate the effect of electrode poisons,  $\Delta E_T - I$  data were obtained for an alkaline ferro-ferrocyanide solution, which was exposed to air and light for several days. Nickel electrodes used in this study were cleaned in the same manner as described previously, but were not given any cathodic hydrogen discharge treatment. Fig. 12 shows the results for solution No. 1 in the form of  $\Delta E_T$  vs.  $\log Q$  plot. Large chemical polarizations (demonstrated by deviations from the  $\Delta E_{conc}$  line) were obtained in spite of relatively low rotational speeds (up to 56.6 cm/sec). Values of  $\Delta E_{conc} = -59.1$  mV and  $\Delta E_{chem} = -47.9$  mV (hence  $\Delta E_T = -107$  mV) indicated in Fig. 12 (cathodic case) are for an applied C.D. of 12.1 ma/cm<sup>2</sup> and a peripheral speed of 24.6 cm/sec. It is interesting to compare these with a freshly prepared solution (number 9) at about the same C.D.

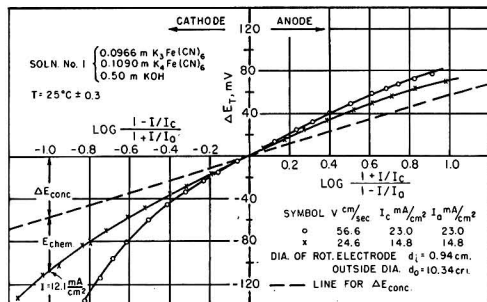


FIG. 12. Total polarization  $\Delta E_T$  vs.  $\log Q$  in case of "inactive electrodes" and presence of air-oxygen.

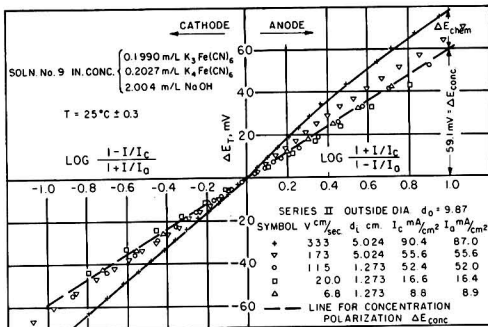


FIG. 13. Total polarization  $\Delta E_T$  vs.  $\log Q$  for high current density electrolysis.

and rotational speed.<sup>16</sup> Thus at a  $I = 12 \text{ ma/cm}^2$  and  $V = 20 \text{ cm/sec}$ , a total cathodic polarization ( $\Delta E_T$ ) of only  $-43.5 \text{ mv}$  was measured for solution number 9.<sup>17</sup> The corresponding concentration polarization was calculated to be  $-47.1 \text{ mv}$ .<sup>18</sup> Hence no measurable chemical polarization was determined in this case, while at the same C.D. in the case of the poisoned electrode,  $\Delta E_{\text{chem}}$  represented about 45% of total electrode polarization.

With regard to the ferro-ferriicyanide couple the following conclusions may be drawn on the basis of the present study.

(A) Only freshly prepared and deaerated alkaline potassium ferri- and ferrocyanide solutions should be used with a maximum possible exclusion of light. The electrode (platinum or nickel) should be given a cathodic hydrogen treatment prior to each experiment.

(B) With the above precaution a reasonably small  $\Delta E_{\text{chem}}$  is associated with the electrolytic redox reaction. The amount of  $\Delta E_{\text{chem}}$  involved depends on the magnitude of the  $I_a/i_o$  ratio, i.e., on the rate of stirring (on which  $I_a$  depends). For rotating electrodes up to a peripheral velocity of 115 cm/sec, the electrode reaction is predominantly mass transfer controlled and the chemical polarization is negligibly small. The above peripheral velocity corresponds to a Reynolds number of 11,000. It should be reasonable to assume that in many other types of flow up to  $R_d = 11,000$  a negligible  $\Delta E_{\text{chem}}$  may be expected for the ferri-ferrocyanide couple.

(C) Under conditions (see above) at which the total electrode polarization is almost entirely represented by concentration polarization, the general mass transfer correlation for rotating cylinders (equation VII) can be used to predict  $\delta$ ,  $I_c$ , or  $I_a$ , and  $\Delta E_{\text{conc}}$  (see equations X, XI, and IV). Conversely, from a given measured polarization,  $c_i$  of the reacting ion may be calculated at an applied current density.

To illustrate the latter point, calculations of  $\delta$ ,  $I_c$ ,  $I_a$ , and  $\Delta E_{\text{conc}}$  have been carried out below for a rotating electrode in an alkaline potassium ferro-ferriicyanide solution. To facilitate comparison with

<sup>16</sup> The difference in concentrations of the reacting ions between solutions number 1 and 9 (a factor of 2) does not significantly affect this comparison, primarily because the ratio  $I_a/i_o$  is independent of the bulk concentration of the reacting ion.

<sup>17</sup> See footnote (15).

<sup>18</sup> Actually the absolute value of  $\Delta E_T$  cannot be smaller than that of  $\Delta E_{\text{conc}}$ . Whenever this seems to be the case, it must be attributed not only to experimental inaccuracies, but also to the possibility that achievement of a steady state polarization of the electrode was not quite complete. Fortunately in no case were these deviations very serious.

experimental measurements the physical data for one of the systems studied were used.

*Illustrative example.* Assumed solution: (Equivalent to solution No. 9) 0.1976M  $\text{K}_3\text{Fe}(\text{CN})_6$ , 0.2027M  $\text{K}_4\text{Fe}(\text{CN})_6$ , 2.004M NaOH.

Data:  $d_i = 1.273 \text{ cm}$ ;  $S = 300 \text{ rpm}$ ;  $V = \frac{S}{60} \pi d_i = \frac{300}{60} \times 3.1416 \times 1.273 = 20.0 \text{ cm/sec}$ ;  $R_d = 1,789$ ; temperature,  $25^\circ\text{C}$ ;  $\nu = 1.423 \times 10^{-2} \text{ cm}^2/\text{sec}$ ;  $D_{\text{ferri}} = 0.454 \times 10^{-5} \text{ cm}^2/\text{sec}$ ;  $D_{\text{ferro}} = 0.390 \times 10^{-5} \text{ cm}^2/\text{sec}$ ;  $c_{\text{ferri}} = 0.1976 \times 10^{-3} \text{ moles/cc}$ ;  $c_{\text{ferro}} = 0.2027 \times 10^{-3} \text{ moles/cc}$ .

*Diffusion Layer Thickness,  $\delta$ :* From equation (XI):

$$\delta_{(\text{cm})} = 12.64 d_i^{0.30} V^{-0.70} \nu^{0.344} D^{0.356}$$

Hence for the cathodic case:

$$\begin{aligned} \delta_{\text{ferri}} &= 12.64 (1.273)^{0.30} (20.0)^{-0.70} \\ &\quad (1.423 \times 10^{-2})^{0.344} (0.454 \times 10^{-5})^{0.356} \\ &= 4.840 \times 10^{-3} \text{ cm} \\ \delta_{\text{ferro}} &= 12.64 (1.273)^{0.30} (20.0)^{-0.70} \\ &\quad (1.423 \times 10^{-2})^{0.344} (0.390 \times 10^{-5})^{0.356} \\ &= 4.585 \times 10^{-3} \text{ cm} \end{aligned}$$

*Limiting Current Densities:* Cathodic limiting C.D.,

$$\begin{aligned} I_c &= \frac{nFD}{\delta} c_{\text{ferri}} \\ &= \frac{1 \times 96,500 \times (0.453 \times 10^{-5})}{4.840 \times 10^{-3}} \times (0.1976 \times 10^{-3}) \\ &= 17.89 \times 10^{-3} \text{ amp/cm}^2 = 17.89 \text{ ma/cm}^2 \end{aligned}$$

as compared to experimentally determined

$$\begin{aligned} I_c &= 16.6 \text{ ma/cm}^2 \\ \text{Deviation} &= 7.6\% \end{aligned}$$

Anodic limiting C.D.,

$$\begin{aligned} I_a &= \frac{nFD}{\delta_{\text{ferro}}} c_{\text{ferro}} \\ &= \frac{1 \times 96,500 \times (0.390 \times 10^{-5})}{4.585 \times 10^{-3}} \times (0.2027 \times 10^{-3}) \\ &= 16.64 \times 10^{-3} \text{ amp/cm}^2 = 16.64 \text{ ma/cm}^2 \end{aligned}$$

as compared to experimentally determined

$$\begin{aligned} I_a &= 16.4 \text{ ma/cm}^2 \\ \text{Deviation} &= 1.5\% \end{aligned}$$

*Concentration Polarization at Applied C.D. of 10 ma/cm<sup>2</sup>:*

$$\begin{aligned} \text{Cathodic } \Delta E_{\text{conc}} &= 59.1 \log \frac{1 - I/I_c}{1 + I/I_a} \\ &= 59.1 \log \frac{1 - 10/17.89}{1 + 10/16.64} \\ &= -33.1 \text{ mv} \end{aligned}$$

as compared to the experimentally measured total cathodic polarization

$$\Delta E_T = -33.0 \text{ mv}$$

$$\begin{aligned} \text{Anodic } \Delta E_{\text{conc}} &= 59.1 \log \frac{1 + I/I_c}{1 - I/I_a} \\ &= 59.1 \log \frac{1 + 10/17.89}{1 - 10/16.64} \\ &= +34.9 \text{ mv} \end{aligned}$$

as compared to the experimentally measured total anodic polarization

$$\Delta E_T = 32.8 \text{ mv}$$

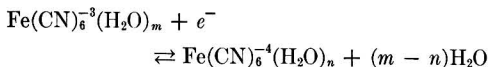
Hence chemical polarization is negligible for these cathodic and anodic runs, and prediction of  $\Delta E_T$  is possible. It should be noted that the general mass transfer correlation enables prediction of limiting currents and concentration polarization even when chemical polarization is large; however, then the total electrode polarization could not be calculated.

The ferro-ferricyanide couple can thus be used conveniently to study mass transfer in liquids for various types of geometries and hydrodynamic conditions. The advantages of using an electrolytic redox reaction over solid dissolution for purposes of studying rates of mass transfer are: (a) achievement of steady state in a relatively short time; (b) direct control of rates, i.e., applied current (This is not possible in case of solids.); (c) preservation of smooth interfacial surface throughout the experiment; (d) higher accuracy and convenience in determination of rates of mass transfer.

The present study has proved that, when properly carried out, the ferro-ferricyanide electrode reactions may be considered to remain predominantly under mass transfer control up to stirring rates corresponding to  $R_d = 11,000$ . However, chemical polarization is essentially present whenever finite currents are passed, and becomes significant at high stirring rates. The reason Essin and coworkers (30) could claim that electrolytic reactions of the ferri-ferrocyanide couple involve only concentration polarization is that their experiments were carried out at low stirring rates.

Under proper experimental conditions, when concentration polarization is accounted for, the ferri-ferrocyanide couple is not far from thermodynamic equilibrium, i.e.,  $\Delta F^*$  is not very large. For the electrochemical reaction which takes place at the electrode interface itself, Lewartowicz (43) discussed two rate-determining steps. One step involves electron transfer at the interface of the electrode, the other the change in hydration of the ion under-

going recharge. For the ferri-ferrocyanide couple this may be expressed as:



Numerous investigators (46-48) have found that an ion is more hydrated the larger its charge and the smaller its radius. Hence, activation energy of the total process is composed of energy necessary for electron passage between ion and electrode and of hydration energy. The latter depends only on the state of hydration of oxidized and reduced ions, but the former is probably the one which is affected by presence of electrolytic poisons adsorbed at the electrode surface. Lewartowicz's experiments (43) on  $\text{Fe}^{+3}/\text{Fe}^{+2}$ ,  $\text{Ce}^{+4}/\text{Ce}^{+3}$  and quinone/hydroquinone couples have shown a small chemical polarization to be involved in each case. His results support in a general sense the above discussed mechanism of the electrolytic redox reaction.

It seems reasonable that electrode reactions involving only electron transfer and change in degree of ion hydration would involve small activation energies, compared to reactions involving breaking or formation of chemical bonds.

#### ACKNOWLEDGMENT

The authors wish to acknowledge the support of the Office of Naval Research. Appreciation is due to Mr. Lawrence Wolf and Mr. James Worley for assistance with experimental measurements.

Any discussion of this paper will appear in a Discussion Section to be published in the December 1954 issue of the JOURNAL.

#### REFERENCES

1. M. EISENBERG, "Studies on the Role of Ionic Diffusion and Mass Transfer in Electrode Processes," M.S. Thesis, University of California, Berkeley (1951).
2. C. W. TOBIAS, M. EISENBERG, AND C. R. WILKE, *This Journal*, **99**, 359C (1952).
3. C. WAGNER, *ibid.*, **95**, 161 (1949).
4. C. R. WILKE, M. EISENBERG, AND C. W. TOBIAS, *ibid.*, **100**, 513 (1953).
5. B. LEVICH, *Acta Physicochim. U.R.S.S.*, **17**, 257 (1942).
6. J. N. AGAR, *Disc. Faraday Soc.*, **1**, 26 (1947).
7. C. S. LIN, E. B. DENTON, N. S. GASKILL, AND G. L. PUTNAM, *Ind. Eng. Chem.*, **45**, 2136 (1951).
8. C. S. LIN, R. W. MOULTON, AND G. L. PUTNAM, *Ind. Eng. Chem.*, **45**, 636 (1953).
9. G. I. TAYLOR, *Phil. Trans. Roy. Soc. London*, **223**, 289 (1923); *Proc. Roy. Soc. London*, **A151**, 494 (1935).
10. SHIH-I PAI, NACA Tech. Note 892 (1943).
11. T. THEODORSEN AND A. REGIER, NACA Report 793 (1945).
12. I. M. KOLTHOFF AND J. J. LINGANE, "Polarography," 2nd ed., Interscience Publishing Co., New York (1952).
13. T. TSUKAMOTO, T. KAMBARA, AND I. TACHI, *J. Electrochem. Assoc. Japan*, **18**, 386 (1950).

14. E. BRUNNER, *Z. physik. Chem.*, **47**, 56 (1904).
15. W. NERNST AND E. S. MERRIAM, *Z. physik. Chem.*, **53**, 235 (1905).
16. A. EUCKEN, *Z. Elektrochem.*, **38**, 341 (1932).
17. T. KAMBARA AND T. TSUKAMOTO, *J. Electrochem. Assoc. Japan*, **18**, 356 (1950).
18. B. ROALD AND W. BECK, *This Journal*, **98**, 277 (1951).
19. H. SALZBERG AND C. V. KING, *ibid.*, **97**, 290 (1950).
20. C. V. KING AND F. S. LANG, *ibid.*, **99**, 295 (1952).
21. C. V. KING AND N. MAYER, *ibid.*, **100**, 473 (1953).
22. R. GLICKSMAN, H. MOUQUIN, AND C. V. KING, *ibid.*, **100**, 580 (1953).
23. C. V. KING AND M. SHACK, *J. Am. Chem. Soc.*, **57**, 1212 (1935).
24. C. V. KING AND W. H. CATHCART, *ibid.*, **59**, 63 (1937).
25. C. V. KING AND P. L. HOWARD, *Ind. Eng. Chem.*, **29**, 75 (1937).
26. C. FREDENHAGEN, *Z. anorg. Chem.*, **29**, 396 (1902).
27. G. JUST, *Z. physik. Chem.*, **63**, 513 (1908).
28. G. GRUBE, *Z. Elektrochem.*, **18**, 189 (1912); **20**, 334 (1914).
29. W. L. H. MOLL, *Z. physik. Chem.*, **A175**, 353 (1936).
30. O. ESSIN, S. DERENDIAYER, AND N. LADYGIN, *J. Appl. Chem. (U. R. S. S.)*, **13**, 971 (1940).
31. W. R. CARMODY AND J. J. ROHAN, *Trans. Electrochem. Soc.*, **83**, 241 (1943).
32. J. V. PETROCELLI AND A. A. PAOLUCCI, *This Journal*, **98**, 291 (1951).
33. J. MATUSCHEK, *Chem. Ztg.*, **25**, 601 (1901).
34. S. IMORI, *Z. anorg. u. allgem. Chem.*, **167**, 145 (1927).
35. I. M. KOLTHOFF AND E. A. PEARSON, *Ind. Eng. Chem., Anal. Ed.*, **3**, 381 (1931).
36. I. M. KOLTHOFF AND N. H. FURMAN, "Volumetric Analysis," Vol. II, p. 427, J. Wiley and Sons, New York (1929).
37. F. SUTTON, "Volumetric Analysis," 12th ed., p. 235, Blakiston and Co., Philadelphia (1935).
38. J. S. ANDERSON AND K. SADDINGTON, *J. Chem. Soc.*, **1949**, S381.
39. M. EISENBERG, C. W. TOBIAS, AND C. R. WILKE, Technical Report No. 2, Nonr 222 (06). To be published in *Chem. Eng. Progr.* in 1954.
40. J. V. PETROCELLI, *This Journal*, **98**, 187 (1951).
41. T. H. CHILTON AND A. P. COLBURN, *Ind. Eng. Chem.*, **26**, 1183 (1934).
42. H. GERISCHER, *Z. Elektrochem.*, **54**, 362 (1950); **55**, 98 (1951).
43. E. LEWARTOWICZ, *J. chim. phys.*, **49**, 557, 564, 573 (1952).
44. H. EYRING, S. GLASSTONE, AND K. J. LAIDLER, *J. Chem. Phys.*, **7**, 1053 (1939).
45. M. LE BLANC, *Abhandl. Bunsen Ges.*, No. 3 (1910).
46. H. BRINTZINGER AND CH. RATANARAT, *Z. anorg. u. allgem. Chem.*, **222**, 113 (1935).
47. H. SACHSSE, *Z. Elektrochem.*, **40**, 531 (1934).
48. G. SUTRA, *J. chim. phys.*, **43**, 189 (1946).

## NOMENCLATURE

Symbol	Definition	Units
$c_o$	Concentration of reacting ions in the bulk of the solution	mole/cc
$c_i$	Concentration of reacting ions at the electrode interface	mole/cc
$c_{ferri}$	Bulk concentration of ferri-ferrocyanide ions	mole/cc
$c_{ferro}$	Bulk concentration of ferrocyanide ions	mole/cc
$d_i$	Diameter of the inner rotating electrode	cm
$D$	Diffusion coefficient of species $k$	cm <sup>2</sup> /sec
$\Delta E_T$	Total polarization	mv
$\Delta E_{conc}$	Concentration polarization	mv
$\Delta E_{chem}$	Chemical polarization	mv
$f$	Friction factor	dimensionless
$F$	Faraday equivalent	96,500 coulomb/equiv
$\Delta F^*$	Standard free energy change of activation	ergs/mole
$h$	Planck constant	$6.624 \times 10^{-27}$ erg-sec/molecule
$h'$	Height of cell	cm
$i$	Total current	amp
$i_o$	Exchange current density	amp/cm <sup>2</sup>
$I$	Current density	ma/cm <sup>2</sup>
$I_a$	Anodic limiting current density	ma/cm <sup>2</sup>
$I_c$	Cathodic limiting current density	ma/cm <sup>2</sup>
$I_L$	Limiting current current density, generally	amp/cm <sup>2</sup>
$j_D'$	Modified Chilton-Colburn j-number	dimensionless
$k$	Boltzmann constant, $1.3805 \times 10^{-6}$	erg/ <sup>o</sup> K molecule
$k_a$	Mass transfer coefficient at the anode	cm/sec
$k_c$	Mass transfer coefficient at the cathode	cm/sec
$k_L$	Mass transfer coefficient, generally	cm/sec
$n$	Number of electrons exchanged in electrode reaction	

## NOMENCLATURE—Continued

Symbol	Definition	Units
$N$	Rate of mass transfer	mole/cm <sup>2</sup> -sec
$r_i$	Radius of rotated inner electrode	cm
$r_o$	Internal radius of outer electrode	cm
$R_{(1)}, R_{(2)}$	Resistance	ohms
$R$	Universal gas constant	$8.313 \times 10^7$ erg/ <sup>o</sup> K-mole
$t_i$	Transference number of the reacting ion	
$T$	Temperature	<sup>o</sup> K
$V$	Peripheral velocity at the rotating cylinder	cm/sec
$ZCP$	Zero current potential (static potential difference between an investigated electrode and the reference cell)	mv

## Greek symbols

$\alpha, \beta$	Fractions of electrical potential difference across the activation energy barrier acting in the cathodic and anodic direction respectively	
$\delta$	Thickness of diffusion layer	cm
$\kappa$	Electrical conductivity of a solution	ohm <sup>-1</sup> cm <sup>-1</sup>
$\mu$	Dynamic viscosity	g/cm-sec
$\nu$	Kinematic viscosity	cm <sup>2</sup> /sec
$\rho$	Density	g/cm <sup>3</sup>

## Dimensionless groups

$Q = \frac{1 \mp I/I_c}{1 \pm I/I_a}$	Ratio used in $\Delta E_{conc}$ calculations (upper sign for cathodic case, lower for anodic)	
$R_d = \frac{Vd_i}{\nu}$	Reynolds number based on diameter of rotating inner cylinder	
$Sc = \frac{\nu}{D_k}$	Schmidt number for mass transfer of species $k$	

# Electrochemical Polarization of Titanium in Aqueous Solutions of Sodium Chloride<sup>1</sup>

NORMAN HACKERMAN AND COLBY D. HALL, JR.<sup>2</sup>

*Department of Chemistry, The University of Texas, Austin, Texas*

## ABSTRACT

Cathodic and anodic polarization curves for titanium in neutral NaCl solutions were determined over the range  $0.02 \mu\text{a}/\text{cm}^2$  to  $0.01 \text{ amp}/\text{cm}^2$ . These were derived from steady-state values of time-potential curves measured by the direct method using a thermionic amplifier to limit current in the potential measuring circuit to  $10^{-12}$  amp.

On open circuit the potential increased from  $-0.25$  volt (saturated calomel scale) to about  $+0.2$  volt. As little as  $0.1 \mu\text{a}/\text{cm}^2$  cathodic considerably decreased rate and extent of change, while anodic treatment of the same intensity increased these effects. At  $1 \text{ ma}/\text{cm}^2$  hydrogen overvoltage was  $0.84$  volt and oxygen overvoltage was  $0.96$  volt. Tafel slopes were  $0.15$  and  $0.14$ , respectively. In aerated solution the effect of salt concentration between  $0.5$  and  $2M$  was almost wholly that caused by change in oxygen solubility.

The anodic time-potential curves can be divided into three parts: (a)  $E$  increases linearly with time at a rate proportional to current density; (b)  $E$  is constant with time, and oxygen is evolved continuously; (c)  $E$  increases rapidly to about  $+10$  volts after some hours for current densities in excess of  $1 \text{ ma}/\text{cm}^2$ ; a visible surface film forms and a few deep pits appear, but there is no oxygen evolution. Results are considered on the basis of oxide formation and of chemisorbed oxygen atoms.

## INTRODUCTION

Titanium is being studied here as part of a general investigation into characteristics of passive metals. This metal does not fit fully either the category typified by aluminum or by chromium. A careful study of its properties as a working electrode was indicated and resulted in the work reported here as well as in an analysis of the anodic charging process (1).

Although considerable work has been done on polarization of some of the newly available uncommon metals, much of it appears in reports and relatively little in the open literature.<sup>3</sup>

## EXPERIMENTAL METHOD

Polarization measurements were made by the direct method. Apparatus used provided for concurrent measurements in six polarization cells, which were contained in a thermostat bath held at  $30^\circ\text{C}$ .

*Polarization cells.*—Each cell consisted of an open-top glass jar  $16 \times 21$  cm,  $32$  cm deep, containing  $5.0$  liters NaCl solution, and an electrode assembly consisting of the metal, an input electrode, and a saturated calomel electrode. The  $2.52$  cm diameter titanium

coupon was cast in a plastic wafer, polished by hand on  $2$  to  $2/0$  metallographic emery paper, rubber with filter paper moistened with  $95\%$  ethyl alcohol, and wiped carefully with clean, dry lens tissue. The wafer was inserted into a machined plastic holder provided with an electrical connection to the back of the coupon. The holder was sealed water-tight by application of melted ceresin wax. The platinum auxiliary electrode, consisting of  $6$  turns of platinum wire around a  $6$ -mm glass tube, was located  $7$  cm in front of the center of the face of the coupon. The calomel half-cell vessel was a  $2$ -cm glass tube with a bent side arm drawn out to a capillary tip and filled with  $2\%$  agar-saturated KCl gel. The three electrodes were mounted on a plastic support. The calomel electrode vessel could be rotated to vary the distance of the capillary tip from the face of the coupon. The electrode support was itself supported by a brass rod passing through a bracket which was clamped to the horizontal beam of a modified circular path apparatus (2). This rotated electrode assemblies in a circle  $2.54$  cm in diameter, in the plane of the coupon face at  $26.5$  rpm, and gave the coupons a linear velocity of  $3.5$  cm/sec.

*Electrical circuits.*—Six polarization cells were connected in parallel to a  $4$ – $12$ -volt battery source for cathodic measurements, or  $4$ – $50$  volts for anodic measurements. Current for each cell was controlled by a series resistance made up of combinations of  $1/2$ -watt composition type resistors, some being provided with shorting switches, and one or two variable

<sup>1</sup> Manuscript received March 20, 1953. This paper was prepared for delivery before the Philadelphia Meeting, May 4 to 8, 1952.

<sup>2</sup> Present address: Dowell, Incorporated, Tulsa, Oklahoma.

<sup>3</sup> For example, in a series of progress reports to the U. S. Atomic Energy Commission by D. S. McKinney and J. C. Warner of Carnegie Institute of Technology.

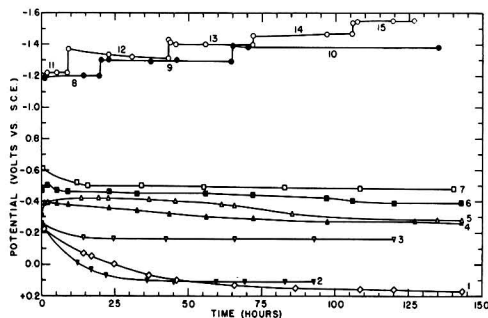


FIG. 1. Time-potential curves for cathodic polarization of titanium in aerated 0.5M NaCl at 30°C. Curve-current density in amp/cm<sup>2</sup>: 1—0.0; 2— $2 \times 10^{-8}$ ; 3— $6 \times 10^{-8}$ ; 4— $1 \times 10^{-6}$ ; 5— $2 \times 10^{-6}$ ; 6— $4 \times 10^{-6}$ ; 7— $4 \times 10^{-5}$ ; 8— $2 \times 10^{-4}$ ; 9— $4 \times 10^{-4}$ ; 10— $1 \times 10^{-3}$ ; 11— $2 \times 10^{-4}$ ; 12— $6 \times 10^{-4}$ ; 13— $2 \times 10^{-3}$ ; 14— $4 \times 10^{-3}$ ; 15— $1 \times 10^{-2}$ .

2-watt resistors. Current was read by measuring *IR* drop across a calibrated wire-wound resistor in series with the cell, and was held constant within less than 1% of the nominal value.

Potential of the titanium coupon with respect to the saturated calomel electrode was measured by an L & N thermionic amplifier and Type K-2 potentiometer. The former limited current drawn in the potential-measuring circuit to  $10^{-12}$  amp or less, even when the potentiometer was not balanced, and thus prevented disturbance of the measured polarizing current during measurements at very low current densities. For measuring potentials in excess of the maximum range of the potentiometer, dry cells, calibrated to  $\pm 1$  mv, were connected in series with the potentiometer. All potentials are given on the saturated calomel electrode scale.

**Materials.**—Coupons were cut from Remington titanium sheet, 1.6 mm thick. Spectrographic analysis<sup>4</sup> showed over 99% titanium, with 0.725% carbon, 0.25% iron, and 0.005% other elements.

Surface areas were determined by krypton adsorption at 78°K, and from this the coupons as prepared were found to have a roughness factor of  $2.2 \pm 0.2$ .<sup>5</sup> All current densities are given in terms of apparent or projected area.

Solutions were made with analytical reagent grade NaCl and distilled water. They were unbuffered, and had a pH of 6–7. The NaCl contained 3 ppm iron, which was essentially completely precipitated during a run, giving about 1 mg of Fe(OH)<sub>3</sub> in 5 liters 0.5M solution. The colloidal precipitate trav-

elled by electrophoresis to the anode, and therefore caused no interference on a cathodically polarized coupon. Solutions used in anodic runs were made iron-free by dissolving NaCl in the minimum volume of water, aerating for 12 hr, filtering through fritted glass, and diluting to desired concentration.

All anodic polarization measurements and most cathodic measurements were made in solutions which were kept saturated with air by means of a fritted glass gas dispenser. A glass chimney prevented air bubbles from coming in direct contact with the electrodes. Some measurements of cathodic polarization were made in solutions designated as "air-free." For these runs, one of the jars was fitted with a flexible plastic film cover, sealed on with masking tape. The solution was boiled, cooled under nitrogen, and forced into the polarization cell by nitrogen pressure. During the run, purified nitrogen (4) was bubbled through the solution. A porous aluminum cup around the platinum anode prevented oxygen from getting into the main part of the solution around the cathodic coupon. A more rigorous exclusion of oxygen was not required in these measurements for reasons stated in the Discussion.

**Correction for *IR* drop in the solution.**—In order to prevent errors due to blocking of part of the coupon surface by the tip of the reference electrode, the capillary tip was kept 2.0 cm from the face of the coupon. The potential at that point differs from that at the coupon surface only by the *IR* drop for the polarizing current passing through the 2 cm of solution. This *IR* drop was negligible except at high current densities, for which corrections were made. Potentials were measured in 0.5M NaCl at several distances from 2.0 cm to the surface, the latter measurement being taken immediately after touching the electrode tip to the surface. These points were found to lie on a smooth curve. The effective value of *R* was found by dividing the potential difference from 2.0 cm to the surface by the polarizing current. This was used in calculating the correction for other current densities in 0.5M NaCl, and corresponding values of *R* for 0.1M and 2.0M NaCl were calculated from ratios of specific resistances of solutions.

#### Cathodic Polarizations

Typical time-potential curves at several current densities for cathodically polarized titanium are shown in Fig. 1. Points marked with the same symbol represent measurements on the same coupon in a continuous run. In describing the curves a potential becoming more positive, i.e., moving down, is said to be increasing.

On open circuit and up to  $0.06 \mu\text{a}/\text{cm}^2$  the initial potential is  $-0.25$  volt and increases slowly to a constant value after a day or more (6 days at zero

<sup>4</sup> National Spectrographic Laboratories, Inc., Cleveland, Ohio.

<sup>5</sup> Surface areas were also determined by polarization capacity measurements (3) and led to a roughness factor of  $10 \pm 3$ . The gas adsorption area is considered to be more reliable at present.



current). Generally, at low cathodic current densities, the initial increase in potential is more rapid the lower the current density.

The most noticeable characteristic in the range  $1-4 \mu\text{a}/\text{cm}^2$  is the long time needed for constant potential—more than 6 days. Initial potentials are more negative the higher the current density, and decrease during the first few hours. Between 10 and  $60 \mu\text{a}/\text{cm}^2$ , after a comparatively rapid increase for several hours, a slow increase takes place for as long as 10 days.

In the range 0.1 to  $0.16 \text{ ma}/\text{cm}^2$  potentials do not become sufficiently steady to plot, varying from average values at first by as much as  $\pm 0.1$  volt in less than a minute and, at the end, by  $\pm 0.03$  volt. Average initial and final values (48 hr) were as follows:

$\text{ma}/\text{cm}^2$	volt	volt
0.1	-0.6	-0.6
0.12	-0.5	-1.10
0.14	-0.65	-1.15
0.16	-1.06	-1.17

Curves 8, 9, and 10 were obtained in a single run on the same coupon, as were curves 11-15. The length of time for which the current was held at each value was arbitrary, being at least long enough for the potential to become constant. At these high current densities, the potential does not change greatly from its initial value and becomes constant in a short time. When current is increased to a new constant value, the potential immediately decreases to a more negative value. Usually it then increases slightly but becomes essentially constant in a few hours.

At  $0.2 \text{ ma}/\text{cm}^2$  the rapid variation of potential has an amplitude of  $\pm 0.02$  volt. The amplitude of the swings decreases, at higher current densities, to about  $\pm 0.001$  volt at  $10 \text{ ma}/\text{cm}^2$ .

Time-potential curves for 0.1 and  $2.0M$  NaCl show the same general features as those of Fig. 1. At about the same current densities, curves for the three concentrations show no greater dissimilarities than do curves of duplicate runs at the same concentration.

*Effect of NaCl concentration.*—Cathodic polarization curves for titanium in aerated 0.1, 0.5, and  $2.0M$  NaCl solutions are shown in Fig. 2. Each solid point represents the constant potential finally attained by a coupon held at the same current density from the start of the run. Each open point represents a constant potential attained by a coupon at the designated current density after previous polarization at one or more other current densities.

The polarization curve for  $0.5M$  NaCl was established with especial care. Enough points were

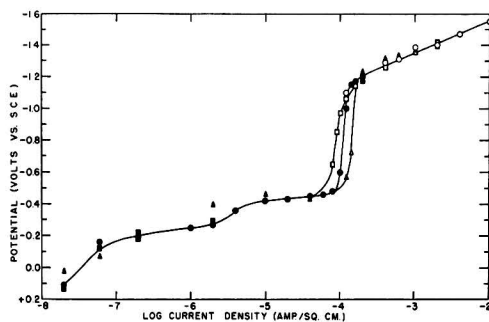


FIG. 2. Cathodic polarization curves for titanium in aerated NaCl solutions at  $30^\circ\text{C}$ . (Solid points give potential at original current density and open points at altered current density.)  $\blacktriangle$   $\Delta$ — $0.1M$ ;  $\bullet$   $\circ$ — $0.5M$ ;  $\blacksquare$   $\square$ — $2.0M$ .

determined to establish that curves for the three concentrations were essentially the same. They are drawn as identical except near  $0.1 \text{ ma}/\text{cm}^2$ . The open circuit potentials cannot be shown in Fig. 2 because the current density scale is logarithmic. These potentials for 0.1, 0.5, and  $2.0M$  solutions are  $+0.18$ ,  $+0.17$ , and  $+0.2$  volt, respectively.

At the three lowest current densities, the curve is drawn through weighted average values of the potentials for the three different concentrations. Deviations of individual points average less than  $0.03$  volt. From  $1-40 \mu\text{a}/\text{cm}^2$  the curve is drawn through the points for  $0.5M$  solution. Reality of the wave drawn in the curve in this region is considered later.

Near  $0.1 \text{ ma}/\text{cm}^2$  a rapid decrease in potential occurs, but at a lower current density for more concentrated solutions. At higher current densities, the logarithmic polarization curve is linear. The slope, corresponding to the constant  $b$  in the Tafel equation, is  $0.204$  volt/log unit.

Most points above  $80 \mu\text{a}/\text{cm}^2$  were measured on a coupon which was polarized successively to several different current densities. One coupon was polarized in  $0.1M$  NaCl for 157 hr at  $0.12 \text{ ma}/\text{cm}^2$ , for 28 hr at  $0.14 \text{ ma}/\text{cm}^2$ , and then for about 20 min each at decreasing current densities from  $2-0.4 \text{ ma}/\text{cm}^2$ . A coupon in  $2.0M$  solution was started at  $0.2 \text{ ma}/\text{cm}^2$  which was increased successively through the other values to the maximum,  $2 \text{ ma}/\text{cm}^2$ . It was returned to the initial current, where it then had the same potential as before. The remaining points were determined at decreasing current densities. For  $0.5M$  solution, points from  $0.2 \text{ ma}/\text{cm}^2$  upward were determined in two runs. It may be noted that points at  $0.4$  and  $1 \text{ ma}/\text{cm}^2$ , which are from the same run, are slightly off the straight line, but would lie on a line parallel to it. The remaining points, all from the other run, fall very closely on the line.

At  $0.2 \text{ ma}/\text{cm}^2$ , hydrogen is evolved slowly on ti-

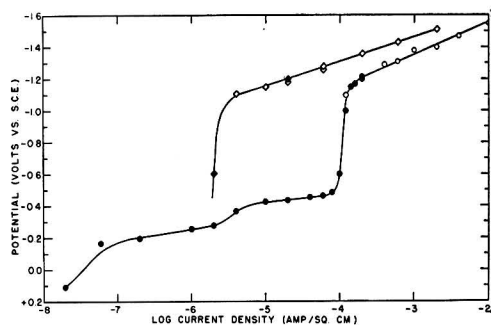


Fig. 3. Cathodic polarization curves for titanium in 0.5M NaCl at 30°C. (Solid points give potential at original current density and open points at altered current density.)  
 ◆ ◇—air-free solution; ● ○—aerated solution.

tanium. Visible bubbles do not form on the surface, but large bubbles gather on the wax coating around the edge of the coupon. At higher current densities small bubbles are evolved continuously from the entire coupon surface. After long polarization at high current density, the titanium surface becomes darkened and very hard.

*Effect of oxygen concentration.*—Cathodic polarization curves for titanium in aerated and in air-free 0.5M NaCl solutions are shown in Fig. 3. The curve for the aerated solution is that for 0.5M NaCl in Fig. 2. The other was determined in two separate runs, one from 2 to 60  $\mu\text{a}/\text{cm}^2$  and the other from 20  $\mu\text{a}/\text{cm}^2$  on up. Agreement of the overlap data is very good. The slope of the linear portion is 0.154 volt/log unit.

The experimental arrangement in the air-free runs prevented observation of hydrogen evolution, but coupons were darkened and surfaces hardened just as in corresponding aerated runs.

#### Anodic Polarization

All anodic polarization measurements were made in aerated 0.5M NaCl solution. Time-potential curves were measured at constant current densities from 0.02  $\mu\text{a}/\text{cm}^2$  to 6.0  $\text{ma}/\text{cm}^2$ . Corresponding charging curves have been given previously (1). The curves show that potential increases linearly with time, at a rate proportional to current density, until a constant potential is reached at which oxygen is evolved. The charge required to reach the oxygen evolution potential is approximately the same for all current densities from 0.06 to 20  $\mu\text{a}/\text{cm}^2$ , the average being 0.0145 coulomb/cm<sup>2</sup>. At current densities above 1  $\text{ma}/\text{cm}^2$ , after several hours at the oxygen evolution potential, a second increase of potential begins. Visible oxygen evolution ceases, and the potential rises at an increasing rate to about +10 volts, where it becomes erratic but generally constant, and a visible oxide film develops.

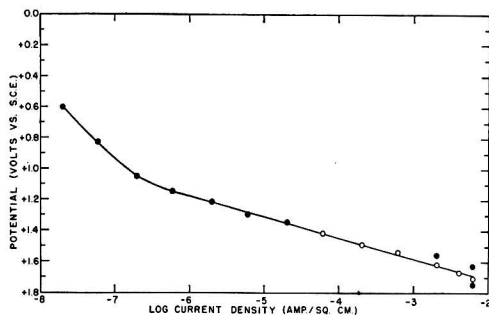


Fig. 4. Anodic polarization curve for titanium in aerated 0.5M NaCl at 30°C. (Solid points give first constant potential reached at original current density. Open points give constant potential at altered current density.)

The anodic polarization curve for titanium in aerated 0.5M NaCl solution is shown in Fig. 4. Each solid point represents the first constant potential reached by a coupon polarized at a constant current density. Each open point represents the constant potential attained by a coupon at the indicated current density after previous polarization to a constant potential at a lower current density. For the latter points, the time of polarization was not long enough for the second increase of potential to have begun when the reading was made.

All experimental points touch the straight line except for the solid points at the two highest current densities. Of these, the one at the less positive potential represents the coupon mounted in the recessed holder.

Below 0.6  $\mu\text{a}/\text{cm}^2$  the curve bends toward less positive potentials. Because of the logarithmic current density scale, the zero-current or open-circuit potential cannot be plotted. This value is +0.17 volt.

Polarization decay on open circuit and the charging process on repolarization are discussed elsewhere (1).

#### DISCUSSION

*Cathodic polarization.*—The usual cathodic reactions in aqueous solutions containing no other reducible material are reduction of dissolved O<sub>2</sub> to OH<sup>-</sup>, possibly in steps involving H<sub>2</sub>O<sub>2</sub>, and reduction of H<sup>+</sup> to H<sub>2</sub>. The former reaction occurs at a less negative potential, and therefore precedes hydrogen evolution as current density is increased. Results indicate that a titanium cathode in neutral NaCl solution follows this expected behavior at current densities above 0.1  $\mu\text{a}/\text{cm}^2$ . Below this the effects are related to those produced by anodic polarization. In the current density range 0.1 to 100  $\mu\text{a}/\text{cm}^2$  the electrode reaction apparently is reduction of O<sub>2</sub>. The sharp break in the curves near 100  $\mu\text{a}/\text{cm}^2$  represents the limiting diffusion current (i.e., current density)

for oxygen under the particular conditions of the experiment. At higher current densities, and more negative potentials, hydrogen is evolved.

In order to establish that the diffusion wave represents the limiting diffusion current of oxygen, rather than that of some other substance, a portion of the polarization curve was measured in an air-free solution. For this purpose it was not necessary to use elaborate measures for rigid exclusion of oxygen. It was sufficient to reduce oxygen concentration of the solution considerably below that of an air-saturated solution. Curves in Fig. 3 show that the limiting diffusion current,  $I_d$ , was lowered from 100  $\mu\text{a}/\text{cm}^2$  in the aerated solution to 2  $\mu\text{a}/\text{cm}^2$  in the air-free solution.

The only apparent effect of variation of NaCl concentration is a small change in the limiting diffusion current of  $\text{O}_2$ . Since the limiting diffusion current of a substance is proportional to its concentration,  $I_d$  for  $\text{O}_2$  should be proportional to the solubility of oxygen from air in various concentrations of salt solutions. The following table gives concentrations of  $\text{O}_2$  under conditions of the experiment, calculated from data for oxygen solubility (5):

NaCl conc	0.1	0.5	2.0M
$\text{O}_2$ conc	2.23	1.93	$1.18 \times 10^{-4}M$
$I_d$ (obs)	1.3	1.0	$0.8 \times 10^{-4}$ amp/cm <sup>2</sup>
$I_d$ (calc)	1.15	1.00	$0.61 \times 10^{-4}$ amp/cm <sup>2</sup>

The values of  $I_d$  (calc) are proportional to the  $\text{O}_2$  solubilities, taking the value for 0.5M NaCl as the standard. Agreement for 0.1M and 2.0M solutions is fairly good, considering that points for these concentrations were determined by a somewhat different procedure from those for 0.5M solution.

From the ratio of diffusion currents in aerated and in air-free solutions, and the solubility of oxygen in 0.5M NaCl, the concentration of oxygen in air-free solutions was  $4 \times 10^{-6}M$ , corresponding to an oxygen partial pressure of 3 mm.

At current densities larger than the oxygen limiting diffusion current, the potential follows the Tafel equation for hydrogen overvoltage. In aerated solutions at all three concentrations of NaCl, the potential is given by the equation

$$E = -1.97 - 0.204 \log I, \quad (\text{I})$$

where  $I$  is current density in amp/cm<sup>2</sup>. In the air-free solution, the equation is

$$E = -1.93 - 0.154 \log I. \quad (\text{II})$$

Since hydrogen overvoltage depends on current actually involved in hydrogen evolution rather than on total current, the relation of  $I - I_d$  to  $E$  for aerated solutions would better represent the hydrogen

overvoltage. A plot (not shown) of  $E$  vs.  $\log(I - I_d)$  is linear from 0.01–1 ma/cm<sup>2</sup> and lies parallel to the line for air-free solution, at potentials 0.11 volt more positive. With this correction, the slope for hydrogen overvoltage in aerated solution agrees with that in the air-free solution. The difference between this slope, 0.15, and the usual Tafel slope of 0.12 may be attributed to the presence of concentration polarization effects in the unbuffered NaCl solution.

Hickling and Salt (6) state that for current densities greater than ten times  $I_d$  the presence of dissolved oxygen has no effect on hydrogen overvoltage. In the present work, both the  $\log I$  and the  $\log(I - I_d)$  curves for aerated solutions, which coincide above 10  $I_d$ , differ by about 0.1 volt from the curve for air-free solution. There is no apparent explanation for this lack of agreement. The air-free curve, however, probably is a good representation of hydrogen overvoltage on titanium. The reversible hydrogen potential here is -0.63 volt and the hydrogen overvoltage on titanium thus is given by

$$\omega = 1.30 + 0.154 \log I. \quad (\text{III})$$

At 1 ma/cm<sup>2</sup> the overvoltage is 0.84 volt, placing titanium with lead and mercury with respect to its very high overvoltage.

After prolonged rapid evolution of hydrogen on titanium, the surface of the metal was darkened and became very hard. Polishing by hand on No. 2 emery paper removed the tarnish and left a bright surface, which in some instances contained numerous very small pits. However, it was necessary to use a motor-driven metallographic polishing wheel and fresh emery paper in order to remove the hardened surface layer and expose unaltered metal. It appears that hydrogen evolution on titanium produces some sort of hydride, either a compound or a solid solution, to an appreciable depth. The solubility of hydrogen in titanium is high; according to Bornelius (7) it is higher than in palladium, and hydride formation is not unexpected.

At current densities below the oxygen limiting diffusion current, the cathode reaction is reduction of  $\text{O}_2$  to  $\text{OH}^-$ . Under conditions of the experiment, the reversible potential of this reaction is +0.60 volt, so that the overvoltage for oxygen reduction is 0.85 volt at 1  $\mu\text{a}/\text{cm}^2$ . If the polarization curve were drawn as a straight line from 0.1 to 100  $\mu\text{a}/\text{cm}^2$ , the slope would be 0.11 volt/log unit. Thus, it may be that reduction of oxygen follows an overvoltage law similar to that for hydrogen or oxygen evolution, and with about the same value for the constant  $b$  in the Tafel equation.

The small wave shown in Fig. 3 near 4  $\mu\text{a}/\text{cm}^2$  seems to be real. Points shown represent the steady potentials reached after prolonged polarization. A

similar wave would be present at about the same current density if either the initial potentials or the most negative potentials attained at each current density were plotted. After coupons polarized at 1 and 4  $\mu\text{a}/\text{cm}^2$  reached their steady potentials (167 hr), both were changed to 2  $\mu\text{a}/\text{cm}^2$ , and in 48 hr both reached potentials within 0.01 volt of the value obtained at the same current density in a previous run. Points at 10 and 40  $\mu\text{a}/\text{cm}^2$  are for 250 hr runs, and gave no indication of becoming appreciably more positive.

Time-potential curves of points on the wave are shown in Fig. 1, curves 4, 5, and 6. The increase of potential begins sooner, the lower the current density. If the wave represented the limiting diffusion current of some depolarizer being formed by electrolysis, the increase of potential would occur sooner at a higher current, since the concentration of this substance would increase more rapidly at the higher current. This eliminates both hydrogen peroxide and chlorine as possible depolarizers. Chlorine is also ruled out by the fact that the cathode potential at the wave is about  $-0.3$  volt. For a limiting diffusion current of 4  $\mu\text{a}/\text{cm}^2$ , the concentration of the depolarizer must be about  $7 \times 10^{-6}M$ . For this concentration of  $\text{Cl}_2$  (or  $\text{HClO}$ ) in 0.5M chloride, the reversible potential is  $+0.9$  volt, and the chlorine electrode does not usually show large overvoltages. It is possible that the wave is in some way associated with a change from the two-electron reaction for reduction of  $\text{O}_2$  to  $\text{H}_2\text{O}_2$  to the four-electron reaction for reduction of  $\text{O}_2$  to  $\text{H}_2\text{O}$  as the potential is made more negative. It is not clear in what manner this change of reaction would be expected to affect time-potential behavior.

The polarization curve in Fig. 2 is probably typical of the behavior of titanium in many other aerated salt solutions not containing reducible ions. Since electrode processes which control potential do not involve ions of the dissolved salt, the only effects of using a different salt or changing concentration should be those resulting from differences in  $\text{pH}$  or oxygen solubility. The entire curve should be shifted to potentials 0.06 volt more negative for each increase of one  $\text{pH}$  unit, and vice versa. This would not hold true, however, in strongly acidic solutions. Titanium is corroded in fairly concentrated acids, and its polarization behavior under such conditions would be expected to differ considerably from that in neutral solutions. The general form of cathodic curves for many other noncorroding metals in aerated salt solutions probably is similar to that for titanium. Curves would be shifted in potential by different overvoltages for reduction of oxygen or for evolution of hydrogen.

**Anodic polarization.**—Oxygen overvoltage follows the Tafel equation from 0.2  $\mu\text{a}/\text{cm}^2$  to 6  $\text{ma}/\text{cm}^2$ , the

highest current density measured. The potential, for solutions of  $\text{pH} = 6.2$ , is given by

$$E = 1.98 + 0.134 \log I, \quad (\text{IV})$$

where  $I$  is in  $\text{amp}/\text{cm}^2$  of projected area. The reversible oxygen potential at  $\text{pH} = 6.2$  is  $+0.63$  volt, so that oxygen evolution overvoltage is given by

$$\omega = 1.35 + 0.134 \log I. \quad (\text{V})$$

The overvoltage is 0.95 volt at 1  $\text{ma}/\text{cm}^2$ , and 0.55 volt at 1  $\mu\text{a}/\text{cm}^2$ . The Tafel slope of 0.134 is close to 0.12, which is the theoretical value for oxygen overvoltage as well as for hydrogen overvoltage.

Anodic polarization of metals has been studied largely with respect to oxygen overvoltage and mechanism of oxygen evolution. Adam (8) says that a complete film of oxygen is present on an electrode from which oxygen is being evolved. However, the form of oxygen on the metal surface is in question; it may be chemisorbed, or a metal oxide film may be formed. The situation is not necessarily the same for all metals.

A rather full analysis of this anodic process has already been given (1). The potential reached on open circuit ( $+0.2$  v) is essentially the same as that found when the metal polarized to the oxygen evolution potential is permitted to decay on breaking the circuit. From the charging curves and the true area (r.f. = 2.2) it is found that the equivalent of three layers of oxygen atoms will have been deposited before oxygen evolution occurs. If the oxygen is not discharged but remains as either  $\text{OH}^-$  or  $\text{O}^=$ , this amounts to about 9 equivalent layers. The calculations assume hexagonal close packing and use 0.74 Å as the covalent radius of oxygen or 1.4 Å as the radius of either ion. The hydroxyl ion is highly polarizable and conceivably could pack so as to give fewer layers.

It is not likely that charged particles can be packed in so closely, so in the case of the oxide ion it would necessarily be assumed that a very thin metal oxide layer formed ( $<50$  Å) before oxygen evolution started. However, it is then not clear why the open circuit potential after polarization should be about  $+0.2$  volt since the Ti,  $\text{TiO}_2$  potential under these conditions would be about  $-1.6$  volts. However, it is not reasonable to postulate three layers of chemisorbed oxygen atoms.<sup>6</sup>

Hence, these data still do not permit an unequivocal choice between chemisorption or oxide formation as the first step prior to oxygen evolution (and incidentally, as the primary reason for the passivity of titanium). There is the possibility that the charge goes into forming a double layer involving a mono-

<sup>6</sup> Chemisorbed because on repolarization only a minute fraction of the original charge is needed to bring the metal back to the oxygen evolution potential (1).

layer of any one of the three particles, with the excess leaking off continuously into the metal or into the solution. Clearly, experimental evidence of the form of the attached particle is needed in order to resolve the question.

#### ACKNOWLEDGMENT

The authors are pleased to take this opportunity to thank Mr. N. Komodromos of these laboratories for the gas adsorption area measurements.

Any discussion of this paper will appear in a Discussion Section to be published in the December 1954 issue of the JOURNAL.

#### REFERENCES

1. C. D. HALL, JR., AND N. HACKERMAN, *J. Phys. Chem.*, **57**, 262 (1953).
2. O. B. J. FRASER, D. E. ACKERMAN, AND J. W. SANDS, *Ind. Eng. Chem.*, **19**, 337 (1927).
3. C. WAGNER, *This Journal*, **97**, 71 (1950).
4. L. MEITES AND T. MEITES, *Anal. Chem.*, **20**, 984 (1948).
5. "The Corrosion Handbook," (H. H. Uhlig, Editor), p. 1147, John Wiley & Sons, Inc., New York (1948).
6. A. HICKLING AND F. W. SALT, *Trans. Faraday Soc.*, **37**, 319 (1941).
7. G. BORELIUS, *Metallwirtschaft*, **8**, 105 (1929).
8. N. K. ADAM, "The Physics and Chemistry of Surfaces," 3rd ed., p. 326, Oxford University Press, London (1941).

# The Nature of the Zinc-Containing Ion in Strongly Alkaline Solutions<sup>1</sup>

THEDFORD P. DIRKSE

Calvin College, Grand Rapids, Michigan

## ABSTRACT

The nature of the zinc-containing ion in strongly alkaline solutions was determined by measuring electrode potentials of zinc in such solutions under equilibrium conditions. Galvanic cells were used in which junction potentials were practically eliminated. Results indicate that in the concentration range of approximately 1-7*M* potassium hydroxide all the zinc is in the form of a zincate ion,  $Zn(OH)_4^{2-}$ . The standard free energy of formation of this ion is  $-206.2$  kcal.

## INTRODUCTION

The question as to whether zinc, when dissolved in strong alkalis, is present as a zincate ion,  $(ZnO_2)^{-}$  or as a hydrogen zincate ion  $(HZnO_2)^{-}$  has received a fair share of attention. An attempt to answer this question has been made by many investigators, and a variety of techniques have been used. Hildebrand and Bowers (1) studied weakly alkaline solutions using a potentiometric titration technique. They found justification for presence of the hydrogen zincate ion only. However, Britton (2), using the same technique, was unable to confirm the presence of either ion. Bodländer (3) measured electrical potentials of cells containing solutions of zinc in aqueous sodium hydroxide. He interpreted the behavior of the zinc electrode to indicate presence of the hydrogen zincate ion at all concentrations. Later Kunschert (4) used a similar method and concluded that zinc existed as the zincate ion in the more strongly alkaline solutions. Bodländer concurred in this interpretation and retracted his earlier conclusions.

The work reported here was undertaken in an attempt to shed some light on this problem by means of a potentiometric study similar to that of Kunschert (4), but using cells in which junction potentials are negligible. The potential of the zinc electrode in alkaline solutions containing zinc will be dependent on activities of zinc-containing ions, hydroxyl ions, and water in the solution. The generalized equation for this reaction may be written as

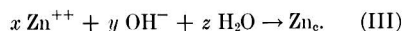


where  $Zn_c$  represents the complex ion formed. It is possible, however, that the water in this reaction is a product rather than a reactant. But, as is shown later, evidence favors the equation as given.

This reaction may be considered as taking place in stages



followed by



At equilibrium, the potential of reaction (II) is

$$E_{Zn} = E_{Zn-Zn^{++}}^0 - (RT/nF) \ln (Zn^{++})/(Zn) \quad (IV)$$

(The terms in parentheses refer to activities of the species indicated.) Assuming that activity of metallic zinc is unity, this becomes

$$E_{Zn} = E_{Zn-Zn^{++}}^0 - 0.0295 \log (Zn^{++}) \quad (V)$$

at 25°C. The equilibrium constant for reaction (III) is

$$K = \frac{(Zn_c)}{(Zn^{++})^x(OH^-)^y(H_2O)^z} \quad (VI)$$

Solving for  $(Zn^{++})$  and substituting in (V),

$$E_{Zn} = E_{Zn-Zn^{++}}^0 - (0.0295/x) \log (Zn_c) \\ + (0.0295/x) \log K + (0.0295y/x) \log (OH^-) \\ + (0.0295z/x) \log (H_2O) \quad (VII)$$

The object now is to evaluate  $x$  and  $y$ . No attempt is made to evaluate  $z$  because it is doubtful whether degree of hydration can be expressed exactly.

If the activities of hydroxyl ions and water are held constant while the activity of the zinc complex ion is varied and the temperature is held at 25°C, equation (VII) assumes the form

$$E_{Zn} = K' - (0.0295/x) \log (Zn_c) \quad (VIII)$$

where  $K'$  includes all the constant terms. This is an equation for a straight line having a slope of  $-0.0295/x$ , from which the value of  $x$  can be determined.

## EXPERIMENTAL

From a stock solution of zinc oxide in aqueous potassium hydroxide, a given amount was pipetted into each of several volumetric flasks. Each sample was then diluted to the mark with a potassium hydroxide solution, a different concentration being used in each flask. This gave a series of solutions in which zinc molarity was the same but hydroxyl ion concentration varied. Several such series were prepared.

Analysis of these solutions for hydroxyl ion concentration was carried out as follows. A known excess of hydrochloric acid was added, and solutions were back-titrated with a standard sodium hydroxide solution. Alkalinity of solutions so determined includes both the free hydroxyl ion concentration and hydroxyl ion content of the zinc complex. The latter must be known to evaluate the former. Since the nature of the zinc complex was not known, several possibilities were considered, e.g.,  $\text{Zn}(\text{OH})_2$ ,  $\text{Zn}(\text{OH})_3^-$ , and  $\text{Zn}(\text{OH})_4^{2-}$ . The value for free hydroxyl ion concentration depends on which of these zinc complexes is assumed to be present. All three possibilities were considered, but these had only a slight effect on the evaluation of  $x$ , as shown below. The mean activity of the hydroxyl ion was determined by applying the data of Akerlof and Bender (5). The assumption is made that the presence of dissolved zinc does not appreciably affect the activity of free hydroxyl ions. All solutions were fairly concentrated with respect to potassium hydroxide so that the zinc complex ion contributed little to the total ionic strength.

A clean zinc electrode and the bridge of a reference electrode consisting of mercury, mercuric oxide, and a 20% potassium hydroxide solution were placed in each solution. The zinc potential was measured against this reference electrode at  $25 \pm 0.2^\circ\text{C}$ . A large scale plot was made of  $E_{\text{Zn}}$  vs.  $\log(\text{OH}^-)$  for each series of solutions. Then a given value of  $\log(\text{OH}^-)$  was chosen, and  $E_{\text{Zn}}$  in each series was read from the graph for this value of  $\log(\text{OH}^-)$ . This gave  $E_{\text{Zn}}$  with varying zinc concentration but constant hydroxyl ion activity. Activity coefficients of the zinc complex were assumed to be the same in all such selected solutions since the ionic strength of these solutions is almost wholly due to free potassium hydroxide. The activity of water was also assumed to be constant in such a case since it is related to hydroxyl ion activity (5). No correction was made for the junction potential between the reference electrode and the solution. This potential depends on hydroxyl ion activity in the solution, and since in plotting  $E_{\text{Zn}}$  vs. zinc ion concentration the hydroxyl ion activity was held constant, all values on such a plot would have been affected by the same amount,

and the slope would have remained unchanged. The varying amounts of zinc ion may have changed hydroxyl ion activity slightly, but for present purposes this effect is assumed to be negligible.

Several values of  $\log(\text{OH}^-)$  were chosen and the results are shown on Fig. 1. Lines for the various series are approximately parallel, the average slope varying from  $-0.031$  to  $-0.029$ , depending on which species of zinc complex is assumed to be present in solution. This gives a value of 1 for  $x$ .

Determination of  $y$  proved to be more difficult. The method finally adopted was as follows. An H-type cell with a sintered glass disk in the cross piece was used. An aqueous solution of potassium hydroxide was placed in one compartment, and a hydrogen electrode was inserted in this solution. In the other compartment was placed a sample of the same potassium hydroxide solution to which some zinc oxide was added, and a clean zinc electrode was inserted. This cell was of the type



and  $E_{\text{cell}} = E_{\text{Zn}} - E_{\text{H}_2}$ , when both electrode reactions are written as oxidation processes. Since zinc oxide concentration was not large in any case, it was assumed that it did not significantly affect the mean hydroxyl ion activity, and thus did not bring about an appreciable junction potential. EMF values for this cell were measured at  $25^\circ \pm 0.2^\circ\text{C}$ . Hydrogen was purified in the usual way, and fresh electrodes were used for each run. Zinc electrodes appeared to behave reversibly since constant and reproducible values were obtained within a few minutes after the zinc electrode was inserted.

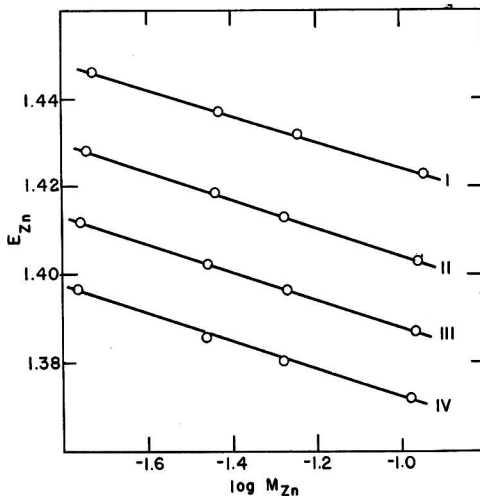


FIG. 1. Variation of  $E_{\text{Zn}}$  with  $\log M_{\text{Zn}}$  at constant hydroxyl ion activity.  $\log a_{\text{OH}^-}$  for curve I is 1.75; curve II, 1.40; curve III, 1.10; curve IV, 0.80.

EMF of the hydrogen electrode was calculated from the mean activity of hydroxyl ion using data of Akerlof and Bender (5); emf of the cell was measured, and  $E_{Zn}$  was calculated from these two values. Several different concentrations of potassium hydroxide were used, and for each concentration a large scale plot was made of  $E_{Zn}$  vs. molarity of the zinc. Then a given molarity of zinc was chosen and  $E_{Zn}$  values for this concentration were read from the plot for various concentrations of potassium hydroxide. Small concentrations of zinc were chosen so that the mean hydroxyl ion activity would not be affected to a large extent. For a constant value of zinc concentration, equation (VII) becomes

$$E_{Zn} = K'' + 0.0295y \log (\text{OH}^-) + 0.0295z \log (\text{H}_2\text{O}) \quad (\text{IX})$$

where

$$K'' = E_{Zn-Zn^{++}}^0 + 0.0295 \log K - 0.0295 \log (Zn_c) \quad (\text{X})$$

Equation (IX) has three unknowns in it:  $K''$ ,  $y$ , and  $z$ .

To evaluate these, certain values were assumed for  $z$  and inserted in equation (IX). The most reasonable values for  $z$  seemed to be 2, 3, or 4. Upon substituting these in equation (IX), the term  $[E_{Zn} - 0.0295z \log (\text{H}_2\text{O})]$  was plotted against  $\log (\text{OH}^-)$ . According to equation (IX) this should give a straight line having a slope of  $0.0295y$ , from which  $y$  can be evaluated. In order to obtain this straight line, however, it is necessary that  $K''$  be constant over the concentration range studied. The only term that might vary with changing hydroxyl

ion concentration is the term  $\log (Zn_c)$ . It is possible that the activity coefficient of this species of ion may not be constant over this range of ionic strengths, even though the molarity of the species is a constant. However, when the term

$$[E_{Zn} - 0.0295z \log (\text{H}_2\text{O})]$$

is plotted against  $\log (\text{OH}^-)$ , reasonably straight lines are obtained (see Fig. 2). Using the slopes of these lines to evaluate  $y$ , one obtains values varying from 3.86 to 4.06. This means that the zinc-containing ion is a divalent zincate ion, and it substantiates the work of Kunschert (4).

Some idea as to the role of water in the formation of this zinc complex may also be determined by the use of equation (IX). As far as water is concerned there are three possibilities: (a) it is a reactant, and equation (IX) is correct; (b) it is a product, and the last term in equation (IX) becomes

$$[-0.0295z \log (\text{H}_2\text{O})];$$

(c) it is neither product nor reactant, and the last term in equation (IX) drops out. The correct possibility can be determined by choosing several  $E_{Zn}$  values at constant  $\log (Zn_c)$ . In plotting  $E_{Zn}$  vs.  $\log (\text{OH}^-)$  the lines obtained will bend toward the  $\log (\text{OH}^-)$  axis at higher values of  $\log (\text{OH}^-)$  if the water is a reactant. These lines will bend toward the  $E_{Zn}$  axis if water is a product, and the lines will be straight if water is neither product nor reactant. Several such lines are shown on Fig. 3. These all bend toward the  $\log (\text{OH}^-)$  axis indicating that water is a reactant rather than a product in the formation of the zinc complex.

At lower hydroxyl ion activities, the activity of water is high and is approaching a constant value. From equation (IX) then, it is evident that as the activity of the hydroxyl ion approaches zero, the slope of the lines in Fig. 3 should become straight

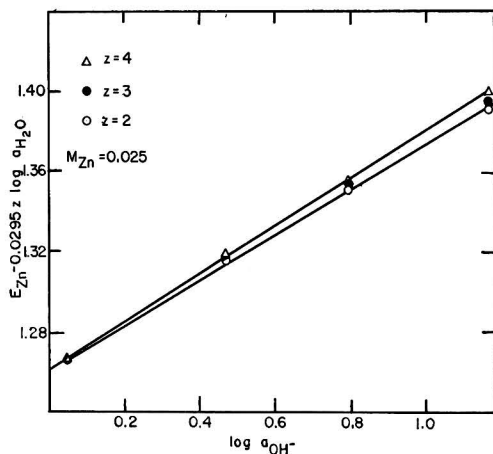


FIG. 2. Variation of  $E_{Zn} - 0.0295z \log (\text{H}_2\text{O})$  with  $\log a_{\text{OH}^-}$ . The mean activity of the  $\text{OH}^-$  ion in KOH solutions is used.

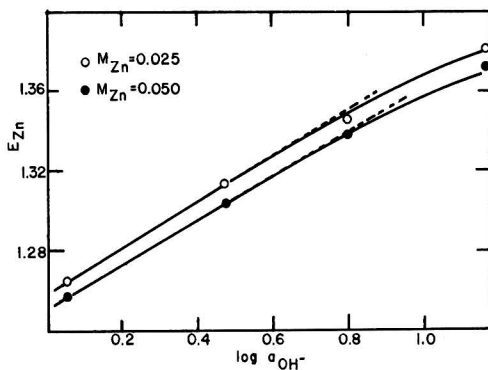
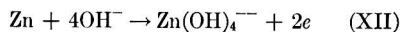


FIG. 3. Variation of  $E_{Zn}$  with  $\log a_{\text{OH}^-}$ . The mean activity of the  $\text{OH}^-$  ion in KOH solutions is used.

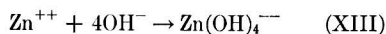


and should be a multiple of 0.0295. These limiting slopes are about 0.116, which approaches 0.118, the value the slope should have if  $y$  has a value of 4. This is a check on the value of  $y$  as determined above.

Having thus determined the values of  $x$  and  $y$ , equation (I) becomes



Making an appropriate plot, the value of  $E^0$  for this reaction is found to be 1.211 volts. From this,  $\Delta F_{298}^0$  for this reaction is  $-55.85$  kcal. Using the accepted free energy values for the hydroxyl ion,  $\Delta F_{298}^0$  for the zinc complex ion is  $-206.2$  kcal. Substituting this value and other standard free energy values,  $\Delta F_{298}^0$  for reaction (XIII) is  $-20.7$  kcal and the formation constant



of the zinc complex from  $\text{Zn}^{++}$  is  $1.4 \times 10^{15}$ . This is about half the value given by Latimer (6). However,

he makes the assumption that water is a product of the reaction rather than a reactant.

#### ACKNOWLEDGMENT

The author wishes to acknowledge with thanks the help of Mr. S. Schuldiner and Drs. J. J. Lander and Carl Wagner in the preparation of this paper, and the generosity of the Office of Naval Research in giving financial support to this work.

Any discussion of this paper will appear in a Discussion Section, to be published in the December 1954 issue of the JOURNAL.

#### REFERENCES

1. J. H. HILDEBRAND AND W. G. BOWERS, *J. Am. Chem. Soc.*, **38**, 785 (1916).
2. H. T. S. BRITTON, *J. Chem. Soc.*, **127**, 2120 (1925).
3. G. BODLÄNDER, *Ber.*, **36**, 3933 (1903).
4. F. KUNSCHERT, *Z. anorg. Chem.*, **41**, 337 (1904).
5. G. C. AKERLOF AND P. BENDER, *J. Am. Chem. Soc.*, **70**, 2366 (1948).
6. W. M. LATIMER, "Oxidation Potentials," p. 156, Prentice-Hall, Inc., New York (1938).



## SURFACE REACTIONS OF STEEL IN DILUTE $\text{Cr}^{+6}\text{O}_4$ SOLUTIONS: APPLICATIONS TO PASSIVITY

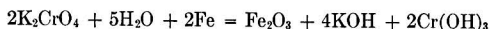
R. A. Powers and Norman Hackerman (pp. 314-319)

M. J. PRYOR<sup>1</sup>: The adsorption theory of inhibition by chromate has undergone several modifications since it was first suggested. Originally<sup>2</sup> it was supposed that inhibition was simply due to adsorption of a monolayer of chromate ions, "in such a manner that they satisfied the secondary valency forces of the iron ions but did not disrupt the metal lattice." Even in the earlier work of Uhlig<sup>2</sup> it was admitted that films thicker than a monomolecular layer were formed during passivation, but no protective action was ascribed to them. In view of the fact that the authors are now postulating adsorption of chromate ions on top of an incomplete oxide layer as well as adsorption on bare and presumably anodic areas, it would appear pertinent to determine what sound experimental evidence there is to support the adsorption theory of inhibition. The crux of any argument between an adsorption theory and a film theory of inhibition can be stated as follows. If inhibition is due to a monolayer of adsorbed chromate ions, then passivation of an originally film-free iron surface should yield only a "film" of monomolecular thickness. If, however, it can be demonstrated that an appreciably thicker film is formed, then it is clear that an adsorbed monolayer is not preventing corrosion since thickening of the film can only occur if the monolayer is not protective; if this is the case, inhibition must be ascribed to causes other than adsorption. With this in mind, it is apparent that the authors could have performed more critical experiments by starting with film-free iron surfaces instead of iron surfaces already carrying an air formed oxide film.

It has been shown by means of electron diffraction<sup>3</sup> that passivation of initially film-free iron specimens by solutions of potassium chromate resulted in the formation of thin films composed mainly of  $\gamma\text{-Fe}_2\text{O}_3$ ; the thickness of the films appeared to increase with increasing time of exposure of the specimens to the passivating solution and, after two days' immersion, achieved an estimated thickness of 150 Å–200 Å, based on the apparent surface area of the specimens. The thickness of passivity films calculated on the real surface area of the specimens was undoubtedly less, probably around 50 Å–70 Å, but there is absolutely no doubt that they were considerably thicker than a monolayer. For instance, films could be detached from the metal by a suitable film stripping reagent and were then visible to the naked eye. They could be handled relatively easily and could be mounted on small grids and identified by electron diffraction. Identification of

stripped films was supported by electron diffraction identification of the films while still attached to the metal<sup>3</sup> and has later been confirmed, using a stripping technique which permits isolation of passivity films without bringing specimens into contact with air after passivation.<sup>4</sup> Since the isolation of films was carried out in air-free nonaqueous solutions there was no chance of film formation during the stripping process.

Films formed by chromate, on examination by normal electron diffraction methods, show no constituent other than oxide.<sup>3</sup> This means that any second phase is present in amounts less than approximately 10%. Other work<sup>5</sup> has shown that chromium, either as chromic compounds or as chromate, is undoubtedly present but in smaller amounts than the stoichiometric quantity expected from a reaction such as:



Evidently the major portion of the passivity film is formed by the heterogeneous interaction of dissolved oxygen and the iron surface, despite the fact that the rate of interaction of chromate ions with ferrous ions in neutral solutions is greater than that of dissolved oxygen and ferrous ions. It has been suggested<sup>6</sup> that the function of the chromate is largely confined to repairing those areas where the oxide film is discontinuous. It is agreed that the first step in this localized film repairing is the absorption of chromate ions into the steel surface. It is believed, however, that the reaction does not stop at this point but is followed by oxidation of the iron and reduction of the chromate ion.

Distribution of chromium in passivity films has not been previously determined; consequently, the work of the authors is timely. However, distribution of ferric phosphate in passivity films formed in sodium orthophosphate<sup>7, 8</sup> and of lepidocrocite in films formed in sodium hydroxide<sup>9</sup> has been investigated. Both of these are anodic inhibitors and, although they are nonoxidizing anions with respect to iron, it has been suggested that the mechanism of inhibition is not dissimilar to that of chromate.<sup>6</sup> The size of the inclusions of ferric phosphate and lepidocrocite is of the order of 1–2  $\mu$  in diameter

<sup>3</sup> J. E. O. MAYNE AND M. J. PRYOR, *J. Chem. Soc.*, **1949**, 1831.

<sup>4</sup> M. J. PRYOR, Unpublished work.

<sup>5</sup> D. M. BRASHER AND E. R. STOVE, *Chemistry & Industry*, **1952**, 171.

<sup>6</sup> M. J. PRYOR AND M. COHEN, *This Journal*, **100**, 203 (1953).

<sup>7</sup> M. J. PRYOR, F. BROWN, AND M. COHEN, *This Journal*, **99**, 452 (1952).

<sup>8</sup> J. W. MENTER, *Compt. rend. du Premier Congrès International de Microscopie Electronique Paris (1950)*; Editions de la *Rev. opt. Paris* (1952).

<sup>9</sup> J. E. O. MAYNE, J. W. MENTER, AND M. J. PRYOR, *J. Chem. Soc.*, **1950**, 3229.

<sup>1</sup>Kaiser Aluminum & Chemical Corporation, Spokane, Wash.

<sup>2</sup>H. H. UHLIG, *Offic. Dig. Federation of Paint & Varnish Production Clubs*, **313**, 660 (1952).

and they were present in amounts of between 2-10% of the passivity film (excluding a few results on acid washed surfaces in solutions on the borderline between passivity and inhibition where the phosphate contents were higher). The distance separating the inclusions was, on the average, between 5-7  $\mu$ . Whereas it cannot be assumed arbitrarily that distribution of chromium compounds would be on a similar scale, convincing evidence concerning the distribution of these compounds in passivity films will not be obtained unless experiments, sensitive enough to pick up heterogeneity on this scale, are carried out. This is not easy to do by radioautographic means, since heterogeneity of the nature indicated above would be equivalent to a large number of point sources separated by very small distances (5-7  $\mu$ ).

Therefore, there are two questions that I would like to ask the authors on their radioautographs. These are:

1. What was the magnification of the radioautograph of the passive surface?
2. What was the emulsion thickness and approximate grain size of the plate used for the radioautograph of the passive surface?

The exclusion of these details from the experimental section makes it difficult to determine the value of the radioautograph of passive surfaces. To prove conclusively that the distribution of activity is homogeneous, the grain size of the emulsion would have to be of the order of 2-3  $\mu$  and the emulsion thickness of the same order. To the best of my knowledge, characteristics of this nature can only be obtained by painted emulsions which, I believe, are not produced commercially. Plates of highest resolving power available commercially have a resolving power of the order of 1000 lines/mm. These plates might be just sensitive enough to detect heterogeneity of the nature indicated above when examined under high magnification.

It may be that the radioautographic techniques used by the authors were carried out in this manner; if they were, their conclusions are valid; if such was not the case, the arguments advanced in the discussion are unconvincing.

Two other points in this paper require some qualification. Firstly, the reference to the work of Robertson<sup>10</sup> on tungstate and molybdate is misleading. It was pointed out in the discussion to this paper<sup>11, 12</sup> that tungstate and molybdate had been proved to be nonoxidizing anions only in 1N sulfuric acid which has a considerable stabilizing influence on ferrous ions. Experiments reported in this discussion<sup>11</sup> and later published in the JOURNAL<sup>6</sup> show that tungstate and molybdate have mild oxidizing properties toward ferrous ions in neutral solutions where they are effective as anodic inhibitors. Unlike chromate, however, they are not sufficiently powerful oxidizing agents to inhibit corrosion in deaerated solutions.

Secondly, I would like to ask the authors why they measured contact potentials instead of solution potentials. It is granted that the interpretation of either measure-

ment is not easy, but the interpretation of contact potentials would seem to suffer from the additional disadvantage that specimens have to be removed from the passivating solution and exposed to the atmosphere before a measurement can be made. Is there, therefore, some special advantage to contact potential measurement which outweighs this disadvantage?

To sum up these comments, it is evident that during the last ten years a considerable volume of experimental work on anodic inhibitors has been carried out. To explain these observations in a satisfactory manner requires, of necessity, a relatively comprehensive theory; to say inhibition is due to adsorption, or to precipitation, or to film-formation is not enough. It must be shown how a particular theory best explains the available data. It appears that the adsorption theory is not consistent with a large volume of data published by many other corrosion investigators. Few will disagree that adsorption of chromate ions at anodic areas is one step in the inhibitive process. However, the writer disagrees that the reaction stops at this point, but believes that adsorption of chromate takes place only at small anodic areas and is followed by oxidation of the iron and reduction of the inhibitor anion.

R. A. POWERS AND NORMAN HACKERMAN: In answer to Dr. Pryor's specific questions, the radioautographs shown were actual size, and were taken at various times during the investigation on both Kodak nuclear track plates and Kodak No-Screen X-ray film. The particular radioautograph shown for a passive surface was obtained using x-ray film, and was specified as showing only the apparent uniform distribution of Cr<sup>51</sup>. There was no pretense of having shown uniformity on an absolute scale, nor would one expect it in view of the heterogeneous nature of surfaces and surface reactions. One should not confuse the term "monolayer" with absolute uniformity, since "layers" exist primarily as the result of calculations based on values of absolute surface area and mass of reactant retained on the surface. We refer rather to "equivalent monolayers" which implies no predetermined distribution. Note also that the distribution of activity was not one of the seven factors on which our conclusions were based.

The measurement of contact potential has the inherent advantage that it measures irreversible changes in the electrical properties of a surface independently of the media or conditions producing the change. They can thus be more directly related to the structure or composition of the surface than can solution potentials. Contact potential measurements also permit comparison of surface conditions before and after exposure to passivating or other environments, which solution potentials do not. They may also be applied to gaseous and nonaqueous systems. It is true that transfer of specimens from passivating solution to air for measurement produces secondary changes in potential. In fact, measurement of contact potentials in dry, oxygen-free nitrogen, shows that secondary changes such as these can be minimized.<sup>13</sup> However, in the case of steel from chromate solutions,

<sup>13</sup> L. L. ANTES AND N. HACKERMAN, *J. Appl. Phys.*, **22**, 1395 (1951).

<sup>10</sup> W. D. ROBERTSON, *This Journal*, **98**, 94 (1951).

<sup>11</sup> M. J. PRYOR AND M. COHEN, *This Journal*, **98**, 513 (1951).

<sup>12</sup> P. DELAHAY, *This Journal*, **98**, 514 (1951).

these changes were slow enough to follow with ease and were always constant in magnitude, so that there is no valid reason to question the significance of the values used.

The reported work on the passivation of iron and steel by chromates is primarily limited to experiments of three types: (a) oxide-free surfaces and solutions containing dissolved air; (b) air oxidized surfaces and deaerated solutions; or (c) air oxidized surfaces and solutions containing dissolved air. In the references cited by Dr. Pryor, and in his discussion of the subject paper, there are no explicit statements or descriptions of film stripping and electron diffraction work with both oxide-free surfaces and deaerated solutions.

Hackerman and Hurd<sup>14</sup> have reported on the reaction between steel and deaerated dichromate-acetic acid solutions. In these solutions, up to 60% of the original dichromate (300–450 ppm) was reduced before the rate of reduction leveled off after 90–100 hr. In the presence of air, however, there was no measurable change in dichromate concentration and no apparent change in appearance of the steel in contrast to the dark reddish-brown film formed in air-free solutions.

These data illustrate the point that there is no necessity, and perhaps no valid reason, to postulate a universal mechanism for the passivation of steel by hexavalent chromium. The authors have advanced a mechanism which is derived from, and self-consistent with, the behavior of oxide-bearing steel and chromium in dilute chromium-VI solutions containing dissolved oxygen—the most common condition under which passivity is observed. If one admits the possibility that the heterogeneous reaction between iron and dissolved oxygen takes precedent over any reaction between iron and chromium-VI,<sup>14, 15</sup> then the concept of inhibitor adsorption onto an oxidized surface applies to the cases cited by Dr. Pryor for oxide-free surfaces and aerated chromate solutions.<sup>16</sup>

The amounts of chromium found firmly fixed to a passive steel or chromium surface were such that one would not expect them to be detected by normal electron diffraction examination of stripped oxides, so that in this sense we agree with the experiments of Mayne and Pryor.<sup>16</sup> The  $48 \times 10^{-8}$  gram of chromium retained per cm<sup>2</sup> of oxide-bearing steel surface passivated in  $1 \times 10^{-3}M$  sodium chromate of pH 7.5 corresponds to approximately 8% of the weight of a  $\gamma$ -Fe<sub>2</sub>O<sub>3</sub> film 200 Å in thickness. In this connection, it is worth pointing out that the amount of chromium retained by an oxide-bearing steel surface passivated in chromium-VI solutions is a sensitive function of solution pH, and possibly other variables. Hence, one is not justified in making inclusive statements regarding the amount of chromium that should or should not be associated with such surfaces. For example, little

or no firmly fixed chromium is associated with steel surfaces passivated in  $10^{-3}M$  chromate solution of pH 11, while approximately  $100 \times 10^{-8}$  g/cm<sup>2</sup> are retained at pH 4. In the case of chromium surfaces in  $10^{-4}M$  solution, retention of chromium from solution is limited not only by pH, but by the ratio of surface to solution volume, and the concentration of anions such as sulfate and chloride.<sup>17</sup> Data like these call attention to the fact that, in order to have meaning, any statement made concerning the character of a passive surface should be carefully modified by the conditions under which passivation was produced, e.g., state of the initial surface, solution concentration, pH, oxygen content, etc.

#### ANODIC FORMATION OF COATINGS ON MAGNESIUM, ZINC, AND CADMIUM

Kurt Huber (pp. 376–382)

H. J. WRIGHT<sup>18</sup>: What are the compositions of some of the anodically formed coatings on magnesium?

How are these affected by traces of chlorides, phosphates, sulfides?

We need to know if the metal oxides on magnesium are resistant to polyphosphates, etc., under anodic conditions.

KURT HUBER: The experiments described in my paper dealing with the anodic behavior of magnesium were performed in solutions prepared with purest NaOH. Therefore, no predictions can be made at present concerning the effect of traces of chlorides, phosphates, and sulfides on these anodically formed coatings.

However, Flückiger in his doctoral research work [Reference (2) of my paper] investigated the anodic formation of coatings on magnesium in aqueous solutions of Na<sub>3</sub>PO<sub>4</sub> and NH<sub>4</sub>F as well as in various polishing baths. After isolation, the composition of these coatings was determined by x-ray and electron diffraction methods.

In 4*N* Na<sub>3</sub>PO<sub>4</sub>, coatings were formed in which MgO, Mg(OH)<sub>2</sub>, and occasionally Mg<sub>3</sub>(PO<sub>4</sub>)<sub>2</sub>·4H<sub>2</sub>O could be detected. MgO predominated, particularly with short formation periods (1 min at 10–40 volts), while Mg(OH)<sub>2</sub> became the principal component after longer formation periods. In an analogous manner, MgO, Mg(OH)<sub>2</sub>, and MgF<sub>2</sub> were formed in 2*N* NH<sub>4</sub>F solution.

The change in composition of the coatings with increasing periods of anodic treatment seems to indicate in these cases as well that MgO is produced as the primary product, and that then in a subsequent reaction it is hydrated or converted to an insoluble salt. In a polishing bath containing 375 ml H<sub>3</sub>PO<sub>4</sub> (*d* = 1.71) and 625 ml absolute alcohol, coatings containing MgO and Mg(OH)<sub>2</sub> were formed. At higher voltages corresponding to those employed for anodic polishing, magnesium phosphate was also occasionally formed. However, MgO was always the predominant component.

<sup>14</sup> N. HACKERMAN AND R. M. HURD, *This Journal*, **98**, 51 (1951).

<sup>15</sup> M. J. PRYOR AND M. COHEN, *This Journal*, **100**, 203 (1953).

<sup>16</sup> J. E. O. MAYNE AND M. J. PRYOR, *J. Chem. Soc.*, **1949**, 1831.

<sup>17</sup> N. HACKERMAN AND R. A. POWERS, *J. Phys. Chem.*, **57**, 139 (1953).

<sup>18</sup> Socony-Vacuum Oil Company, 26 Broadway, New York, N. Y.

## FACTORS AFFECTING THE TRANSFORMATION TO GRAY TIN AT LOW TEMPERATURES

R. R. Rogers and J. F. Fydell (pp. 383-387)

F. A. LOWENHEIM<sup>19</sup>: The authors are to be complimented on a most interesting study of a question which appears to be again attracting considerable attention. I question, however, whether the grade of tin which they used for their experiments should be called "commercial." I have no criticism of using for research work the purest materials which can be found but, considering that rather small amounts of impurities appear to have large effects on the phenomenon the authors are studying, it may be well to point out that grades of tin available commercially may behave quite differently from that which the authors designate as commercial. For example, the authors' tin contained 0.0005% antimony; commercial tin may contain up to 80 times this amount and still be designated Grade A. Similarly, the authors' tin contained 0.0005% lead; the maximum specification for Grade A is 100 times this amount. Similar remarks would hold for the other impurities cited by the authors. Details of the specification for Grade A tin and for typical analyses of all the leading brands may be found in "Metal Statistics 1952" published by the American Metal Market, page 451. It would be interesting if the authors could fit into their program a study of more typical commercially available tin.

The effect of zinc is of particular interest in view of commercial possibilities of the tin-zinc alloy deposit. It may be pointed out that, although the very small amounts of zinc the authors have studied appear to accelerate the phase transformation, some work which is in progress in the United States shows that zinc in considerably larger amounts acts as an inhibitor. In fact, electrodeposits of the 80% tin-20% zinc alloy show little or no tendency to transform, even when inoculated, after a testing period of six months. I recognize, of course, that 20% zinc is no longer an impurity, but the reversal of the trend should be noted, and it might be interesting to investigate the range of tin-zinc alloy compositions to find at what percentage of zinc this reversal occurs.

R. R. ROGERS AND J. F. FYDELL: In describing the tin used in these experiments we stated that two of the three types were obtained from ordinary commercial sources. It was left to the reader to decide whether or not such tin should be called "commercial."

We agree with Dr. Lowenheim that the composition of commercial tin varies over a comparatively wide range, and the tendency to form gray tin is very different in different parts of this range. This was demonstrated clearly in the present investigation. As stated in our paper, when a small amount of copper was added to Type I tin, containing 0.0005% antimony and 0.0005% lead, the average  $m$  value of the resulting material was 0.342 at  $-29^{\circ}\text{C}$ . On the other hand, when a similar amount of copper was added to Type II tin, containing 0.015% antimony and 0.009% lead, the average  $m$  value was only 0.006 at the same temperature.

We agree also with Dr. Lowenheim's statement that, although a small amount of zinc tends to accelerate the transformation to gray tin, a larger amount of zinc actually acts as an inhibitor. This is brought out clearly by the following data taken from Table IV of our paper:

Composition of tin	$m$ Value
Type I tin + 0.019% zinc.....	0.130
Type I tin + 0.037% zinc.....	0.115
Type I tin.....	0.07
Type I tin + 0.05% zinc.....	0.020

It would appear that the  $m$  value of Type I tin with the addition of approximately 0.040% of zinc would be the same as that of Type I tin alone. When smaller zinc additions (as 0.019 or 0.037%) are made to the tin, the  $m$  value tends to be greater than that figure, but when larger zinc additions (as 0.05%) are made, the  $m$  value tends to be less.

## ATTEMPTS AT THE ELECTROLYTIC INITIATION OF POLYMERIZATION

H. Z. Friedlander, Sherlock Swann, Jr., and C. S. Marvel (pp. 408-410)

GARRETT W. THIESSEN<sup>20</sup>: Relative to reluctance of "free radicals" R·COO, to leave the anode in the Kolbe aqueous electrolysis, work is in progress at Monmouth College, doing the acetate electrolysis between Pt plates at variable frequency. At 60 cycles, only very small amounts of H<sub>2</sub> only are found; even at 1 cycle, the yield of Kolbe gas is highly inhibited. We infer that the CH<sub>3</sub>·COO radical coheres within itself, and adheres to the electrode, for times of the order of one second.

No comment from the authors.

## STRUCTURAL FEATURES OF OXIDE COATINGS ON ALUMINUM

F. Keller, M. S. Hunter, and D. L. Robinson (pp. 411-419)

CHARLES L. FAUST<sup>21</sup>: This is a very interesting discussion to one interested in anodic processes. The electron microscope pictures are certainly excellent.

The quality in eye appeal of an electrobrightened-, anodized-, and dyed-aluminum surface is better than that of abrasively finished and buffed aluminum that is anodized and dyed. This situation suggests that the nature of the starting surface is influential in determining the characteristics of the oxide formed in anodizing. The authors' comments on this point would be of interest.

How does surface distortion, strain, and cold work influence the character of oxide coating vs. that of oxide coating over the nonworked, nonstrained, and undistorted electrobrightened surface?

<sup>20</sup> Monmouth College, Monmouth, Ill.

<sup>21</sup> Battelle Memorial Institute, Columbus, Ohio.

<sup>19</sup> Metal & Thermit Corporation, Rahway, N. J.

The authors state that the ideal electrobrightening treatment would be one in which the oxide layer was dissolved as fast as it was formed. Morize, Lacombe, and Chandron<sup>22</sup> report that aluminum electropolished in perchloric-acetic acid bath has no oxide coating. As evidence of this, the electrode potentials are cited. Assuming that this claim of no oxide is correct, would such an electrobrightened aluminum surface anodize to different oxide-cell size, pore dimensions, etc., than a surface electrobrightened, but containing a thin oxide film or "smudge?" The thin oxide is mentioned on page 418, left column, of the Keller, Hunter, and Robinson paper.

F. KELLER, M. A. HUNTER, AND D. L. ROBINSON: While the appearance of anodically coated and dyed aluminum surfaces is dependent on the nature and characteristics of the starting surface, we believe that such differences in appearance are not related to the cell and pore dimensions of the oxide coating. In the case of surfaces which are abrasively finished and buffed, the dull appearance is generally attributed to particles of abrasive or buffing compound which have been incorporated into the surface layer of metal. It is doubtful that surface distortion, strain, or cold work influence the dimensions of the oxide cells because no differences in oxide structure have been observed between coatings applied to annealed aluminum and those applied to hard rolled aluminum.

We would expect a thin oxide film or "smudge" remaining after an electrobrightening treatment to have little or no effect on the dimensions of an anodic oxide film applied subsequently, particularly if the anodic film was of appreciable thickness. When an anodic coating is applied to an aluminum surface which already has an anodic coating applied in a different electrolyte and under different conditions, there is a relatively rapid transition from the cell structure characteristic of the initial coating to that characteristic of the final coating. The time required for this transition is a function of current density and is apparently only slightly longer than that required to establish the cell and pore pattern initially. Thus, the presence of a thin oxide layer remaining from an electropolishing treatment would have no significant effect on the pore and cell dimensions of the major portion of the anodic coating. Inasmuch as such a layer would remain on the outer surface of the anodic layer, however, some difference in appearance might result.

#### DETERMINATION OF CURRENT EFFICIENCY OF DIAPHRAGM ALKALI-CHLORINE CELLS BY GAS ANALYSIS

M. S. Kircher, H. R. Engle, B. H. Ritter, and A. H. Bartlett (pp. 448-451)

RALPH M. HUNTER<sup>23</sup>: I am wondering if you have ever compared the quantities of the three products collected, i.e., measure the collected chlorine and correct for chlorate, chlorine losses in the brine, and other undesired reactions; collect the caustic soda, making corrections for impurities; and collect the hydrogen. Under these conditions, you should account for 35.5 grams of Cl<sub>2</sub>, 40 grams of NaOH,

<sup>22</sup> P. MORIZE, P. LACOMBE, AND G. CHANDRON, *Compt. rend des J. des Etats de Surface*, **34**, 242 (1945).

<sup>23</sup> The Dow Chemical Company, Midland, Mich.

and 1 gram of H<sub>2</sub>. It occurs to me that this might be an excellent method for studying cell operation.

M. S. KIRCHER: In normal plant operation, the quantities of chlorine, caustic soda, and hydrogen produced are measured. It is because of the inaccuracies of these measurements as carried out on a plant scale that the gas analysis measurement of current efficiency was devised.

It would be relatively simple to conduct the measurements which Dr. Hunter suggests on a single cell. We have not done this, but consider that it should be done if a further investigation, such as that done earlier,<sup>24</sup> were undertaken.

#### THE ELECTROCHEMISTRY OF THE FIRST LAYERS OF ELECTRODEPOSITED METALS

T. Mills and G. M. Willis (pp. 452-458)

J. O'M. BOCKRIS<sup>25</sup>: Values obtained by Mills and Willis for the capacity on silver electrodes seem very high indeed.<sup>26</sup> It would be of the utmost interest to learn if these authors could obtain any solid evidence with regard to hydrogen atom adsorption from their charging curves; the position in this respect is particularly ambiguous with respect to silver.

T. MILLS AND G. M. WILLIS: Our capacities are comparable with those found by Veselovsky for etched silver (350-400  $\mu\text{F}/\text{cm}^2$ ). We also find similar variations in capacity with the state of the surface, which may be attributed to changes in surface area. We agree with Dr. Bockris that the capacities, even after allowing for a high ratio of real to apparent surface, seem high. This appears to be generally true of the double layer capacities of solid metals when compared with that of mercury. Measurement of true surface area would be of assistance in interpreting results. It is possible that reduction of surface oxide or deposition of adsorbed hydrogen contributes to the high measured capacity.

We have no definite evidence for hydrogen adsorption on silver. The second arrest in alkaline solutions which was found by Veselovsky (and which we have confirmed) was ascribed by him to a strongly bound oxide film. From changing curves *alone* it is not possible to distinguish an oxide film which can only be reduced at highly cathodic potentials from an adsorbed hydrogen film. Removal of oxygen with simultaneous deposition of adsorbed hydrogen is another possibility which cannot be excluded from consideration.

#### SOME PROPERTIES OF TIN-II SULFATE SOLUTIONS AND THEIR ROLE IN ELECTRODEPOSITION OF TIN

II. Solutions with Tin-II Sulfate and Sulfuric Acid Present

C. A. Discher (pp. 480-484)

A. H. DU ROSE<sup>27</sup>: Dr. Graham has suggested the use of fluoride in the sulfate bath to prevent sludging. It has

<sup>24</sup> R. L. MURRAY AND M. S. KIRCHER, *Trans. Electrochem. Soc.*, **86**, 83 (1944).

<sup>25</sup> John Harrison Laboratory, University of Pennsylvania, Philadelphia, Pa.

<sup>26</sup> Cf. Y. VESELOVSKY, *Acta Physicochim.*, **11**, 815 (1939).

<sup>27</sup> The Harshaw Chemical Company, Cleveland, Ohio.

been our experience that, while fluoride will prevent sludging for a time, dependent on the fluoride concentration, it does so by holding the Sn-IV in solution, and the rate of formation of Sn-IV is faster in the presence of fluoride. The effect of Rochelle salts is similar. Copper and iron in the solution accelerate the formation of Sn-IV.

C. A. DISCHER: During my work with Dr. Mathers, we conducted a series of experiments with the sulfate bath in which hydrofluoric acid was substituted for sulfuric acid.<sup>28</sup> Under the conditions used, sludging was not a problem even over relatively long periods of time. However, this approach was discontinued since its merit was not considered sufficient to overcome certain disadvantages inherent in the fluoride type of bath.

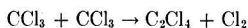
#### MECHANISM OF REACTION OF ALUMINUM AND ALUMINUM ALLOYS WITH CARBON TETRACHLORIDE

Milton Stern and Herbert H. Uhlig (pp. 543-552)

H. G. OSWIN<sup>29</sup>: It would seem that further investigation should be carried out before any reaction mechanisms can be proposed for this system.

While the presence of certain "inhibitors" appears to prevent the initiation of the reaction, this only indicates that the initial steps involve free-radical mechanisms; it does not preclude the possibility of a chemical reaction in later stages. This could, of course, be checked by addition of inhibitors to the system at suitable time intervals.

Presence of C<sub>2</sub>Cl<sub>6</sub> as the sole organic end product is surprising, since other authors,<sup>30</sup> working with systems likely to contain CCl<sub>3</sub> radicals, have failed to detect any hexachloroethane. It seems more likely from this other evidence that C<sub>2</sub>Cl<sub>4</sub> is usually formed,<sup>31</sup> possibly with the formation of chlorine, in some such disproportionation as:



Bowen and Rohatgi,<sup>32</sup> working in the liquid phase, also do not report the formation of any C<sub>2</sub>Cl<sub>6</sub>.

I should also like to know the ratio of the end products C<sub>2</sub>Cl<sub>6</sub>/AlCl<sub>3</sub>. This would probably provide a very good indication of the mechanism.

Presumably, in the proposed mechanism the chain-propagating process is  $\text{AlCl}_3 + \text{CCl}_4 \rightarrow \text{AlCl}_3^+ [\text{CCl}_3]^- + \text{Cl}$ . The induction period of the reaction is then affected by the concentration [AlCl<sub>3</sub>]. It would be interesting to observe how the addition of AlCl<sub>3</sub> to the system would affect the induction period.

Finally, it would be worthwhile investigating the reaction from a photochemical viewpoint to see whether it could be initiated by a direct photolysis or a photosensitized method.

<sup>28</sup> F. C. MATHERS AND C. A. DISCHER, *Proc. Indiana Acad. Sci.*, **56**, 141 (1946).

<sup>29</sup> National Research Council, Ottawa, Ontario, Canada.

<sup>30</sup> H. SCHUMACHER AND K. WOLFF, *Z. physik. Chem.*, **B25**, 161 (1934).

<sup>31</sup> H. F. SMYSER AND H. M. SMALLWOOD, *J. Am. Chem. Soc.*, **55**, 3499 (1933).

<sup>32</sup> E. J. BOWEN AND K. K. ROHATGI, *Disc. Faraday Soc.*, **14**, 146 (1953).

MILTON STERN AND H. H. UHLIG: Many of the questions raised by Mr. Oswin are answered directly in the text of the paper. For example, compounds effective as inhibitors were found also effective after the reaction had started, as is described on page 550. Also, detailed discussion of the effect of aluminum chloride on the induction period is found on page 541 and in reference (1). There is, of course, no difference between the reaction mechanism we propose and that of a chemical reaction, and we feel that sufficient data have now been assembled to establish that the reaction depends on a chain sequence in which free radical species participate.

We did not state in our paper that C<sub>2</sub>Cl<sub>6</sub> is the sole organic reaction product, but only that our work, confirming other investigators, proves it to be the major product. However, as we have indicated in the abstract and also in the text beginning page 550, it would be quite unusual, if not exceptional, to find a free radical reaction which produces no side products. Accordingly, a complex residue of by-products was found, but no measurable quantities of chlorine were evolved during the reaction. It should be emphasized that where reactions with lower activation energy are possible, trichloromethyl radicals may be consumed by processes other than dimerization (formation of C<sub>2</sub>Cl<sub>6</sub>). This is generally the case in the systems which Oswin has quoted. On the other hand, Melville, Robb, and Tutton<sup>33</sup> have shown that trichloromethyl radicals may be involved in dimerization as the predominant termination reaction, or they may react with other available species, depending on the concentrations and substances present. For the aluminum-carbon tetrachloride reaction, where no third organic material is available for combination with trichloromethyl radicals, it is readily understood why hexachloroethane is the major end product.

We agree that the reaction should prove fruitful from the standpoint of the photochemist, and hope that sometime this phase of the problem will be investigated by those familiar with photochemistry.

W. W. SMELTZER<sup>34</sup>: Stern and Uhlig suggest that vacuum treatment at 400°C for 7 hr does not damage the oxide film on aluminum and, thus, will not account for the shorter delay in the aluminum-carbon tetrachloride reaction. It has not been established whether the crystalline structure of the oxide may have an effect on the duration of this induction period. Heating at 400°C may cause crystallization of the amorphous oxide to gamma-alumina, as the diffraction studies of Brouckère<sup>35</sup> show that this crystalline form of alumina occurs in the oxide film after 6 hr of heating in air at 400°C. Also, Hass<sup>36</sup> found that gamma-alumina crystals form at temperatures less than 400°C on the (III) face of evaporated oriented aluminum films, although a temperature of 450°C was required to

<sup>33</sup> H. MELVILLE, A. ROBB, AND R. TUTTON, *Disc. Faraday Soc.*, **14**, 150 (1953).

<sup>34</sup> Aluminium Laboratories Limited, Kingston, Ontario, Canada.

<sup>35</sup> L. DE BROUCKÈRE, *J. Inst. Metals*, **71**, 131 (1945).

<sup>36</sup> G. HASS, *Optik*, **1**, 134 (1946).

initiate crystallization of the amorphous oxide on polycrystalline aluminum films.

It has been suggested by Hass<sup>37</sup> that this crystallization of the oxide may produce cracks in the oxide film. If this is valid, then the decrease in induction time for specimens heated at 400°C in vacuum may be partially caused by formation of a less protective film by crystallization of the amorphous oxide.

The conclusion of Stern and Uhlig that water and, perhaps, oxygen in the oxide are probably responsible for the induction period, would be strengthened if it is proven that crystallization of the amorphous oxide does not occur with heating of specimens at 400°C in vacuum for 7 hr, or if specimens with either an amorphous or crystalline thin oxide film exhibit the same characteristic behavior.

MILTON STERN AND H. H. UHLIG: In answer to W. W. Smeltzer, heating the oxide film on aluminum undoubtedly causes some structural changes, including recrystallization and perhaps the production of cracks. However, these changes do not explain decrease of the induction period after vacuum treatment. For example, similar oxides heated in air would be expected to undergo a similar structural change; yet, for specimens so treated, the induction period is either the same or somewhat greater than for the untreated specimens. Increase in thickness of oxide films on heating does not balance any supposed loss of protection through structural change, because anodized films equal to or thicker than the oxide films produced by heating are also not very effective in extending the induction period. On the other hand, our experiments show clearly the marked effect of water and oxygen on delaying the reaction. Since natural oxide films on aluminum contain water and perhaps oxygen as well, both of which are removed by vacuum treatment, it is more likely that these factors account for the observations rather than a mechanism based on cracking of the film.

M. J. PRYOR<sup>38</sup>: The authors have presented an interesting interpretation of their data on the corrosion of aluminum alloys in carbon tetrachloride by suggesting that the reaction is initiated by the formation of  $\cdot\text{CCl}_3$  free radicals. The  $\cdot\text{CCl}_3$  free radical is one that has been generated with relative ease in carbon tetrachloride solutions by photolysis. If the interaction of aluminum and carbon tetrachloride proceeds by a free radical mechanism, then it should be possible to initiate the reaction by photolysis. Have any experiments of this nature been carried out by the authors?

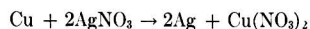
MILTON STERN AND H. H. UHLIG: We agree with M. J. Pryor that there should be considerable effect of radiation on the reaction, and that studies of this kind would be both interesting and valuable. Although we excluded light from the reaction vessels in which our experiments were carried out, we made no systematic effort to determine the magnitude of the effect.

### RATE OF DISPLACEMENT OF SILVER FROM AQUEOUS SILVER NITRATE BY ZINC AND COPPER

Richard Glicksman, H. Mouquin, and Cecil V. King (pp. 580-585)

H. J. AXON AND P. A. CARTWRIGHT<sup>39</sup>: We were particularly interested in this paper since we have recently studied the reaction between solid copper and aqueous  $\text{AgNO}_3$  solution under static conditions, and have also done a few experiments with rotating specimens of the type described by King and his coworkers. In the "rotating specimen" experiments, using a copper cylinder with peripheral speed 4500  $\text{cm min}^{-1}$  (900 rpm) and 0.1M  $\text{AgNO}_3$ , we found that silver tended to adhere to randomly distributed areas of the rotating copper, thus producing erratic values of  $k$ . When the rotating specimen was continuously scraped with a light glass scraper, a consistent value of 0.78 was obtained for the rate constant  $k$ . Considering the different concentration and geometry in the two investigations, this value is in reasonable agreement with Fig. 4 of the paper.

We would also like to relate the results of our experiments with "stationary" specimens to some of the gaps in the literature which have been pointed out in the paper. For stationary conditions we have found that the replacement process in the  $\text{Cu}/0.1\text{M AgNO}_3$  system may be described by the equation



to an accuracy better than 1%, in general, the actual loss of weight of solid copper being 1% greater than that calculated from an analysis of the silver ions remaining in solution. We are convinced that most of this discrepancy is due to the mechanical loss of small particles of copper from the corroded specimen, but have detected the simultaneous evolution of hydrogen during the reaction. Special care is required to detect this hydrogen, since in our experiments we estimate that the deposition of 1 gram of metallic Ag is associated with the evolution of only  $\sim 2$  ml  $\text{H}_2$  at N.T.P.

A further possible, but again small, contribution to the 1% discrepancy noted above is associated with the redeposition of copper onto previously deposited silver. We suspect that this redeposition of copper takes place at cathode areas of differential aeration cells, the anode process of which would be the solution of copper from the main specimen. It is certain that artificially accentuated differential aeration increases the amount of redeposited copper. Spectrographic tests of the silver crystals before and after washing with dilute  $\text{HNO}_3$  show that the copper deposit is superficial, and microscopic examination of the silver crystals suggests that the copper is deposited onto actively growing surfaces of the depositing silver, and, having deposited, prevents further growth of silver on that particular surface.

RICHARD GLICKSMAN, H. MOUQUIN, AND CECIL V. KING: We are very much pleased with the information supplied by H. J. Axon and P. A. Cartwright, which adds materially to the available knowledge about these displacement reactions.

<sup>39</sup> Metallurgy Department, University of Manchester, Manchester, U. K.

<sup>37</sup> G. HASS, *Verhandl. deut. physik. Ges.*, **22**, 1 (1941).

<sup>38</sup> Kaiser Aluminum and Chemical Corporation, Spokane, Wash.





## The Problem of Correct Thermal Insulation of Bottom Linings of Aluminum Furnaces

J. Wleugel<sup>1</sup> and O. C. Böckman<sup>2</sup>

### Introduction

Designers of aluminum furnaces are well aware that the thermal insulation of bottom linings for aluminum furnaces must be adjusted to the intended operating conditions of the furnaces, viz., current density of the anode, furnace voltage, and the distance between the anode and the metal bath acting as cathode. In this paper, a theoretical analysis of the problem is attempted, based on some measurements on operating furnaces and on thermochemical data for the reduction of alumina to aluminum metal.

### Stating the Problem

The main characteristics of furnace operation are: (a) furnace voltage, in this paper designated  $E$ ; (b) total direct current  $I$ , and the current density of the anode  $I/A$ ; (c) distance between the anode and metal bath, designated  $d$ ; (d) current efficiency, designated  $s$ ; (e) specific energy consumption, expressed in kw-hr/kg metal produced, designated  $r$ .

These five quantities are naturally interrelated and their relationships involve certain electrochemical and physical quantities: (f) heat of reaction, or change of enthalpy, of the cell reaction



(g) change of free energy, or equivalently, the equilibrium decomposition voltage of  $\text{Al}_2\text{O}_3$  under operating conditions; (h) effects of irreversibilities, or overvoltage; (i) different ohmic voltage drops: in the outer circuit (bus bars), in the anode and cathode, and in the electrolytic bath between the anode and cathode; (j) heat generation accompanying these different ohmic voltage drops; and (k) different heat losses of the furnace: heat conducted through the furnace bottom lining, through the anode, radiant heat losses from the bath especially when charging the alumina, and the heat content of anode gases and metal produced.

Two main aspects of the problem have to be discussed: (A) the energy balance of the furnace, and (B) actual voltage drops.

While a knowledge of the actual voltage drops is required to arrive at a true picture of the electrolytic process, the problem of correct heat insulation is solved mainly by proper application of the energy balance.

Heat losses represent a waste of energy, and any reduction in the heat losses per kg metal produced naturally turns out to be a gain in the energy efficiency of the process. By increasing the thermal insulation, heat losses may be reduced. However, the practical operation of the furnace imposes certain limitations as to the amount of insulation that may be applied.

A reduction in heat losses requires an equivalent reduction

in heat generation in order to maintain the correct temperature of the bath. Generation of heat may be regulated mainly by regulating the distance between anode and cathode, and by regulating the total current, or, equivalently, the current density of the anode.

With a given current density, the effect of a reduction of heat generation by reducing the anode-cathode distance is complicated by a second phenomenon, viz., the current efficiency will simultaneously be reduced, especially at low values of anode-cathode distances. A reduction in current efficiency naturally will result in an increase in specific energy consumption.

Thus we find that two effects are opposed: when reducing the anode-cathode distance, the heat generated is reduced, which permits an increase in thermal insulation, but, at the same time, the current efficiency is reduced. It will be demonstrated that minimum specific energy consumption is obtained when these two opposing effects are properly balanced. Calculation of the conditions for the proper balancing of the two opposing effects provides means for the determination of the correct thermal insulation of aluminum furnaces.

In the discussions to follow, actual voltage drops will be calculated to arrive at a true picture of the process. Aspects of current efficiency have then to be considered, and lastly an energy balance will be set up to demonstrate the conditions for the minimum specific energy consumption.

### Actual Voltage Drops

Actual voltage drops of a number of 33-kamp and 18-kamp furnaces have been determined in the following manner.

By constant current the anode is lowered successively until complete short-circuiting and the furnace voltage at different positions of the anode is noted. It is presumed that measurements are carried out so rapidly that the cell does not change its temperature during measurements. Measurements of different furnaces, all of them operating at the same current density, show a remarkable conformity. A good average of the measurements is given in Fig. 1.

It is seen that at first the furnace voltage decreases along a straight line as the anode is lowered. At a certain point, a sudden voltage drop of about 1.6 volts is observed. By further lowering the anode, a slight decrease in furnace voltage is noted until a constant value of about 1.4 volts is obtained.

This voltage characteristic of the furnace may be explained by assuming that direct contact between the anode and the metal bath at first is obtained in a single point, or at least in a restricted area. When this contact is established, electrolysis is interrupted and the voltage drop observed corresponds roughly to the decomposition voltage of the electrolysis. Complete short-circuiting is obtained when the total working surface of the anode is in direct contact with the metal bath, this condition being established by further lowering of the anode. The short-circuiting voltage of the furnace thus pro-

<sup>1</sup> A/S Norsk Aluminium Company, Oslo, Norway.

<sup>2</sup> Elektrokemisk A/S, Oslo, Norway.

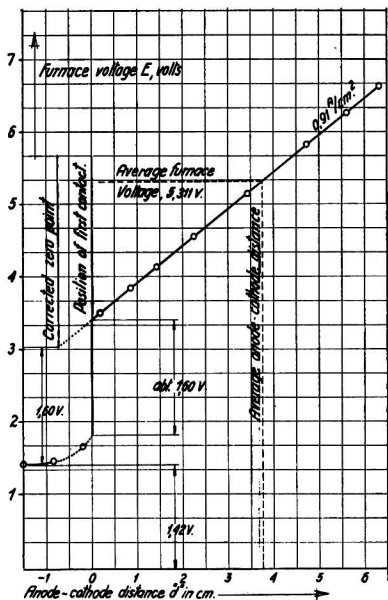


FIG. 1. Average experimental voltage characteristic of 33 kamp and 18 kamp aluminum furnaces.

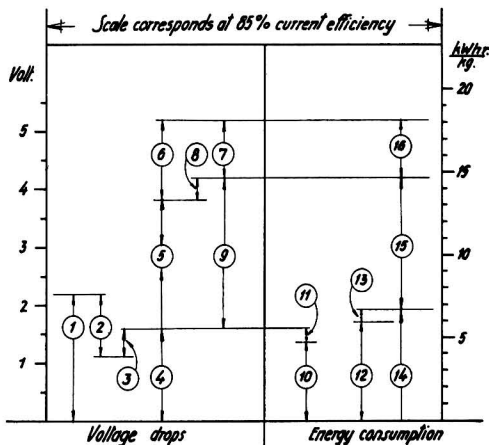


FIG. 2. Energetics of alumina reduction. 1—Decomposition voltage of alumina; 2—depolarizing effect of carbon; 3—over-voltage; 4—actual decomposition voltage; 5—voltage drop in bath; 6—voltage drop in current supply; 7—waste voltage drop in current supply; 8—useful voltage drop in current supply; 9—total useful voltage drop; 10—energy equivalent of decomposition voltage; 11—energy equivalent of current losses; 12—heat of reaction; 13—heat content of metal and gases; 14—total heat requirements of reaction; 15—useful heat generation; 16—waste heat generation in current supply.

vides a value for the combined voltage drops in anode and cathode, with their outer circuit for current supply. It is seen that this value is about 1.4 volts.

The measured value 1.6 volts for decomposition voltage checks well with measurements made by other investigators (1-3). It may be worth while to notice, however, that this value includes effects of irreversibilities, known as overvoltage. Calculations by the third law of thermodynamics (1, 4-7), as well as direct measurements in laboratory (1, 2, 6, 8, 9) have established the decomposition voltage of alumina at 1000°C to be about 2.2 volts. The depolarizing effect of the

carbon anode may be calculated from the free energy of formation of CO and CO<sub>2</sub> to be about 1.1 volts (7). The equilibrium value of the decomposition voltage is then 2.2 - 1.1 = 1.1 volts, which, compared with the measured values of 1.6 volts, shows an overvoltage of about 0.5 volt.

Combining the short-circuiting voltage and the actual decomposition voltage, we get 1.4 + 1.6 = 3.0 volts, while the furnace voltage usually is 4.5-5.0 volts. The difference is made up of the voltage drop in the electrolytic bath between the anode and the metal bath acting as a cathode.

These voltage relationships are demonstrated in Fig. 2.

### Current Efficiency

By the normal operation of aluminum furnaces aluminum is deposited with a current efficiency of 85-90%. No completely satisfactory theory has as yet been put forward to explain the mechanism of current losses. Grünert (10) and Pearson and Waddington (9) have given evidence for the view that current losses are caused by a simultaneous deposition of sodium metal. Possibly, monovalent aluminum may exist in the cryolite bath, and in some way play a part in current losses.

Fortunately, a knowledge of the mechanism of current losses is not needed for this analysis. Here it is enough to know the magnitude of current losses, and the variation of current losses with the distance between the anode and the aluminum bath acting as cathode.

Current losses also depend on the temperature and composition of the bath, and possibly on other factors. These factors do not affect our problem, as we postulate constant temperature and composition of the bath and consider other possible factors also to be unaltered.

In our calculations, current density is varied, and possibly variation in current density may affect the current efficiency of the electrolysis. At the moment, we have no data, however, to demonstrate this effect, and for this reason we consider current efficiency to be independent of current density. For our analysis, then, current efficiency may be considered to depend only on the anode-cathode distance.

It is well known that current efficiency decreases rapidly as this distance is lowered under a critical value of about 4 cm. Naturally, determination of current efficiency at different anode-cathode distance is difficult, as the measurements require operation of the furnace over a period of time sufficiently long, during which it is difficult to maintain constant operating conditions. The following figures have been obtained, however.

Distance anode-metal bath	Determined current efficiency	Values used for later calculations
cm	%	%
3	72-76	73
3.75		83.0
4	84-89	85
5	89-94	90
6	91-95	92
7	92-96	92.5

The distance between anode and metal bath given above is measured by lowering the anode until the first contact with metal bath is obtained. No zero point correction is introduced here (see Discussion of zero point correction).

As will be seen, the measured values allow for a fairly wide latitude. Accordingly, values selected for our calculations are somewhat uncertain, but, at the moment, we have no better values.

### Energy Balance

When setting up an energy balance with the aim of providing means for calculating the conditions of minimum specific energy consumption, three main groups of energy dissipations must be distinguished.

#### Heat of Reaction

Energy consumed by the electrode reaction is equivalent to the heat of the net cell reaction



The heat of reaction depends on the composition of anode gases. With a gas composition of 65% CO<sub>2</sub> and 35% CO, the authors have calculated the heat of reaction at 1000°C to be 276.0 kcal/gram mole of alumina (7). This corresponds to 5.94 kwhr/kg Al. The sensible heat content of anode gases and of produced metal is a permanent loss and may logically be added to the heat of reaction. This addition amounts to 0.73 kwhr/kg Al under the assumed operating conditions, giving a total of 6.67 kwhr/kg Al.

For any furnace operating under these conditions, the energy consumed by the electrochemical reaction may be found by multiplying the number of kg metal produced with 6.67 kwhr/kg Al. To be correct, for furnaces operating under other conditions, viz., with other anode gas compositions, a slight correction of this value has to be introduced. This correction, however, is so small that in this paper it is neglected.

Actual decomposition voltage, multiplied by total direct current through the furnace, and by current efficiency, may be interpreted as the power input to the furnace directly converted to chemical energy. This power input may, by dividing with the metal production, be expressed as a specific energy consumption, and gives the figure 4.77 kwhr/kg Al. This figure, being less than the energy requirements of reaction, shows that a part of the energy requirements of the reaction must be supplied from other sources. Assuming that the power input associated with the current losses is fully recovered as useful heat and a current efficiency of 85%, which gives an additional energy supply, corresponding to 0.83 kwhr/kg, we get a total of 5.60 kwhr/kg. Even this figure is less than the energy requirements of the reaction. The difference, or 1.07 kwhr/kg, must then be supplied by heat generated by ohmic resistance, mainly in the bath.

This comparison of energy requirements of the reaction with actual decomposition voltage is demonstrated in Fig. 2.

#### Generation of "Useless Heat"

The power input to the furnace, not required for covering the heat of reaction and the sensible heat of anode gases and metal produced, is dissipated to the surroundings as heat losses. The power input, which corresponds to the voltage drops in the anode and cathode, in part contributes toward heating the electrolytic bath, and in part it is generated where it may be considered to be of no use. The short-circuiting voltage of the furnaces measured is 1.4 volts, which corresponds to the combined voltage drops of anode and cathode. Of this, we may estimate that 0.4 volt will contribute to the heating of the bath and 1.0 volt generates useless heat.

For measured furnaces we get the power input generating useless heat by multiplying this 1.0 volt by the total current.

#### Generation of "Useful Heat"

Total power input to the furnace may be calculated by multiplying the total furnace voltage by the total furnace current. By subtracting from the total power input the items

calculated under heat of reaction and generation of useless heat, we get the heat generation necessary to maintain the correct temperature of the bath. This power input is dissipated as heat losses from the furnace bottom by heat conduction through the furnace lining and by radiant heat losses from the bath, especially during the charging of alumina.

The heat generation equivalent to this power input may be called the generation of "useful heat," as this heat generation is effectively utilized in keeping the bath at correct temperature.

It will be seen that we now have arrived at a quantity very important for our reasoning. By using data from furnaces in actual operation, the generation of useful heat may be calculated for this particular installation and operating conditions. We may then calculate the effect of changing the operating conditions, or of changing the heat insulation of the furnace bottom on the specific energy consumption.

### Specific Energy Consumption

The following data serve as basis for our calculations.

A number of 33-kamp furnaces of the same design operating under the same conditions have for a long period of operation produced metal with a specific energy consumption of 19.1 kwhr/kg, as calculated from the weight of metal produced and the readings of the kwhr-meter of the series. Unfortunately, no kamp hr- or kvolt hr-meter were used, but frequent readings of the total series current and voltage established a reasonable value for the current efficiency to be 83.0%.

It may be shown that current efficiency  $s$ , specific energy consumption  $r$ , and furnace voltage  $E$  are related to each other by the equation

$$E = 0.3354 \cdot r \cdot s$$

when  $E$  and  $r$  are expressed in volts and kwhr/kg, respectively, and  $s$  is given as a fraction. The measured values given above then correspond to an average furnace voltage of 5.31 volts, which checks well with the average voltage of the series according to the frequent readings.

These figures, by the nature of their derivation, include the time when anode effects occur. During the anode effects the power input to the furnace is greatly increased, which, to a large extent, is converted into useful heat. For our purpose then it seems logical to include the time when anode effects occur, and the figure 5.31 volts will be used as an average furnace voltage.

According to the voltage characteristic of the furnace (Fig. 1), this average furnace voltage corresponds to an average distance between anode and cathode of 3.75 cm. This checks well with actual measurements of this distance for the furnaces in question as measured by lowering of the anode until the first contact with the metal bath.

It is not quite correct to use the average furnace voltage in combination with the voltage characteristic of Fig. 1 since the former includes anode effects and the latter is based on the normal operation of the furnaces. The main purpose of our investigation is, however, to demonstrate the effect of changing the operating conditions on specific energy consumption. It is felt that, although theoretically not correct, this simplification does not invalidate our conclusions as to the effects of changing the operating conditions. It must be stressed, however, that the actual figures given refer to this particular installation and the general methods of attendance used. For other installations and methods of attendance, other figures will result. It is thought, however, that the trend

of the figures may be more generally valid. To demonstrate this trend is the main purpose of our investigation.

We then arrive at the following fundamental data for the furnaces measured:

Furnace voltage, $E$ . . . . .	5.31 volts
Current, $I$ . . . . .	33.0 kampf
Current density, $I/A$ . . . . .	0.91 amp/cm <sup>2</sup>
Current efficiency, $s$ . . . . .	83.0 %
Specific energy consumption, $\tau$ . . . . .	19.1 kwhr/kg
Average anode-cathode distance, $d$ . . . . .	3.75 cm

By using these data and the furnace characteristic shown in Fig. 1, together with the relationship found between current efficiency and anode-cathode distance, we may construct lines showing the specific energy consumption at different total currents, or, equivalently, at different current densities. Thermal insulation is supposed to be unaltered. To maintain the correct temperature of the bath, the change in total current has to be compensated for by an equivalent change in anode-cathode distance, to give a constant generation of useful heat.

Suppose the thermal insulation is changed to give a different loss of heat at correct temperature of the bath. We may then repeat our calculations with the new value for the generation of useful heat.

In the calculations to follow, the 33-kampf furnaces, which have supplied the fundamental data, are supposed to operate at different operating conditions and with different thermal insulation of the furnace bottom. Similar calculations may be performed using data obtained from the operation of furnaces of other designs and of other sizes, generation of necessary useful heat being naturally dependent on furnace design and on furnace size as well as on the method of furnace attendance.

To carry out these calculations, we must first determine the generation of useful heat with the normal heat insulation of the furnace. This is done in the following manner:

Furnace current	= 33.0 kampf
Current efficiency	= 83.0%
Metal production 33.0 kampf · 0.83 · 0.3354 kg/kampf hr	= 9.18 kg/hr
Heat of reaction 9.18 kg/h · 6.67 kwhr/kg	= 61.1 kw
"Useless heat" generation 1.00 volt · 33.0 kampf	= 33.0 kw
By addition	94.1 kw
Furnace voltage	= 5.31 volt
Total power input 5.31 volts · 33.0 kampf	= 175.2 kw
Useful heat generation by difference 175.2 - 94.1	= 81.1 kw
Specific energy consumption 175.2 kw/9.18 kg/h	= 19.1 kwhr/kg.

Our calculations are carried out for five different cases:

(A) The insulation of the furnace bottom is reduced, necessitating 40% increase in the generation of useful heat, or a total generation of useful heat of  $81.1 \cdot 1.40 = 113.7$  kw.

(B) 20% increase of said heat generation, or  $81.1 \cdot 1.20 = 97.4$  kw.

(C) Normal insulation.

(D) 20% reduction of said heat generation by properly increased insulation, giving  $81.1 \cdot 0.80 = 64.9$  kw.

(E) 40% reduction of said heat generation, giving  $81.1 \cdot 0.60 = 48.7$  kw.

The voltage characteristic is naturally influenced by the current density of the electrolysis. The observed voltage characteristic, at a current density of 0.91 amp/cm<sup>2</sup>, therefore has to be transformed to voltage characteristics at other current densities.

This transformation raises the problem of the choice of correct zero point for the distance between the anode and the metal bath. Obviously, the first point of contact is not the correct zero point because this point indicates the minimum distance which is less than the average distance.

A reasonable correction for the zero point may be obtained

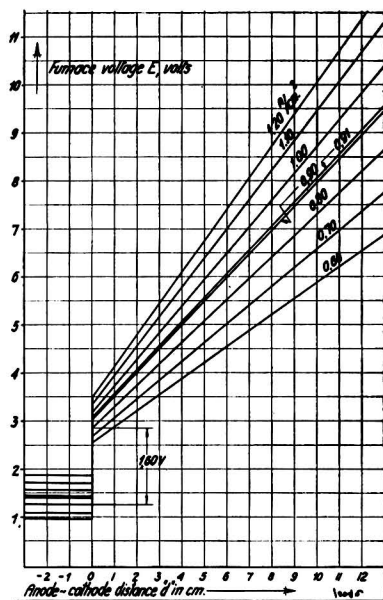


FIG. 3. Voltage characteristics of different current densities, corrected zero point.

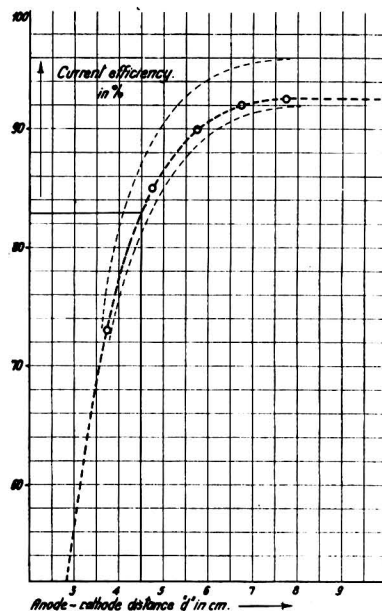


FIG. 4. Current efficiency, viz., anode-cathode distance, corrected zero point.

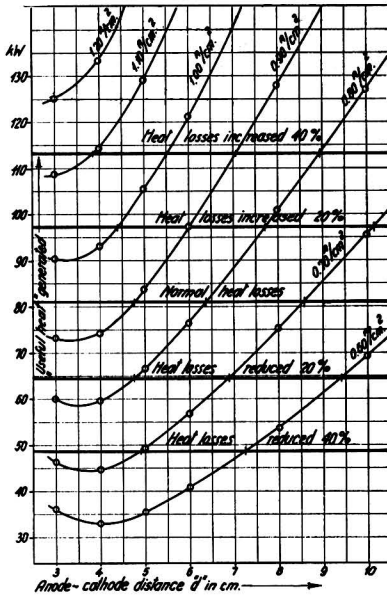


FIG. 5. Comparison of useful heat generated and heat losses from bottom lining.

in the following manner. The short-circuiting voltage may be considered as representing the voltage drops in the current supply under normal operating conditions. By adding the actual decomposition voltage, we arrive at  $1.4 + 1.6 = 3.0$  volts, which should be the furnace voltage at zero distance just before contact between anode and metal is obtained, assuming plane surfaces. By extrapolating the straight line of the voltage characteristic (Fig. 1) down to 3.0 volts, we arrive at a zero point correction of 0.75 cm. This correction is applied in all the later calculations.

The voltage characteristics at different current densities are given in Fig. 3. It may be seen from this figure that the short-circuiting voltage too is influenced by a change in current density. It is assumed that a constant proportion of the short-circuiting voltage is contributing to the generation of useful heat.

The current efficiency at different distances between the anode and metal bath with zero point correction introduced is given diagrammatically in Fig. 4.

By repeating the calculation of useful heat generation, assuming different current densities and different anode-cathode distances, we arrive at Fig. 5. From this graph, the correct anode-cathode distance may be found for different values of useful heat generation, corresponding to different thermal insulations of the furnace.

In this manner, an energy balance is set up for every hypothetical operation of the furnace indicated by the circles of Fig. 5. For the same hypothetical operating conditions, the specific energy consumption is calculated as given by the open circles in Fig. 6. The dotted lines indicate the current densities.

For each current density and furnace insulation (Fig. 5) the correct anode-cathode distance giving the correct generation of useful heat is noted and these values are introduced into Fig. 6, black circles. The circles representing the same furnace insulation are connected by fully drawn lines. These

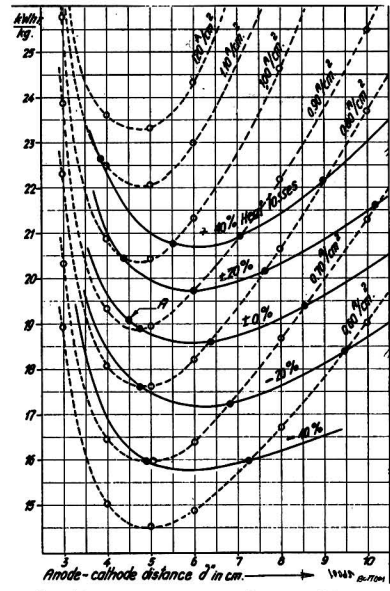


FIG. 6. Specific energy consumption at different current densities and different heat losses from furnace bottom.

lines then represent the actually possible operating conditions of the furnace without altering the insulation.

The operating conditions of the furnaces that have provided the fundamental data are represented in Fig. 6 by the black circle marked A.

### Discussion

From Fig. 6 it may be seen how the two opposing effects act. At small distances between the anode and the metal bath the specific energy consumption increases rapidly with a decrease in this distance. This effect is caused by the rapid decrease in current efficiency with a decrease in the anode-cathode distance at low values of this distance.

On the other hand, specific energy consumption increases but slowly with an increase in the anode-cathode distance above 6-7 cm, at constant insulation.

It may be seen further that an increase or a decrease in the amount of insulation applied imposes a change in operating conditions with accompanying changes in specific energy consumption. An increase in furnace insulation generally tends to reduce specific energy consumption. This increase in furnace insulation has to be compensated for by a decrease in anode-cathode distance or in current density. If the anode-cathode distance, however, turns out to be small, the increased insulation may result in an increase in specific energy consumption, as indicated by the left side of Fig. 6. This fact points to the danger of overinsulating the furnaces.

For a given installation, a change in current density results in a change in metal production. When considering the application of the relationship given in Fig. 6 to an installation actually operating, the problem of total metal production must be paid due attention.

When planning new installations, however, the relationships given may serve as a guide in the choice of proper operating data. With a given total metal production, the choice of current density will influence the linear dimensions of the furnaces, and consequently the installation costs. A

balance must here be struck on economic considerations of installation cost, viz., cost of operation.

Results of this analysis may, naturally, be anticipated by common sense and practical experience. It is thought, however, to be of some value to give a quantitative evaluation of the relationships to supplement the qualitative reasoning of common sense and practical experience.

#### References

1. M. DE K. THOMPSON AND R. G. SEYL, *Trans. Electrochem. Soc.*, **64**, 321 (1933).
2. I. W. CUTHBERTSON AND J. WADDINGTON, *Trans. Faraday Soc.*, **32**, 745 (1936).
3. G. MORITZ, U. S. Dept. of Commerce PB 70023, March 8, 1944.
4. P. DROSSBACH, *Z. Elektrochem.*, **34**, 206 (1928).
5. P. DROSSBACH, *ibid.*, **36**, 179 (1930).
6. W. D. TREADWELL AND L. TEREBSI, *Helv. Chim. Acta*, **16**, 922 (1933).
7. National Bureau of Standards, Selected Values of Chemical Thermodynamic Properties, Series III.
8. P. DROSSBACH, *Z. Elektrochem.*, **40**, 605 (1934).
9. T. G. PEARSON AND J. WADDINGTON, *Discussions Faraday Soc.*, **1**, 307 (1947).
10. E. GRÜNERT, *Z. Elektrochem.*, **48**, 393 (1942).



## News Notes in the Electrochemical Field

### Gordon Research Conferences, August 16-20

The Gordon Research Conferences, sponsored by the American Association for the Advancement of Science, for 1954 will be held from August 16-20 at New Hampton School, New Hampton, New Hampshire.

The Gordon Research Conferences were established to stimulate research in universities, research foundations, and industrial laboratories. This purpose is achieved by an informal type of meeting consisting of the scheduled lectures and free discussion groups. Sufficient time is available to stimulate informal discussions among the members of a Conference. Meetings are held in the morning and in the evening, Monday through Friday, with the exception of Friday evening. Afternoons are available for recreation, reading, resting, or participation in discussion groups as the individual desires.

The purpose of the program is not to review the known fields of chemistry, but primarily to bring experts up to date as to the latest developments, analyze the significance of these developments, and to provoke suggestions as to underlying theories and profitable methods of approach for making new progress. In order to protect individual rights and to promote discussion, it is an established rule of each Conference that all information presented is not to be used without specific authorization of the individual making the contribution, whether in formal presentation or in discussion. No publications are prepared as emanating from the Conferences.

The morning sessions, Monday through Friday, are scheduled from 9:00 A.M. to 12:00 Noon, Eastern Daylight Saving Time. The second session of each day is held in the evening from 7:30 to 10:00 P.M., Monday through Thursday. There are no Friday evening meetings.

Individuals interested in attending the Conference are requested to send applications to the Director. Each ap-

plicant must state the institution or company with which he is connected and the type of work in which he is most interested. Attendance at each Conference is limited to 100. Communications should be addressed to W. George Parks, Director, Department of Chemistry, University of Rhode Island, Kingston, Rhode Island. From June 15 to September 1, 1954, mail should be addressed to Colby Junior College, New London, New Hampshire.

Shown below are the programs for the 1954 Conference on the Chemistry and Physics of Metals.

#### Chemistry and Physics of Metals

G. J. Dienes, *Chairman*  
J. C. Fisher, *Vice Chairman*

##### Mechanical Properties of Metals

###### *Monday, August 16*

- H. Brooks—Electronic Theory of Cohesion and Elastic Constants.
- C. Wert—Anelasticity of Metals.
- J. R. Low—Microstructure and Fracture.
- E. W. Hart—Role of Dislocations in Plastic Deformation.
- B. E. Warren—X-Ray Measurements of Cold Work Distortion.
- M. Bever—Stored Energy.

###### *Tuesday, August 17*

- E. Parker—Work Hardening and Substructure.
- J. Washburn—Work Hardening and Substructure.
- R. W. Cahn—Mechanical Twinning.
- H. B. Huntington—Variation of Elastic Constants with Temperature and Pressure.
- R. W. Powers—Internal Friction due to Impurities.

###### *Wednesday, August 18*

- E. Montroll—Frequency Spectrum of Vibrations of Crystal Lattices.

- A. Nowick—Internal Friction Effects Produced by Dislocations.
- L. Zernow—Plastic Deformation and Fracture at Very High Strain Rates.
- T. H. Blewitt and R. R. Coltman—The Deformation of Copper Single Crystals.
- C. E. Dixon—Low Temperature Irradiation and Plastic Deformation.
- R. H. Pry—Electrical Resistivity.

###### *Thursday, August 19*

- J. H. Koehler—On the Production of Vacancies and Interstitials during Cold Work.
- J. J. Gilman—Cooperative Dislocation Motion.
- F. C. Frank—Dislocation in Real Crystals.
- K. Lucke—Strain Hardening in Face Centered Cubic Metals.

###### *Friday, August 20*

- R. Truell—The Use of Ultrasonics in the Study of Solid State Problems.
- T. Vreeland, D. S. Wood, and D. S. Clark—Delay Time in Yielding.
- R. Smoluchowski—Structure of Grain Boundaries.

### Annual Meeting of Engineering Educators

Over 1,500 engineering educators will attend the Annual Meeting of the American Society for Engineering Education on June 14-18 at the University of Illinois, Urbana, Ill. Educators and distinguished engineers from other countries who are visiting in the United States are cordially invited to attend this meeting.

The meetings will include conferences sponsored by the Engineering College Administrative Council and the Engineering College Research Council, which are two component organizations of the ASEE. The theme of the conference this year, "Evaluation of Engineering Education," will feature a thorough analysis of all phases of engineering education. This will conclude

a two-year study on Evaluation of Engineering Education undertaken by the society.

The Engineering College Research Council and Engineering College Administrative Council will hold a joint dinner to commemorate the 50th Anniversary of the founding of Engineering Experiment Stations in engineering colleges, a movement which has contributed very substantially to research progress in this country. The speaker at this dinner will be Dr. Lee DuBridg, President of California Institute of Technology.

There will be over 100 individual conference programs arranged by the numerous divisions, committees, and councils of the society.

Foreign guests who wish to attend the Conference should write to Professor Robert K. Newton, ASEE Housing Chairman, University of Illinois, Urbana, Ill., for information and reservations.

### **Pennsalt Chemicals Creates New Operating Divisions**

To provide more logical product grouping, better customer service, and a suitable pattern of organization for expected future growth, the Pennsylvania Salt Manufacturing Company will establish two new operating divisions, it was announced by President George B. Beitzel.

These new components—the Industrial Chemicals and Chemical Specialties Divisions—will function as complete operating units responsible for both the manufacture and sale of their respective products. Other units already operating on this basis are the Pennsylvania Salt Manufacturing Company of Washington, Sharples Chemicals Inc., and Pennsalt International Corporation.

The change-over will be made gradually during a period of approximately a year, and most changes will be at top and middle management levels.

### **New G. E. Wire Probe**

A tiny platinum wire one-thirtieth as thick as a human hair is being used at the General Electric Company's Research Laboratory in Schenectady, N. Y., to detect thin films which interrupt electrical contacts between metal surfaces.

Formed into a loop by scientists at the laboratory, the thin wire can be

employed to detect finger prints and other films built up by oxidation or tarnishing. Even invisible films can frequently be detected.

When compressed against a surface, the resilient platinum probe ferrets out films on the most highly buffed and machined surfaces. Measurement of the pressure exerted with a micrometer suggests the type of film present and its electrical strength.

Developed by Robert H. Savage and Dr. Donald G. Flom, the wire probe has been used at times to replace difficult chemical means for analyzing such films. These chemical techniques, it was pointed out, often destroy or damage the surface, while the delicate probe does not affect it.

### **Michigan State Alumni to Meet**

The Michigan State College alumni in the electroplating field are planning a breakfast reunion in connection with the annual meeting of the American Electroplaters' Society, to be held in New York City during July. All former students of Professor D. T. Ewing are invited, together with other alumni who are interested in the electrodeposition of metals. Announcements will be sent to all Michigan State alumni known to be in this field, but since such lists are necessarily incomplete, requests for further notification should be sent in promptly. Reunion plans are being handled by C. Fred Gurnham, Head of the Department of Chemical Engineering, Michigan State College, East Lansing, Mich.

### **Ionic Pump Developed by G. E.**

Two General Electric scientists have built a simple experimental air pump with no moving parts, which can produce a vacuum as high as one billionth of normal atmospheric pressure, similar to that in x-ray tubes and TV picture tubes.

According to Dr. A. M. Gurewitsch and Dr. W. F. Westendorp, of the company's Research Laboratory, Schenectady, N. Y., the device, known as an ionic pump, may eventually simplify exhaustion of radio tubes and other widely-used vacuum tubes in the process of manufacture.

Pumps presently used for the purpose involve streams of oil or mercury vapor, which are not required in the new device.

## **Symposium on Electrochemical Processes and Their Applications to Indian Industry**

A symposium on "Electrochemical Processes and Their Applications to Indian Industry" was held at Karaikudi on March 27 and 28 under the auspices of the Central Electrochemical Research Institute, Karaikudi. It was divided into four sections: (a) electrometallurgy and electrothermal processes, (b) electrolytic processes, inorganic and organic, (c) batteries, electrodeposition and electropolishing, (d) miscellaneous. Nearly 60 papers were presented, covering all the branches of electrochemistry. The members of the India Section of The Electrochemical Society contributed 25 papers; the authors were: A. Joga Rao, S. L. Chawla, H. V. K. Udupa, N. Subramanian, K. Seshadri, V. Aravamuthan, T. Banerjee, T. L. Rama Char, and B. A. Shenoy. Professor M. S. Thacker, Chairman of the India Section, participated in the proceedings.

There was a good gathering drawn from research laboratories, electrochemical industries, and government establishments all over India. The discussions that followed the papers were extremely interesting. The program was rounded off with social functions.

T. L. RAMA CHAR,  
*Regional Editor, India*

---

## **SECTION NEWS**

---

### **Chicago Section**

The Chicago Section held its monthly meeting at the Chicago Engineers Club on Friday, February 5. Dr. Malcolm Dole spoke to the Section on the effects of reactor irradiation on the chemical and physical properties of polyethylene. Despite the prevailing cold weather there was a good turnout of local electrochemists.

Dr. Dole described the experiments he had performed, briefly discussed the equipment involved, and elaborated on the results obtained and the theories involved. In general, reactor irradiation was found to break carbon to hydrogen and carbon to carbon bonds, and to result in a certain amount of increased polymerization and chemical unsaturation of the plastic.

Samples of polyethylene were irradiated in the Argonne National Laboratory CP-3' reactor. Chemical and



physical measurements were made before and after irradiation. Products given off due to irradiation bond rupture included hydrogen and short chain saturated and unsaturated hydrocarbons. The increased chemical unsaturation of polyethylene caused by irradiation was measured by determining the amount of hydrogen which was evolved and by measuring the amount of unsaturation before and after irradiation by the bromine addition reaction.

In the discussion which followed, it was pointed out by Dr. Dole that experimental evidence indicated that a majority of the bonds which were broken were located in the side chains. This led to increased linkages through these short chains, and the development of a higher molecular weight plastic. It was further pointed out that increased polymerization caused increased viscosity and increased the softening and melting point temperatures.

In conclusion, Dr. Dole answered questions raised from the floor and discussed at greater length several theories he had developed relating to the chemical reactions of polyethylene taking place under irradiation.

A. H. ROEBUCK, *Secretary*

### Cleveland Section

The Cleveland Section met on April 13 at the Cleveland Engineering Society. Following the dinner, Mr. Quilan, a representative of the Cleveland Technical Societies Council, spoke on behalf of the proposed new Cleveland Engineering Center.

Dr. L. W. Niedrach of the Knolls Atomic Power Laboratory, Schenectady, was guest speaker. His topic was "Atomic Power, Present and Future." Existing nuclear reactors were described and a comparison made between the homogeneous and heterogeneous types. Dr. Niedrach discussed development work which will be required to achieve an economically feasible reactor, including improvements in design and operation, chemical processing of materials, and utilization of by-products. Atomic energy was considered relative to its position among the world's energy resources. Finally, an interesting comparison was given between a nuclear reactor power plant and a conventional coal powered generating station.

The annual Cleveland Section Award to an outstanding student of the colleges in the Cleveland area was presented at

this meeting. This year the award went to Warren Krause of Cleveland, a student at Western Reserve University.

MERLE E. SIBERT, *Secretary*

### New York Metropolitan Section

The guest speaker for the April 7 meeting of the New York Metropolitan Section was Mr. George F. Weaton, whose subject was "Electrothermic Zinc." The history of electrothermic zinc smelting was reviewed and the process in use at the smelter of the St. Joseph Lead Company at Josephstown, Pa., described.

In 1885 the Cowles Brothers in England attempted to smelt zinc in a small horizontal retort about 10 in. in diameter and 5 ft long, in which the charge of zinc-bearing material mixed with carbon was used as a resistor to supply heat for the reduction. Development work was started in 1893 in Sweden, resulting in a commercial plant built in 1903. By 1918 there were 22 furnaces of 500 hp each in operation. It appears that the major fault with this installation was in the method used to condense the zinc vapors. The best results showed these furnaces using 2.95 kwhr/lb of zinc. Many other people experimented with electric furnaces for smelting zinc and the inefficiency of the available condensers was an important cause of failure.

Development work on the electrothermic smelting of zinc was started by the St. Joseph Lead Company in 1926. Mr. E. C. Gaskill brought to the company a very small model and soon built an 18-in. diameter unit. This furnace was operated for several short periods, and while it was not a successful unit it encouraged the company to build a furnace 48 in. in diameter. The adoption of a rotary table at the bottom solved the problem of disposing of the residue. The top section of the furnace, originally used as a preheater, caused trouble and a separate heater was designed. The furnace was built originally with six electrodes at top and bottom, but these were soon reduced to three. The furnace was later enlarged to 57 in. in diameter. During this time the furnace had been operated to produce zinc oxide.

In the reduction of zinc oxide by carbon, the temperature must reach about 1050°C before the rate of reaction is satisfactory for commercial operation. The vapors produced consist of equal volumes of zinc vapor and carbon

monoxide. Zinc vapor has a great affinity for oxygen, so condensation of metal must be conducted in an atmosphere devoid of oxidizing agents. The further development of the electric furnace depended on the development of an efficient condenser capable of handling the large volume of vapors produced. The vacuum type condenser which was developed by the company made today's large scale production of electrothermic zinc possible.

After the formal talk, slides showing views of the plant at Josephstown were shown and discussed. A film showing the mining and concentration of the ore was also presented.

KENNETH B. MCCAIN,  
*Secretary-Treasurer*

### Washington-Baltimore Section

At the March 18, 1954 meeting of the Washington-Baltimore Section, Dr. Bernard Rubin of the National Bureau of Standards gave an excellent talk on "Galvanic Cells with Fused Salts."

The development of galvanic cells using solid-molten electrolytes was traced from the fuel cell of Jablohoff in 1877 to the present day. Two advantages of these cells were cited: (a) their extended shelf-life while the electrolyte is in the solid state, (b) the compactness and ease of handling as a result of the absence of water. The cell Mg/NaOH/MnO<sub>2</sub>, C was discussed with particular emphasis on the nature of the electrolyte and the nature of the cathode material. A review of the thermodynamic data necessary for calculating emf's of reversible thermal cells was given, and a new electrochemical series for the elements was derived. Several notable exceptions to the aqueous series were pointed out. With the newer sources of heat energy now available, thermal cells show great promise as sources of electrical energy.

FIELDING OGBURN, *Secretary*

Dr. J. O'M. Bockris gave a highly stimulating lecture entitled "Research Vistas in Electrochemistry" at the April 15 meeting of the Washington-Baltimore Section. Dr. Bockris observed that after a period of reduced activity in electrochemical research the field has now become more active again. He ascribed the loss of interest which occurred during the 30's and early 40's to discouragement resulting from the inapplicability of Debye-Huckel Theory

and "Nernstian" thermodynamics to many important electrochemical processes. The application of the kinetic-molecular approach, as typified by the Eyring absolute rate theory, to electrochemical problems has proved fruitful and provided a new impetus to research in electrochemistry.

Examples of how the kinetic-molecular approach has resulted in significant advances in our understanding of hydrogen overvoltage and of the structure of molten silicates were cited.

Dr. Bockris indicated his belief that the kinetic-molecular approach to the electrochemistry of fused salt, non-aqueous systems, and concentrated aqueous solutions will yield new knowledge in the field of solution theory and structure of ionic liquids.

At the same meeting, the following officers were elected to serve for the 1954-1955 term:

*Chairman*—Fielding Ogburn, National Bureau of Standards, Washington, D. C.

*Vice-Chairman*—D. T. Ferrell, Jr., Naval Ordnance Laboratory, Washington, D. C.

*Secretary-Treasurer*—Jeanne B. Burbank, Naval Research Laboratory, Washington, D. C.

FIELDING OGBURN, *Secretary*

---

## PERSONALS

---

H. M. FISHER, technical supervisor of the Pennsylvania Salt Manufacturing Company's Natrona, Pa., plant, has been named technical assistant to the manager of Pennsalt's Calvert Works, Calvert City, Ky.

J. S. MACNAIRN, formerly research associate at Massachusetts Institute of Technology, Cambridge, Mass., has joined the engineering staff of the Chrysler Corporation, Detroit, Mich.

ROBERT A. STAUFFER, vice-president and director of research of the National Research Corporation, Cambridge, Mass., has been elected to the Board of Directors of the company. He is also vice-president and a director of the Vacuum Metals Corporation, jointly owned by the Crucible Steel Company of America and the National Research Corporation.

CHRISTOPHER L. WILSON recently became director of research at the Hudson Foam Plastics Corporation, Yonkers, N. Y. Formerly a professor in the Department of Chemistry at Ohio State University, Columbus, Dr. Wilson still retains a part-time position there.

VERNON A. LAMB, assistant chief of the Electrodeposition Section, National Bureau of Standards, Washington, D. C., has received the Department of Commerce Silver Medal for Meritorious Service. The award was made for outstanding contributions and distinguished leadership in development engineering in the field of electro-deposition.

EMILIO JIMENO of the University of Madrid, Spain, has recently been awarded the title of Doctor in Engineering "honoris causa" by the Engineering College of Hannover, Germany, for his contributions in chemistry, metallurgy, and corrosion.

GEORGE F. HERRMANN is now associated with S. W. Farber, Inc., Bronx, N. Y. In his position as chemical engineer he is responsible for all chemical operations involved in the manufacture of "Farberware" stainless steel aluminum clad kitchen utensils, aluminum giftware, and brass holloware with chrome on nickel plate. Mr. Herrmann was previously chemical engineer at Ronson Art Metal Works, Inc., Newark, N. J.

CHARLES A. THOMAS AND CARROLL A. HOCHWALT, president and vice-president, respectively, of the Monsanto Chemical Company, St. Louis, Mo., were among officers re-elected to the Board of Directors of the company for the coming year.

HOWARD ADLER, chemical director at Victor Chemical Works, Chicago, Ill., has been elected to the company's newly-created position of vice-president in charge of chemical research.

CLIFFORD A. HAMPPEL, chemical engineer, Homewood, Ill., and president of the Chicago Technical Societies Council, is a member of the commission named by Chicago's Mayor to nominate appointees for membership on the Chicago Board of Education.

## KARL M. LEUTE

Karl M. Leute, President of the Lithium Corporation of America, Inc., and also President of the Manganese Chemicals Corporation, both of Minneapolis, Minn., died on March 24, 1954, in Phoenix, Ariz.

Mr. Leute was born in Duluth, Minn., and was active in that city, as well as Detroit, Minneapolis, and Knoxville, in various enterprises. In 1937 he founded the Electro Manganese Corporation and erected the first successful commercial plant for the production of electrolytic manganese. The Metalloy Corporation, which was later to become the Lithium Corporation of America, Inc., was founded by Mr. Leute in 1942. In the ensuing 12 years he built the company into the leading factor in the lithium field. He formed the Manganese Chemicals Corporation in 1950 to produce manganese compounds from low-grade ores in Minnesota. This company had recently erected a plant at Riverton, Minn.

Less than two weeks prior to his death, Mr. Leute had announced plans on the part of Lithium Corporation to erect a \$7,000,000 plant for the expanded production of Lithium products at Bessemer City, N. C. Following completion of the arrangements for this project, Mr. Leute had gone to Phoenix for a vacation.

It has been announced that operations of the Lithium Corporation will continue unchanged. The Board of Directors of the company have appointed Herbert W. Rogers, Secretary of the corporation, to assume the duties of President of Lithium Corporation of America, Inc.

Mr. Leute became a member of The Electrochemical Society in 1940. He also held memberships in various technical societies, including The American Chemical Society, The American Institute of Mining & Metallurgical Engineers, and the American Society for Metals.

He is survived by his wife, Mayme, a daughter, Mrs. Rome Riebeth, and two grandchildren.

### Mention the Journal

When making purchases from our advertisers, please be sure to mention that you saw the ad in the JOURNAL.

---

## LETTER TO THE EDITOR

---

### Journal Advertising

Dear Sir:

The increased amount of advertising in the JOURNAL gives some of us a more comfortable feeling, since we know that the very high cost of printing has to be paid for out of Society income. Obviously, the greater the share of this cost which can be borne by advertising income, the less drain there is on membership dues, interest, and other sources of income.

There is nothing improper about having advertising in a technical journal, providing it does not interfere with the proper function of the publication. This function is to distribute and preserve scientific information. It is accomplished best if adequate funds are available to provide space for prompt publication of all worthwhile manuscripts.

Advertising does not interfere with the function of the JOURNAL as long as skillful editing separates technical writing and advertising in such a way that continuity is preserved, and so that binding of the permanent, technical record can easily be made independent of ephemeral matter. It would be objectionable, for example, to have advertising intercalated with technical writing; it is not objectionable, however, to have end sections or central sections devoted to advertising.

Let us welcome the advertisers. They are also members of our Society. Their company's advertising itself is literature, which to be effective in its own purpose must be at least of temporary interest to the reader. Let us do all other things which can insure a permanent, adequate, well-edited, dignified, and solvent journal.

J. F. GALL

Pennsylvania Salt Manufacturing Co., Philadelphia, Pa.

---

## MEETINGS OF OTHER ORGANIZATIONS

---

AMERICAN SOCIETY FOR TESTING MATERIALS, 57th Annual Meeting, Hotel Sherman, Chicago, June 13-18, will include the 11th Exhibit of Testing and Scientific Apparatus and Labora-

tory Supplies, and the 9th Photographic Exhibit with the theme Materials, Testing, and Research.

L'ALUMINIUM FRANCAIS and LA SOCIETE CHIMIQUE DE FRANCE, Scientific Congress and Exhibition, Paris, June 14-19, celebrating centenary of the first production of industrial aluminum in France by Henry Sainte-Claire Deville. Program and other relevant information available from the Secretary, L'Aluminium Francais, 23 Rue Balzac, Paris (8e), France.

CHEMICAL INSTITUTE OF CANADA, 37th Annual Conference and Exhibition, Royal York Hotel, Toronto, June 21-23; 2nd Western Regional Conference, Vancouver, B. C., Sept. 10-11.

INSTRUMENT SOCIETY OF AMERICA, third annual Analytical Instrument Clinic to be held in conjunction with the First International Instrument Congress and Exposition, Philadelphia, Sept. 13-15. Advance registration required. For registration forms and further information write Dr. Axel H. Peterson, Mellon Institute, 4400 Fifth Ave., Pittsburgh 13, Pa.

FIRST INTERNATIONAL INSTRUMENT CONGRESS AND EXPOSITION, Philadelphia, Sept. 13-24.

THIRD SALON DE LA CHIMIE ET DES MATIERES PLASTIQUES, Paris, Dec. 3-12.

---

## BOOK REVIEWS

---

TEMPERATURE MEASUREMENT IN ENGINEERING, by H. Dean Baker, E. A. Ryder, and N. H. Baker, Vol. I. Published by John Wiley & Sons, Inc., New York, and Chapman and Hall Limited, London, 1953. 179 pages, \$3.75.

The preface states "The object in this two-volume work is to provide in convenient non-mathematical form the information necessary to the engineer who wishes to measure temperature. An effort has been made to include all those specific details essential to actual execution, while refraining from encumbering the space with material of infrequent application or of the nature of background theory. . . . Volume I deals primarily with thermocouple technique. . . ."

The book gives many references to the literature, is well indexed, and contains many fine detailed drawings of practical thermocouple installations.

However, the reaction of this reviewer is generally unfavorable. The "how" is overemphasized relative to the "why." The first four chapters (33 pages) are intended as theory for both volumes, and are inadequate. More mathematics would strengthen the book without troubling any engineer. Students will learn little nor retain the various methods described in later chapters. British units are used throughout, rather than metric. Much of the text is excessively detailed. For example, in Chapter 9 (21 pages) dealing with drilling holes to insert thermocouples into samples, the following occurs:

"If a hole is drilled, the required depth of the hole is the distance, from the most accessible point on the surface from which the leads are to emerge, to the interior point at which temperature is to be measured. The diameter of the hole must be sufficient to accommodate the sensitive element and the leads.

"The larger the diameter of the hole, the greater will be the disturbance in temperature distribution within the body, because of the existence of the hole and of the thermocouple installation. Error in measurement is thereby greater for a larger diameter hole and less for a smaller diameter hole. The required diameter of hole is that which will just accommodate the installation. With thermocouples, the size of the sensitive element and leads, i.e., of the bead and lead wires, can be made very small by using small diameter wires."

Most of page 123 is occupied by a drawing of a hypodermic used to inject  $\text{CCl}_4$  into a hole to wash out chips formed in drilling, and nearly all of page 126 by a description of method for removing broken drills. Very few engineers will need such discussion.

GEORGE E. MOORE

---

### Correction

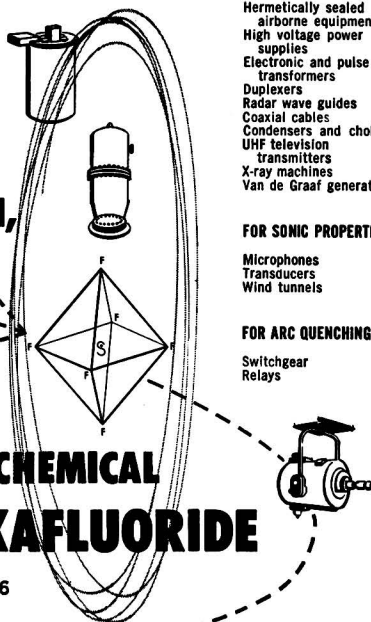
ROBERT D. NUTTING continues his association with E. I. du Pont de Nemours and Company, Inc., Newport, Del., as research supervisor in the Chemical Division of the Pigments Department.

SCHRADE F. RADTKE is director of the Metallurgical Research Laboratories of the Reynolds Metals Company, Richmond, Va.

**Wherever Liquid  
or Gaseous  
Insulation is used,  
consider . . .**

# GENERAL CHEMICAL SULFUR HEXAFLUORIDE

SF<sub>6</sub>



#### FOR DIELECTRIC STRENGTH

Hermetically sealed  
airborne equipment  
High voltage power  
supplies  
Electronic and pulse  
transformers  
Duplexers  
Radar wave guides  
Coaxial cables  
Condensers and chokes  
UHF television  
transmitters  
X-ray machines  
Van de Graaf generators

#### FOR SONIC PROPERTIES

Microphones  
Transducers  
Wind tunnels

#### FOR ARC QUENCHING

Switchgear  
Relays

### Read the Facts!

**WITH THREE TIMES THE DIELECTRIC STRENGTH** of nitrogen and equaling oil at modest pressure, Sulfur Hexafluoride provides a safe and convenient means of insuring reliable operation, increased power and voltage output, compact design and ease of maintenance of electronic equipment.

**INERT, NON-TOXIC, NON-FLAMMABLE AND EXTREMELY STABLE,** Sulfur Hexafluoride is easy and safe to handle. Its vapor pressure changes but slightly over a wide temperature range. One of the heaviest known gases, SF<sub>6</sub> has only a slight tendency to diffuse into the atmosphere when equipment is being filled or recharged. Small amounts of air do not materially affect its dielectric strength. That means making repairs or filling apparatus becomes a simple operation.

**FIND OUT MORE** about SF<sub>6</sub>. Send in this coupon and get your free copy of the technical bulletin on this remarkable new dielectric gas. Specifying your intended use will enable us to make helpful suggestions on the most effective way of using Sulfur Hexafluoride in your equipment.

### Send today!



**GENERAL CHEMICAL DIVISION, Allied Chemical & Dye Corporation**  
40 Rector Street, New York 6, N. Y.

Please send my free copy of your Sulfur Hexafluoride Technical Bulletin No. SF6A.

Name \_\_\_\_\_

Title \_\_\_\_\_

Organization \_\_\_\_\_

Address \_\_\_\_\_

City \_\_\_\_\_ Zone \_\_\_\_\_ State \_\_\_\_\_

I am interested in this product for \_\_\_\_\_ (specify end use) \_\_\_\_\_ JE-6

GENERAL CHEMISTRY, AN INTRODUCTION TO DESCRIPTIVE CHEMISTRY AND MODERN CHEMICAL THEORY, by Linus Pauling, 2nd ed. Published by W. H. Freeman and Co., San Francisco, 1953. xii + 710 pages, 193 illustrations. \$6.00.

A reviewer of the first edition of this book (1947) said that the student who could "make the grade" in mastering its contents would really have something worth while; and one might almost wonder what would be left for him to learn in the field. There was, of course, much more material available, and some of it is found in this second edition; there are over 50% more square inches of print, on more and larger pages. The author estimates that the book contains about 10% more material than is needed in a one year college course. Most teachers (to say nothing of students) will think him much too optimistic.

The book can only be recommended as a text for the superior and serious student who has an excellent background in high school chemistry, physics, and mathematics. It is too bad that Professor Pauling did not drop any pretense of writing for the beginner, since so much elementary definition and detail is missing anyway. Written exclusively for the superior group with previous experience, the text could have been kept to a more reasonable length, the lack of logical presentation would not be so obvious, and the book could assume its true stature as an excellent text on a somewhat advanced level.

As in the first edition, there is no "historical approach" to chemical theory. Assuming somewhat more prior knowledge than just that "every boy knows about atoms," why not start with authentic, modern description of the atom and its constituent particles, the molecule, x-rays, crystals and crystallography, radioactivity, the nature of electricity, quantum theory? On the other hand, it seems difficult, illogical, and unnecessary to try to derive elementary chemical theory from the pertinent experiments of physics alone. Historically, the experiments were just not planned that way; they were designed with current chemical knowledge fully in mind. The suggestion of discrete electrical particles hinged on atomic theory, not the other way round. The first experiments on x-ray diffraction were a test of the nature of the rays rather than of the crystals. More modern and advanced chemical theory is, of course, completely interwoven with physical theory.

The laws of stoichiometry and their significance in the development of chemistry are, as before, relegated to two pages of "Historical Remarks" in fine print (pp. 150, 151). The virtues of rigorous argument, of inductive and deductive logic are extolled, but the student will have to look closely for their application. There are, nevertheless, well written paragraphs on the nature of scientific theory, on the matter of precise and imprecise definition, on the value of "successive approximation" in theory as measurements become more exact, on the meaning of temperature, on the distinction between daltonides and berthollides, on the reality of the fundamental particles.

The chemist will feel on surer ground after he reaches Chapter 9 (p. 192). From this point on he has an excellent textbook in general and physical chemistry. There will not be too much disagreement about the order of presentation of elements and their compounds, and of theory. To be sure, some teachers would prefer more analytical properties, more description of industrial processes, especially more suggestions for lecture demonstrations and laboratory experiments. Many will feel that the theory goes too far into semi-advanced physical chemistry. All will feel that the chapters are well written, except that information is often anticipated and not given until later, if at all. As is to be expected from the author, the electronic and spacial structure of molecules, the nature of and variation in covalent bonding are not merely described; the concepts are integrated and applied throughout. The author's electronegativity scale of the elements is presented and used in a logical manner. The concept of resonance is plausibly introduced. The numerous illustrations (drawn by Roger Hayward) are very helpful and are much more interesting and attractive than line drawings.

The author has a disconcerting way of assuming acquaintance with important concepts which may (or may not) be discussed later; and is not always consistent with definitions. For instance, *erg* and *electron volt* are defined early and used consistently; *calorie* is not defined or illustrated in simple examples. One learns that a certain bond type is  $x$  kcal more stable than another, but energy in chemical reactions and the relation to spontaneity are not treated until Chapter 31 (p. 633). (In Chapter 32, the distinction between enthalpy and free energy is admirably discussed, in a qualitative

way.) Knowledge of the nature of equilibrium is needed long before adequate discussion is given. One feels that Chapters 5 and 6, on the Periodic System, should be written in some reverse order, with properties first, classification later. In Chapter 1, a *constituent* is defined as a *phase*, but this definition is never used again; the electron is a constituent of matter, aluminum is a constituent of minerals, bromine is the photochemically active constituent of a mixture with hydrogen. On p. 319 *steady state* is synonymous with true equilibrium; on p. 417 it denotes a time-independent flow of heat or matter.

Most chapters include several worked-out examples. The student is encouraged to reason each problem out rather than to use a formula or a set method. Numerous problems are given at the end of each chapter; the student who works some of them will find them quite appropriate, and will demonstrate that he has learned his lessons.

CECIL V. KING

**CHROMIUM—THE METALLURGY OF THE RARER METALS, No. 1, by A. H. Sully.** Published by Academic Press Inc., New York, and Butterworths Scientific Publications, London, 1954. 272 pages, \$5.50.

This is a comprehensive compendium of the literature on chromium. Students, research workers, and plant operations personnel will find it a handy reference and textbook.

The book opens with a survey of the occurrence and world-wide distribution of chromium ores. Then the methods for preparing ferroalloys, as well as commercial and high purity chromium, are described. The numerous data on the physical properties of pure chromium have been compiled and critically reviewed.

The shaping of chromium by either melting and casting or by hot working is beset with difficulties which can sometimes be by-passed through the use of powder metallurgy methods. The plastic deformation characteristics of chromium are related to the so-called brittle/ductile transition; this is discussed and an explanation proposed.

Since chromium electroplates and diffused alloy layers on metallic materials have extensive commercial use, it is not surprising that about 25% of the book relates to these subjects. The history, methods, theories, and properties of these superficial layers are given. The final portion of the book is devoted

to a discussion of the alloying characteristics of chromium with reference to (a) binary and ternary equilibrium diagrams and (b) the properties of high chromium alloys.

The foreword states that "Chromium" is the first of a series of books on the metallurgy of the "rare metals." Dr. Sully's work has given this worthwhile project an excellent start.

E. S. GREINER

**ZIRCONIUM—METALLURGY OF THE RARER METALS, No. 2, by G. L. MILLER.** Published by Academic Press Inc., New York, 1954. xviii + 382 pages, \$7.50.

The author's preface states "The reason for writing this book was a desire to collate the information on zirconium which has been flowing at an ever increasing rate from the technical press during the last few years." This objective has been adequately carried out. The book gives a digest of the available information on zirconium and an extensive bibliography is appended at the end of each chapter.

This book may be divided more or less naturally into four sections. The first of these contains information on the availability of zirconium ores, the methods of extraction, and the purification procedures used to prepare pure zirconium compounds. Particular emphasis is placed on the removal of hafnium from which zirconium must be freed if it is to be used for nuclear purposes. A number of references to the newer methods of separating these elements by ion exchange and adsorption mechanisms are cited. The data, however, are for laboratory separations and no information is given for production methods.

The second section of the book is concerned with the production of zirconium sponge and with the preparation of ductile zirconium bars. Detailed information for the production of zirconium sponge by the Kroll process is given. Details for the production of ductile zirconium by the Van Arkel process are for small-scale operations, and in discussing quantity production methods the author draws heavily on the related experience with titanium.

A third section of the book gives an excellent survey of the chemical and physical properties of zirconium and its alloys which should be of especial value to the metallurgical engineer interested in exploring the usefulness of these materials.

The last section of the book deals with zirconium melting and fabricating processes. Arc melting processes are discussed in detail. In addition, a good summary of the newer melting techniques is given, some of which are applicable to other metals where high purity is essential. In regard to fabrication, the methods discussed are conventional for reactive metals. Precautions required in handling zirconium are included in this section.

On the whole this book is concise and well written and should be an excellent reference source for the chemist or metallurgist interested in zirconium.

H. C. THEUERER

**CATALYSIS, Volume 1. FUNDAMENTAL PRINCIPLES (Part 1).** Edited by P. H. EMMETT. Published by Reinhold Publishing Corp., New York, 1954. 394 pages, \$10.00.

This is the first volume in a series which is designed to give an account of the physical chemistry of catalysts and catalytic processing. In view of the

rapid advances which have recently been made in the fields of surface chemistry and catalysis, its publication is most timely.

About three quarters of this first volume are devoted to a review of surface chemistry and the remainder to an account of industrial catalysts. Each chapter (of which there are eight) is written by a person who is regarded as a leader in that particular field so that it is not surprising that the book as a whole is well and clearly written.

The first five chapters provide good, up-to-date critical reviews of physical adsorption, measurement of surface areas, chemisorption, and rates of surface reactions and contain about 500 references to the literature, ranging from Langmuir's earliest work to the present time.

The following two chapters describe catalyst carriers, promotion, acceleration, poisons, inhibitors, and catalyst preparation, principally from an industrial point of view. While there is no doubt that these are two valuable chapters, many readers may have

preferred that they be included in a later volume.

The final chapter gives a concise account of the relationships between magnetic and catalytic properties of materials.

The book can be recommended to anyone interested in catalysis and surface chemistry, and will form a valuable part of all reference libraries.

J. T. LAW

**DIE METALLURGIE DER FERROLEGIERUNGEN.** Edited by R. Durrer and G. Volkert. Published by Springer, Berlin, Goettingen, Heidelberg, 1953. Price 72.00 DM, about \$16.00.

The last comprehensive treatise on the subject of ferroalloy production is the one of the Frenchman Coutagne, which was printed in 1924, just 30 years ago. This incomprehensible gap has now been filled with the appearance of a book written in German under the direction of two well-known iron and steel electrometallurgists, R. Durrer and G. Volkert. It is astounding that, despite the fact that the United States possesses one of the most powerful ferroalloy industries of the world, no such book ever was written by one or the other of the many specialists of this country. The lethargy in this field is illustrated by the almost complete absence of publications on this subject in the *TRANSACTIONS* of this Society. This secrecy is barely understandable when considering that so much of the current U. S. practice originates in foreign countries, such as the Söderberg electrode, the Elchem rotating hearth furnace, the low carbon silicochrome and Perrin processes. The lack of English written textbooks is aggravated by the curious fact that no American university teaches applied electrothermics, so that students who want to introduce themselves to this kind of metallurgy are most seriously handicapped. The new book presents the problems of ferroalloy production from the continental European angle, but American publications, as far as they exist, have duly been reported.

The subject matter of the book has been divided into five different sections, written by 14 different authors, among whom there is one American. Yet inhomogeneity has been mostly avoided, coordination is excellent, and repetitions are few. The first section concerns the general principles of the metallurgy of ferroalloys; the second

# ALSiMAG®

CUSTOM MADE

## TECHNICAL CERAMICS

If your requirements call for materials which must withstand high temperatures, electrical stresses, or the corrosive action of chemicals, one of the many AlSiMag ceramic compositions may be the answer to your problem • If you also need accurately formed shapes, to your own design, which must withstand thermal and mechanical stresses, then it will pay you to contact AlSiMag Headquarters, the American Lava Corporation, to discuss your technical problems on a confidential basis.

**AMERICAN LAVA CORPORATION**

A SUBSIDIARY OF MINNESOTA MINING AND MANUFACTURING COMPANY  
53 RD YEAR OF CERAMIC LEADERSHIP  
CHATTANOOGA 5, TENNESSEE

BRANCH OFFICES IN: Newark, N. J., Syracuse, N. Y., Cleveland, O., Cambridge, Mass., Philadelphia, Penn., St. Louis, Mo., Chicago, Ill., Dallas, Tex., Los Angeles, Cal.

the construction of furnaces and the electrical problems involved, such as those of transformers, electrode regulation, switching arrangements, electrical conditions, wild and blind phases; the third section is written by specialists on electrodes, amorphous, graphite, and Söderberg type, while the next one concerns the specific methods of production of the following ferroalloys: FeCr high and low C, FeCo, FeMn high and low C, FeMo, FeNi, FeP, FeSi, FeTa, FeCb, FeTi, FeV, FeW, and FeSiZr. In the last section new outlooks for ferroalloy production are exposed, especially with regard to the arrival of a potential competitor, the low shaft, oxygen blast furnace.

The highly interesting section IV on the production of ferroalloys refers not only to arc furnace practice, but all other methods are also well reported, such as aluminothermic, silico and metallothermic processes, as well as blast furnace practice; most interesting comparisons are made, especially with regard to respective economic limits. Many details are given as to aluminothermic procedures, which up to now have not been described in the literature.

In spite of the outstanding quality of this book, there may be some critical remarks as to the following points. Despite the fact that so many high class

specialists have been called upon to bring the subject matter up to date, the reader will still be quite bewildered after reading certain chapters as to what is the real present-day practice. This occasional lack of knowledge of the authors is apparent from the fact that the old book of Coutagne is referred to in many places in almost any chapter as a valuable source of information. On the other hand, those authors who are really aware of modern practice have a tendency to overplay their subject and their chapters are bulging over compared to those presenting subject matter of greater importance. For instance, forty pages concern the, no doubt, most interesting German war practice of ferrovanadium production from low vanadium pig iron, as compared with only nine pages on ferrosilicon production. This chapter on German vanadium practice is the best treatise on this matter that has been published. The same observation concerns the reclamation of manganese from slags. However, those engaged at present in this country in winning manganese from similar materials would certainly gain a lot of knowledge just by reading these pages, in which converter practice is condemned in favor of blast furnacing, followed by arc furnace reduction.

In spite of these few hypertrophies it can be said that this book is an invaluable source of information for the electrothermics man, and that it does away with a lot of the secrecy, spread over this field of metallurgy mostly by practitioners with no academic training.

W. J. KROLL

---

## RECENT PATENTS

---

Selected by Fred. W. Dodson, Chairman of the Patent Committee, from the Official Gazette.

March 2, 1954

- Shortsleeve, F. J., and Nicholson, M. E., 2,671,050, Stainless Steel Alloy and Apparatus for Converting Hydrocarbons
- Aten, A. H. W., and Wiechers, S. G., 2,671,055, Process for Electrolyzing Aqueous Liquids
- Sherrick, P. H., 2,671,123, Radiant Heating Furnace
- Bagley, G. D., 2,671,124, Electric Reduction Furnace
- Héraud, A., 2,671,125, Sheath-Insulated Flat-Cell Battery

## MANUSCRIPTS AND ABSTRACTS FOR FALL MEETING

Manuscripts are now being received for the Fall Meeting of the Society, to be held at the Statler Hotel in Boston, October 3, 4, 5, 6, and 7, 1954. Subjects to be covered at the technical sessions will be Battery, Corrosion, Electrodeposition, and Electrothermics.

To be considered for this meeting, triplicate copies of manuscripts or abstracts (not to exceed 75 words in length) must be received at Society headquarters, 216 West 102nd Street, New York 25, N. Y., *not later than July 15, 1954.*

- Ray, C. H., and Sears, J. N., 2,671,153, Electric Control Device and Electrolytic Fluid Therefor  
 Burstain, E., 2,671,154, Infrared Detector  
 Douglas, R. W., and Lindell, O. E., 2,671,156, Method of Producing Electrical Crystal-Contact Devices  
 Morey, W. A., 2,671,181, Servomotor Control Apparatus for Electric Furnaces and the Like  
 Kenty, C., 2,671,184, Flashing Discharge Device  
 Racine, M. J., and Coppel, C. L., 2,671,188, Simplified Metallic Rectifier Assembly

March 9, 1954

- Foyn, K., 2,671,816, Cylindrical Electrode Holder  
 Groddeck, K. B., 2,671,817, Electroactive Radiation Screen  
 Turck, J., 2,671,818, Thermopile  
 Field, B. R., 2,671,819, Lid of Electric Accumulators  
 Herbert, W. S., 2,671,820, Combination Jumper Insulator  
 Macomber, O. B., 2,671,890, Battery Post Terminal

March 16, 1954

- Carlile, F. S., 2,671,944, Apparatus for Manufacturing Battery Grids of Calcium and Lead Alloy  
 Lewin, G., 2,671,954, Vapor Electric Device  
 Malloy, J. E., 2,672,429, Electrical Steel  
 den Hertog, H. J., and Bruin, P., 2,672,438, Hydrochlorination of Unsaturated Organic Compounds by Electrical Discharge  
 den Hertog, H. J., and Bruin, P., 2,672,439, Hydrobromination of Olefinic Compounds by Electrical Discharge  
 den Hertog, H. J., and Bruin, P., 2,672,440, Production of Alcohols from Olefinic Compounds by Electrical Discharge  
 White, R. J., 3,672,441, Electrode for Measuring Ion Concentration in Solutions  
 Wollentin, R. W., and Nagy, R., 2,672,451, Improved Cadmium Halophosphate Phosphors  
 Lamb, R. H., 2,672,491, Electric Arc Furnace and Cover with Electrodes and Feed Conduits  
 Sukacev, L., 2,672,492, Thermopiles  
 Tingle, L., and Brandon, J. M., 2,672,493, Immersion Thermocouple Construction  
 Fleischer, A., 2,672,494, Nickel Oxide-Carbonyl Nickel Sintered Plates

- Fleischer, A., 2,672,495, Sintered Plate for Nickel-Cadmium Secondary Batteries  
 Lubeck, C. H. O., 2,672,496, Inset Plate for Electrodes of Alkaline Accumulators  
 Burns, H. C., and Wilson, H. D., 2,672,497, Method of Producing Storage Batteries  
 Temple, L. M., 2,672,498, Battery Radeke, W. H., 2,672,499, Battery Cell Inspecting and Testing System  
 Ewing, S. P., 2,672,587, Cathodic Protection of Tank Bottoms

March 23, 1954

- Duncan, D. W., and Eustis, P., 2,673,178, Electrolysis of Zinc Chloride  
 Duncan, D. W., and Eustis, P., 2,673,179, Process for the Recovery of Zinc  
 Emanuel, W. A., Sweeney, K. O'N., and Mahoney, J. F., 2,673,180, Production of Electrolytic Zinc  
 Hubert, B., 2,673,227, Electrode Holder with Fluid Control  
 Kistler, S. S., 2,673,228, Induction Furnace with High-Temperature Resistor  
 Khok, M., 2,673,229, Low-Frequency Induction Furnace for Melting Non-ferrous Metals  
 Brennan, J. B., 2,673,230, Battery Separator  
 Kennedy, H. A., 2,673,231, Storage Battery Cap  
 Silsby, C. C., Jr., 2,673,232, Feed Device for Electrolytic Cells  
 Beese, N. C., 2,673,304, Crater Lamp  
 Odell, N. H., 2,673,312, Semiconductor Device

March 30, 1954

- Vonada, E. E., 2,673,836, Continuous Electrolytic Pickling and Tin Plating of Steel Strip  
 Lowe, C. S., and Ricks, H. E., 2,673,837, Electrolytic Production of Fluorobates  
 Booth, F., 2,673,887, Manufacture of Separators for Electric Batteries  
 Melnikoff, N., 2,673,888, Treatment of Storage Battery Plates  
 Lilienfeld, J. E., 2,673,955, Alternating Current Electrolytic Condenser

97. The control is applicable in production processes for electric, steam, and hot water heaters; baths of all kinds; ovens, kilns, and dryers; plastic extrusion presses; and has a number of other uses. Available for wide ranges in temperature and operates on the principle of the change of resistance of a wire-wound sensing element with changes in temperature. The manufacturer will recommend and supply a complete range of control elements for use with the control. Robertshaw-Fulton Controls Co. P-208

LAPP PULSAFEEDER. 24-page, 2-color booklet describes line of PULSAFEEDER diaphragm-type controlled volume pumps. The maintenance-free feature of no stuffing box is stressed; it is also pointed out that PULSAFEEDER, although basically a pump, also functions as a chemical feeder, meter, instrument, filling machine, proportioner, and sampler. Also covered in detail are special liquid handling assemblies. Both manual and automatically-controlled types are described. Several pages are devoted to the Auto-Pneumatic Pulsafeeder, pointing out its adaptability to automatic volume adjustment from commercial pneumatic instruments. Lapp Insulator Co., Inc. P-209

DECADE SHUNT. A low cost micro-microammeter results from combining a Keithley Electrometer and new Decade Shunt, described in a recent 2-page bulletin. The Shunt provides 10 current ranges, permitting full-scale readings over the enormous range of 2 ma down to 2  $\mu$ a, over 100 times the sensitivity of current-sensitive galvanometers. Included in the bulletin are full specifications and circuit schematic diagrams of such typical uses as accurate measurement of photocell currents, capacitance, and extremely high resistances. Keithley Instruments. P-210

## LITERATURE FROM INDUSTRY

ELECTRONIC TEMPERATURE CONTROL. Bulletin gives information on the new electronic temperature control, Series

REGULATED POWER EQUIPMENT CATALOGUE. A new general catalogue is available on the manufacturer's entire standard line of instruments, which includes electronic a-c voltage regulators, regulated d-c sources and "B-Supplies," electronic frequency changers, inverters, magnetic-amplifier d-c sources, and



related equipment. The catalogue provides abundant general information on the operating principles of Sorensen instruments and complete specific data on each instrument; also pictures, general descriptions, electrical and mechanical specifications. Sorensen & Co., Inc.  
P-211

**PORTABLE TEMPERATURE INDICATORS.** 8-page bulletin just issued describes two portable temperature indicators, the Potentiometer Indicator and the Resistance Thermometer. Described in detail are operating adjustments, features of design, test circuits, measuring elements, and instrument specifications. An entire page is devoted to listing the standard scales available, covering temperatures from  $-200^{\circ}$  to  $+2800^{\circ}\text{F}$ . Tables also list the type of thermocouple or resistance bulb recommended for each range, as well as the degrees of temperature indicated by each scale division. Also covered is the use of portable pyrometers in checking installed pyrometric instruments and in replacing potentiometers which are temporarily out of service. The Foxboro Co.  
P-212

**"RUBBER LININGS."** Illustrated, 2-color, 8-page brochure gives information on the advantages and application of rubber lining to steel tanks, drums, pipes, valves, fittings, and pumps. Included are important tables giving the resistance characteristics of MW rubber lining to inorganic acids, salts and alkalies, organic materials, and a wide group of miscellaneous materials. Details on the chemical, abrasive, and temperature resistant qualities of rubber linings and the different types of linings available are also given. Metalweld, Inc.  
P-213

**ELECTROMETER VOLTAGE DIVIDERS.** D-C potentials to 20,000 volts can be measured with a Keithley electrometer and new voltage dividers, presented in a new bulletin. Designated the Models 2006 and 2007, the resistive dividers have division ratios of 100:1 and 1000:1, respectively, maximum inputs of 2000 and 20,000 volts, and input impedances of  $10^{12}$  ohms. Combining an electrometer and new voltage divider results in a high-impedance d-c kilovoltmeter with

## Support Our Advertisers

Since advertisers in the JOURNAL are investing money in our publication, members of the Society have a great opportunity to cooperate in the mutual success of the project. For instance, Society members buy large quantities of products, instruments, and equipment. Whenever an advertiser's products meet company specifications, readers are urged to give preference in their purchases to JOURNAL advertisers.

several unusual features—wide selection of voltage ranges, polarity sensitivity, very short time constant, and unusual portability. Uses include measuring voltages on cathode ray tubes, photomultiplier tubes, radiation equipment, and leakage of high-voltage insulators. Keithley Instruments.  
P-214

**ARITEMP RESINS.** Brochure, including data sheets, describes line of ARITEMP resins for casting and encapsulation of electrical components. These resins are extremely resistant to both high and low temperatures, have excellent mechanical properties, exhibit a marked adhesion to metals, and a high resistance to water vapor transmission. Have excellent electrical properties, which makes them well suited for applications in the electronics industry. Aries Laboratories, Inc.  
P-215

**ELECTRONIC AIR CLEANERS.** 8-page booklet describes electronic air cleaners for homes and smaller commercial and industrial building areas. Discussed are construction features of the horizontal and vertical air-flow units; also specifications, dimensions, size estimation, principle of operation, methods of testing air filter efficiency. Typical commercial and industrial applications are listed. Electro-air Cleaner Co.  
P-216

---

## NEW PRODUCTS

---

**CHROMATE REDUCER.** A new product called "Chromekill 4A" has been announced for destruction of hexavalent chromium in alkaline cleaning and plating solutions. Designed to give a dual action. Contains materials for fast reduction of hexavalent chromium to the harmless trivalent chromium state; also contains more stable reducing agents to give prolonged protection. The material is available as a fine free-flowing powdered mixture and is used in concentrations of the order of  $\frac{1}{4}$  oz./gal. Enthone, Inc.  
N-77

**ENAMEL STRIPPER.** New enamel stripper, nonflammable, mild in odor, and pleasant to use, removes Epoxy type enamels and most other enamels. Suitable for removing enamels from brass and other base metals, including aluminum and steel. The stripper is operated at room temperature; the enamel is removed by a wrinkling action, and the stripper and loosened enamel are removed from the work by means of a water rinse. A water seal is used to reduce evaporating losses. The stripper is supplied as a thin clear liquid in steel drums. Enthone, Inc.  
N-78

**CONDUCTIVITY CELLS.** A new series of electrolytic conductivity cells for use with Dynalog Conductivity Instruments are designed for high and low conductivity measurements, detecting the concentration of acids, bases, and salts in solution. Low-conductivity cells (constants of 1, 0.1, and 0.01) are available in two types, both designed for insertion in a pipeline or a tank. High-conductivity cells (constants of 10 and 100) also furnished in two types, one for insertion, the other a dip type for open tanks. The Foxboro Co.

N-79

**4-WAY VALVE.** Now available is a new hand-and-foot operated 4-way valve with patented built-in, full-capacity, flow-control meters of the Venturi type. Specifically designed for the control of double acting air or hydraulic cylinders. The flow control meters permit full-line volume without loss of pressure. Line-pressure variation will not affect valve function. The valve is also available for remote pilot operation, cam, single or double solenoid, together with time-delay features. Noncorrosive throughout; extremely compact. Airmatic Valve, Inc. N-80

**RECEIVER-INTEGRATOR UNIT.** A receiver-integrator for graphic panels has been designed for use with the company's line of compact Consotrol instruments. A pneumatic-electric instrument, the new Type 224 Receiver-Integrator computes an accurate and continuous total of any process flow and operates a small counter located in the graphic display. Consists of two small, self-contained units: a remote counter and a flow receiver. Available for uniform or square root scales to totalize minute, hourly, or daily rates. Developed chiefly for graphic-type panels, it is equally suited to control cabinet installations where compact instrumentation is desired. The Foxboro Co. N-81

**MICRO-OPTICAL PYROMETER.** An entirely new type of optical pyrometer, known as the Pyro Micro-Optical Pyrometer, has been developed to meet the demand not only for higher degrees of accuracy but also greater versatility in the measurement of temperatures over 700°C (1300°F). Designed particularly for precision temperature measure-

ments in the laboratory, yet sufficiently portable to be used for general plant applications. Capable of measuring targets less than 0.001 in. in diameter and, by means of supplementary lenses, can be adjusted for focal distances varying from 5 in. to infinity. Mountings on table-top and floor type tripods available, and the vernier worm gears permit extremely fine vertical and horizontal adjustments of the telescope. The Pyrometer Instrument Co. N-82

**HOOK-ON VOLT-AMMETER.** New hook-on volt-ammeter is believed to be the first with automatic scale changing. Designated the AK-5, the pocket-size unit is designed to measure current and voltage quickly and accurately. A valuable aid in balancing circuits, tracing faults and grounds, estimating distribution circuits, and diagnosing operating troubles, the volt-ammeter is an essential accessory for engineers, contractors, maintenance and service men, and many others. Has a current range of 5/20/80/350 amperes. Measures a-c voltage in three ranges (150/300/750) without auxiliary equipment, provides accuracy up to 3% of full scale, and withstands a voltage breakdown test of 4000 volts a.c. General Electric Co. N-83

**GLENNITE NONLINEAR DIELECTRICS.** New materials available in thin sheets from 0.002 to 0.025 in. thickness, or as finished units complete with electrodes, leads, and protective coatings. Narrow loop materials have low losses, are suitable for high frequency applications. Square loop bodies have high remanent polarization necessary for memory work. Typical applications: dielectric amplifiers, memory devices, modulation, voltage tuning, frequency doubling, sweep circuits, variable filters. Glenco Corp. N-84

---

## ADVERTISERS' INDEX

American Lava Corporation.	158C
Enthone, Incorporated . . .	Cover 4
General Chemical Division, Allied Chemical & Dye Corp. . . . .	156C
Great Lakes Carbon Copora- tion . . . . .	Cover 2
National Carbon Company 140, 141C	
Torsion Balance Company. . .	142C
Weston Electrical Instrument Corporation. . . . .	144C

---

"ADJUST-A-VUE HANDLE." Manufacturers of the "260" Volt-Ohm-Milliammeter will incorporate a new utility handle on Model 260's. The new handle carries the trade name "Adjust-A-Vue Handle" and permits the technician to set his tester at any convenient viewing angle while he is servicing. Eliminates the use of old-fashioned, bulky, bird cage accessory devices. Stays cleaner in actual service since there are no large dirt-collecting pores in its smooth surface. Constructed of steel coated with tough Durez plastic. Simpson Electric Co. N-85

---

## EMPLOYMENT SITUATION

---

Please address replies to box shown, % The Electrochemical Society, Inc., 216 W. 102nd St., New York 25, N. Y.

### Position Wanted

**ELECTROMETALLURGIST.** B.S., M.S., and Ph.D. degrees in metallurgy. Permanent resident alien. Eight years in nonferrous and corrosion research. Knowledge of corrosion, hydro- and electrometallurgy, radiography, x-ray diffraction, spectro-analysis, and heat treatment. Desires position in research, production, or plant control with opportunity for experience and advancement. Location immaterial. Reply to Box 355.

To receive further information on any New Product or Literature from Industry listed above, send inquiry, with key number, to JOURNAL OF THE Electrochemical Society, 216 West 102nd Street, New York 25, N. Y.

Please print your name and address plainly.

# Sustaining Members of The Electrochemical Society

- Air Reduction Company, Inc., New York, N. Y.  
Ajax Electro Metallurgical Corporation, Philadelphia, Pa.  
Alloy Steel Products Company, Inc., Linden, N. J.  
Aluminum Company of America, New Kensington, Pa.  
Aluminum Company of Canada, Ltd., Montreal, Canada  
American Machine & Foundry Co., Raleigh, N. C.  
American Platinum Works, Newark, N. J. (2 memberships)  
American Potash & Chemical Corp., Los Angeles, Calif.  
American Zinc, Lead and Smelting Company, St. Louis, Mo.  
Armour Research Foundation, Chicago, Ill.  
Auto City Plating Company Foundation, Detroit, Mich.  
Bell Telephone Laboratories, Inc., New York, N. Y.  
Bethlehem Steel Company, Bethlehem, Pa. (2 memberships)  
Buffalo Electro-Chemical Company, Buffalo, N. Y.  
Burgess Battery Company, Freeport, Ill. (4 memberships)  
Canadian Industries Limited, Montreal, Canada  
Chrysler Corporation, Detroit, Mich.  
Columbia-Southern Chemical Corporation, Pittsburgh, Pa.  
Consolidated Mining and Smelting Company of Canada, Ltd., Trail, B. C. (2 memberships)  
Corning Glass Works, Corning, N. Y.  
Crane Company, Chicago, Ill.  
Diamond Alkali Company, Pittsburgh, Pa. (2 memberships)  
Dow Chemical Company, Midland, Mich.  
Wilbur B. Driver Company, Newark, N. J.  
E. I. du Pont de Nemours & Company, Inc., Wilmington, Del.  
Eagle-Picher Company, Joplin, Mo.  
Eaton Manufacturing Company, Stamping Div., Cleveland, Ohio  
Electric Auto-Lite Company, Toledo, Ohio  
Electric Storage Battery Company, Philadelphia, Pa.  
The Eppley Laboratory, Newport, R. I.  
Ford Motor Company, Dearborn, Mich.  
General Chemical Division, Allied Chemical & Dye Corporation, New York, N. Y.  
General Electric Company, Schenectady, N. Y.  
General Motors Corporation, Research Laboratories Division, Detroit, Mich.  
Gould-National Batteries, Inc., Depew, N. Y.  
Graham, Crowley & Associates, Inc., Chicago, Ill.  
Great Lakes Carbon Corporation, Niagara Falls, N. Y.  
Hanson - Van Winkle - Munning Company, Matawan, N. J. (2 memberships)  
Harshaw Chemical Company, Cleveland, Ohio (2 memberships)  
Hooker Electrochemical Company, Niagara Falls, N. Y. (3 memberships)  
Houdaille-Hershey Corporation, Detroit, Mich.  
International Graphite & Electrode Div., Speer Carbon Company, St. Marys, Pa. (2 memberships)  
International Minerals & Chemical Corporation, Chicago, Ill.  
International Nickel Company, Inc., New York, N. Y. (3 memberships)  
Kaiser Aluminum & Chemical Corporation, Division of Metallurgical Research, Spokane, Wash.  
Mathieson Chemical Corporation, Niagara Falls, N. Y.  
McGean Chemical Company, Cleveland, Ohio  
Merck & Company, Inc., Rahway, N. J.  
Metal & Thermit Corporation, New York, N. Y.  
Monsanto Chemical Company, St. Louis, Mo.  
National Carbon Division, Union Carbide and Carbon Corporation, New York, N. Y. (2 memberships)  
National Cash Register Company, Dayton, Ohio  
National Research Corporation, Cambridge, Mass.  
Niagara Alkali Company, Niagara Falls, N. Y.  
Norton Company, Worcester, Mass.  
Pennsylvania Salt Manufacturing Company, Philadelphia, Pa. (2 memberships)  
Phileo Corporation, Lansdale, Pa.  
Philips Laboratories, Inc., Irvington-on-Hudson, N. Y.  
Potash Company of America, Carlsbad, N. Mex.  
Promat Division, Poor & Company, Waukegan, Ill.  
Ray-O-Vac Company, Madison, Wis.  
Rockwell Spring and Axle Company, Coraopolis, Pa.  
Solvay Process Division, Allied Chemical & Dye Corporation, Syracuse, N. Y. (3 memberships)  
Stackpole Carbon Company, St. Marys, Pa.  
Standard Steel Spring Division of the Rockwell Spring and Axle Company, Coraopolis, Pa.  
Stauffer Chemical Company, San Francisco, Calif.  
Sylvania Electric Products Inc., Bayside, N. Y. (2 memberships)  
Sarkes Tarzian, Inc., Bloomington, Ind.  
Tennessee Products & Chemical Corporation, Nashville, Tenn.  
Edylite Corporation, Detroit, Mich. (2 memberships)  
Union Carbide Company, Electrometallurgical Division, New York, N. Y.  
United Chromium, Inc., New York, N. Y.  
Vanadium Corporation of America, New York, N. Y.  
Victor Chemical Works, Mt. Pleasant, Tenn.  
Wagner Brothers, Inc., Detroit, Mich.  
Western Electric Company, Inc., Chicago, Ill.  
Western Electrochemical Company, Los Angeles, Calif.  
Westinghouse Electric Corporation, E. Pittsburgh, Pa.  
Willard Storage Battery Company, Cleveland, Ohio.  
Yardney Electric Corporation, New York, N. Y.

# STRIP

...economically  
...quickly

with

ENTHONE  
metal strippers

platings

coatings

solders

*Enthone*  
AT WORK

ENTHONE  
INCORPORATED

442 ELM STREET

NEW HAVEN, CONNECTICUT

ENTHONE has developed 8 outstanding metal strippers which, without attacking your base metal in any way, quickly and economically strip off defective plated coatings, excess solder, silver brazing metal, and metal smuts.

Where your  
base metal is . . .

STEEL

and you want to strip nickel, copper, silver, zinc or cadmium chemically, use

ENSTRIP "S", an additive for sodium cyanide solutions, or . . . ENSTRIP "A", which is a prepared compound containing sodium cyanide.

where you want to remove copper or nickel coatings electrolytically, use

ENSTRIP 103, an economical alkaline electrolytic stripper containing no cyanide.

COPPER  
or  
STEEL

and you wish to dissolve tin, lead, or tin-lead coatings chemically, use

ENSTRIP "TL", a fast acting, alkaline stripper.

ALUMINUM,  
COPPER  
or  
STEEL

and you want to take off heavy chromium coatings chemically, use

ENSTRIP "CR-5", a rapid, acid type stripper.

COPPER  
ALLOYS

use ENSTRIP "165-S", an additive for acid solutions that will give you quick removal of nickel, tin, zinc, lead or cadmium.

ZINC  
DIE  
CASTINGS

use ENSTRIP "L-88", an acid electrolytic stripper for removing chromium, nickel or copper coatings.

Write directly to Enthone Incorporated, or to your nearest Enthone Service Representative, for further information.

ARDCO, INC.,  
5000 West 73rd Street,  
Chicago 38, Illinois

R. O. HULL & COMPANY,  
1300 Parsons Court,  
Rocky River, Ohio

L. H. BUTCHER COMPANY,  
3628 East Olympic Boulevard,  
Los Angeles, California

\* The Scientific Solution of Metal Finishing Problems